EPA-650/2-73-048b

December 1973

Environmental Protection Technology Series

EVALUATION OF THE FLUIDIZED-BED COMBUSTION PROCESS

VOLUME II - FLUIDIZED-BED BOILER COMBINED-CYCLE POWER PLANT DEVELOPMENT --VOLUME I APPENDICES

Office of Research and Development
U.S. Environmental Protection Agency
Washington, D.C. 20460

EPA-650/2-73-048b

EVALUATION OF THE FLUIDIZED-BED COMBUSTION PROCESS

VOLUME II - FLUIDIZED-BED BOILER COMBINED-CYCLE POWER PLANT DEVELOPMENT--VOLUME I APPENDICES

by

D.L. Keairns, D.H. Archer, J.R. Hamm,
R.A. Newby, E.P. O'Neill, J.R. Smith, and
W.C. Yang

Westinghouse Research Laboratories
Pittsburgh, Pennsylvania 15235

Contract No. 68-02-0217
ROAP No. 21ADB-09
Program Element No. 1AB013

EPA Project Officer: P.P. Turner

Control Systems Laboratory
National Environmental Research Center
Research Triangle Park, North Carolina 27711

Prepared for

OFFICE OF RESEARCH AND DEVELOPMENT
U.S. ENVIRONMENTAL PROTECTION AGENCY
WASHINGTON, D.C. 20460

December 1973

This report has been reviewed by the Environmental Protection Agency and approved for publication. Approval does not signify that the contents necessarily reflect the views and policies of the Agency, nor does mention of trade names or commercial products constitute endorsement or recommendation for use.

ACKNOWLEDGMENTS

The results, conclusions, and recommendations presented in this volume represent the combined work and thought of many persons at Westinghouse and the Office of Research and Development (ORD). Other ORD contractors have freely shared with us their ideas and the results of their research and development effort.

In particular, we want here to express our high regard for and acknowledge the contribution of personnel at Westinghouse Research Laboratories and the personnel at ORD who conceived the overall fluidized bed combustion boiler effort and who have defined, monitored, and supported the efforts of Westinghouse and others on the program. Mr. P. P. Turner, Chief of the Advanced Process Section, has served as project officer on our work. Numerous enlightening and helpful discussions have been held with Mr. Turner; with section members D. Bruce Henschel and Sam Rakes; and with R. P. Hangebrauck, Chief of the Demonstration Projects Branch. Mr. E. J. Vidt participated in the evaluation. Mr. R. E. Brinza, Mr. W. F. Kittle and Mr. C. Spangler assisted in the collection of data.

PREFACE

The Office of Research and Development (ORD) of the United States Environmental Protection Agency has organized and is sponsoring a fluidized bed fuel processing program. Its purpose is to develop and demonstrate new methods for utilizing fossil fuels -- particularly coal and oil -- in utility power plants. These methods should:

- Meet environmental goals for SO_2, NO_x, ash, smoke emissions, and wastes
- Compete economically with alternative means for meeting these abatement goals.

Westinghouse Research, under contract to the Office of Research and Development (ORD) of the Environmental Protection Agency, is carrying out a study to evaluate and develop fluidized bed combustion and oil gasification in air pollution abatement. The goals of this work are

- To identify which fluidized processes might be economically employed in utility power plants or industrial boilers to reduce SO_2, particulate, and NO_x emissions
- To assist in planning and implementing a program to develop the fluidized bed systems deemed effective in air pollution control and economical in steam/power production.

Tasks in the evaluation of fluidized bed combustion set forth by EPA which have been completed at Westinghouse under a previous contract are

- To search the technical and patent literature in fluidized bed combustion, to canvass commercial organizations with expertise pertaining to this field, and to survey the market for industrial boilers and utility power systems

- To design a fluidized bed industrial boiler and two fluidized bed utility power systems -- one 300 MW capacity, the other 600 MW; and to provide performance and cost projections for the equipment designed
- To provide technical consultation and assistance on the ORD fluidized bed fuel processing program, including both combustion and gasification
- To conceptualize a development plant which will prove the configurational or operating features of the fluidized bed boiler designs not confirmed by prior art or experience
- To assess the effectiveness and economics of an atmospheric-pressure, fluidized bed oil gasification-combustion system and to aid in planning for a demonstration installation of such a system.

The results of these surveys, designs, evaluations, and comparisons were published in a three-volume report, "Evaluation of the Fluidized Bed Combustion Process," in November 1971 under contract No. CPA 70-9.

These results provided the basis for the work reported in this four-volume report. Tasks in the evaluation of the fluidized bed combustion process set forth by EPA under contract 68-02-0217 have focused on the development of pressurized fluidized bed combustion for power generation and fluidized bed oil gasification for power generation. These tasks, which are presented here, have included:

- <u>Extensive process evaluation studies of the pressurized fluidized bed combustion system for power generation</u>. These investigations predict the sensitivity of operating and design parameters selected for the base power plant design on plant economics; provide additional experimental data on sulfur removal and sorbent regeneration using

limestones and dolomites; project economics and performance for various sulfur removal systems, both regeneration/sulfur recovery and once-through sorbent; establish a plant operation and control philosophy and evaluate alternative pressurized fluid bed combustion concepts, both economics and performance.

- Preparation of preliminary plans and a cost estimate for a 30 MW (equivalent) pressurized fluidized bed combustion boiler development plant. The design provides sufficient detail to locate a suitable plant site and to obtain a fixed cost bid for the preparation of detailed plans. The plant will provide the capability for studying the remaining technical problems effectively in order to achieve the greatest potential for reducing emissions and for generating economical electrical energy.

- Identification of a project team to demonstrate fluidized bed oil gasification/desulfurization for power generation. A cooperating utility -- New England Electric System -- has been identified to carry out a 50 MW demonstration plant program. Further process evaluation has been carried out and experimental data obtained on sulfur removal and spent stone disposal.

- Evaluation of pressurized oil gasification for combined cycle power generation. Oil gasification process concepts and options have been reviewed, material and energy balances projected, performance projected,and capital and energy costs estimated.

- Provision of technical consultation and assistance on the ORD fluidized bed fuel processing program, including both combustion and gasification processes. Technical and economic comparisons have been carried out on various fluidized bed fuel processing systems and various conventional means of steam/power generation.

Volume I contains new data on pressurized fluid bed combustion and an evaluation of the current technology state. This volume (Volume II) contains the appendices to Volume I. Volume III presents the preliminary design of a 30 MW (equivalent) pressurized fluid bed boiler development plant. Volume IV includes the work on fluidized bed oil gasification/desulfurization.

CONVERSION FACTORS -- ENGLISH TO METRIC UNITS

	English System	Metric Equivalent
Length	in	2.54 cm
	ft	0.305 m
Area	in^2	6.45 cm^2
	ft^2	0.0930 m^2
Volume	in^3	16.39 cm^3
	ft^3	28.32 l
	gal	3.785 l
Mass	oz	28.35 gm
	lb	453.6 gm
	ton	907.2 kg
Pressure	lb/in^2	51.70 mm Hg
	in H_2O	1.865 mm Hg
Temperature	°F	1.8 (°C) + 32
	°R	1.8 °K
Energy	Btu	252 cal
Power	Btu/min	252 cal/min

TABLE OF CONTENTS

ECONOMIC SENSITIVITY

A. Boiler Tube Specifications

B. Supplementary Cost Data

C. Parametric Study of Elutriation Rate from a Fluidized Bed Combustion Boiler

SULFUR REMOVAL SYSTEMS

D. Base Design -- High-Pressure One-Step Process

E. Base Design -- Low-Pressure One-Step Process

F. Base Design -- Two-Step Process

G. Temperature Control and Process Turndown

H. Effect of Boiler Conditions

I. Once-through Process

J. Constant Load Concept

K. Process Comparisons

L. General Study of One-Step Process

M. Low-Sulfur Coal

N. Limestone Wet Scrubber Cost

PLANT OPERATION AND CONTROL

O. Part Load Operation

ALTERNATIVE FLUID BED BOILER CONCEPTS

P. Recirculating Bed Boiler Studies

LIST OF FIGURES

ECONOMIC SENSITIVITY — Page

Appendix A

1. Maximum Allowable Stress for Different Tube Materials — A-3
2. Maximum Required Tube Wall Thickness — A-3
3. Minimum Required Tube Wall Thickness (Bed-Tube Heat Transfer Coefficient 35 Btu/ft^2-hr-°F) — A-7
4. Minimum Required Tube Wall Thickness (Bed-Tube Heat Transfer Coefficient 75 Btu/ft^2-hr-°F) — A-7
5. Minimum Required Tube Wall Thickness (Bed Temperature 1407°F) — A-8
6. Minimum Required Tube Wall Thickness (Bed Temperature 1522°F) — A-8
7. Minimum Required Tube Wall Thickness (Bed Temperature 1636°F) — A-8
8. Minimum Required Tube Wall Thickness (Bed Temperature 1750°F) — A-8

Appendix B

1. Effect of Bed-Tube Heat Transfer Coefficient on the Steam Generator Cost (by Design Bed Temperatures) — B-2
2. Effect of Bed-Tube Heat Transfer Coefficient on the Steam Generator Cost (by Maximum Allowable Bed Depth) — B-2
3. Dependence of the Steam Generator Cost (318 MW) on the Maximum Allowable Bed Depth (Bed Temperature 1750°F) — B-3
4. Dependence of the Steam Generator Cost (318 MW) on the Maximum Allowable Bed Depth (Bed Temperature 1636°F) — B-3
5. Dependence of the Steam Generator Cost (318 MW) on the Maximum Allowable Bed Depth (Bed Temperature 1522°F) — B-3
6. Dependence of the Steam Generator Cost (318 MW) on the Maximum Allowable Bed Depth (Bed Temperature 1407°F) — B-3

		Page
7.	Dependence of the Steam Generator Cost (318 MW) on the Maximum Allowable Bed Depth (Heat Transfer Coefficient 75 Btu/ft^2-hr-°F)	B-4
8.	Dependence of the Steam Generator Cost (318 MW) on the Maximum Allowable Bed Depth (Heat Transfer Coefficient 50 Btu/ft^2-hr-°F)	B-4
9.	Dependence of the Steam Generator Cost (318 MW) on the Maximum Allowable Bed Depth (Heat Transfer Coefficient 35 Btu/ft^2-hr-°F)	B-4
10.	Effect of Bed-Tube Heat Transfer Coefficient on the Steam Generator Cost (1-in. O.D. Tubes)	B-5
11.	Effect of Bed-Tube Heat Transfer Coefficient on the Steam Generator Cost (1-in, O.D. Tubes)	B-5
12.	Dependence of the Steam Generator Cost on the Maximum Allowable Bed Depth (1-in. O.D. Tubes, Bed Temperature 1750°F)	B-6
13.	Dependence of the Steam Generator Cost (318 MW) on the Maximum Allowable Bed Depth (1-in. O.D. Tubes, Bed Temperature 1636°F)	B-6
14.	Dependence of the Steam Generator Cost (318 MW) on the Maximum Allowable Bed Depth (1-in. O.D. Tubes, Bed Temperature 1522°F)	B-6
15.	Dependence of the Steam Generator Cost (318 MW) on the Maximum Allowable Bed Depth (1-in. O.D. Tubes, Bed Temperature 1407°F)	B-6
16.	Dependence of the Steam Generator Cost (318 MW) on the Maximum Allowable Bed Depth (1-in. O.D. Tubes, Bed-Tube Heat Transfer Coefficient 75 Btu/ft^2-hr-°F)	B-7
17.	Dependence of the Steam Generator Cost (318 MW) on the Maximum Allowable Bed Depth (1-in. O.D. Tubes, Bed-Tube Heat Transfer Coefficient 50 Btu/ft^2-hr-°F)	B-7
18.	Dependence of the Steam Generator Cost (318 MW) on the Maximum Allowable Bed Depth (1-in. O.D. Tubes, Bed-Tube Heat Transfer Coefficient 35 Btu/ft^2-hr-°F)	B-7
19.	Effect of Bed-Tube Heat Transfer Coefficient on the Steam Generator Cost (2-in. O.D. Tubes)	B-8
20.	Dependence of the Steam Generator Cost (318 MW) on the Maximum Allowable Bed Depth (2-in. O.D. Tubes, Bed Temperature 1750°F)	B-9

Page

21. Dependence of the Steam Generator Cost (318 MW) on the Maximum Allowable Bed Depth (2-in. O.D. Tubes, Bed Temperature 1636°F) B-9

22. Dependence of the Steam Generator Cost (318 MW) on the Maximum Allowable Bed Depth (2-in. O.D. Tubes, Bed Temperature 1522°F) B-9

23. Dependence of the Steam Generator Cost (318 MW) on the Maximum Allowable Bed Depth (2-in. O.D. Tubes, Bed Temperature 1407°F) B-9

24. Dependence of the Steam Generator Cost (318 MW) on the Maximum Allowable Bed Depth (2-in. O.D. Tubes, Bed-Tube Heat Transfer Coefficient 75 Btu/ft^2-hr-°F) B-10

25. Dependence of the Steam Generator Cost (318 MW) on the Maximum Allowable Bed Depth (2-in. O.D. Tubes, Bed-Tube Heat Transfer Coefficient 50 Btu/ft^2-hr-°F) B-10

26. Dependence of the Steam Generator Cost (318 MW) on the Maximum Allowable Bed Depth (2-in. O.D. Tubes, Bed-Tube Heat Transfer Coefficient 35 Btu/ft^2-hr-°F) B-10

Appendix C

1. Different Combinations of Elutriation Rates for a Dust Loading Equal to that of Westinghouse-Foster Wheeler Basic Design C-3

2. Different Combinations of Elutriation Rates for a Dust Loading Double that of Westinghouse-Foster Wheeler Basic Design C-3

3. Different Combinations of Elutriation Rates for a Dust Loading Triple that of Westinghouse-Foster Wheeler Basic Design C-3

4. Possible Dust Loading from FBC at 0% Carbon Elutriation Rate C-4

5. Possible Dust Loading from FBC at 6% Carbon Elutriation Rate C-4

6. Possible Dust Loading from FBC at 10% Carbon Elutriation Rate C-4

7. Possible Dust Loading from FBC at 15% Carbon Elutriation Rate C-5

8. Possible Dust Loading from FBC at 20% Carbon Elutriation Rate C-5

SULFUR REMOVAL SYSTEMS

Appendix D

1. One-Step Regeneration Process Elements D-2

2. High-Pressure One-Step Regeneration Process Flow Diagram D-5

3. High-Pressure One-Step Regeneration Schematic Flow Diagram D-5

Page

Appendix E

1. Low-Pressure One-Step Regeneration Process Flow Diagram E-3
2. Low-Pressure One-Step Regeneration Process Flow Diagram Sorbent Temperature Control E-4
3. Low-Pressure One-Step Regeneration Schematic Flow Diagram E-5

Appendix F

1. Two-Step Regeneration Process Elements F-2
2. Two-Step Regeneration Material and Energy Balances F-4
3. Two-Step Regeneration Schematic Flow Diagram F-7

Appendix G

1. Dolomite Circulation Effect on Temperature Control -- 2000°F Regenerator G-2
2. Dolomite Circulation Effect on Temperature Control -- 1900°F Regenerator G-2
3. Limestone Circulation Effect on Temperature Control -- 2000°F Regenerator G-3
4. Limestone Circulation Effect on Temperature Control -- 1900°F Regenerator G-3
5. Enthalpy of Regenerator Product Gas G-4
6. Gas Producer Characteristics G-5
7. Gas Producer Fuel Requirement G-7
8. Reducing Gas Temperature G-8
9. One-Step Process Turndown G-11

Appendix H

1. Carbonating Boiler Conditions Flow Diagram H-2
2. Calcining Boiler Conditions Flow Diagram H-2

Appendix I

1. Sorbent Handling and Feeding Costs I-2
2. Once-through Energy Cost I-2

Appendix J

1. Constant Load Concept Flow Diagram J-2
2. Constant versus Variable Load for the Low-Pressure One-Step Process J-3
3. Constant versus Variable Load for the High-Pressure Processes J-5

Page

Appendix K

1. Regeneration Process Investment Comparison K-2
2. Regeneration Process Energy Cost Comparison K-2
3. Energy Cost Comparison: Disposal before Regeneration, $2/ton Dolomite K-3
4. Energy Cost Comparison: Disposal before Regeneration, $5/ton Dolomite K-3
5. Energy Cost Comparison: Disposal before Regeneration, $10/ton Dolomite K-4
6. Energy Cost Comparison: Disposal before Regeneration, $10/ton Dolomite K-4
7. Energy Cost Comparison: Disposal after Regeneration, $2/ton Dolomite K-6
8. Energy Cost Comparison: Disposal after Regeneration, $5/ton Dolomite K-6
9. Energy Cost Comparison: Disposal after Regeneration, $10/ton Dolomite K-7
10. Energy Cost Comparison: Disposal after Regeneration, $15/ton Dolomite K-7

Appendix L

1. One-Step Regeneration Process Elements L-4
2. Regeneration Process Sulfur Load L-13
3. Tail Gas Recycle to Boiler L-14
4. Gas Producer Fuel Requirement L-15
5. Total Regeneration Process Fuel Requirement L-15
6. Effect of Sulfur in Gas Producer Fuel L-18
7. Sulfur Production Rate L-19
8. One-Step Regeneration Process Flow Diagram L-23
9. Regenerator Element Capital Investment L-26
10. Sulfur Recovery Element Capital Investment L-27
11. Tail Gas Handling Element Capital Investment L-28
12. Gas Producing Element Capital Investment L-30
13. Sorbent Circulation Element Capital Investment L-32
14. Energy Cost -- Methane at 10 Atmospheres L-35
15. Energy Cost -- Methane at 5 Atmospheres L-35

Page

16. Energy Cost -- Methane at 2 Atmospheres L-35
17. Energy Cost -- Oil at 10 Atmospheres L-36
18. Energy Cost -- Oil at 5 Atmospheres L-36
19. Energy Cost -- Oil at 2 Atmospheres L-36
20. Energy Cost -- Coal at 10 Atmospheres L-38
21. Energy Cost -- Coal at 5 Atmospheres L-38
22. Energy Cost -- Coal at 2 Atmospheres L-38
23. Energy Cost Comparison -- High-Sulfur Load L-39
24. Energy Cost Comparison -- Medium-Sulfur Load L-39

Appendix M

1. Dependence of the Shell Cost on the Fluidizing Velocity M-5
2. Effect of Bed-Tube Heat Transfer Coefficient on the Steam Generator Cost M-6

Appendix N

1. Energy Cost of a Conventional Coal-Fired Power Plant with Limestone Wet Scrubbing N-2

PLANT OPERATION AND CONTROL

Appendix O

1. Temperature-Energy Diagram for Pressurized Utility Boiler O-4
2. Part Load Characteristics O-7
3. Effect of Design Point Temperature and Percent Excess Air on Plant Turndown Capability O-8

Appendix P

1. Detailed Schematic of the Two-Dimensional Cold Model P-2
2. Two-Dimensional Cold Model with Modified Draft Tube Inlet P-5
3. Dimensions of the Serpentine Copper Rods P-7
4. Experimental Data for Case I and Case II P-10
5. Experimental Data for Case III P-11
6. Experimental Values of Total Air By-Passing P-13
7. Schematic Representation of Flow Characteristics in Vertical Pneumatic Transport P-49

		Page
8.	Comparison between the Experimental Data and the Saturation Carrying Capacity	P-50
9.	Pressure Loss Due to Slugging Transport	P-52

LIST OF TABLES

Page

ECONOMIC SENSITIVITY

Appendix A

1. Boiler Tube Specification A-2
2. Boiler Tube Specification for 1-in. O.D. Tubes A-4
3. Boiler Tube Specification for 2-in. O.D. Tubes A-5
4. Design Metal Temperatures and Tube Material A-6

Appendix C

1. Design Bases for Westinghouse-Foster Wheeler Fluidized Bed Combustion Boiler (318 MW/four-module design) C-2

SULFUR REMOVAL SYSTEMS

Appendix D

1. Design Specifications D-3
2. Design Assumptions D-3
3. Material and Energy Balance -- One-Step Regeneration at High Pressure (1% SO_2) D-6
4. Material and Energy Balance -- One-Step Regeneration at High Pressure (2% SO_2) D-7
5. 1% SO_2 Investment Breakdown, $/kw D-10
6. 2% SO_2 Investment Breakdown, $/kw D-10
7. 1% SO_2 Energy Cost (mills/kWh) D-11
8. 2% SO_2 Energy Cost (mills/kWh) D-11
9. Cost Sensitivity of High-Pressure One-Step Regeneration

Appendix E

1. Design Specifications E-1
2. Design Assumptions E-2
3. Material and Energy Balances - Low-Pressure One-Step Regeneration E-6
4. Low-Pressure One-Step Process Investment Breakdown, $/kw E-8
5. Energy Cost (mills/kWh) E-9
6. Cost Sensitivity of Low-Pressure One-Step Regeneration E-10

Page

Appendix F

1. Design Specifications F-3
2. Design Assumptions F-3
3. Two-Step Regeneration Material and Energy Balance (Process Sulfur Load = 0.03) F-5
4. Two-Step Process Investment Breakdown, $/kw F-8
5. Energy Cost (mills/kWh) F-9

Appendix H

1. Cost Increase for Carbonating Boiler Conditions -- High-Pressure and Low-Pressure Regeneration Processes H-3
2. Cost Increase for Calcining Boiler Conditions -- Two-Step Process H-5

Appendix J

1. Constant Load Concept Energy Costs J-4
2. Constant Load Concept Energy Costs (mills/kWh) J-6

Appendix L

1. Process Specifications L-5
2. Operating and Design Variables L-6
3. Performance Variables L-6
4. Design Options L-7
5. Simplified Variables L-8
6. Ranges of SO_2 Mole Fractions L-10
7. Total Installed Regeneration Process Cost, $/kw L-34
8. Conventional Plant Energy Cost with Limestone Wet Scrubbing L-42
9. Energy Cost Comparison L-42

Appendix M

1. Cost Basis M-1
2. Cost Results with 1 wt% Sulfur Coal M-2
3. Cost Results with No Desulfurization M-3
4. Design Factors Resulting from No Sulfur Removal Requirements M-4

Appendix N

1. Conventional Plant Capital Investment N-3
2. Conventional Plant Energy Cost N-3

Page

PLANT OPERATION AND CONTROL

Appendix O

1. Alternative Turndown Procedures O-2
2. Process Variable Limitations O-5

ALTERNATIVE PRESSURIZED FLUIDIZED BOILER CONCEPTS

Appendix P

1. Particle Size Distribution of the Ottawa Sand Used As Bed Material P-8
2. Experimental Data of Test Series 1 (Case I) P-14
3. Experimental Data of Test Series 2 (Case I) P-15
4. Experimental Data of Test Series 3 (Case I) P-16
5. Experimental Data of Test Series with Tubes in Downcomers (Case II) P-17
6. Experimental Data of Test Series with Tubes in Downcomers (Case II) P-18
7. Experimental Data of Test Series with Tubes in Downcomers (Case II) P-19
8. Experimental Data of Test Series with Boot (Case III) P-20
9. Comparison between Experimental and Calculated Jet Penetration Depth (Case I) P-28
10. Comparison between Experimental and Calculated Jet Penetration Depth (Case II) P-30
11. Comparison between Experimental and Calculated Jet Penetration Depth (Case III) P-32
12. Comparison of Pressure Drop Predictions in the Draft Tube P-34
13. Comparison of Pressure Drop Predictions in the Draft Tube P-36
14. Comparison of Pressure Drop Predictions in the Draft Tube P-38
15. Comparison between Theoretical Predictions and Experimental Values in the Downcomer (Case II) P-40
16. Comparison between Theoretical Predictions and Experimental Values in the Downcomer (Case III) P-42
17. Comparison between the Calculated and the Observed Solid Flow Rate P-44
18. Comparison between the Predicted and the Experimental Solid Recirculation Rate (Case I) P-53

Appendix P (Continued) Page

19. Comparison between the Predicted and the Experimental Solid Recirculation Rate (Case II) P-54

20. Comparison between the Predicted and the Experimental Solid Recirculation Rate (Case III) P-56

A

APPENDIX A

BOILER TUBE SPECIFICATION

The minimum requirement of boiler tube wall thickness is dependent on the design fluid bed temperature, steam temperature in the tube, bed-tube heat transfer coefficient, and the size of the boiler tube. For ferrous tubing up to and including 5 in. outside diameter, the equation used is[1]

$$t = \frac{PD}{2S + P} + 0.005\ D + e \quad , \qquad \text{(A-1)}$$

where

- t = the minimum required wall thickness, inches
- P = the maximum allowable working pressure, psi
- D = the outside diameter of tubes, inches
- S = the maximum allowable stress value at the operating temperature of the metal, psi, and
- e = the thickness factor for expanded tube ends

The maximum allowable stress value, S, was obtained from the ASME Boiler & Pressure Vessel Code[1] and plotted as shown in Figure A-1 for the specific tube materials used in the present design.

The design metal temperature, minimum tube wall thickness, and tube material required for the basic design at bed temperature 1750°F are presented in Table A-1. The minimum wall thickness required for designs at bed temperatures of 1636°F, 1522°F, and 1407°F was calculated using Equation A-1 and is also presented in Table A-1 and Figure A-2 for comparison.

The boiler tube specifications for 1-in. O.D. and 2-in. O.D. tubes are summarized in Tables A-2 and A-3. When the bed-tube heat transfer coefficient changes, the design metal temperature and tube material

TABLE A-1

BOILER TUBE SPECIFICATION
(Bed-Tube Heat Transfer Coefficient = 50 Btu/ft^2-hr-°F)

Tube Location	Tube Outside Diameter, in.	Tube Material	Design Metal Temperature, °F	Minimum Wall Thickness, in.
Bed Temperature 1750°F				
Water walls	2	SA-213-T22	975	0.280
Preevaporator	1-1/2	SA-210-A1	732	0.150
Lower superheater	1-1/2	SA-213-T2	900	0.165
Upper superheater (lower loops)	1-1/2	SA-213-T22	1058	0.318
Upper superheater (upper loops)	1-1/2	SA-213-TP304H	1150	0.238
Reheater	2	SA-213-T22	1122	0.186
Bed Temperature 1636°F				
Water walls	2	SA-213-T22	953	0.249
Preevaporator	1-1/2	SA-210-A1	724	0.149
Lower superheater	1-1/2	SA-213-T2	884	0.160
Upper superheater (lower loops)	1-1/2	SA-213-T22	1038	0.290
Upper superheater (upper loops)	1-1/2	SA-213-TP304H	1136	0.226
Reheater	2	SA-213-T22	1104	0.170
Bed Temperature 1522°F				
Water walls	2	SA-213-T22	935	0.231
Preevaporator	1-1/2	SA-210-A1	717	0.147
Lower superheater	1-1/2	SA-213-T2	870	0.156
Upper superheater (lower loops)	1-1/2	SA-213-T22	1023	0.266
Upper superheater (upper loops)	1-1/2	SA-213-TP304H	1120	0.213
Reheater	2	SA-213-T22	1085	0.150
Bed Temperature 1407°F				
Water walls	2	SA-213-T22	915	0.218
Preevaporator	1-1/2	SA-210-A1	705	0.145
Lower superheater	1-1/2	SA-213-T2	858	0.153
Upper superheater (lower loops)	1-1/2	SA-213-T22	1004	0.246
Upper superheater (upper loops)	1-1/2	SA-213-TP304H	1105	0.200
Reheater	2	SA-213-T22	1067	0.135

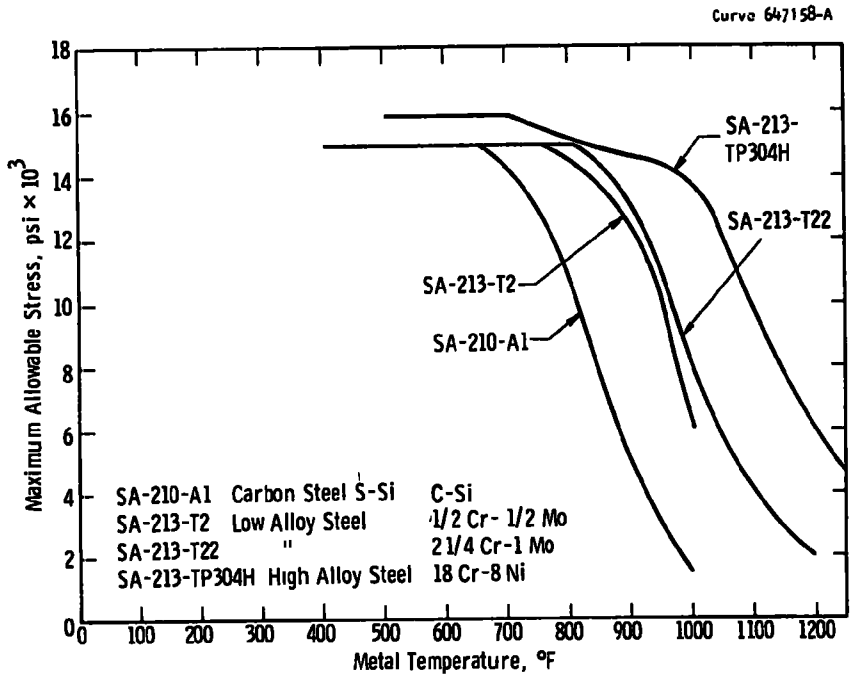

Figure A-1: Maximum Allowable Stress for Different Tube Materials

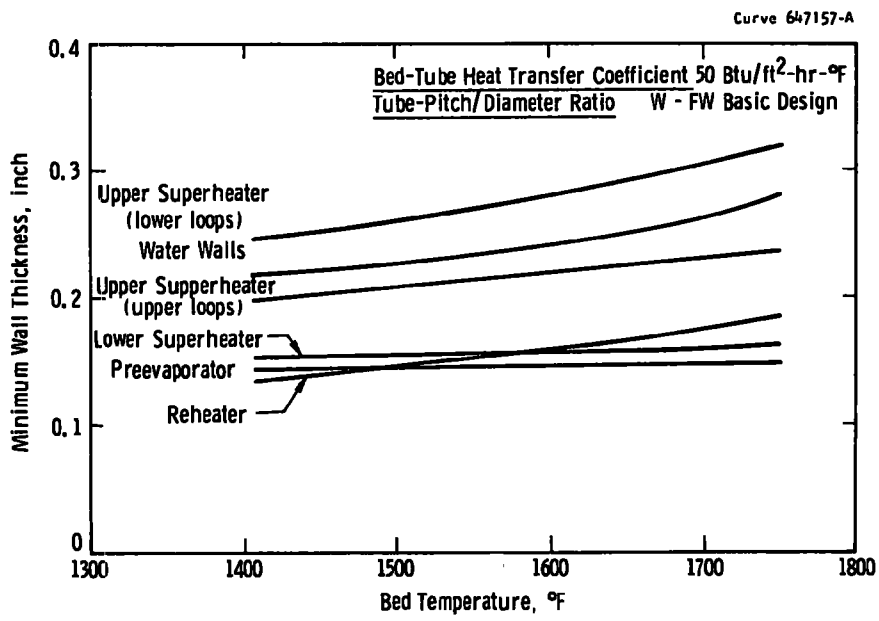

Figure A-2: Minimum Required Tube Wall Thickness

TABLE A-2

BOILER TUBE SPECIFICATION FOR 1" O.D. TUBES
(Bed-Tube Heat Transfer Coefficient = 50 Btu/ft^2-hr-°F)

Tube Location	Tube Outside Diameter, in.	Tube Material	Design Metal Temperature, °F	Minimum Wall Thickness, in.
Bed Temperature 1750°F				
Water walls	1	SA-213-T22	975	0.140
Preevaporator	1	SA-210-A1	732	0.100
Lower superheater	1	SA-213-T2	900	0.110
Upper superheater (lower loops)	1	SA-213-T22	1058	0.212
Upper superheater (upper loops)	1	SA-213-TP304H	1150	0.159
Reheater	1	SA-213-T22	1122	0.093
Bed Temperature 1636°F				
Water walls	1	SA-213-T22	953	0.125
Preevaporator	1	SA-210-A1	724	0.099
Lower superheater	1	SA-213-T2	884	0.107
Upper superheater (lower loops)	1	SA-213-T22	1038	0.193
Upper superheater (upper loops)	1	SA-213-TP304H	1136	0.151
Reheater	1	SA-213-T22	1104	0.085
Bed Temperature 1522°F				
Water walls	1	SA-213-T22	935	0.115
Preevaporator	1	SA-210-A1	717	0.098
Lower superheater	1	SA-213-T2	870	0.104
Upper superheater (lower loops)	1	SA-213-T22	1023	0.177
Upper superheater (upper loops)	1	SA-213-TP304H	1120	0.142
Reheater	1	SA-213-T22	1085	0.075
Bed Temperature 1407°F				
Water walls	1	SA-213-T22	915	0.109
Preevaporator	1	SA-210-A1	705	0.965
Lower superheater	1	SA-213-T2	858	0.102
Upper superheater (lower loops)	1	SA-213-T22	1004	0.164
Upper superheater (upper loops)	1	SA-213-TP304H	1105	0.133
Reheater	1	SA-213-T22	1067	0.068

TABLE A-3

BOILER TUBE SPECIFICATION FOR 2" O.D. TUBES
(Bed-Tube Heat Transfer Coefficient = 50 Btu/ft^2-hr-°F)

Tube Location	Tube Outside Diameter, in.	Tube Material	Design Metal Temperature, °F	Minimum Wall Thickness, in.
Bed Temperature 1750°F				
Water walls	2	SA-213-T22	975	0.280
Preevaporator	2	SA-210-A1	732	0.200
Lower superheater	2	SA-213-T2	900	0.220
Upper superheater (lower loops)	2	SA-213-T22	1058	0.424
Upper superheater (upper loops)	2	SA-213-TP304H	1150	0.318
Reheater	2	SA-213-T22	1122	0.248
Bed Temperature 1636°F				
Water walls	2	SA-213-T22	953	0.332
Preevaporator	2	SA-210-A1	724	0.199
Lower superheater	2	SA-213-T2	884	0.214
Upper superheater (lower loops)	2	SA-213-T22	1038	0.386
Upper superheater (upper loops)	2	SA-213-TP304H	1136	0.302
Reheater	2	SA-213-T22	1104	0.227
Bed Temperature 1522°F				
Water walls	2	SA-213-T22	935	0.308
Preevaporator	2	SA-210-A1	717	0.196
Lower superheater	2	SA-213-T2	870	0.208
Upper superheater (lower loops)	2	SA-213-T22	1023	0.354
Upper superheater (upper loops)	2	SA-213-TP304H	1120	0.284
Reheater	2	SA-213-T22	1085	0.200
Bed Temperature 1407°F				
Water walls	2	SA-213-T22	915	0.291
Preevaporator	2	SA-210-A1	705	0.193
Lower superheater	2	SA-213-T2	858	0.204
Upper superheater (lower loops)	2	SA-213-T22	1004	0.328
Upper superheater (upper loops)	2	SA-213-TP304H	1105	0.266
Reheater	2	SA-213-T22	1067	0.180

change as well (Table A-4). The effects of design bed temperature and bed-tube heat transfer coefficient on the tube wall thickness requirement for the basic design are presented graphically in Figures A-3 through A-8.

TABLE A-4

DESIGN METAL TEMPERATURES & TUBE MATERIAL

Tube Location	Tube Material	Design Metal Temperature, °F Bed Temperature 1750°F	1636°F	1522°F	1407°F
(Bed-tube Heat Transfer Coefficient = 35 Btu/ft^2-hr-°F)					
Water walls	SA-213-T22	928	914	900	885
Preevaporator	SA-210-A1	710	704	695	687
Lower superheater	SA-213-T2	869	859	849	839
Upper superheater (lower loops)	SA-213-T22	1023	1010	998	988
Upper superheater (upper loops)	SA-213-TP304H	1125	1114	1101	1090
Reheater	SA-213-T22	1088	1077	1060	1047
(Bed-tube Heat Transfer Coefficient = 75 Btu/ft^2-hr-°F)					
Water walls	SA-213-T22	1035	1007	981	954
Preevaporator	SA-210-A1	775	765	749	735
Lower superheater	SA-213-T2	947	929	909	889
Upper superheater (lower loops)	SA-213-T22 or SA-213-TP304H	1103	1083	1060	1038
Upper superheater (upper loops)	SA-213-TP304H	1190	1170	1145	1125
Reheater	SA-213-T22	1167	1139	1117	1089

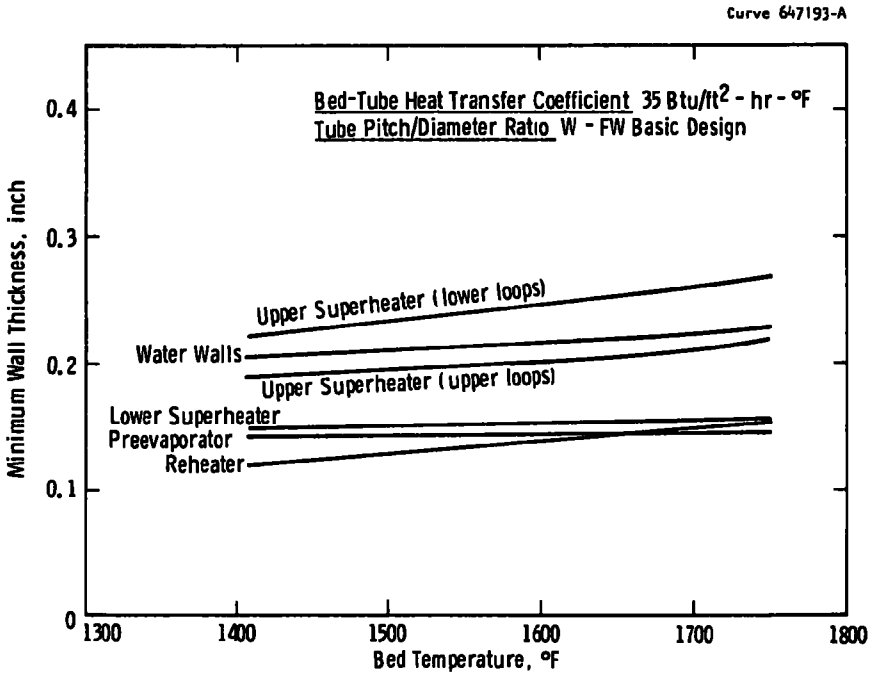

Figure A-3. Minimum Required Tube Wall Thickness

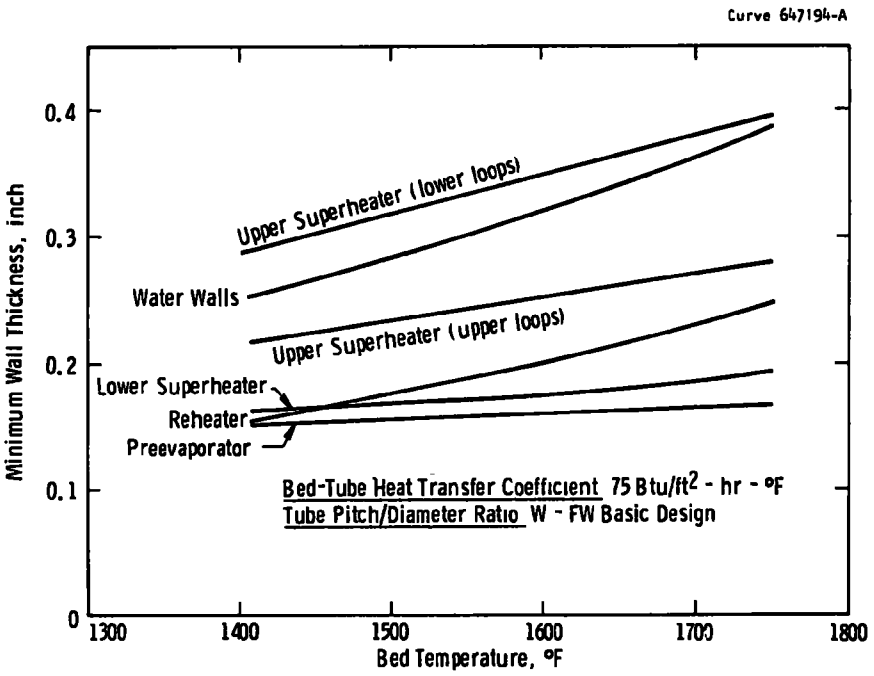

Figure A-4: Minimum Required Tube Wall Thickness

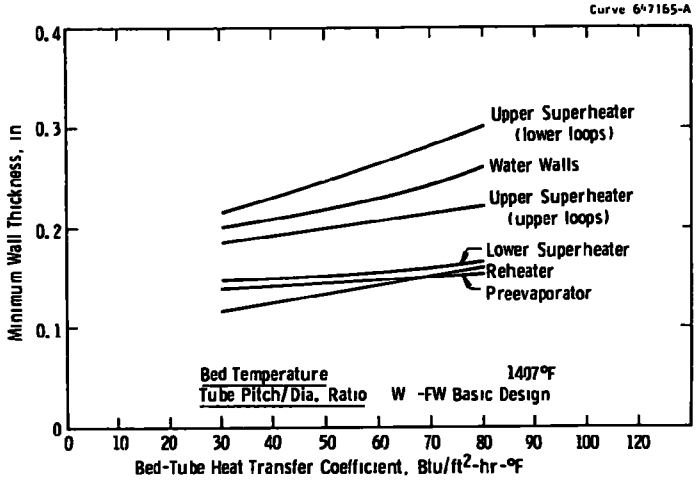

Figure A-5 Minimum Required Tube Wall Thickness

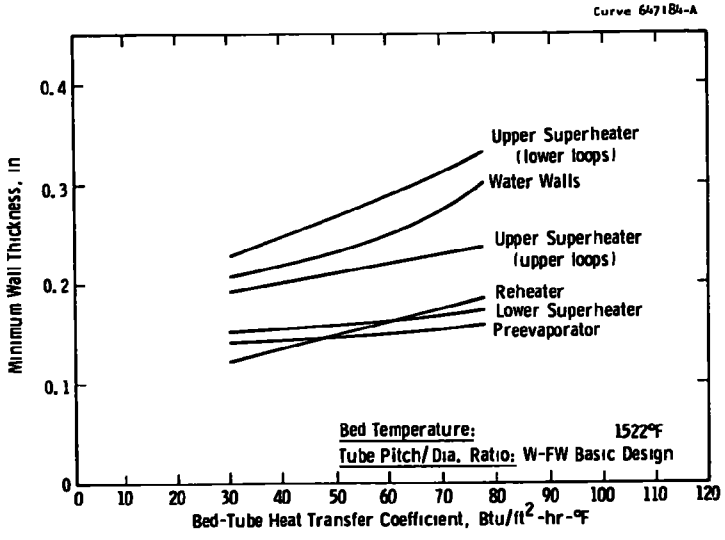

Figure A-6. Minimum Required Tube Wall Thickness

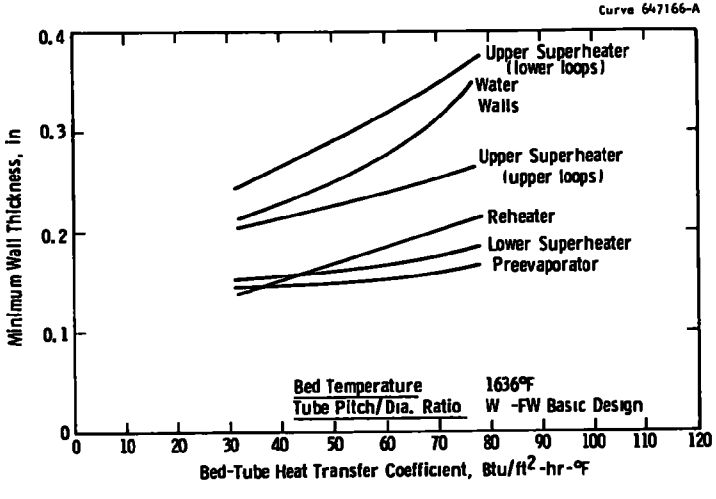

Figure A-7: Minimum Required Tube Wall Thickness

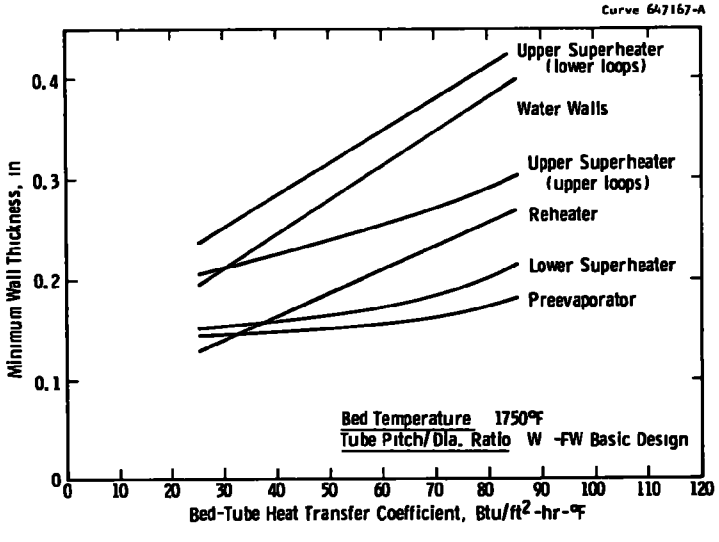

Figure A-8. Minimum Required Tube Wall Thickness

REFERENCES

1. ASME Boiler and Pressure Vessel Code, Power Boilers, Section I, 1971.

B

APPENDIX B

SUPPLEMENTARY COST DATA

The effects of operating conditions and boiler design on the total boiler cost have been discussed in detail in Volume I, Section 2. To complete the evaluation, the cost information is also presented in the following figures to show the interacting effects of the tube pitch/diameter ratio, the bed-tube heat transfer coefficient, the maximum allowable bed depth, and the design bed temperature:

Figure B-1 shows the effect of the bed-tube heat transfer coefficient on the steam generator cost at different design bed temperatures. The tube pitch/diameter ratio is similar to that of the Westinghouse-Foster Wheeler basic design.

Figure B-2 shows the effect of the bed-tube heat transfer coefficient on the steam generator cost at two maximum allowable bed depths (20 feet and unrestricted). The tube pitch/diameter ratio is similar to that of the Westinghouse-Foster Wheeler basic design.

Figures B-3 to B-6 present the effect of the maximum allowable bed depth on the steam generator cost at a constant bed temperature and with the bed-tube heat transfer coefficient as a parameter. The tube pitch/diameter ratio is similar to that of the Westinghouse-Foster Wheeler basic design.

Figures B-7 to B-9 present the effect of the maximum allowable bed depth on the steam generator cost at a constant bed-tube heat transfer coefficient and with the design bed temperature as a parameter. The tube pitch/diameter ratio is similar to that of the Westinghouse-Foster Wheeler basic design.

The same series of figures was also prepared for 1-in. O.D. tubes at H = 4 in. and V = 2 in. (Figures B-10 to B-18) and 2-in. O.D. tubes at H = 8 in. and V = 4 in. (Figures B-19 to B-26).

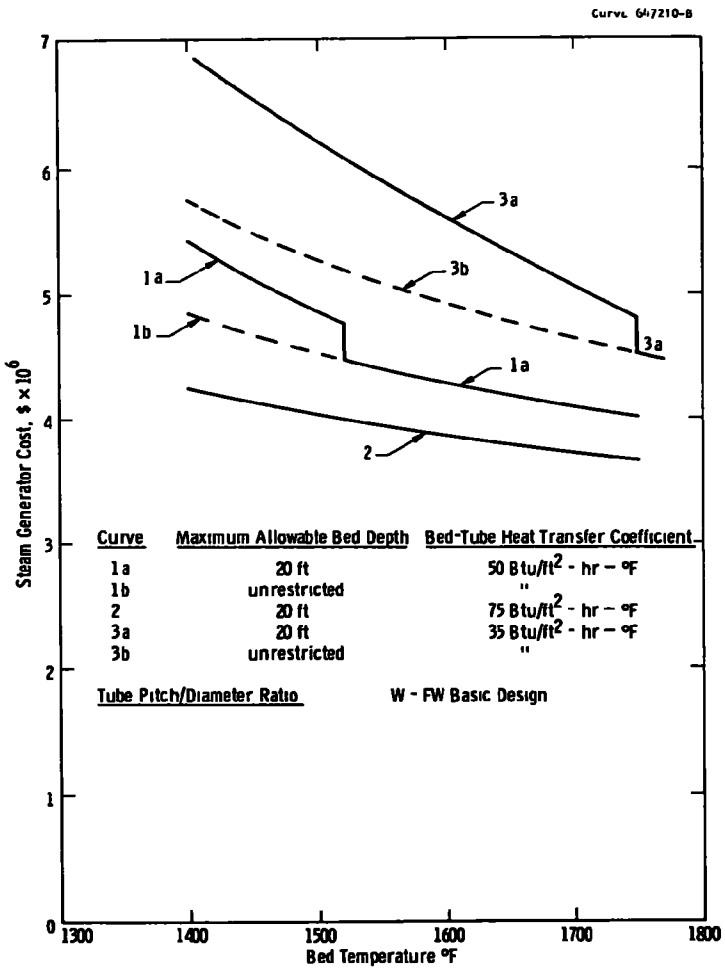

Figure B-1: Effect of Bed-Tube Heat Transfer Coefficient on the Steam Generator Cost (not including erection)

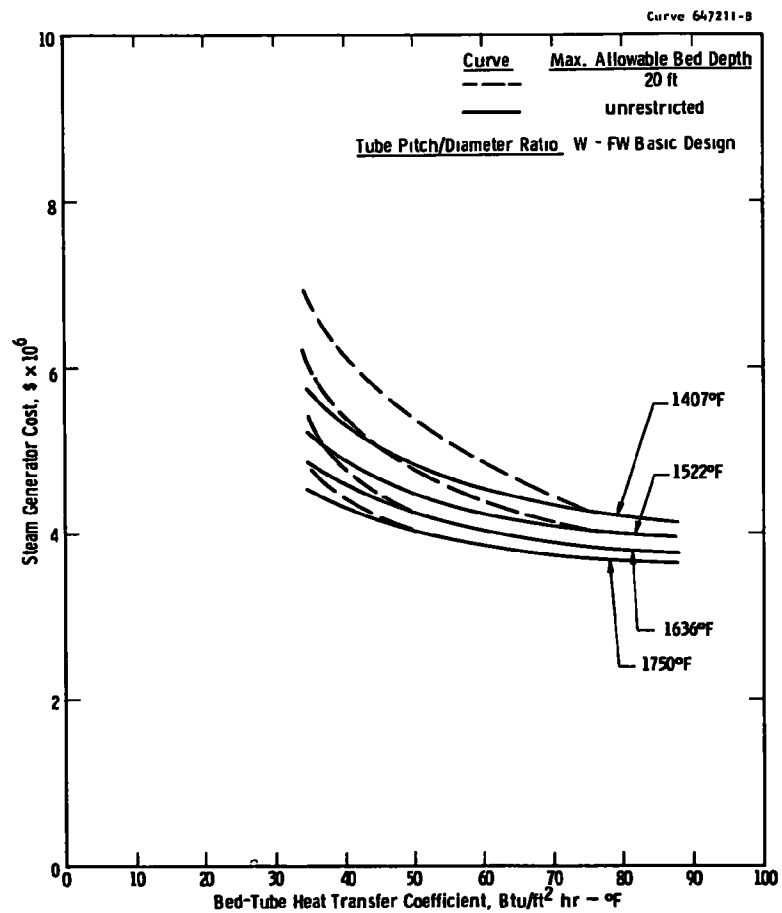

Figure B-2. Effect of Bed-Tube Heat Transfer Coefficient on the Steam Generator Cost (not including erection)

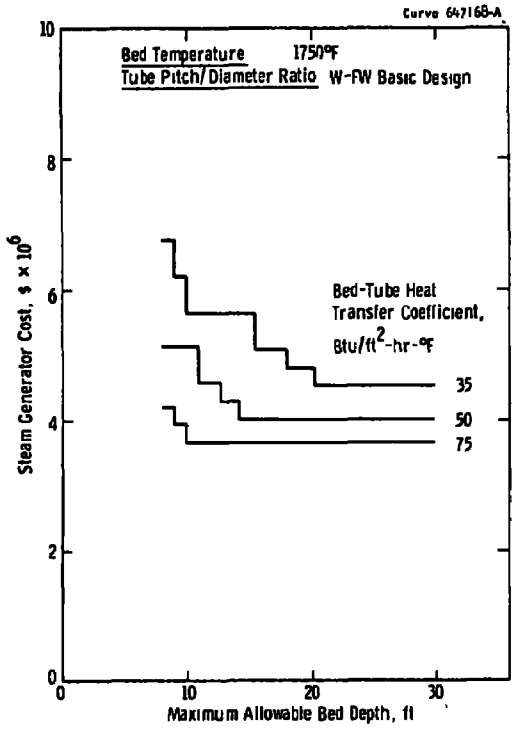

Figure B-3 Dependence of the Steam Generator Cost (318 MW) on the Maximum Allowable Bed Depth (not including erection)

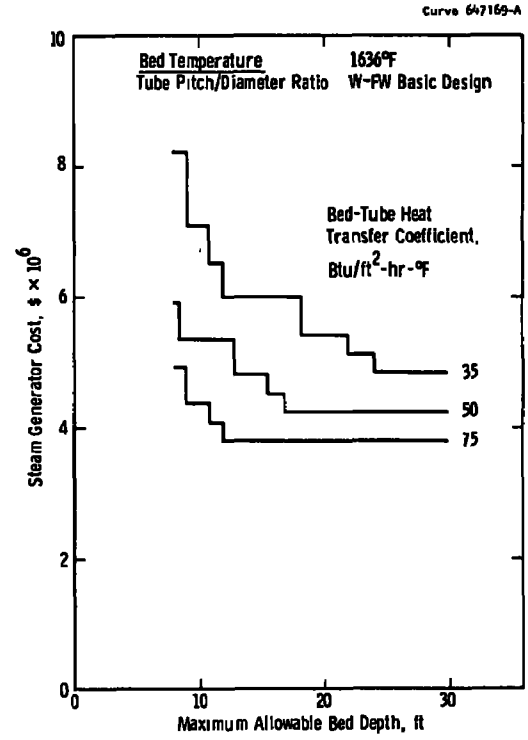

Figure B-4: Dependence of the Steam Generator Cost (318 MW) on the Maximum Allowable Bed Depth (not including erection)

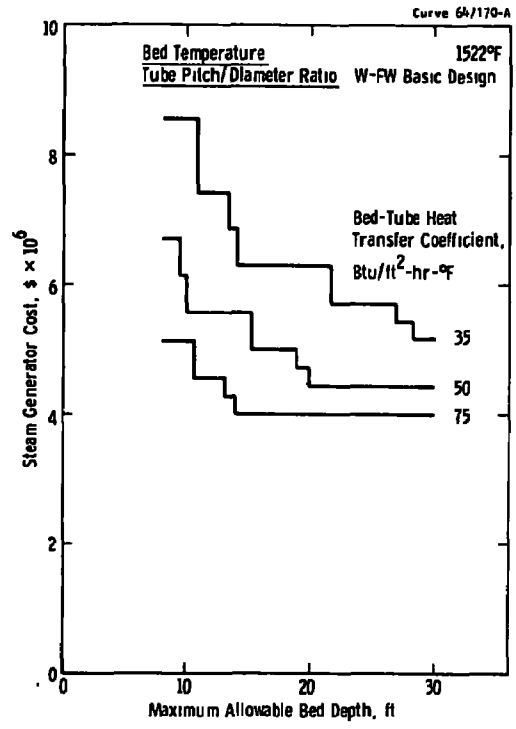

Figure B-5 Dependence of the Steam Generator Cost (318 MW) on the Maximum Allowable Bed Depth (not including erection)

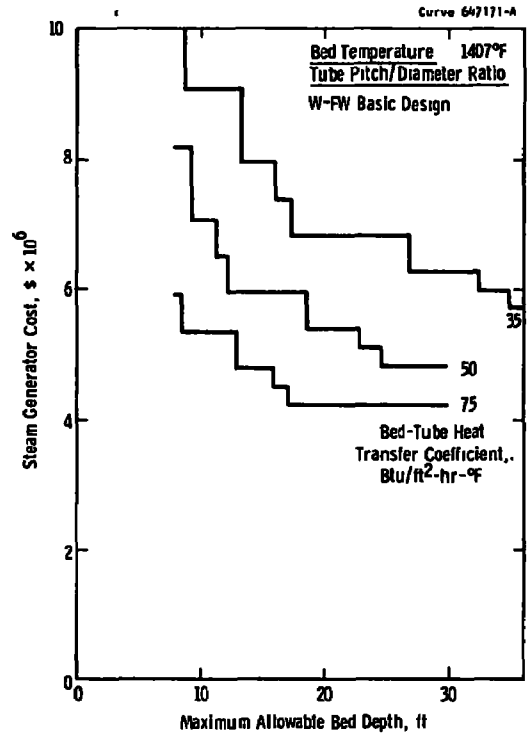

Figure B-6: Dependence of the Steam Generator Cost (318 MW) on the Maximum Allowable Bed Depth (not including erection)

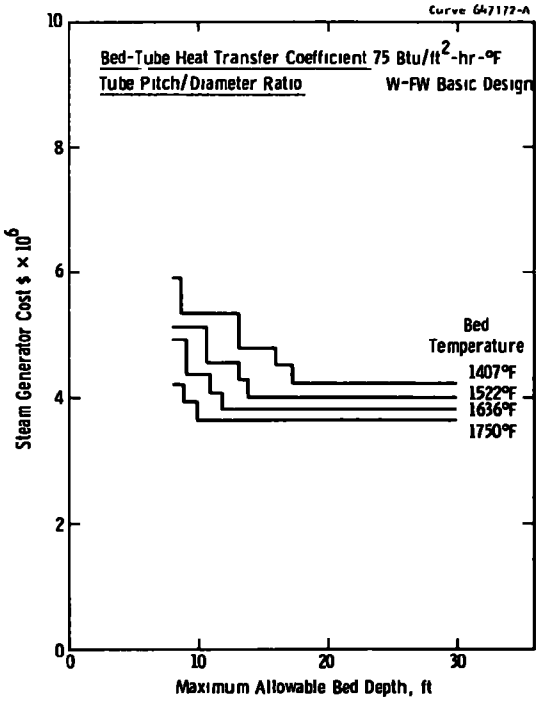

Figure B-7 Dependence of the Steam Generator Cost (318 MW) on the Maximum Allowable Bed Depth (not including erection)

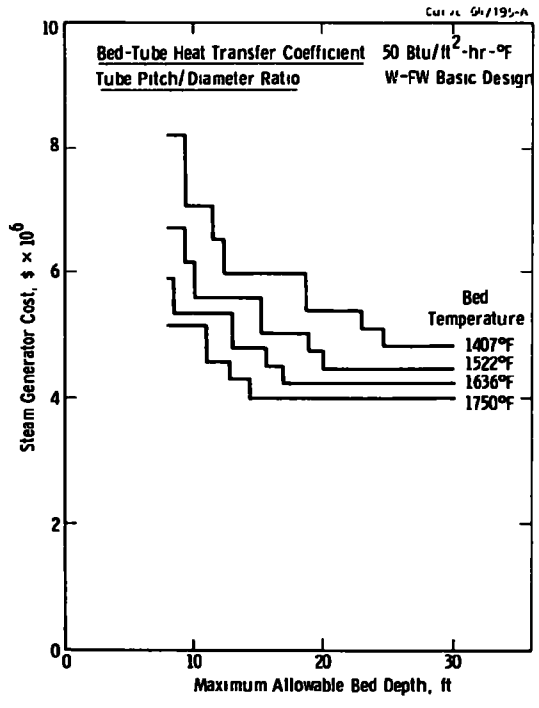

Figure B-8: Dependence of the Steam Generator Cost (318 MW) on the Maximum Allowable Bed Depth (not including erection)

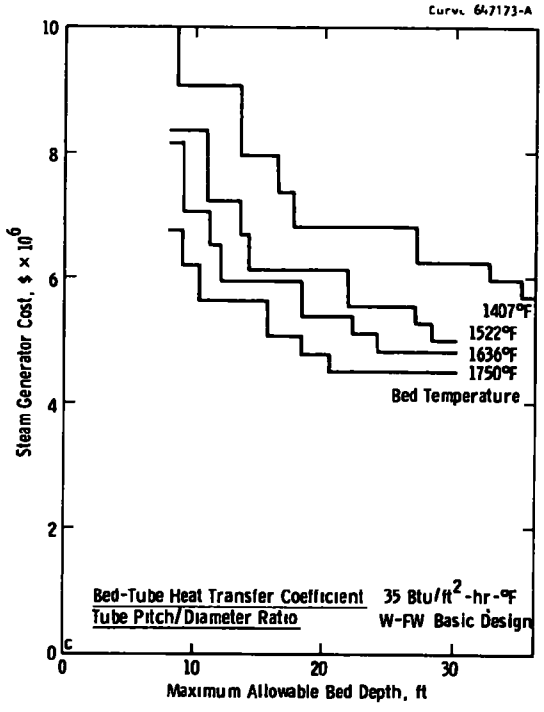

Figure B-9 Dependence of the Steam Generator Cost (318 MW) on the Maximum Allowable Bed Depth (not including erection)

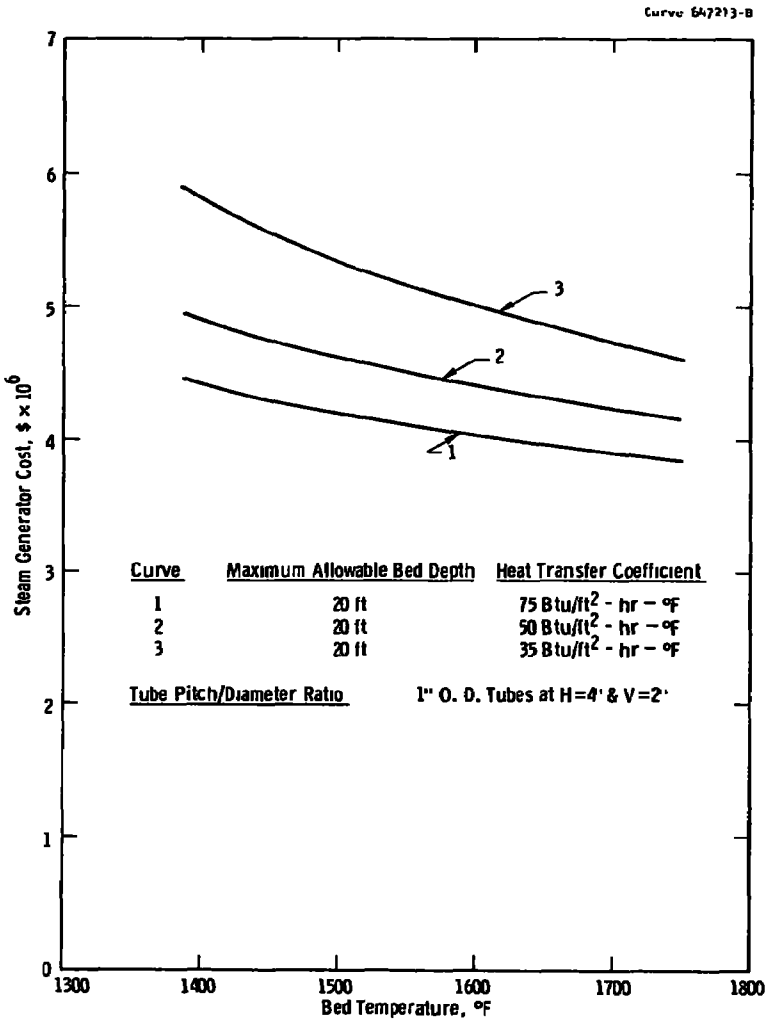

Figure B-10: Effect of Bed-Tube Heat Transfer Coefficient on the Steam Generator Cost (not including erection)

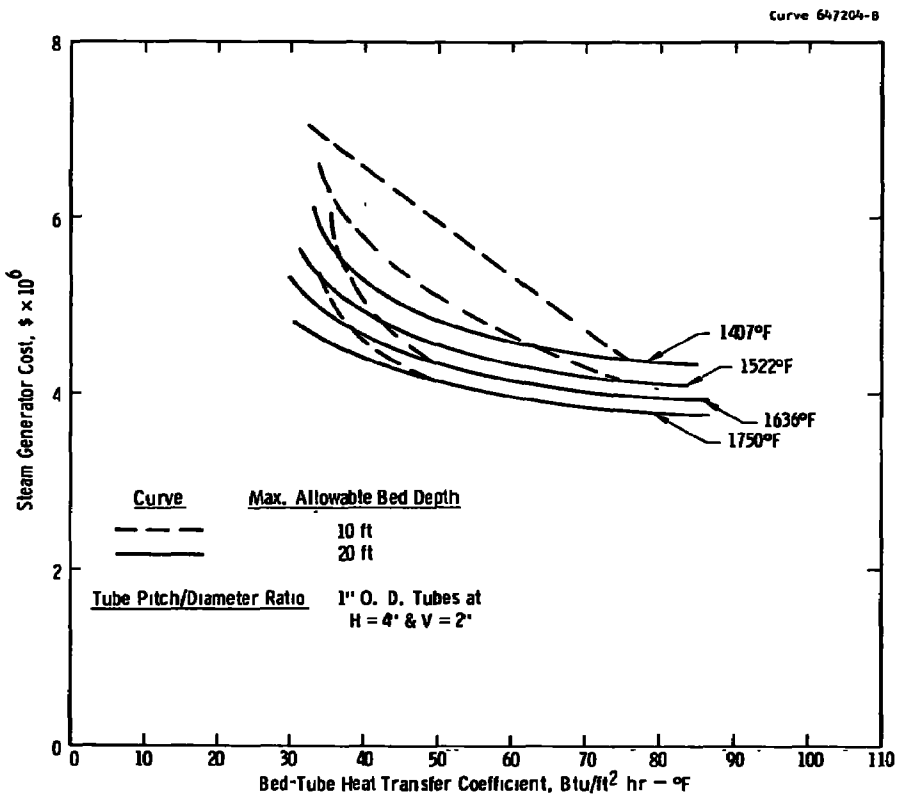

Figure B-11: Effect of Bed-Tube Heat Transfer Coefficient on the Steam Generator Cost (not including erection)

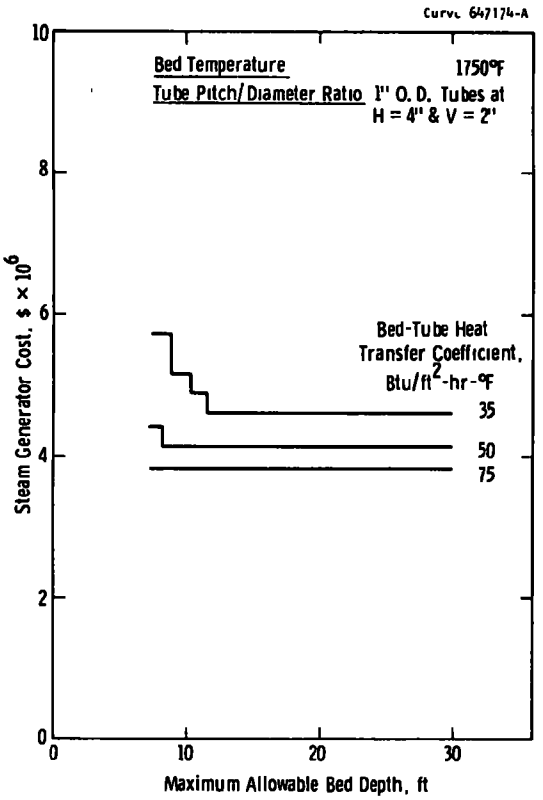

Figure B-12 Dependence of the Steam Generator Cost (318 MW) on the Maximum Allowable Bed Depth (not including erection)

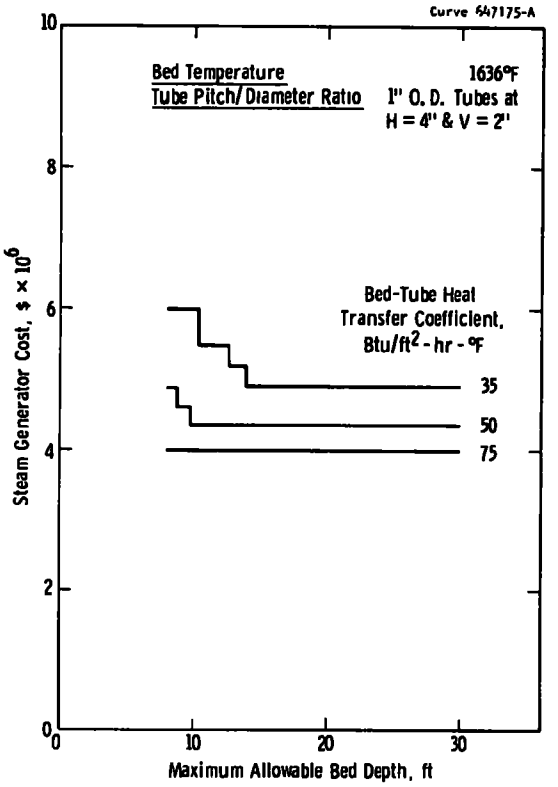

Figure B-13· Dependence of the Steam Generator Cost (318 MW) on the Maximum Allowable Bed Depth (not including erection)

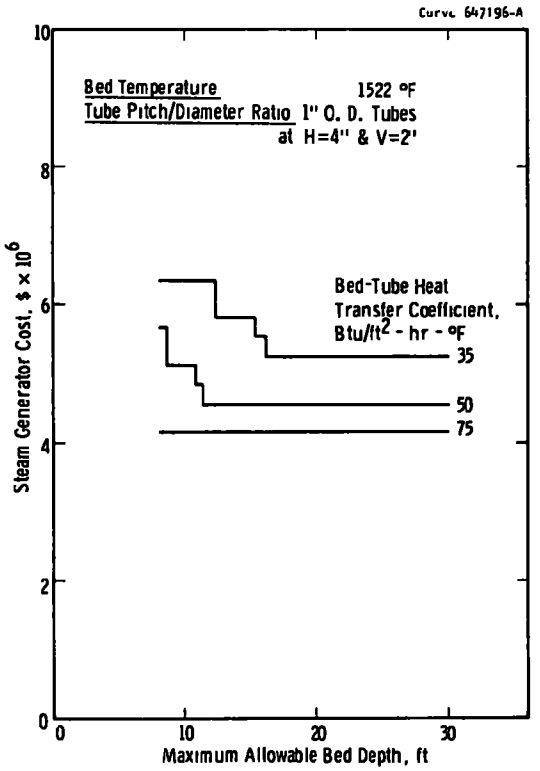

Figure B-14· Dependence of the Steam Generator Cost (318 MW) on the Maximum Allowable Bed Depth (not including erection)

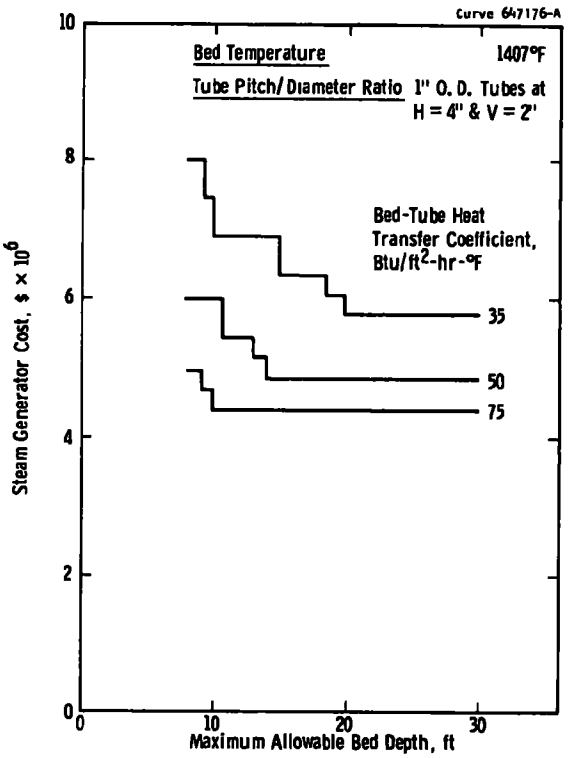

Figure B-15· Dependence of the Steam Generator Cost (318 MW) on the Maximum Allowable Bed Depth (not including erection)

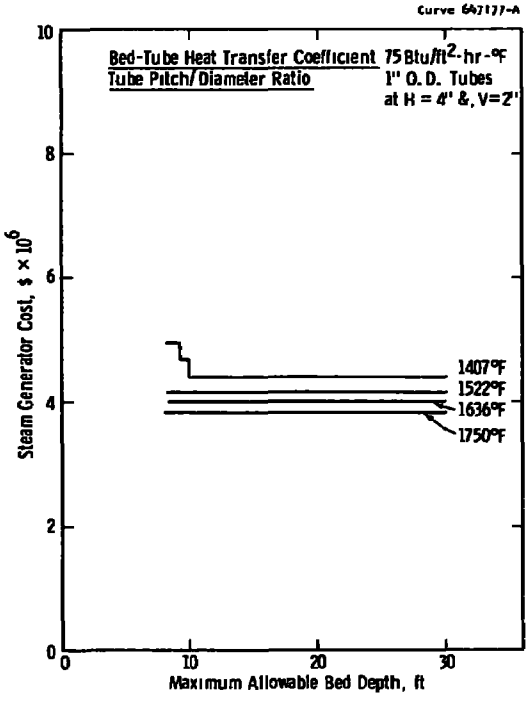

Figure B-16: Dependence of the Steam Generator Cost (318 MW) on the Maximum Allowable Bed Depth (not including erection)

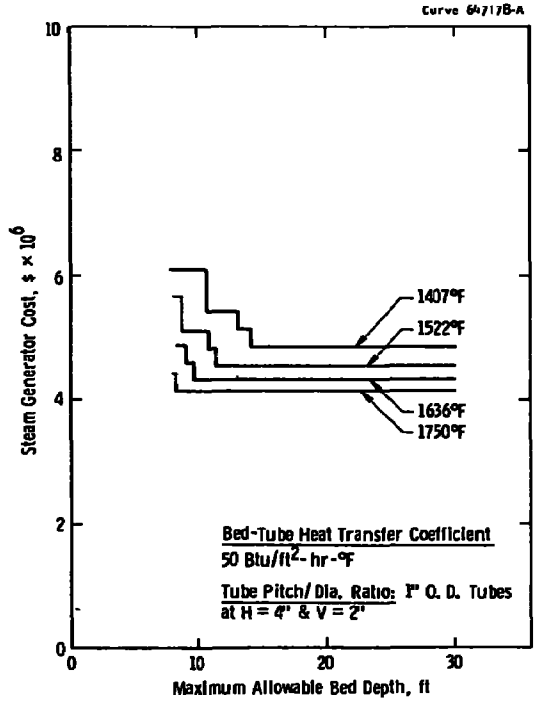

Figure B-17: Dependence of the Steam Generator Cost (318 MW) on the Maximum Allowable Bed Depth (not including erection)

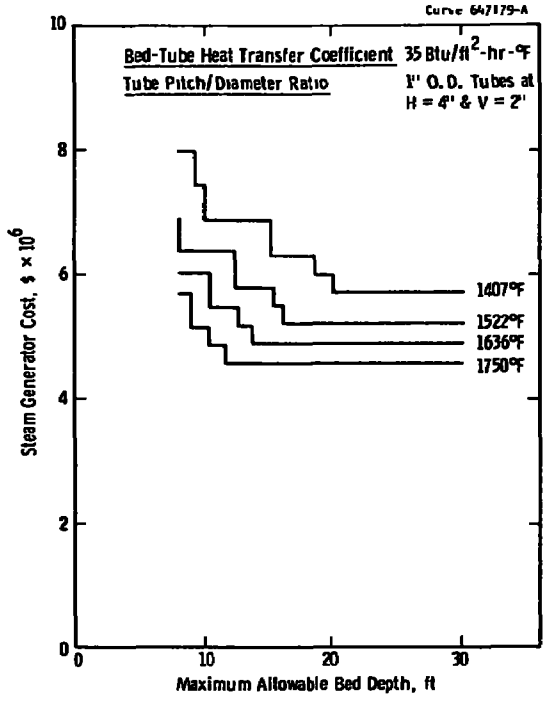

Figure B-18: Dependence of the Steam Generator Cost (318 MW) on the Maximum Allowable Bed Depth (not including erection)

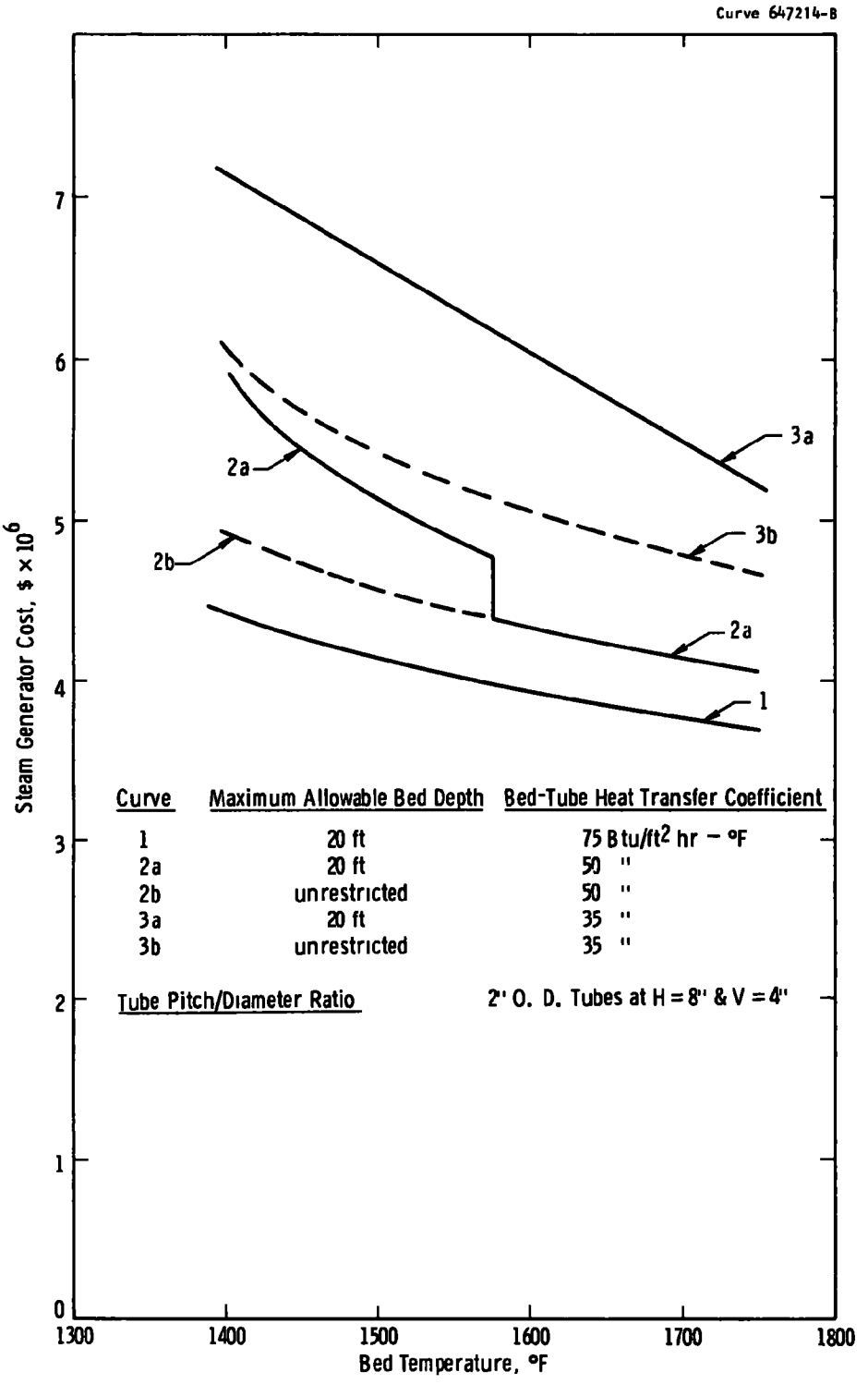

Figure B-19: Effect of Bed-Tube Heat Transfer Coefficient on the Steam Generator Cost (not including erection)

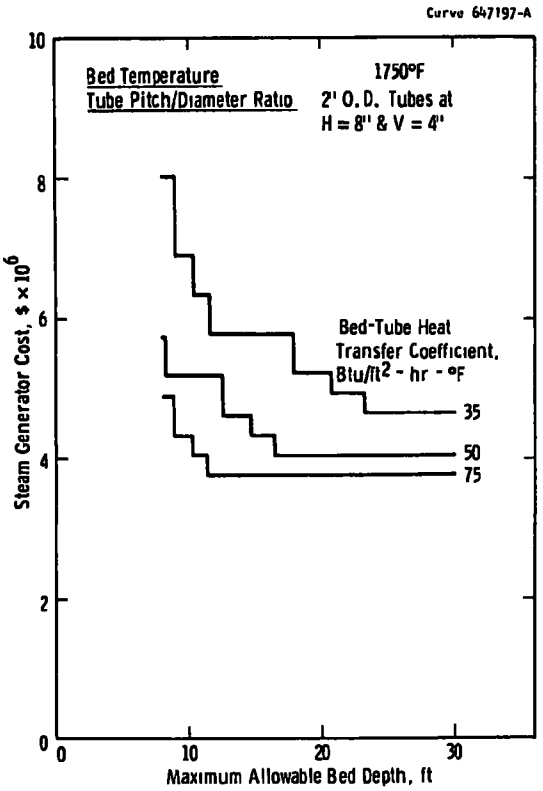

Figure B-20: Dependence of the Steam Generator Cost (318 MW) on the Maximum Allowable Bed Depth (not including erection)

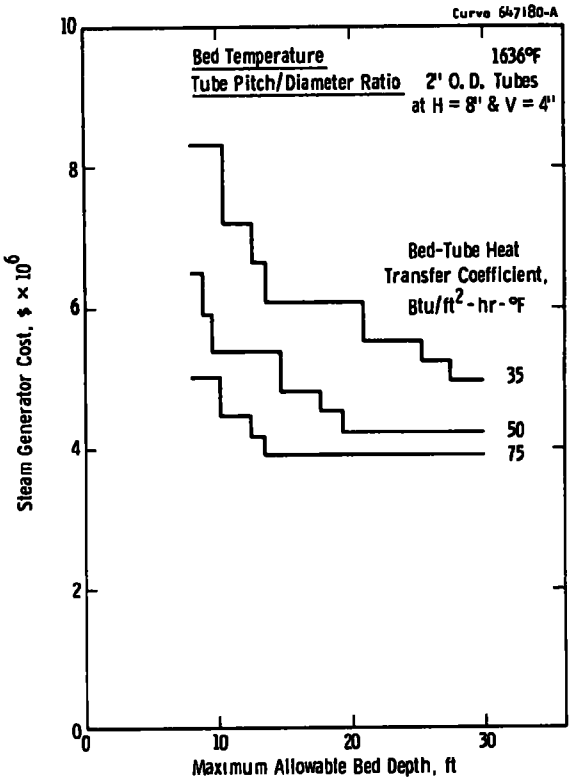

Figure B-21. Dependence of the Steam Generator Cost (318 MW) on the Maximum Allowable Bed Depth (not including erection)

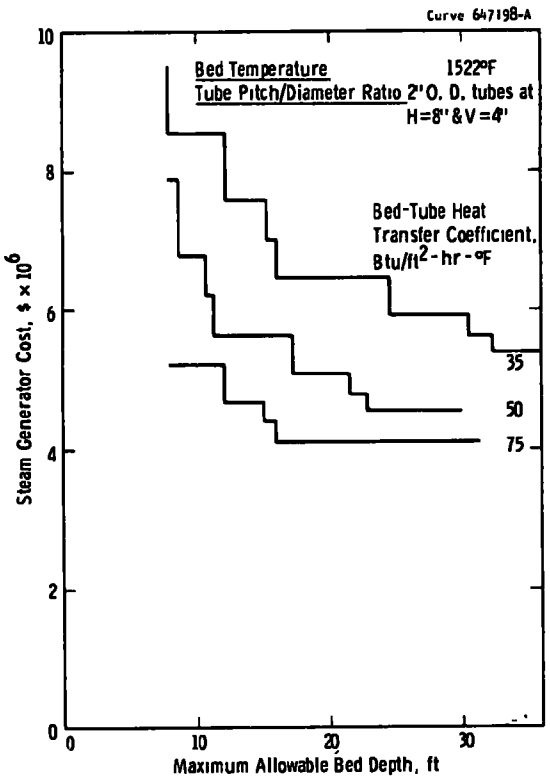

Figure B-22: Dependence of the Steam Generator Cost (318 MW) on the Maximum Allowable Bed Depth (not including erection)

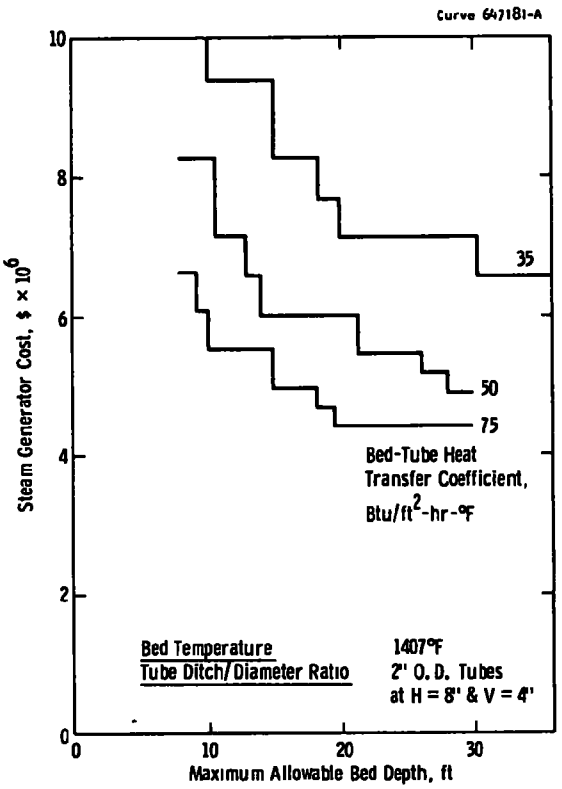

Figure B-23: Dependence of the Steam Generator Cost (318 MW) on the Maximum Allowable Bed Depth (not including erection)

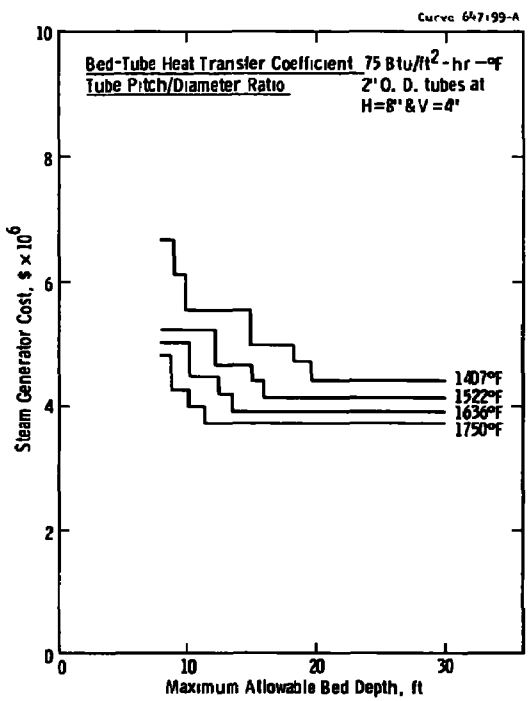

Figure B-24. Dependence of the Steam Generator Cost (318 MW) on the Maximum Allowable Bed Depth (not including erection)

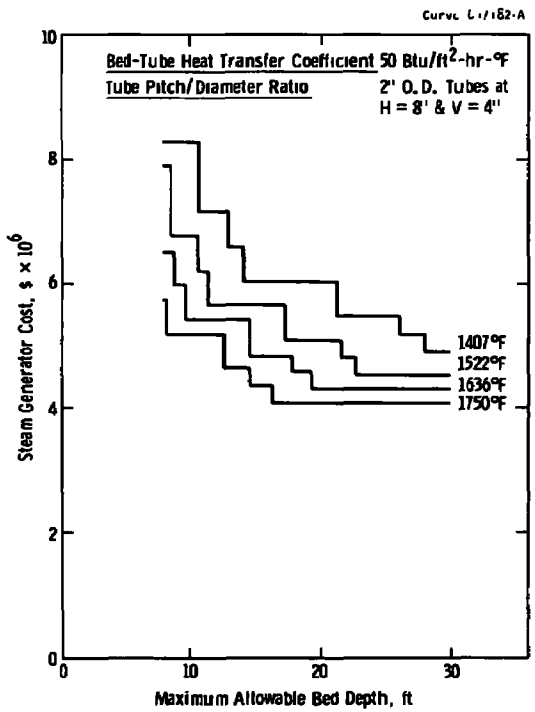

Figure B-25. Dependence of the Steam Generator Cost (318 MW) on the Maximum Allowable Bed Depth (not including erection)

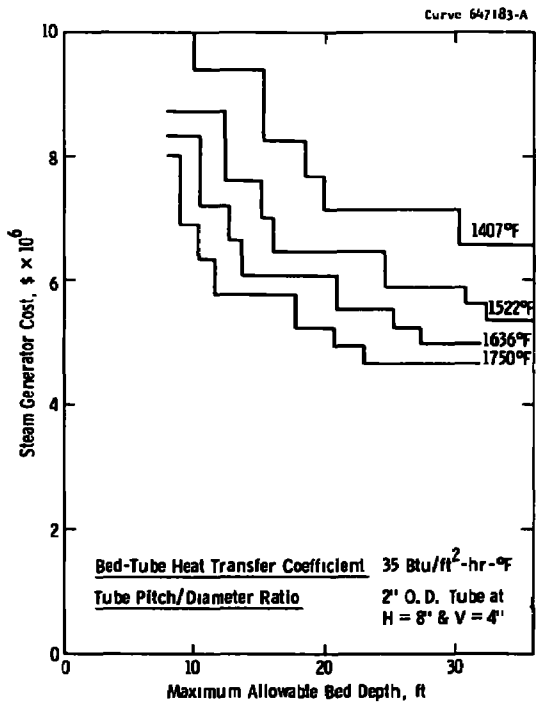

Figure B-26. Dependence of the Steam Generator Cost (318 MW) on the Maximum Allowable Bed Depth (not including erection)

C

APPENDIX C

PARAMETRIC STUDY OF ELUTRIATION RATE FROM A FLUIDIZED BED COMBUSTION BOILER

A parametric study of the elutriation rate from the fluidized bed combustion boiler (Westinghouse-FW basic design) was performed. The design bases for the Westinghouse-FW basic design are summarized in Table C-1. To generate a dust loading identical to that projected for the Westinghouse-Foster Wheeler fluidized bed boiler (7 grains/SCF from the combustor), an infinite number of combinations is possible, as shown in Figure C-1. The basic design specification of this boiler is shown as a point which represents an 8.5% ash coal with 6% carbon elutriation rate and 0.7% dolomite elutriation rate. (The design assumed six times the stoichiometric Ca/S ratio.) For the same coal, a 0% carbon elutriation rate will require a 5.3% dolomite elutriation rate to produce the same dust loading. For a coal of 13.4% ash, the elutriated ash alone will give the same dust loading with 0% carbon and dolomite elutriation rate. Similar diagrams are presented for cases which double and triple this basic design dust loading (Figures C-2 and C-3). The data from Figures C-1 to C-3 are cross-plotted in Figures C-4 to C-8 for a constant carbon elutriation rate to illustrate the possible dust loading for coals of different ash content and stone loss.

TABLE C-1

DESIGN BASES FOR WESTINGHOUSE-FW
FLUIDIZED BED COMBUSTION BOILER (318 MW-4 MODULE DESIGN)

Coal feed (ash content = 8.5%)		53,910 lb/hr-module
Air feed		586,500 lb/hr-module
Dolomite feed plus make-up		44,500 lb/hr-module
Ca/S ratio		6
Dust loading from primary bed		7 grains/SCF
Composition:	Carbon	31.9%
	Ash	63.4%
	Dolomite	4.6%

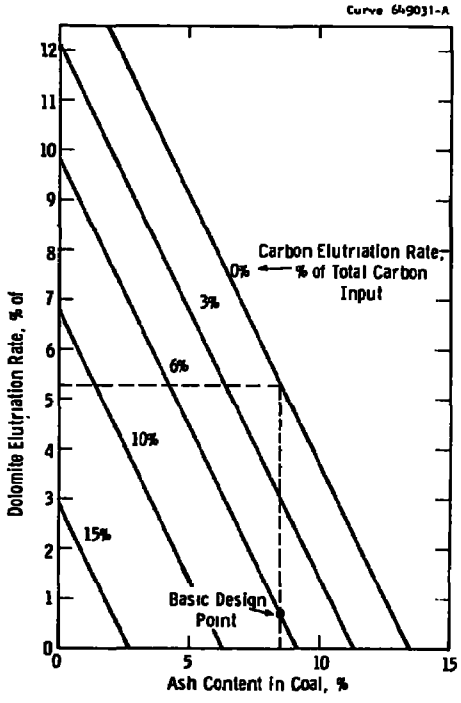

Figure C-1: Different Combinations of Elutriation Rates for a Dust Loading Equal to That of Ⓦ-FW Basic Design

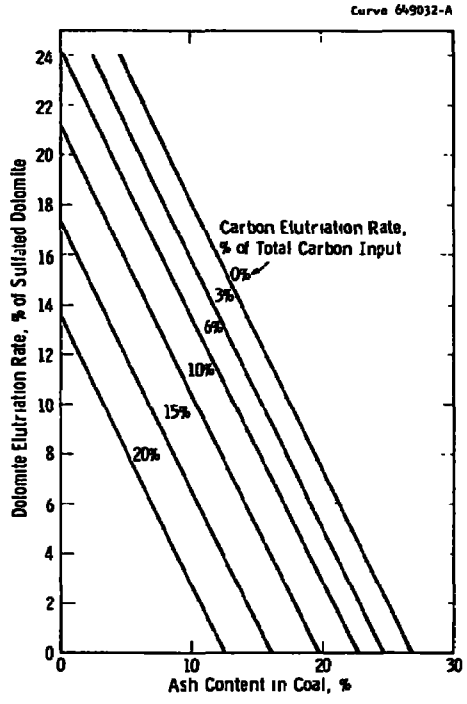

Figure C-2. Different Combinations of Elutriation Rates for a Dust Loading Double That of Ⓦ-FW Basic Design

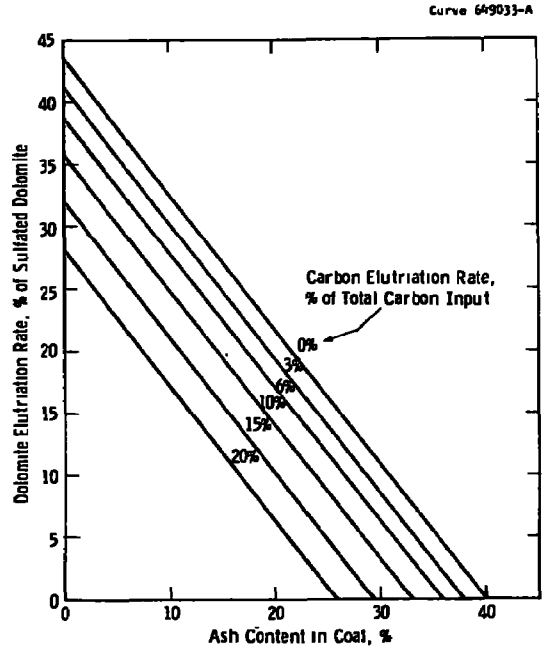

Figure C-3: Different Combinations of Elutriation Rates for a Dust Loading Triple That of Ⓦ-FW Basic Design

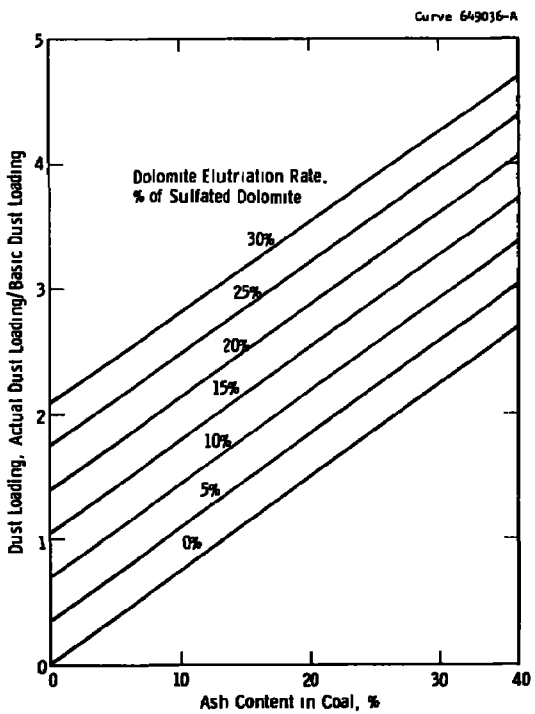

Figure C-4 Possible Dust Loading from FBC at 0% Carbon Elutriation Rate

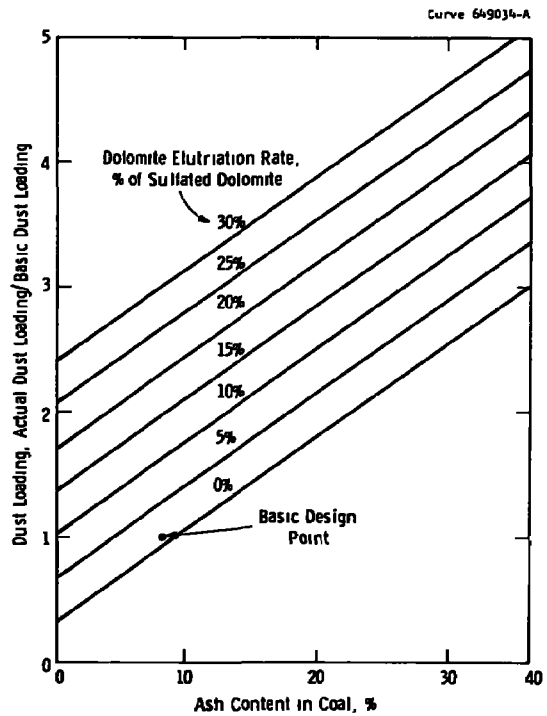

Figure C-5: Possible Dust Loading from FBC at 6% Carbon Elutriation Rate

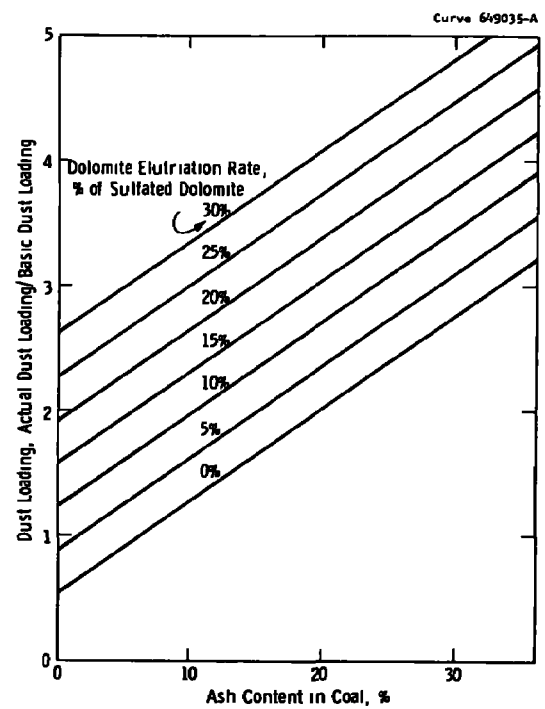

Figure C-6. Possible Dust Loading from FBC at 10% Carbon Elutriation Rate

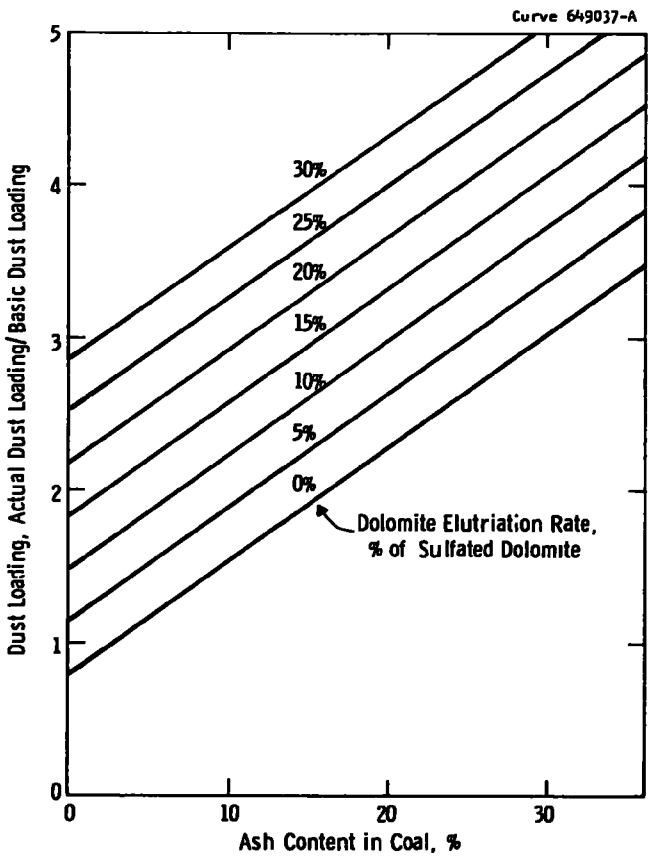

Figure C-7: Possible Dust Loading from FBC at 15% Carbon Elutriation Rate

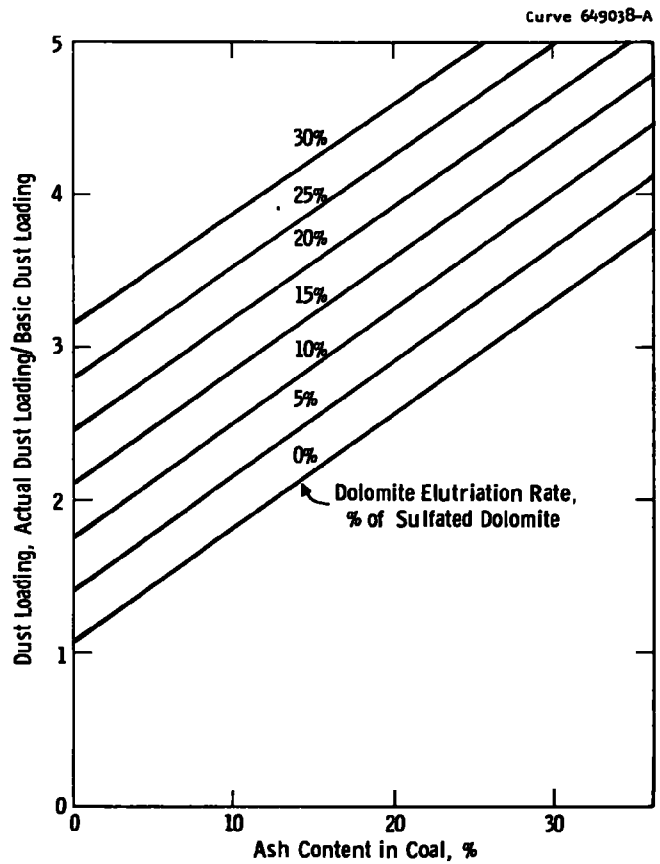

Figure C-8: Possible Dust Loading from FBC at 20% Carbon Elutriation Rate

D

APPENDIX D

BASE DESIGN-HIGH PRESSURE ONE-STEP PROCESS

PROCESS DESCRIPTION

The one-step dolomite/limestone regeneration process consists of a single fluidized bed reaction vessel in which utilized dolomite/limestone ($CaSO_4$) from the pressurized fluid bed boiler (coal-fired) is reacted with a H_2/CO reducing gas to produce CaO and SO_2. The reaction

$$CaSO_4 + \left\{\begin{matrix} H_2 \\ CO \end{matrix}\right\} \rightleftarrows CaO + \left\{\begin{matrix} H_2O \\ CO_2 \end{matrix}\right\} + SO_2 \qquad \text{(D-1)}$$

requires temperatures on the order of 2000°F to produce high levels (1 to 15%) of SO_2 at reasonable rates. The SO_2 equilibrium concentration is favored by reduced pressure, since it is inversely proportional to the total pressure. The competing reaction

$$CaSO_4 + 4 \left\{\begin{matrix} H_2 \\ CO \end{matrix}\right\} \rightleftarrows CaS + 4 \left\{\begin{matrix} H_2O \\ CO_2 \end{matrix}\right\} \qquad \text{(D-2)}$$

also occurs to produce the unwanted product CaS.

The regenerated dolomite/limestone is returned to the fluid bed boiler with the required amount of fresh dolomite/limestone to supplement the regenerated sorbent's reduced activity. The SO_2 stream from the regenerator is sent to a sulfur recovery plant in which sulfuric acid or elemental sulfur is produced.

The high-pressure (10 atmosphere) one-step regeneration process is broken down into five interrelated elements: a regenerator element, a reducing-gas producer element, a sulfur recovery element, a tail gas handling element, and a sorbent circulation element. These elements and their relationship to one another are shown in Figure D-1. The simple block flow diagram indicates the basic streams in the process. Fuel, air, and/or steam are converted to a H_2CO reducing gas in the reducing gas

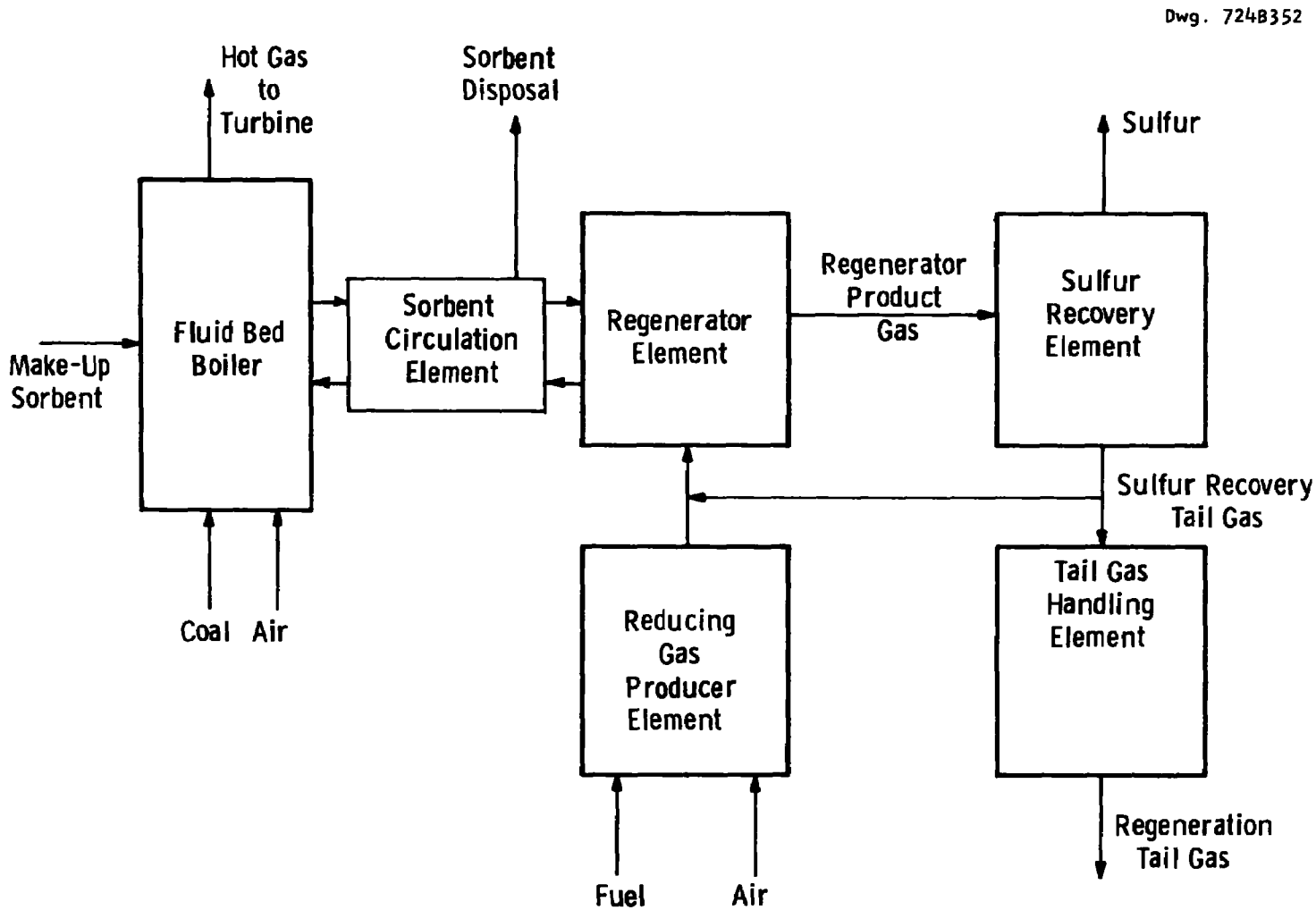

Figure D-1: One-Step Reqeneration Process Elements

producer element. This reducing gas is combined with tail gas recycled from the sulfur recovery element to make up the reducing gas provided to the regenerator. Utilized sorbent from the fluid bed boiler is transported to the regenerator element to produce a regenerated sorbent and an SO_2 stream. The regenerator product gas is processed in the sulfur recovery element, with the sulfur recovery tail gas being either recycled to the regenerator or processed in the tail gas handling element. The performance and design of these five regeneration process elements are interrelated in a complex manner.

SPECIFICATIONS AND ASSUMPTIONS

The high-pressure one-step regeneration base design is founded on the following specifications and assumptions.

TABLE D-1

DESIGN SPECIFICATIONS

Fixed coal rate	430,000 lb/hr (∿ 635 MW)
Sorbent type	dolomite
Boiler sulfur removal	95%
Variable process sulfur loads	0.01, 0.03, 0.06
Recycle of tail gas to boilers	
Recovery of elemental sulfur by methane reduction of SO_2	
Reducing-gas production from coal (methane for sulfur recovery)	
Four regenerator vessels (one for each boiler module)	

TABLE D-2

DESIGN ASSUMPTIONS

Regenerator pressure	10 atm
Regenerator temperature	2000°F
SO_2 mole fraction in regenerator product	1 and 2% cases
$CO + H_2$ mole fraction in reducing gas	1.5 and 3%, respectively
Sulfur recovery efficiency	95%
Dolomite utilization in boiler	30%
Dolomite utilization after regeneration	10%
Dolomite make-up rate	1 mole Ca/mole S
Fluidization velocity	5 ft/sec
Boiler condition	calcination
Dolomite temperature to regenerator	1200°F
Calcium sulfide in regenerated dolomite	0%
Ash in utilized dolomite from boilers	0%
Heat losses from regenerator neglected	

MATERIAL AND ENERGY BALANCES

Material and energy balances for the process streams indicated in Figure D-2 are shown in Tables D-3 and D-4, for the 1% and 2% SO_2 cases, respectively. The basis for Tables D-3 and D-4 is a process sulfur load of 0.03. The energy balance indicates that the process is essentially balanced -- the steam raised from the hot regenerator gas is sufficient to provide the auxiliary power requirements of the process. Thus, the regeneration process has a negligible effect on the electrical output of the power plant.

EQUIPMENT

The major equipment items considered in the base design of the high-pressure one-step regeneration process are shown in Figure D-3.

Regenerator Element

The regenerator element consists of four regenerator vessels (V5). Each regenerator vessel is followed by a multistage particulate clean-up unit (V6). The regenerator vessels have been assumed to be 35 ft in total height with operation at a fluidization velocity of 5 ft/sec. Carbon steel shells with refractory lining and insulation and a refractory distributor plate have been utilized in the design. The particulate control equipment used for each module is a two-stage Ducon cyclone followed by an Aerodyne unit. The cyclones are enclosed in refractory lined pressure shells.

Sorbent Circulation Element

The sorbent circulation element consists of four identical modules to circulate dolomite pneumatically between each boiler-regenerator combination. Each circulation module collects utilized dolomite from the boiler through four transport lines into a single hold vessel (V2). The utilized dolomite is then injected into the circulation line using the Petrocarb injection system (V3). Regenerated dolomite leaves the

Dwg. 724867

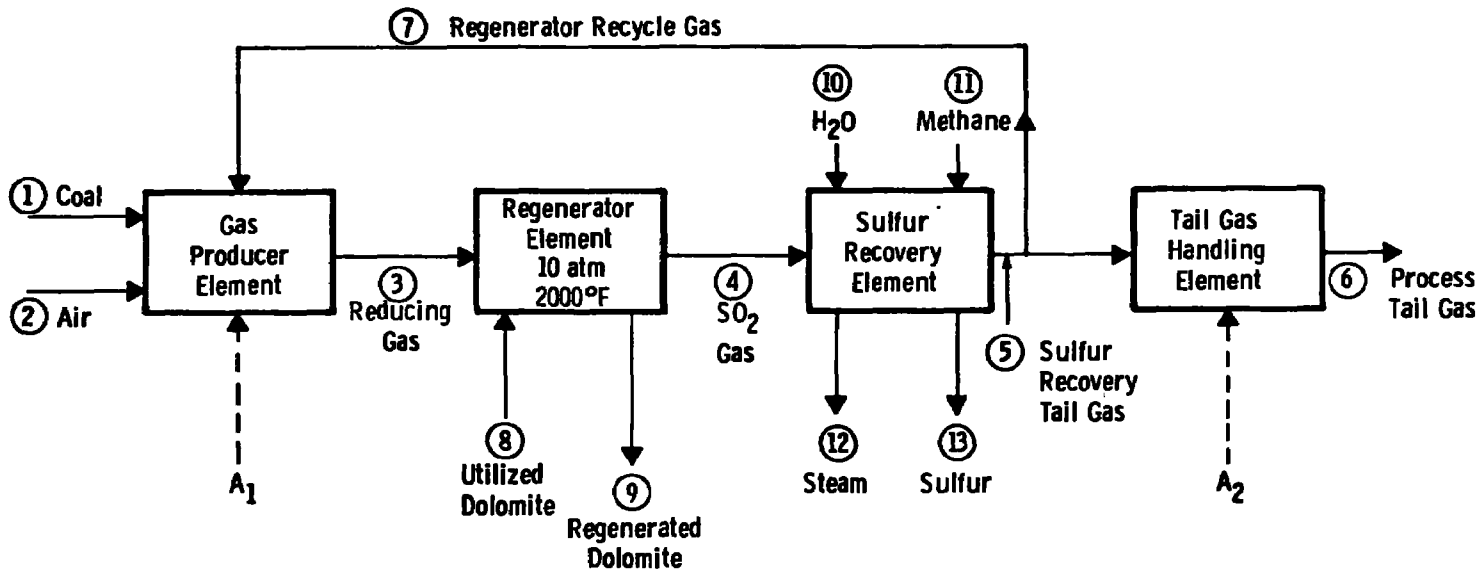

Figure D-2: High-Pressure One-Step Regeneration Process Flow Diagram

TABLE D-3

MATERIAL AND ENERGY BALANCES -- ONE-STEP REGENERATION AT HIGH PRESSURE (1% SO_2)[a]

Stream	Conditions Temperature, °F	/	Pressure, psia	Moles/Hr	Enthalpy, Btu/lb. Fuel[b]	Comments
1. Coal	100	/	165	57,100 lb/hr	1725[c]	85% thermal efficiency in coal partial combustor
2. Air	600	/	165	16,500	139	92% of stoichiometric combustion of coal
3. Reducing Gas	2250	/	150	40,000	1594	1.5% H_2 + CO assumed requirement ΔH_R = -104 Btu/lb fuel in regenerator
4. SO_2 Gas	2000	/	140	40,300	1404	1% SO_2
5. Sulfur Recovery Tail Gas	300	/	135	40,600	172 (+53)[d]	ΔH_R = -40 Btu/lb fuel in Claus plant
6. Process Tail Gas	400	/	155	18,000	84 (+23)[d]	recycled to boiler
7. Regenerator Recycle Gas	400	/	155	22,600	108 (+30)[d]	
8. Utilized Dolomite	1200	/	150	2015 moles Ca	change in sensible heat, ΔH = 86	50% MgO, 15% $CaSO_4$, 35% CaO
9. Regenerated Dolomite	2000	/	150	2015 moles Ca		50% MgO, 5% $CaSO_4$, 45% CaO
10. Water	100	/	-	411,000 lb/hr	---	
11. Methane	100	/	140	310	214	
12. Steam	750 350	/ /	600 75	354,000 lb/hr (600#) 67,000 lb/hr (75#)	1270	1110 Btu/lb fuel - 600 psia, 750°F steam 160 Btu/lb fuel - 75 psia, 350°F steam
13. Sulfur	200	/	135	435	---	95% Claus sulfur removal efficiency assumed
A_1 Auxiliary Power	36,400 H.P.					70% compressor efficiency
A_2 Auxiliary Power	2,100 H.P.					70% compressor efficiency
Sorbent Transport Power	600 H.P. (boosting 10 atm transport gas) or 5,600 H.P. (compressing atm press. trans. gas)					

[a] Basis:
Process sulfur load = 0.03
Boiler coal rate = 430,000 lb/hr.

[b] BTU per lb coal fed to the fluid bed boilers.

[c] Based on 13,000 Btu/lb coal.

[d] Heat of combustion in parentheses.

TABLE D-4

MATERIAL AND ENERGY BALANCES -- ONE-STEP REGENERATION AT HIGH PRESSURE (2% SO_2)

Stream	Conditions Temperature, °F	/	Pressure, psia	Moles/Hr	Enthalpy, Btu/lb Fuel[a]	Comments
1. Coal	100°F	/	165 psia	34,800 lb/hr	1050[b]	85% thermal efficiency in coal partial combustor
2. Air	600	/	165	9,400	80	87% of stoichiometric combustion of coal
3. Reducing Gas	2500	/	150	19,800	892	3% H_2 + CO , ΔH_R = -104 Btu/lb Fuel
4. SO_2 Gas	2000	/	140	20,150	702	2% SO_2
5. Sulfur Recovery Tail Gas	300	/	135	20,440	92 (+50)[c]	ΔH_R = - 40 Btu/lb Fuel in Claus plant
6. Process Tail Gas	400	/	155	10,740	52 (+25)[c]	Recycled to boiler
7. Regenerator Recycle Gas	400	/	155	9,700	49 (+25)[c]	
8. Utilized Dolomite	1200	/	150	2015 moles Ca	change in sensible heat, ΔH = 86	50% MgO, 15% $CaSO_4$, 35% CaO
9. Regenerated Dolomite	2000	/	150	2015 moles Ca		50% MgO, 5% $CaSO_4$, 45% CaO
10. Water	100	/	-	210,000 lb/hr	---	
11. Methane	100	/	140	291	200	
12. Steam (Total)	750 350	/ /	600 75	179,000 lb/hr (600#) 31,000 lb/hr (75#)	650	561 Btu/lb Fuel - 600 psia, 750°F steam 89 Btu/lb Fuel - 75 psia, 350°F steam
13. Sulfur	200	/	135	414	---	95% Claus sulfur removal efficiency
A_1 Auxiliary Power	20, 400 H.P.					70% compressor efficiency
A_2 Auxiliary Power	1, 200 H.P.					70% compressor efficiency
Sorbent Transport Power	600 H.P. (boosting 10 atm trans. gas) or 5,600 H.P. (compressing atm press. trans. gas)					

[a] Btu per lb coal fed to the fluid bed boilers

[b] Based on 13,000 Btu/lb coal

[c] Heat of combustion in parentheses

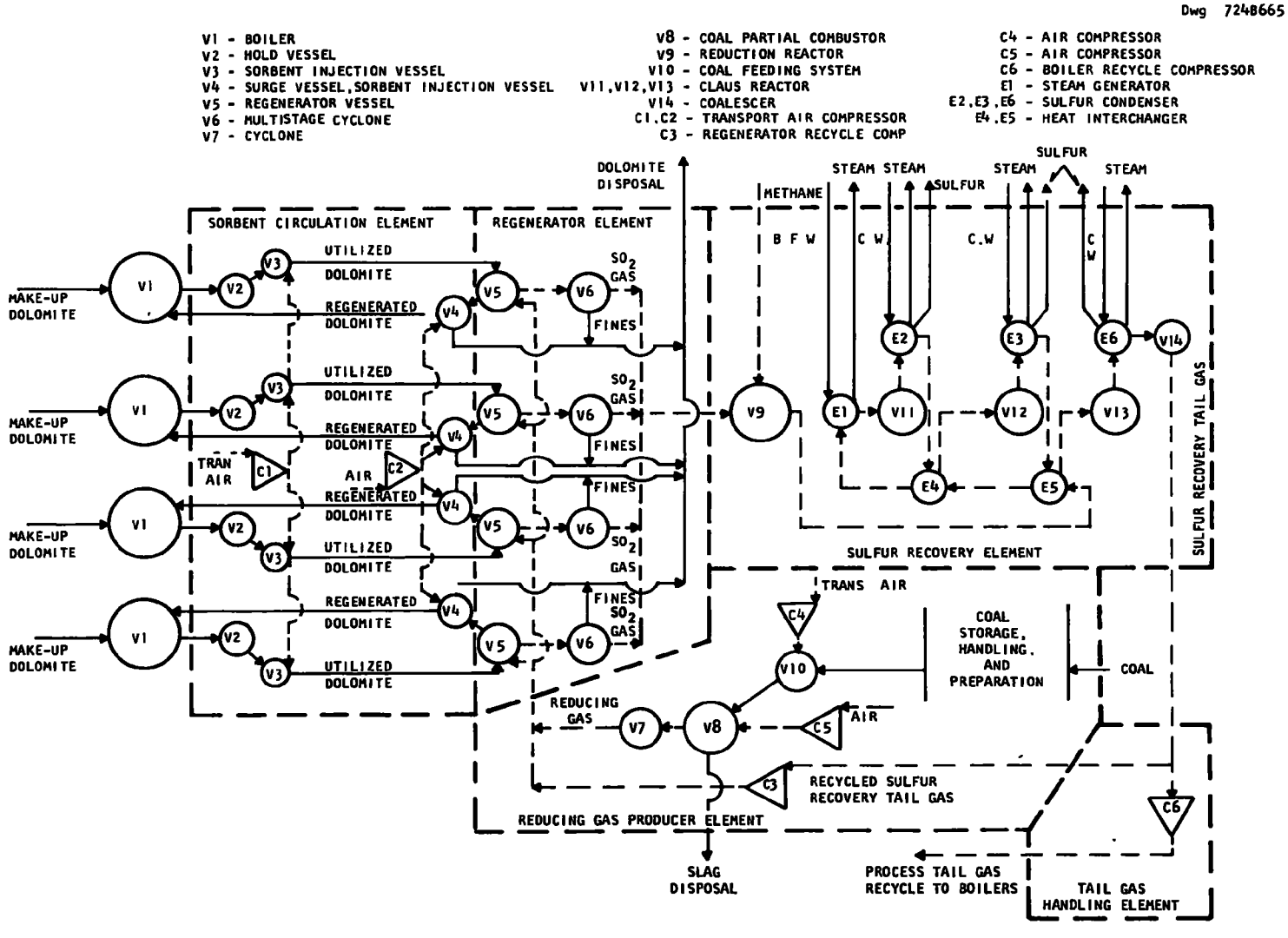

Figure D-3: High-Pressure One-Step Regeneration Schematic Flow Diagram

regenerator and enters a distribution vessel (V4). The dolomite is distributed to four lines and injected into the transport lines returning the sorbent to the boiler beds. Waste dolomite may be withdrawn from either the hold vessels or the distribution vessels (shown in Figure D-3 for disposal. A pair of air compressors is required for transporting the sorbent (C1,C2). Air at about 175 psia is required for transport.

Reducing-Gas Producer Element

A single gas producer module is required for generation of the reducing gas. Coal storage, handling and preparation are required, though some of the equipment required may be integrated with the main coal supply system. In the high-pressure one-step regenerator the levels of hydrogen and carbon monoxide required for regeneration are so low (1.5-3.0%) 3.0%) that it is assumed that reducing gas can be produced by operating a slagging combustor (V8) at slightly below stoichiometric combustion conditions. Coal is fed to the slagging partial combustor using a Petrocarb feeding system (V10). Compression of combustion air is also needed (C5). The reducing gas passes through a single stage cyclone (V8) and is mixed with recycled tail gas by means of recycle compressor C3.

Sulfur Recovery Element

The sulfur recovery element is a three-stage Claus process (V11,V12,V13) with a portion of the entering SO_2 stream reduced to H_2S by means of a catalytic reaction with methane (V9). The sulfur recovery element is described in a previous report by Shell.[1] Other possibilities exist for sulfur recovery such as an Allied Chemical process which is nearer commercial development than the process assumed here.[2]

Tail Gas Handling Element

In the case of the high pressure one-step regeneration process the tail gas handling element consists of a compressor (C6) which recycles the tail gas to the fluid bed boilers. It has been assumed that

no modification to the boilers is necessary to handle the recycled gas, though this may be a large stream relative to the boiler air rate.

CAPITAL INVESTMENT BREAKDOWN

The breakdown by element of the capital investments for the 1 and 2% SO_2 cases is shown in Tables D-5 and D-6. Investments are given in $/kw based on 635 MW of plant capacity.

TABLE D-5

1% SO_2 INVESTMENT BREAKDOWN, $/kw

Element	Process Sulfur Load		
	0.06	0.03	0.01
Regenerator Element	11.2	7.6	3.4
Sulfur Recovery Element	6.7	4.1	1.9
Tail Gas Handling Element	2.8	1.6	0.9
Dolomite Circulation Element	2.5	1.5	0.6
Gas Producer Element	37.4	22.0	11.3
TOTAL PROCESS	60.6	36.8	18.1

TABLE D-6

2% SO_2 INVESTMENT BREAKDOWN, $/kw

Element	Process Sulfur Load		
	0.06	0.03	0.01
Regenerator Element	7.6	4.1	2.3
Sulfur Recovery Element	5.0	3.2	1.5
Tail Gas Handling Element	1.8	1.0	0.5
Dolomite Circulation Element	2.5	1.5	0.6
Gas Producer Element	24.0	14.8	6.8
TOTAL PROCESS	40.9	24.6	11.7

The costs given in Tables D-5 and D-6 are based on the following:

- Mid-1973 costs
- Interest during construction and general items and engineering not included. These items are added to obtain the total power plant cost.

ENERGY COSTS

The energy cost contribution of the high-pressure one-step regeneration process to the total power plant cost is shown in Tables D-7 and D-8. These costs were obtained on the following basis:

- Interest during construction at 7-1/2% per year
- Capital charges at 15%
- O&M at 5%
- 70% capacity factor
- No credit for recovered sulfur
- Coal at 45¢/MM Btu
- Methane at 80¢/MM Btu
- Dolomite at $2/ton.

The base design fluid bed combustion power plant would have a total energy cost of 11.3 mills/kWh plus the regeneration process energy cost shown in the tables.

TABLE D-7

1% SO_2 ENERGY COST (mills/kWh)

	Process Sulfur Load		
	0.06	0.03	0.01
Capital Charges plus O&M	2.27	1.38	0.68
Fuel Cost	1.30	0.65	0.22
Dolomite Cost	0.24	0.12	0.04
TOTAL	3.81	2.15	0.94

TABLE D-8

2% SO_2 ENERGY COST (mills/kWh)

Capital Charges plus O&M	1.53	0.92	0.44
Fuel Cost	0.88	0.44	0.15
Dolomite Cost	0.24	0.12	0.04
TOTAL	2.65	1.48	0.63

SENSITIVITY OF RESULTS

The sensitivity of the cost results for the high-pressure one-step regeneration process with respect to the various parameters which apply to the process are summarized in Table D-9. The variables which have been investigated by the base case study are the process sulfur load, the SO_2 mole fraction, and the boiler condition (calcining or carbonating). The effect of the dolomite cost and make-up rate on the plant energy cost is shown in Appendix H. Some of the design and operating variables considered in Table D-9 are also investigated in the general study of Appendix L.

The capital cost of each of the five process elements are considered in Table D-9, in addition to the total process capital investment. The sensitivity of the regeneration process fuel cost to the variables is also indicated in the table. The quantitative statements in Table D-9 refer to the case of 0.03 process sulfur load and indicate a comparison with the base case results with all parameters fixed at the base value but the parameter in question.

PAGE NOT

AVAILABLE

DIGITALLY

REFERENCES

1. Shpall, R. T. Shell Development Company, "Claus Technical and Economic Study," National Air Pollution Control Administration, OAP Contract EHSD-71-45 (1972).

2. "Evaluation of the Fluidized Bed Combustion Process," Westinghouse Research Laboratories, Office of Research and Monitoring, EPA, Contract No. 68-02-0217 and 68-02-0605, Thirty-Seventh Monthly Progress Report, p. 23, April 1973.

E

APPENDIX E

BASE DESIGN -- LOW-PRESSURE ONE-STEP REGENERATION PROCESS

PROCESS DESCRIPTION

The same chemistry and basic flow diagram applies for the low-pressure one-step regeneration process as for the high-pressure one-step process. The same five process elements are identified as in the high-pressure process: the regenerator element, the sorbent circulation element, the reducing-gas producer element, the sulfur recovery element, and the process tail gas handling element. The characteristics and performance of the five elements are different from the high-pressure case, however, and the motive for examining the low-pressure one-step regeneration process is indicated by the results of Appendix L as having the potential for a much higher concentration of SO_2 in the regenerator product.

PROCESS SPECIFICATIONS AND ASSUMPTIONS

The low-pressure one-step regeneration base design is founded on the following set of specifications and assumptions. The sensitivity of the cost results to these assumptions and specifications are considered in this appendix and in Appendix L.

TABLE E-1

DESIGN SPECIFICATIONS

Fixed coal rate	430,000 lb/hr
Sorbent type	dolomite
Boiler sulfur removal	95%
Variable process sulfur loads	0.01, 0.03, 0.06
Incineration of process tail gas	
Recovery of elemental sulfur by methane reduction of SO_2	
Reducing gas produced from coal (methane for sulfur recovery)	
Four regenerator vessels (one for each boiler module)	

TABLE E-2

DESIGN ASSUMPTIONS

Regenerator pressure	1 atm
Regenerator temperature	1900°F
SO_2 mole fraction in regenerator product	10%
$CO + H_2$ mole fraction in reducing gas	16.5%
Sulfur recovery efficiency	95%
Dolomite utilization in boiler	30%
Dolomite utilization after regeneration	10%
Dolomite make-up rate	1 mole Ca/moles S
Fluidization velocity	5 ft/sec
Boiler condition	calcination
Dolomite temperature to regenerator	1900°F
Calcium sulfide in regenerated dolomite	0%
Ash in utilized dolomite from boilers	0%
Heat losses from regenerator neglected	

MATERIAL AND ENERGY BALANCES

Material and energy balances for the low pressure one-step regeneration process streams in Figures E-1 and E-2, are shown in Table E-3. Temperature control and process turndown of the low-pressure process are discussed in Appendix G. Figure E-2 represents the process streams required to preheat the sorbent to 1900°F, and Figure E-1 deals with the remainder of the regeneration process. Somewhat more steam is produced in the low-pressure one-step process than is required to generate the process auxiliary power. The effect of the regeneration process on the power plant electrical output is neglected.

EQUIPMENT DESCRIPTION

The major equipment items considered in the base design of the low pressure one-step regeneration process are shown in Figure E-3.

Regenerator Element

The regenerator element follows the same basic design used in the high-pressure case: four regenerator vessels (V13), refractory lined, are each in series with a multistage cyclone (V14) to remove fines from the SO_2 gas.

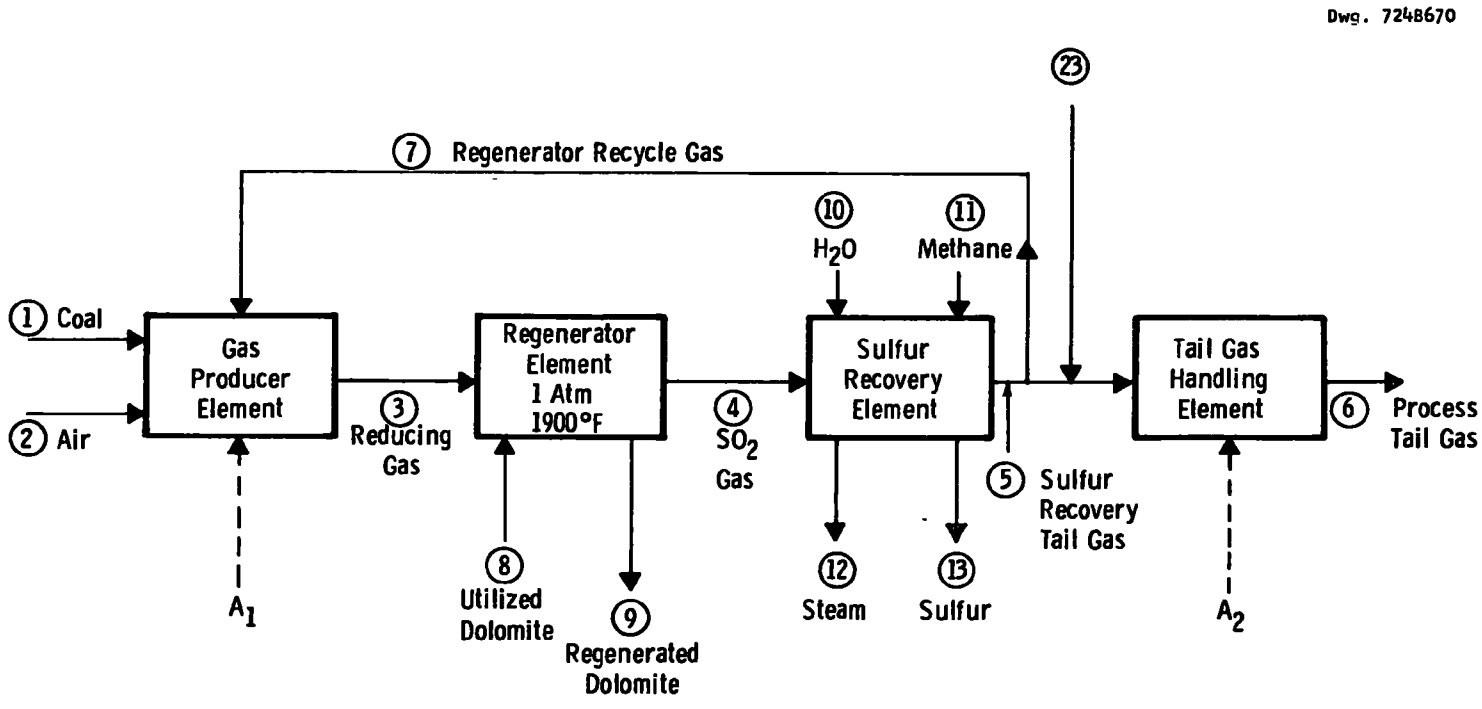

Figure E-1: Low-Pressure One-Step Regeneration Process Flow Diagram

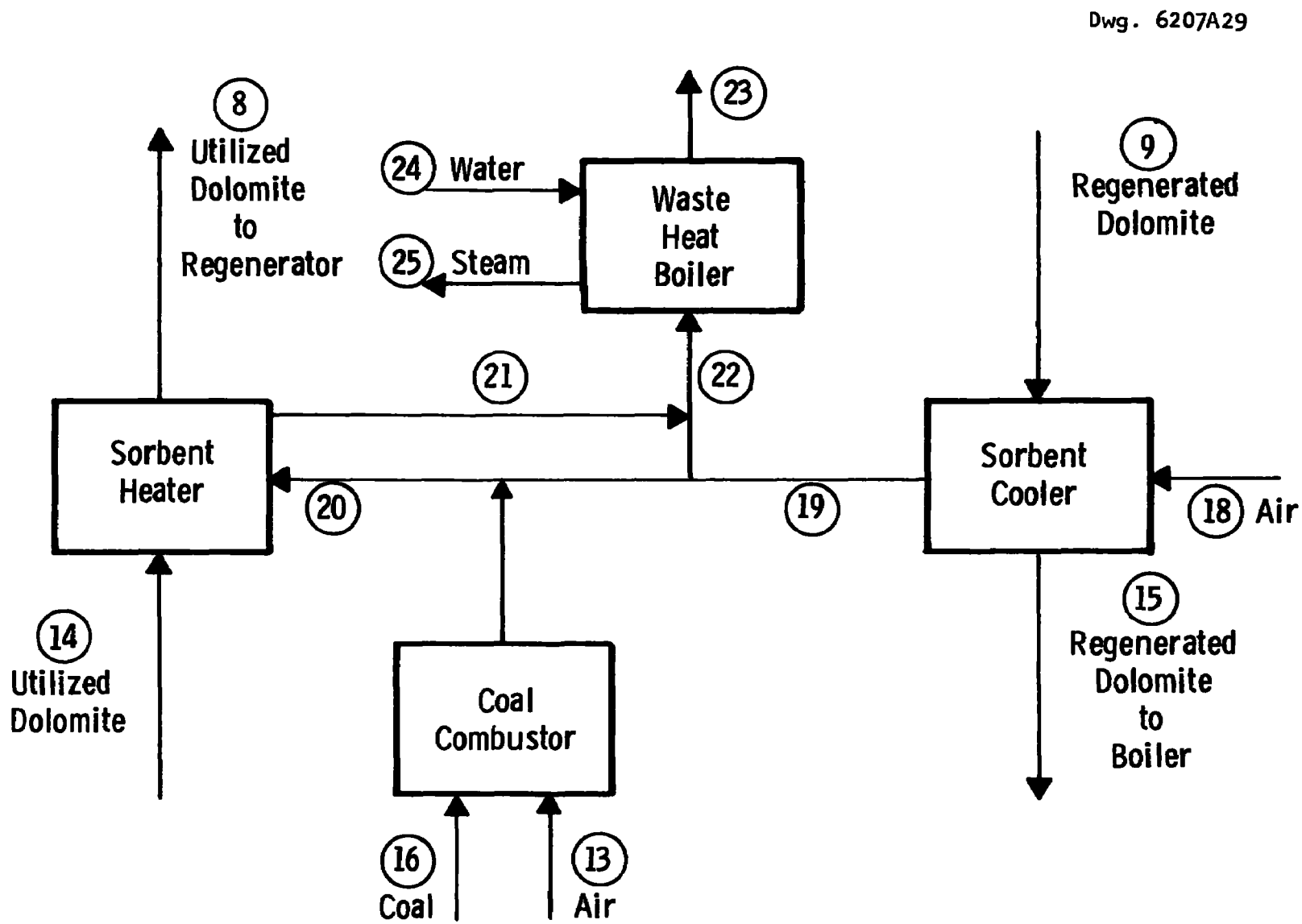

Figure E-2: Low-Pressure One-Step Regeneration Process Flow Diagram — Sorbent Temperature Control

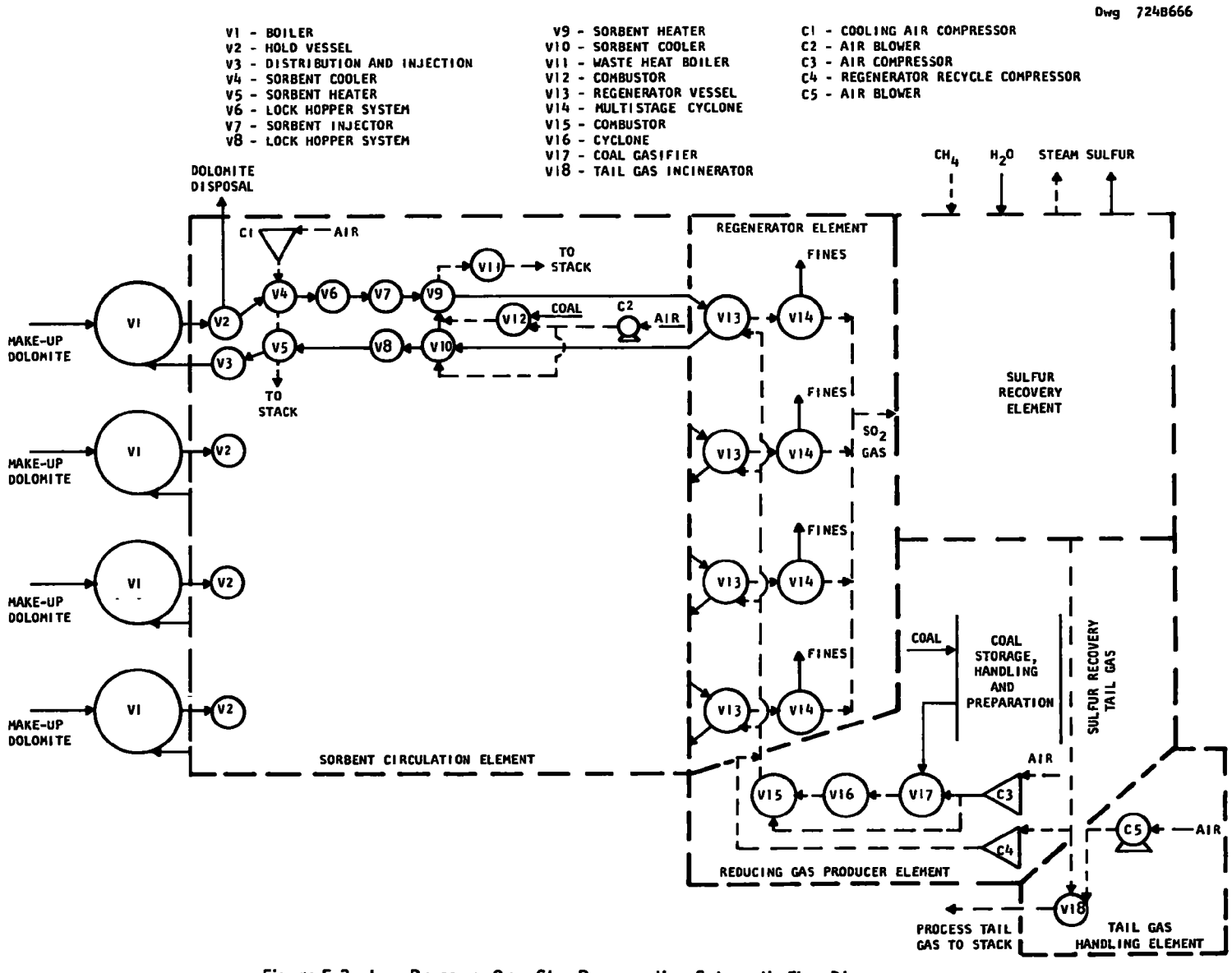

Figure E-3: Low-Pressure One-Step Regeneration Schematic Flow Diagram

TABLE E-3

MATERIAL AND ENERGY BALANCES -- LOW-PRESSURE ONE-STEP REGENERATION

Stream	Conditions °F / psia	Moles/Hr (unless indicated otherwise)	Enthalpy, Btu/lb Fuel	Comments
1. Coal	200°F / 20 psia	12,750 lb/hr	385	85% thermal efficiency in coal gasifier
2. Air	200 / 20	2,500	2	63% of stoichiometric combustion of coal
3. Reducing Gas	3150 / 17	3,630	210	16.5% H_2 + CO assumed requirement ΔH_R = -104 Btu/lb fuel in generator
4. SO_2 Gas	1900 / 16	4,030	126	10% SO_2
5. Sulfur Recovery Tail Gas	300 / 15	4,300	12 (+47)	H.V. of unused CH_4 in parenthesis ΔH = -40 Btu/lb fuel in Claus plant
6. Process Tail Gas	700 / 15	3,640 + 5,700	---	combustion of sulfur plant tail gas with no CH_4 addition and combination with stone heating tail gas
7. Regenerator Recycle Gas	300 / 15	660	3 (+7)	
8. Utilized Dolomite	1900 / 20	2015 moles Ca	change in sensible heat, ΔH = -23	50% MgO, 15% $CaSO_4$, 35% CaO
9. Regenerated Tail Gas	1900 / 15	2015 moles Ca		50% MgO, 5% $CaSO_4$, 45% CaO
10. Water	100 / --	51,000 lb/hr	---	
11 Methane	100 / 16	270	186	
12. Steam	750 / 600 350 / 75	43,000 lb/hr 8,000 lb/hr	 154	135 Btu/lb fuel - 600 psia, 750°F steam 19 Btu/lb fuel - 75 psia, 350°F steam
13. Sulfur	200 / 15	395	---	95% efficient Claus plant
14. Utilized Dolomite	1200 / 20	2015 moles Ca	change in sensible heat ΔH = 99	
15 Regenerated Dolomite	800 / 15	2015 moles Ca	change in sensible heat ΔH = 157	
16. Coal	200 / 15	3430 lb/hr	104	
17. Air	100 / 30	1083	---	
18. Air	100 / 25	4360	---	
19. Air	1800 / 20	4360	157	
20. Heating Gas	2300 / 20	4750	221	
21. Heater Flue Gas	1300 / 17	4750	121	
22. Hot Tail Gas	1400 / 17	5700	156	
23 Cold Tail Gas	300 / 15	5700	27	
24 Water	800 / 200	46,000 lb/hr	10	
25 Steam	750 / 600	46,000 lb/hr	139	

Sorbent Circulation Element

The sorbent circulation element used in the base design requires a system of lock hoppers to transport the dolomite pneumatically between the 10 atmosphere boilers and the 1 atmosphere regenerators. Cooling of the hot sorbent is required in order to meet the temperature limitations of the system valves (V4, V10). The Petrocarb design for pressurized feeding of solids was applied (V6, V7, V3, V10). Heating of the dolomite to 1900°F before it enters the regenerator is carried out by using the hot gas from the sorbent cooler (V10) combined with the hot combustion products supplied by a coal combustor (V12). Energy from the sorbent heater is recovered in a waste heat boiler (V11). Stone for disposal is withdrawn from the hold vessels (V2). High-temperature valves and/or a dense phase transport scheme could reduce the complexity of this element.

Reducing-Gas Producer Element

A single fixed-bed type coal gasifier (V17) is used to supply reducing gas to the regenerator. The gasifier product is combusted with sufficient air in a combustor (V15) to provide the proper reducing-gas composition and temperature when it is combined with the tail gas recycle stream. Compressor (C3) provides the required air for gasification and partial combustion. Compressor (C4) handles the tail gas recycle stream. Coal storage, handling, and preparation are also accounted for.

Sulfur Recovery Element

The same sulfur recovery concept has been applied to the low-pressure one-step regeneration process as was used for the high-pressure case. The SO_2 product from the regenerator is partially reduced to H_2S by the catalytic reaction of methane. This step is followed by a three-stage Claus system.

Tail Gas Handling Element

The tail gas from the sulfur recovery plant is split into a regenerator recycle stream and an incineration stream. Blower (C5) provides the air required to incinerate the tail gas in the incinerator (V18).

CAPITAL INVESTMENT BREAKDOWN

The capital cost breakdown by elements is given in Table E-4 The costs are in 1973 dollars and do not include interest during construction or general items and engineering.

TABLE E-4

LOW-PRESSURE ONE-STEP PROCESS INVESTMENT BREAKDOWN, $/kw

Element	Process Sulfur Load		
	0.06	0.03	0.01
Regenerator Element	8.2	5.6	2.2
Sulfur Recovery Element	5.4	3.1	1.5
Tail Gas Handling Element	0.6	0.4	0.2
Dolomite Circulation Element	25.3	14.7	6.8
Gas Producer Element	8.1	4.1	2.7
TOTAL PROCESS	47.6	27.9	13.4

About 60% of the dolomite circulation element cost is for heating the dolomite prior to regeneration, waste heat recovery, and coal combustion to supply hot gas to the dolomite heater.

ENERGY COST

The energy cost contribution of the low-pressure one-step regeneration process is shown in Table E-5. Costs have been obtained on the basis:

- Interest during construction at 7-1/2%
- Capital charges at 15%
- Operating and maintenance at 5%

- 70% capacity factor
- No credit for recovered sulfur
- Coal at 45¢/MM Btu
- Methane at 80¢/MM Btu
- Dolomite at $2/ton.

The total fluid bed combustion power plant would have an energy cost of 11.3 mills/kWh, plus the regeneration process energy cost shown in Table E-5.

TABLE E-5

ENERGY COST (mills/kWh)

	Process Sulfur Load		
	0.06	0.03	0.01
Capital Charges plus O&M	1.79	1.05	0.50
Fuel Cost	0.46	0.23	0.08
Dolomite Cost	0.24	0.12	0.04
TOTAL	2.49	1.40	0.62

SENSITIVITY OF RESULTS

The sensitivity of the cost results for the low-pressure one-step regeneration process with respect to the various parameters which apply to the process are summarized in Table E-6. Numerical results in the table refer to a process sulfur load of 0.03.

PAGE NOT

AVAILABLE

DIGITALLY

F

APPENDIX F

BASE DESIGN -- TWO-STEP REGENERATION PROCESS

PROCESS DESCRIPTION

The two-step sorbent regeneration requires two fluidized bed reactors to carry out the conversion of calcium sulfate to calcium carbonate. In the first step calcium sulfate is reduced to calcium sulfide by the reaction

$$CaSO_4 + 4\begin{pmatrix} CO \\ H_2 \end{pmatrix} \rightleftarrows CaS + 4\begin{pmatrix} CO_2 \\ H_2O \end{pmatrix}$$

at about 1500°F and 10 atmospheres. The second step converts calcium sulfide to calcium carbonate by the reaction

$$CaS + H_2O + CO_2 \rightleftarrows CaCO_3 + H_2S$$

at about 1250°F and 10 atmospheres. The regenerated sorbent is recycled to the boilers while the H_2S stream is sent to a sulfur recovery plant. The two-step regeneration process provides a low-temperature route to regenerated sorbent.

Figure F-1 illustrates the elements of the two-step process. The process consists of seven elements -- the calcium sulfate reducer element, the H_2S generator element, the reducing-gas producer element, the CO_2 recovery element, the sulfur recovery element, the tail gas handling element, and the sorbent circulation element. Reducing gas for the first step sulfate reduction is provided by the reducing-gas producer element, while CO_2 for the second step calcium carbonate production is provided by recovering CO_2 from stack gas and recycled sulfur recovery tail gas. Tail gases from the calcium sulfate reducer element and the CO_2 recovery element are incinerated or recycled to the fluid bed boilers in the tail gas handling element. The sorbent circulation element carries out the function of circulating the sorbent between the fluidized boiler

Dwg 6202A67

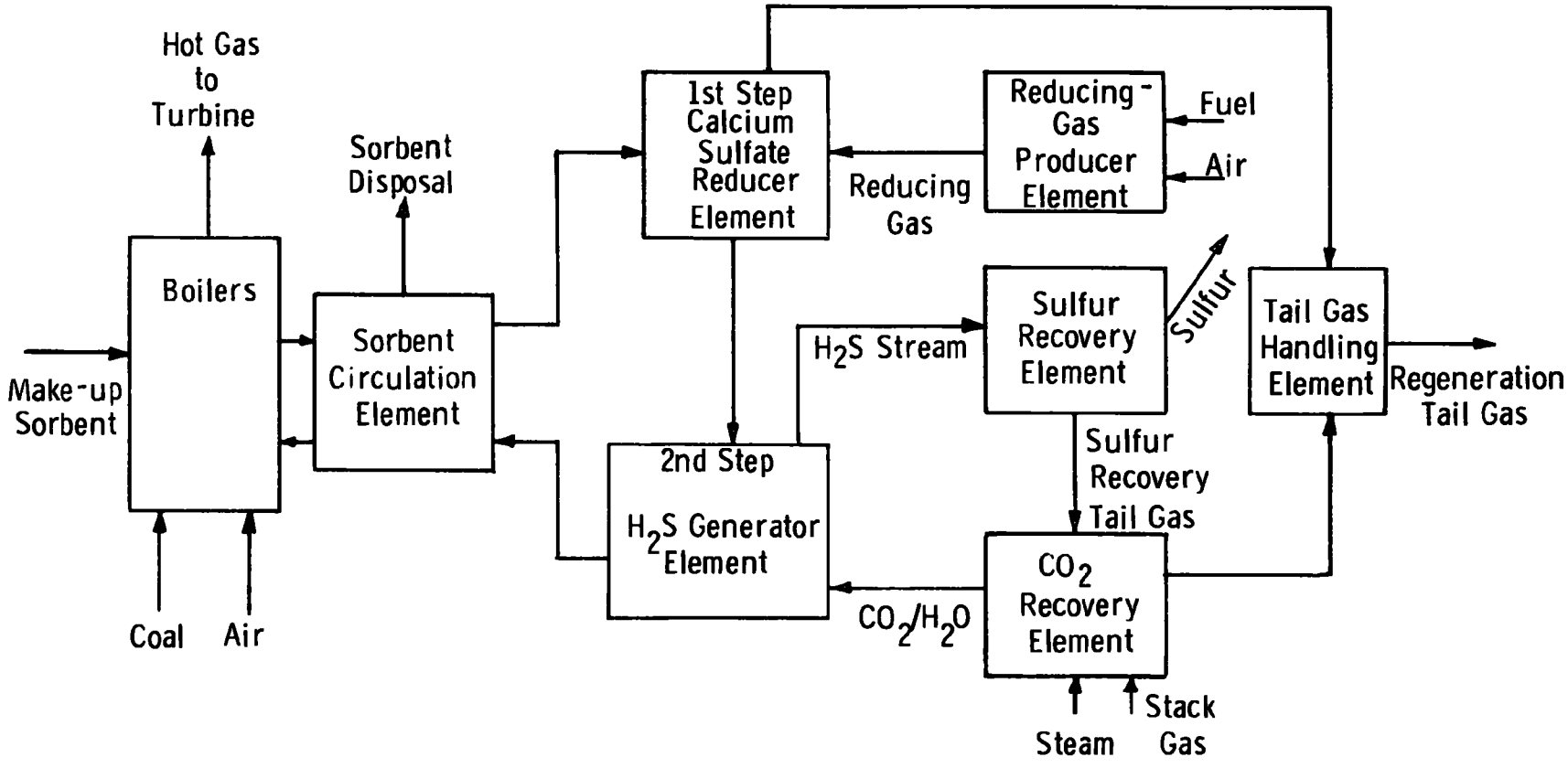

Figure F-1: Two-Step Regeneration Process Elements

and the regeneration process. Elemental sulfur is recovered in the sulfur recovery elements.

SPECIFICATIONS AND ASSUMPTIONS

The base design for the two-step regeneration process follows from the set of specifications and assumptions shown in Tables F-1 and F-2.

TABLE F-1

DESIGN SPECIFICATIONS

Fixed coal rate	430,000 lb/hr (∿ 635 MW)
Sorbent type	dolomite
Boiler sulfur removal	95%
Variable process sulfur loads	0.01, 0.03, 0.06
Recycle of tail gas to boilers	
Recovery of elemental sulfur by Claus reaction	
Reducing-gas production from coal	
Four regenerator modules	

TABLE F-2

DESIGN SPECIFICATIONS

$CaSO_4$ reducer pressure	9 atm
$CaSO_4$ reducer temperature	1500°F
H_2S generator pressure	11 atm
H_2S generator temperature	1250°F
H_2S mole fraction	3%
$CO + H_2$ mole fraction in reducing gas	30%
Sulfur recovery efficiency	95%
Dolomite utilization in boiler	30%
$CaSO_4$ reduced in reducer vessel	100%
Dolomite utilization after H_2S generator	10%
Ash in utilized dolomite	0%

MATERIAL AND ENERGY BALANCES

Material and energy balances for the two-step process streams shown in Figure F-2 are listed in Table F-3. The process is nearly self-balanced: the steam generated by the process is sufficient to provide the required auxiliary power. Temperature control and process turndown is discussed in Appendix G.

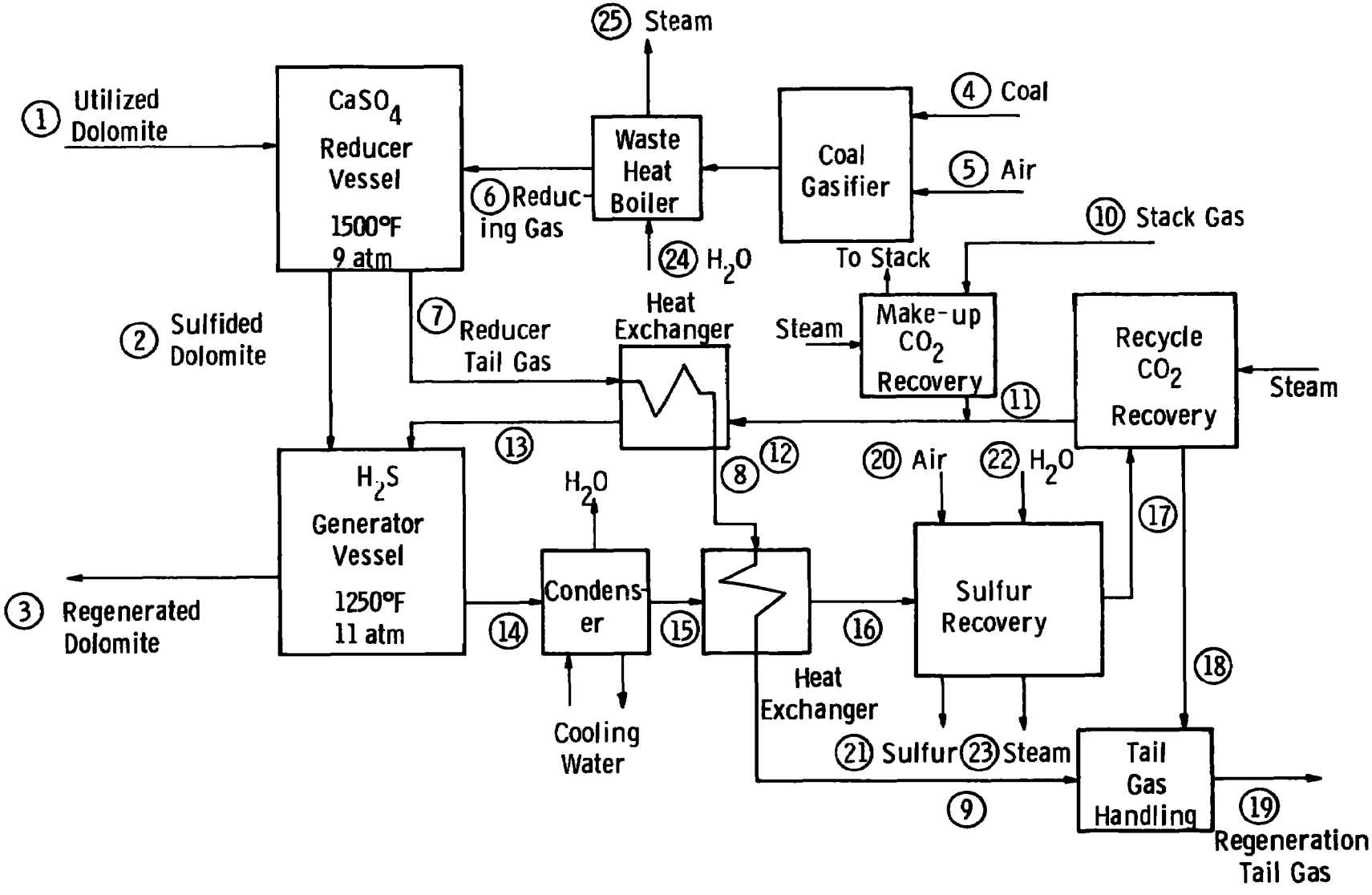

Figure F-2: Two-Step Regeneration Material and Energy Balances

TABLE F-3

TWO-STEP REGENERATION MATERIAL AND ENERGY BALANCE (Process Sulfur Load = 0.03)

Stream	Temperature, °F	Pressure, psia	Moles/Hr	Comments
1. Utilized Dolomite	1200	150	4,030 moles Ca	50% MgO, 15.0% $CaSO_4$, 35.0% $CaCO_3$
2. Sulfided Dolomite	1500	165	4,030 moles Ca	50% MgO, 15.0% CaS, 35.0% $CaCO_3$
3. Regenerated Dolomite	1250	160	4,030 moles Ca	50% MgO, 5.0% CaS, 45.0% $CaCO_3$
4. Coal	200	150	38,600 lb/hr	
5. Air	600	150	6,550	
6. Reducing Gas	1900	135	7,750	30% H_2 + CO
7. Reducer Tail Gas	1500	132	7,750	
8. Reducer Tail Gas	1100	128	7,750	
9. Reducer Tail Gas	300	124	7,750	
10. Stack Gas	300	15	7,500	16% CO_2
11. CO_2 Make-Up	600	170	2,150	50% CO_2, 50% H_2O
12. CO_2 Reactant Gas	600	170	13,800	50% CO_2, 50% H_2O
13. CO_2 Reactant Gas	710	165	13,800	50% CO_2, 50% H_2O
14. H_2S Gas	1250	160	13,400	3% H_2S
15. H_2S Gas	110	157	8,000	5% H_2S
16. H_2S Gas	850	153	8,000	5% H_2S
17. Sulfur Recovery Tail Gas	300	147	8,100	
18. CO_2 Recovery Tail Gas	400	140	1,600	
19. Regenerator Tail Gas	600	155	9,350 (to boiler)	
20. Air	600	155	650	
21. Sulfur	100	150	400	
22. Water	100	210	5.5×10^4 lb/hr	
23. Steam	saturated	200	5.5×10^4 lb/hr	
24. Water	100	2400	6×10^4 lb/hr	
25. Steam	1000	2400	6×10^4 lb/hr	

EQUIPMENT DESCRIPTION

Figure F-3 shows the major equipment items considered in the two-step process base design.

$CaSO_4$ Reducer Element

Four refractory lined pressure vessels (V5), each in series with a multistage cyclone (V7), make up the $CaSO_4$ reducer element. The reactor and cyclone design is similar to the design used in the one-step process.

H_2S Generator Element

As in the $CaSO_4$ reducer element, four pressure vessels (V6) in series with multistage cyclones (V8) comprise the H_2S generator element.

Sorbent Circulation Element

The sorbent circulation element is identical to the pneumatic transport scheme used in the high-pressure one-step regeneration process.

Reducing-Gas Producer Element

The reducing-gas producer element consists of a fixed-bed coal gasifier (V10) with a cyclone particulate control unit (V9) followed by a waste heat boiler (E4) for temperature control of the $CaSO_4$ reducer. Compressed air for partial combustion of the coal is supplied by compressor C1. The Petrocarb coal feeding system (V11) is used. Coal storage, handling, and preparation are included.

CO_2 Recovery Element

The CO_2 recovery element consists of a pair of hot carbonate CO_2 recovery processes. One process recovers CO_2 from stack gas to make up for CO_2 consumed in the H_2S generation, and the other recovers CO_2 from

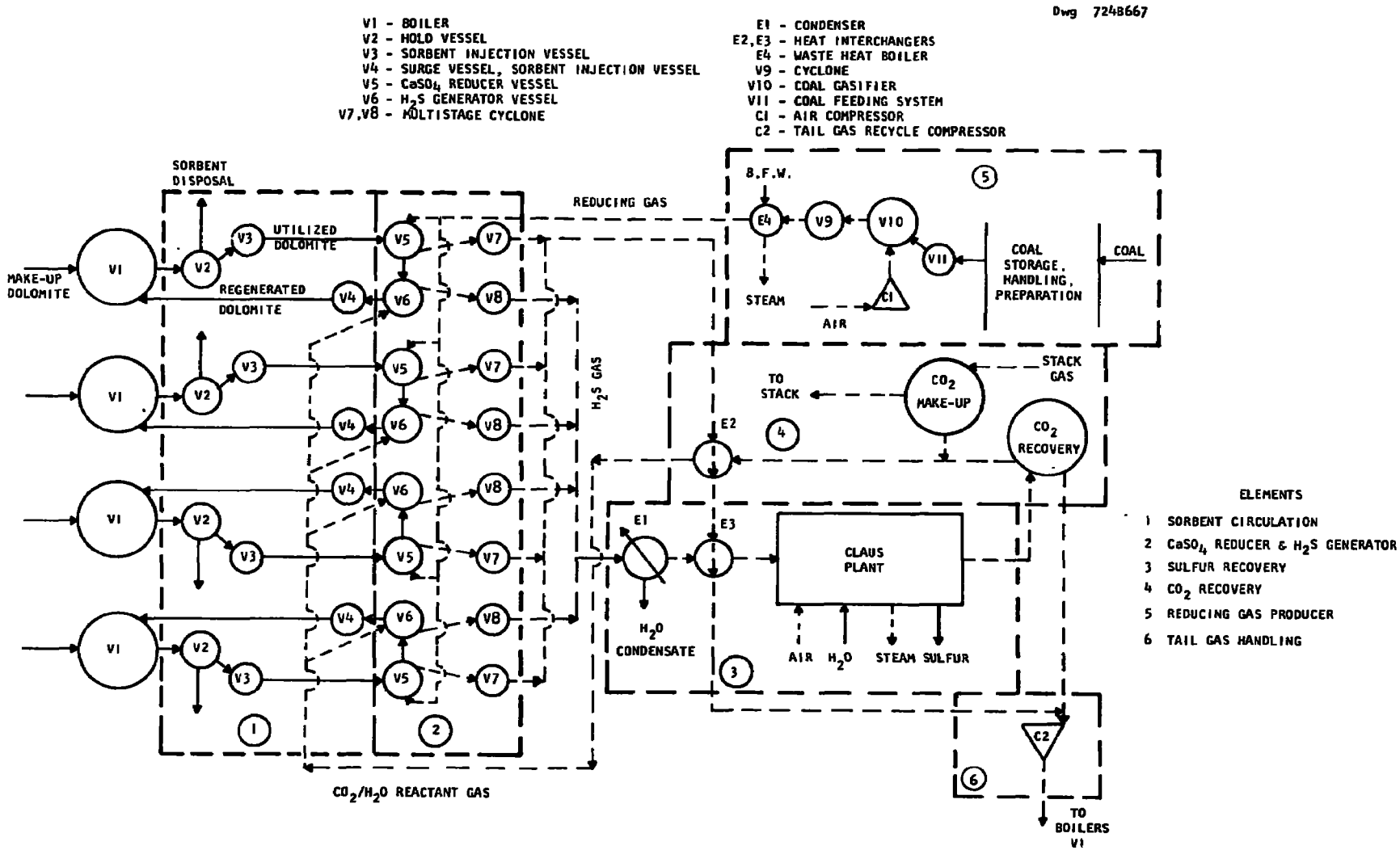

Figure F-3: Two-Step Regeneration Schematic Flow Diagram

the sulfur recovery element tail gas. The combined CO_2/H_2O stream from the two CO_2 recovery processes is heated in exchange (E2) before entering the H_2S generators.

Sulfur Recovery Element

The sulfur recovery element recovers elemental sulfur from the H_2S stream in a Claus plant. The H_2S stream from the H_2S generator element is cooled to condense out excess water in exchange (E1) and preheated before entering the Claus plant in exchanger (E3).

Tail Gas Handling Element

The process tail gas is recycled to the fluid bed boilers by means of compressor (C2). No boiler modifications have been assumed.

CAPITAL INVESTMENT BREAKDOWN

Table F-4 gives the capital investment for the two-step regeneration process broken down by element. The investments are given in $/kw based on 635 MW of total plant capacity.

TABLE F-4

TWO-STEP PROCESS INVESTMENT BREAKDOWN

Element	Process Sulfur Load		
	0.06	0.03	0.01
Reducing Gas Producer	39.2	22.8	9.7
$CaSO_4$ Reducer	2.4	1.6	0.9
H_2S Generator	2.9	2.0	1.1
Dolomite Circulation	4.3	2.6	1.0
Sulfur Recovery	9.0	5.8	2.8
Tail Gas Handling	0.9	0.6	0.3
CO_2 Recovery	18.0	10.6	5.2
TOTAL PROCESS	76.7	46.0	21.0

ENERGY COST

The energy cost for the two-step process has been computed on the same basis as the other regeneration processes examined. The breakdown is shown in Table F-5.

TABLE F-5

ENERGY COST (mills/kWh)

Cost	Process Sulfur Load 0.06	0.03	0.01
Capital Charges plus O&M	2.88	1.72	0.80
Fuel Cost	0.73	0.37	0.12
Dolomite Cost	0.24	0.12	0.04
TOTAL	3.85	2.21	0.96

SENSITIVITY OF RESULTS

The sensitivity of the cost results for the two-step regeneration process is similar to the high-pressure one-step process behavior. The most important variables in the two-step process are the H_2S concentration in the H_2S generator product stream and the change in dolomite utilization, $X_S^B - X_S^R$. Other variables have a secondary effect.

G

APPENDIX G

TEMPERATURE CONTROL AND PROCESS TURNDOWN

TEMPERATURE CONTROL -- ONE-STEP PROCESS

Temperature control of the one-step regeneration process is accomplished by adjustment of the air/fuel ratio in the gas producer element and adjustment of the rate of sulfur recovery element tail gas recycle to the regenerator. In addition to providing the proper regenerator temperature, the gas producer air/fuel ratio and the tail gas recycle stream must provide the proper $CO + H_2$ concentration in the regenerator reactant gas stream. The regenerator energy balance is sensitive to the dolomite circulation rate, the dolomite inlet temperature, the SO_2 mole fraction in the regenerator product stream, and the regenerator temperature.

Figures G-1 and G-2 represent the effects of the dolomite circulation rate, the dolomite utilization, and the dolomite inlet temperature on the regenerator heat load. The change in the sorbent enthalpy across the regenerator is shown as a function of the change in the sorbent utilization, $X_S^B - X_S^R$, for dolomite utilizations in the boiler of 0.5, 0.3, and 0.15. Curves for inlet dolomite temperatures of 200 to 1900°F are shown. Figure G-1 represents a bed temperature of 2000°F and G-2 represents a 1900°F regenerator temperature. Figures G-3 and G-4 show the case of limestone as a sorbent rather than dolomite.

Figure G-5 represents the enthalpy of the regenerator product gas as a function of the SO_2 mole fraction. Curves for a regenerator temperature of 1900°F and 2000°F are shown. The total heat to be supplied by the gas producer element is then the sum of the regenerator product enthalpy, the change in the enthalpy of the sorbent stream, and the heat of the regenerator reaction (3.47 M Btu/lb sulfur converted if no CaS is formed).

Figures G-6, G-7 and G-8 indicate some gas producer operating characteristics as a function of the regenerator heat requirement.

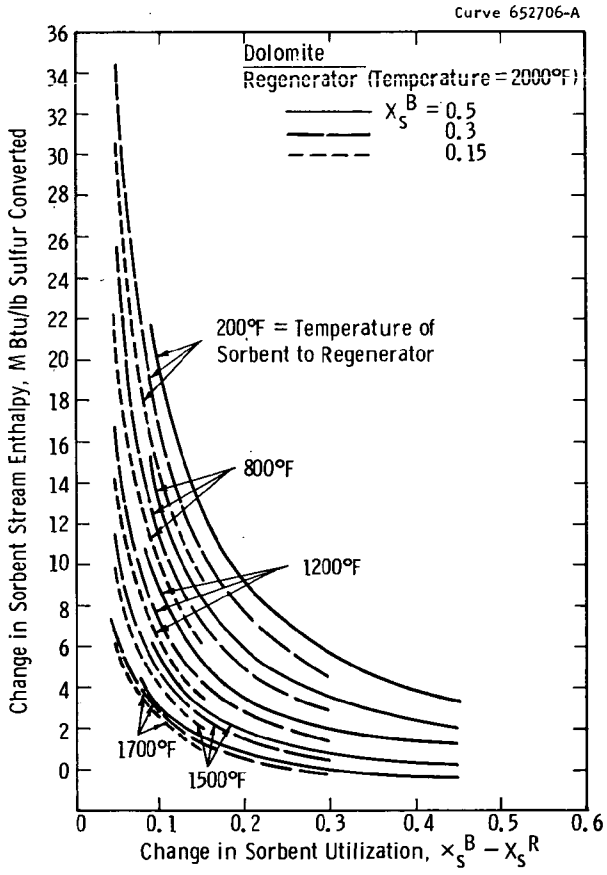

Figure G-1: Dolomite Circulation Effect on Temperature Control — 2000°F Regenerator

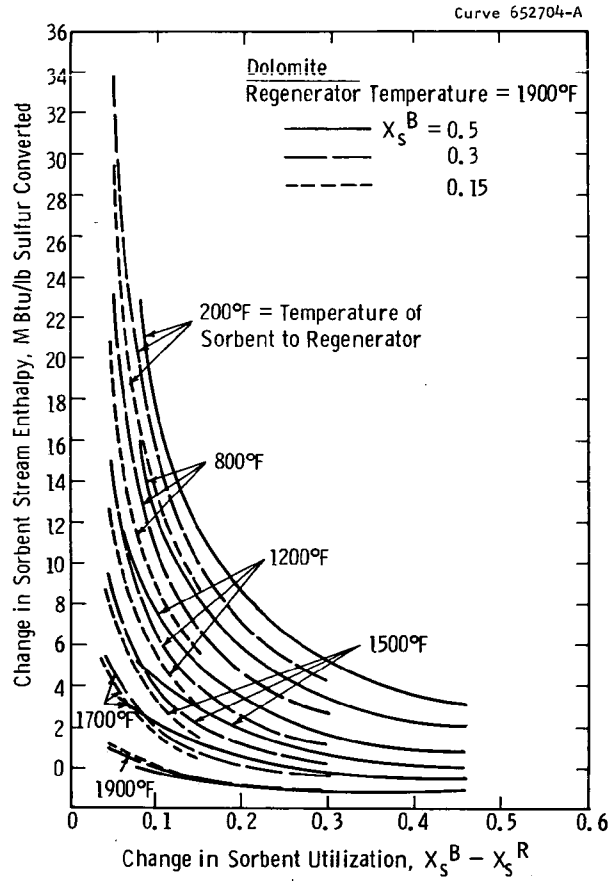

Figure G-2: Dolomite Circulation Effect on Temperature Control — 1900°F Regenerator

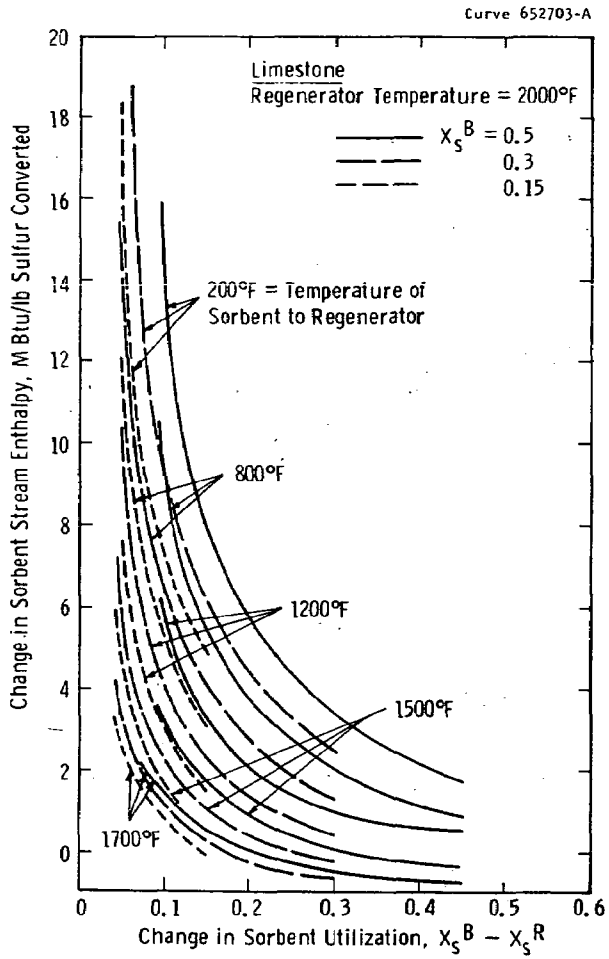

Figure G-3: Limestone Circulation Effect on Temperature Control – 2000°F Regenerator

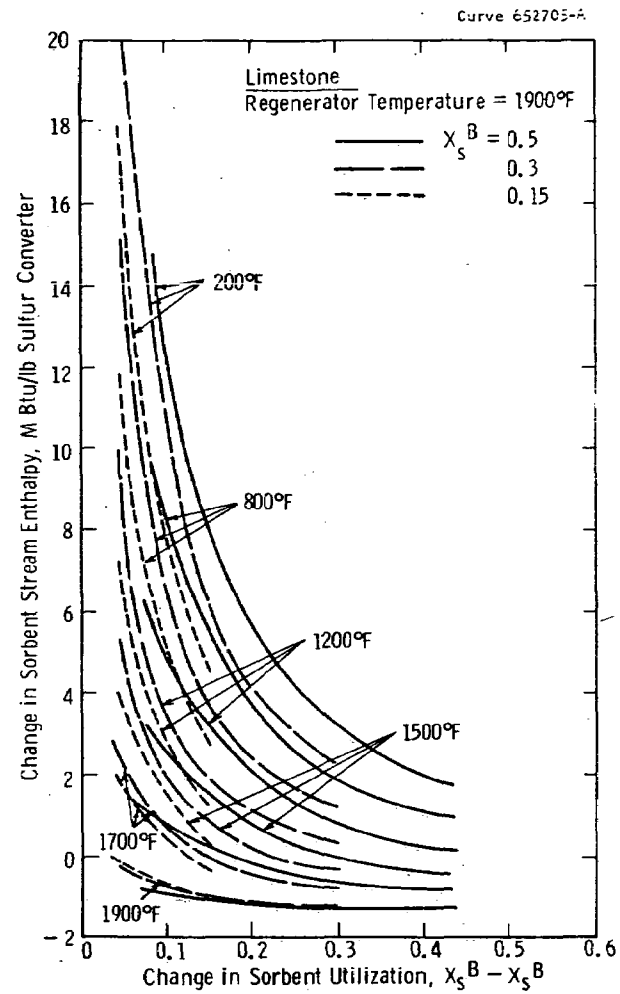

Figure G-4: Limestone Circulation Effect on Temperature Control – 1900°F Regenerator

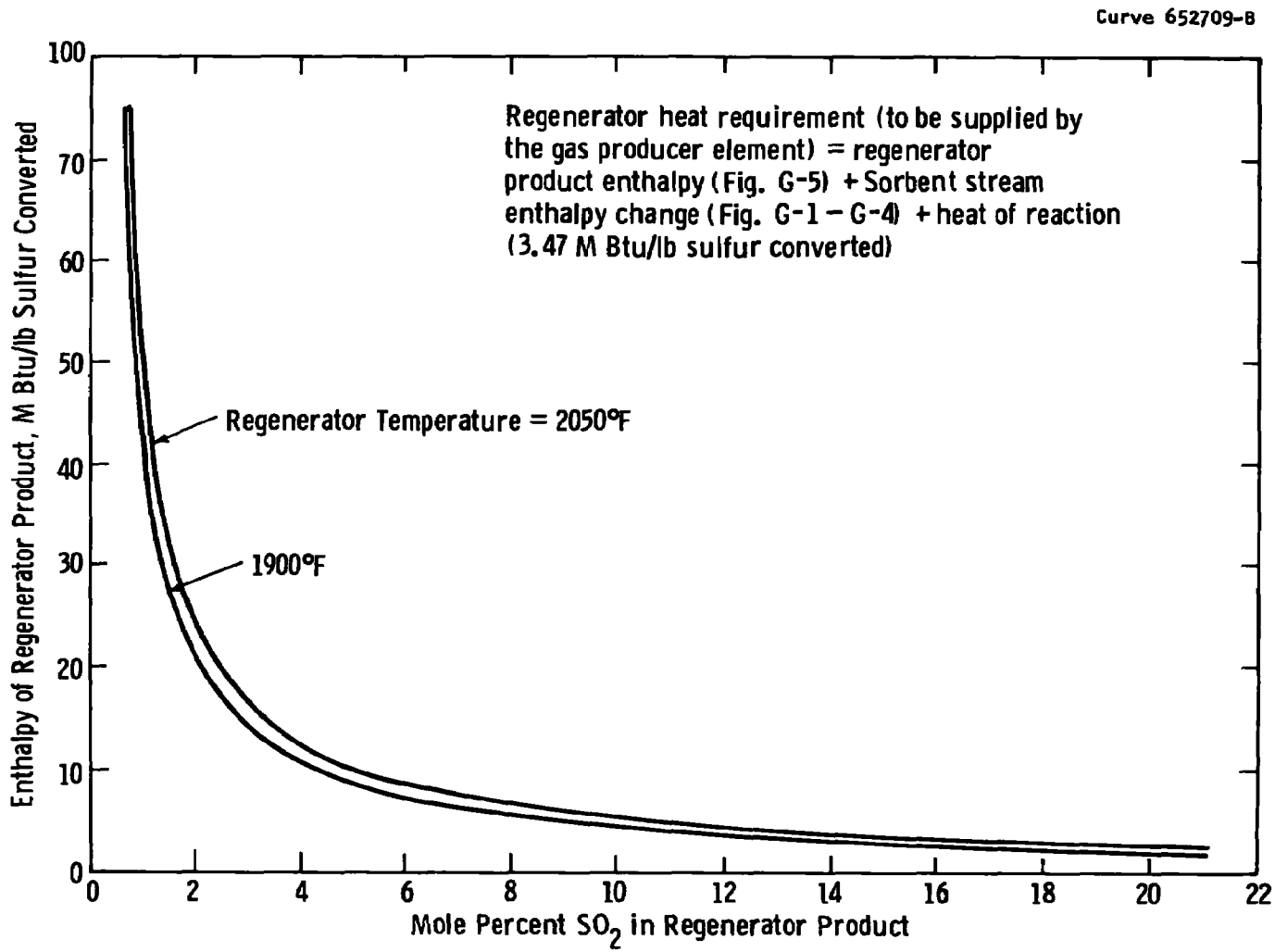

Figure G-5: Enthalpy of Regenerator Product Gas

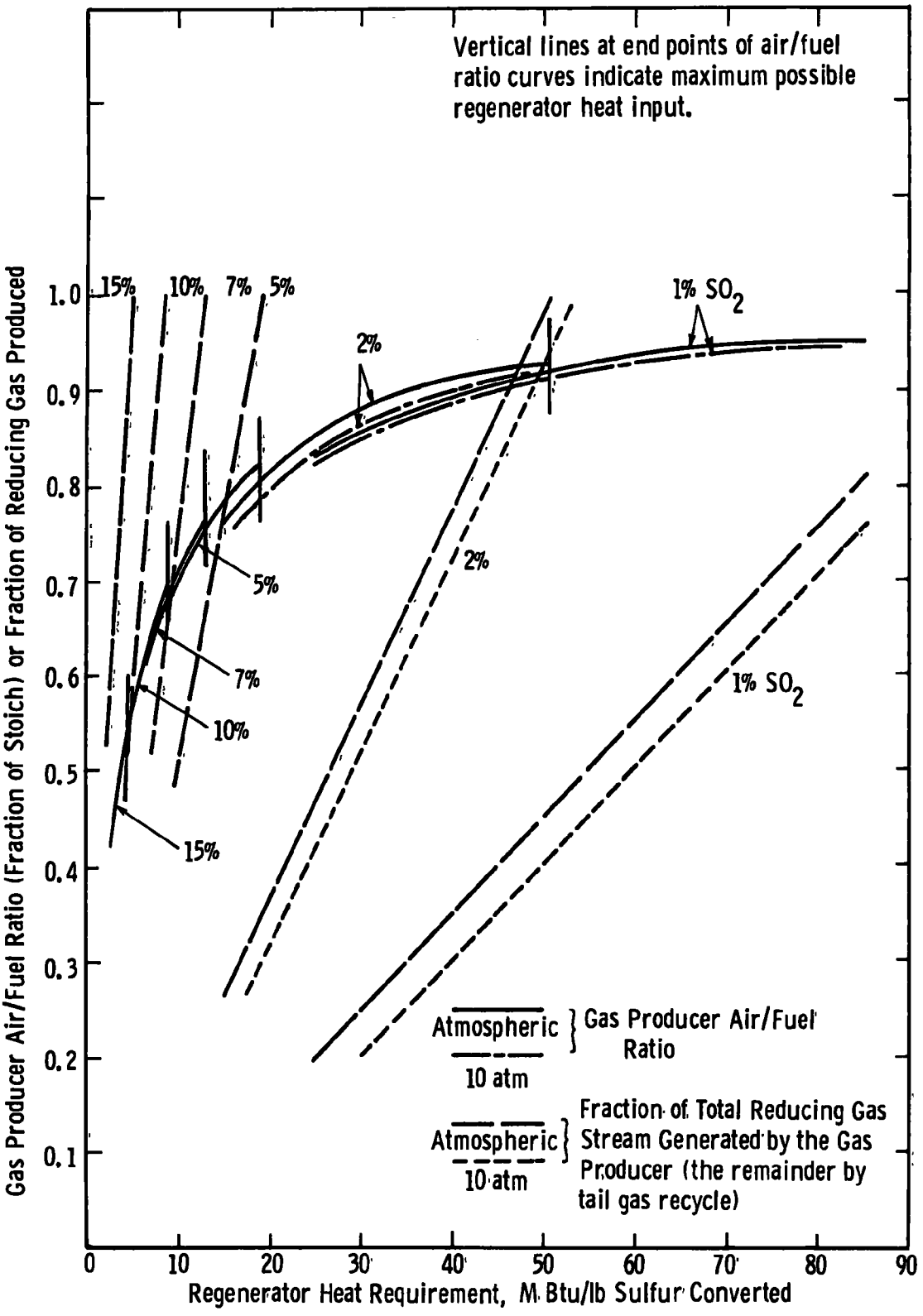

Figure G-6: Gas Producer Characteristics

Figure G-6 shows the gas producer air/fuel ratio (fraction of stoichiometric) and the fraction of the total reducing gas stream which is produced by the gas producer (the remainder being recycled from the sulfur recovery element) as a function of the regenerator heat requirement. Curves of constant SO_2 mole fractions of 1, 2, 5, 7, 10, and 15% are shown with pressures of 1 and 10 atmospheres. The maximum feasible heat requirement for each of the SO_2 mole fractions is also indicated. A general assessment of the figures (G-1 to G-6) indicates that SO_2 mole fractions greater than about 15% will not be feasible under most operating conditions. The only alternatives in order to achieve SO_2 mole fractions greater than 15% would be to heat the incoming sorbent to a high temperature (> 2000°F) or to provide heat transfer surface for heating the vessel, but these alternatives are probably not feasible.

Figure G-7 shows the fuel required to maintain the regenerator temperature and provide the proper reducing gas as a function of the regenerator heat requirement. The amount of fuel (coal) is expressed as the fraction of the boiler fuel input divided by the process sulfur load. Curves of constant SO_2 mole fraction (1, 2, 5, 10, and 15%) are shown with regenerator pressures of 1 and 10 atmospheres.

Figure G-8 shows the temperature of the regenerator reducing gas as a function of the regenerator heat requirement. Curves of constant SO_2 mole fraction are shown.

Figures G-7 and G-8 with Figures G-1 to G-6 indicate that lower SO_2 mole fractions require higher fuel requirements and thus lower plant efficiencies, while higher SO_2 mole fractions require higher reducing-gas temperatures and thus more severe design conditions. For this reason the 1 atmosphere one-step process is operated with a regenerator temperature of 1900°F and with preheat of the inlet dolomite to 1900°F. Temperature control of the high-pressure (low SO_2 mole fraction) process is simpler than that of the low-pressure (high SO_2 mole fraction) process.

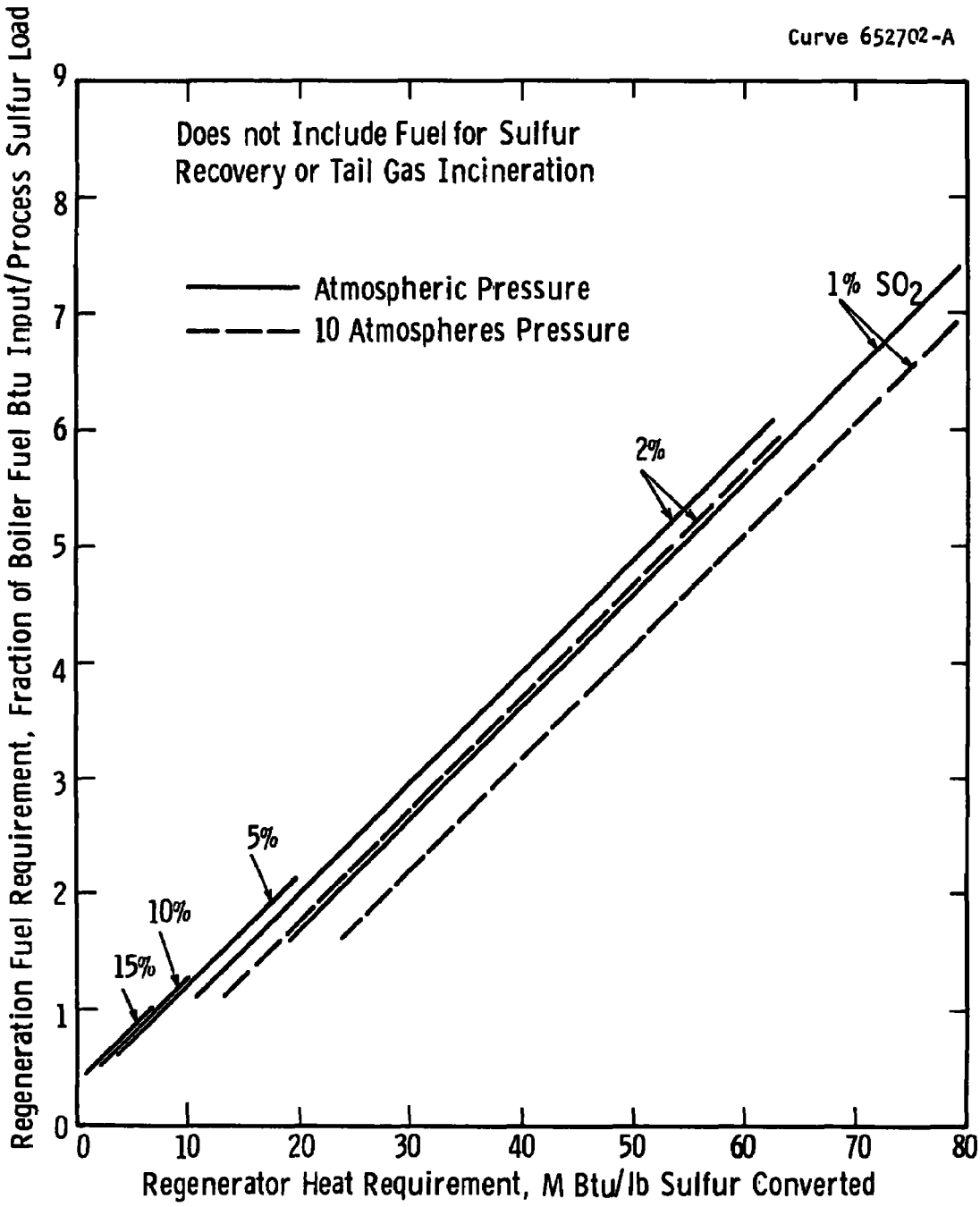

Figure G-7: Gas Producer Fuel Requirement

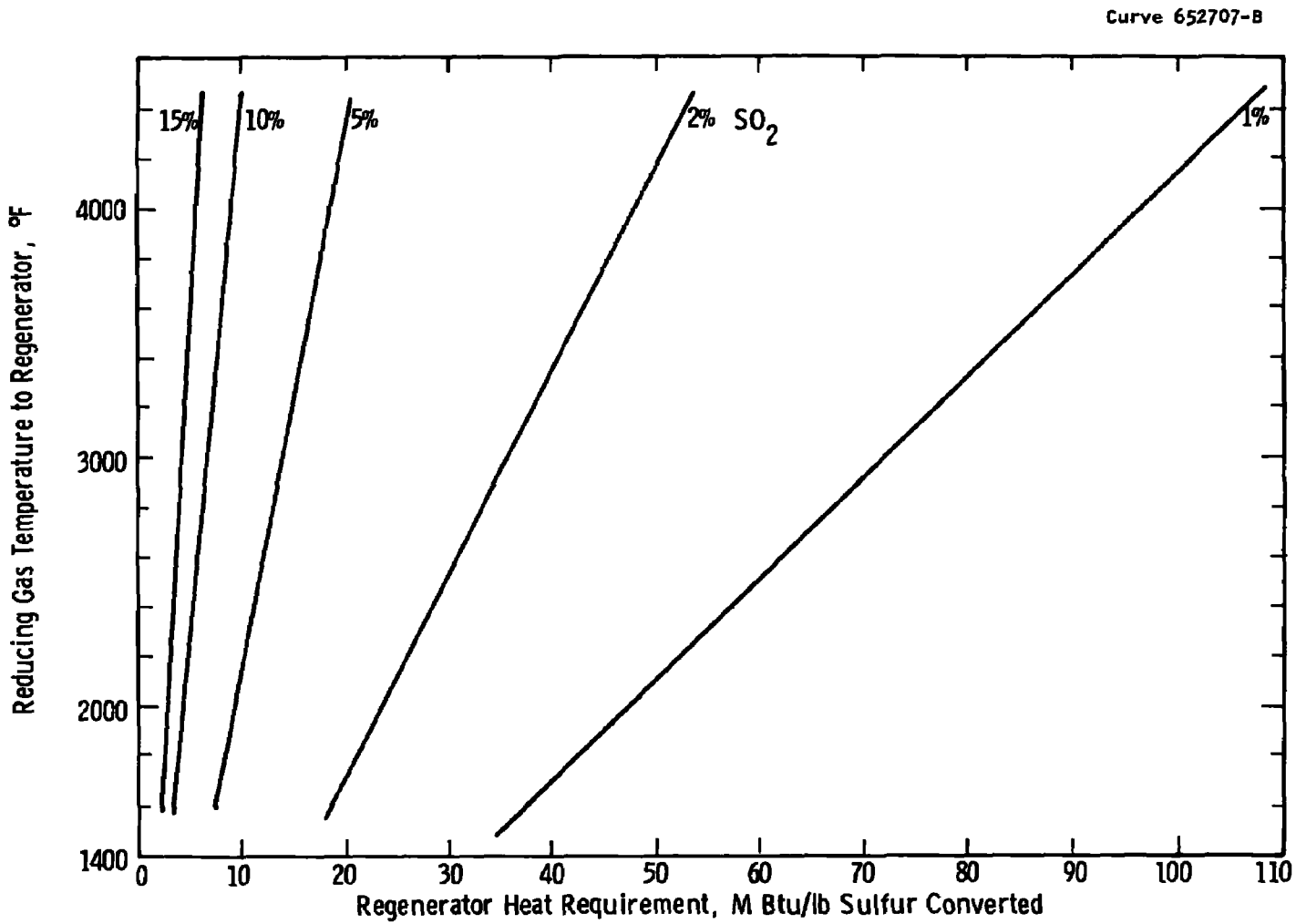

Figure G-8: Reducing-Gas Temperature

TEMPERATURE CONTROL -- TWO-STEP PROCESS

The two-step regeneration process is a low-temperature process (when compared to the one-step process). As such, the complications in dealing with extremely high-temperature gas streams, which exist in the one-step regeneration process, are not important considerations in the two-step process. The temperatures of the $CaSO_4$ reducer and the H_2S generator should be controllable by using waste heat boilers and heat exchangers to regulate the temperature of the reducing gas and the CO_2/H_2O reactant gas. Because process temperature control appears feasible with the two-step process, detailed parametric studies, as were performed for the one-step process, have not been carried out.

PROCESS TURNDOWN -- ONE-STEP PROCESS

Various possibilities exist for changing the regeneration process load in response to a change in the boiler load. It is assumed that the SO_2 mole fraction in the regenerator product should remain nearly constant at all loads in order to maintain the performance of the sulfur recovery element. In the interest of simplifying the control system and the design of the sorbent circulation element, it is assumed that the sorbent circulation rate should be constant for all loads. Then, the only way to keep the SO_2 mole fraction constant during turndown is to reduce the fluidization velocity in proportion to the load, or to maintain a constant fluidization velocity and adjust the regenerator pressure and temperature with the load change in order to achieve a constant SO_2 mole fraction. The latter option is much too complex, so the option of fluidization velocity reduction has been chosen. In order to maintain fluidization of the regenerator during turndown, multiple vessels are required. Four regenerator vessels have been specified in the base designs, though two may be sufficient.

Since the sorbent circulation rate is constant during turndown and the reducing-gas volume flow rate is being reduced with reduced load, the temperature of the reducing gas must increase with reduced load to

maintain the regenerator temperature. This behavior is demonstrated in Figure G-9. The reducing-gas temperature is shown as a function of the percent turndown. Curves of constant SO_2 mole fraction are shown. The extent of temperature increase is seen to become a greater problem with the case of high-SO_2 concentrations than it is for the low-concentration cases. With four regenerator modules the percent turndown of each vessel need not exceed 50 percent, so the high temperature problem is reduced.

The four-module concept allows each of the four boiler modules to be coupled with a single regenerator module so that the regenerator module can follow the load of the individual boiler module.

PROCESS TURNDOWN -- TWO-STEP PROCESS

Due to the low temperature of the two-step regeneration process the power plant load follow using a fixed sorbent circulation rate should be accomplished without the high-temperature complications found in the one-step process. Using four modules, the $CaSO_4$ generator and H_2S generator performance should easily be maintained during turndown. Fewer modules could be considered. The two-step process turndown has not been studied in detail.

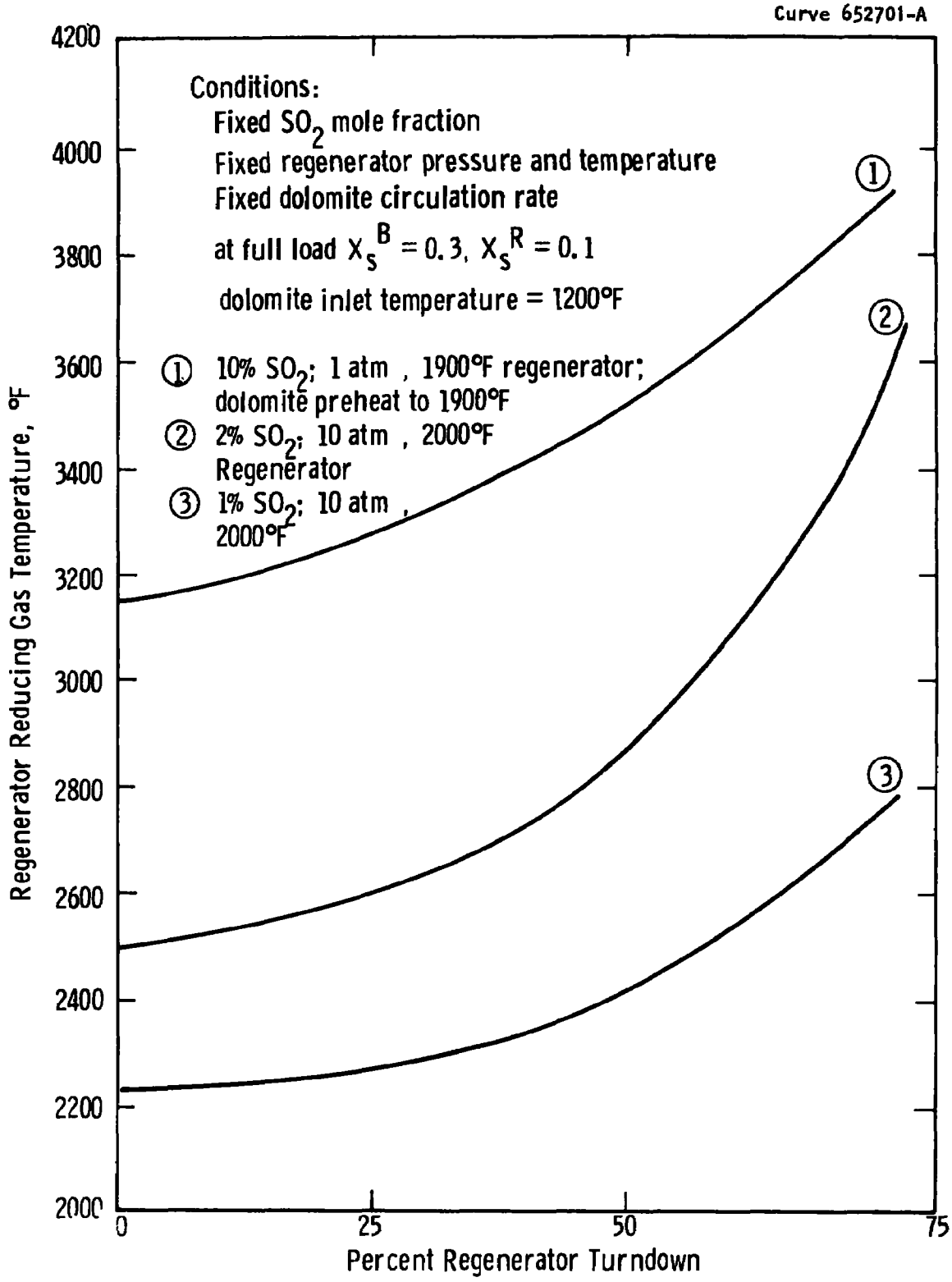

Figure G-9: One-Step Process Turndown

H

APPENDIX H

EFFECT OF BOILER CONDITIONS ON REGENERATION PROCESS COST

CARBONATING BOILER CONDITIONS -- ONE-STEP PROCESS

If the conditions in the fluid bed boilers (temperature, pressure, CO_2 concentration) are such that the dolomite in the bed is in the carbonated form ($MgO \cdot CaCO_3$), then the base design and cost for the high-pressure and low-pressure one-step regeneration processes must be reevaluated. Because the one-step regenerator operating conditions will always lead to calcination of the dolomite, and because the endothermic nature of the calcination reaction would not permit simultaneous maintenance of the regenerator temperature and the SO_2 mole fraction, the process must be altered to a form such as is shown in Figure H-1. In the flow diagram sufficient coal to calcine the dolomite and heat it to 1900°F in a separate fluidized calcining vessel is combusted in a slagging coal combustor. The remainder of the 430,000 lb/hr coal feed is fed to the fluidized bed boilers, along with the hot combustion gases from the calcining vessel. Air from the main combustion air compressor must be boosted about 2 atmospheres for combustion in the slagging combustor.

At the base design dolomite circulation rate, the coal rate needed for 100% calcination of the dolomite corresponds to 80% of the total plant coal rate with a process sulfur load of 0.06. The alteration to the base design is then extremely large. Table H-1 estimates the increase in the capital investment and the energy cost above the base design for the high-pressure and low-pressure one-step processes. The process sulfur load and the percent recarbonation in the fluid bed boilers are parameters in the table. The specification and cost basis used in Table H-1 are identical to those used in the base costs.

Even if carbonating conditions do not exist in the boilers during full load, the change in boiler conditions during turndown may lead to carbonation of the sorbent. This is a critical point to

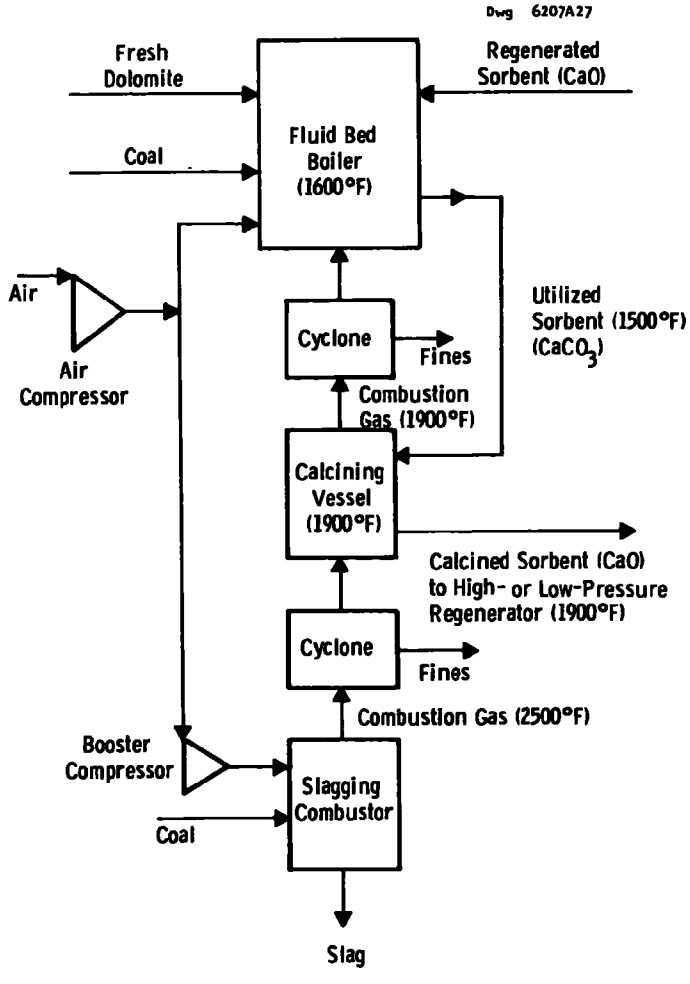

Figure H-1: Carbonating Boiler Combination Flow Diagram

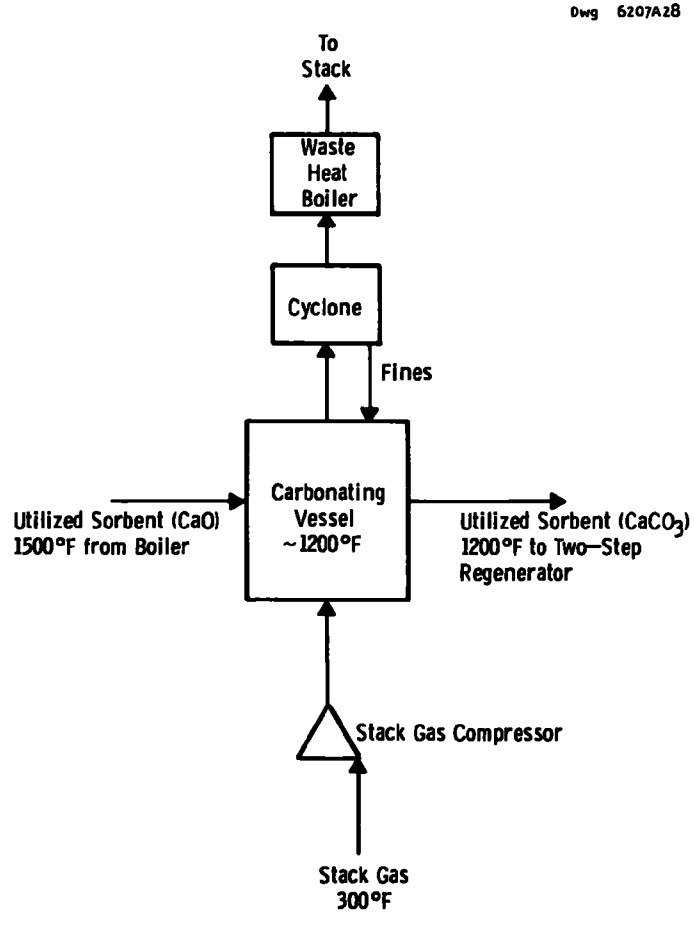

Figure H-2: Calcining Boiler Conditions Flow Diagram

TABLE H-1

COST INCREASE FOR CARBONATING BOILER CONDITIONS - HIGH-PRESSURE AND LOW-PRESSURE REGENERATION PROCESSES

Process Sulfur Load	Increase in Capital Investment, $/kW		Increase in Energy Cost, mills/kWh	
	100% Recarbonation	50% Recarbonation	100% Recarbonation	50% Recarbonation
0.01	13.5	9.0	0.45	0.30
0.03	29.0	19.5	0.86	0.57
0.06	46.0	30.0	1.35	0.90

consider in the process design. In addition to the large cost increase in the low pressure and high-pressure one-step regeneration processes if carbonation takes place in the boiler, the drastic increase in the process complexity must also be acknowledged.

The costs in Table H-1 are extremely sensitive to the dolomite circulation rate, in addition to the process sulfur load and the percent recarbonation. The process cost increase should change with the circulation rate in exactly the same manner as it changes with the process sulfur load. Low circulating rates, or identically high $X_S^B - X_S^R$, are advantageous in all cases.

CALCINING BOILER CONDITIONS -- TWO-STEP PROCESS

If the conditions in the fluid bed boilers are such that the dolomite in the bed is in the calcined form (MgO · CaO) then the base design and cost of the two-step regeneration process must be re-evaluated. The conditions in the two-step regeneration process will always lead to carbonation of the dolomite, and, because of the highly exothermic nature of the carbonation reaction and the large quantity of CO_2 consumed, temperature control of the H_2S generator would not be feasible. Carbonation of the dolomite must be carried out before the regeneration process in a separate vessel.

Figure H-2 shows the major equipment required to carry out the carbonation step using stack gas as the CO_2 source. Stack gas compressed to 10 atmospheres is reacted directly with the utilized dolomite in a fluidized bed at about 1200°F. The 1200°F gas produced is cleaned in a cyclone and then cooled in a waste heat boiler to recover some useful energy. Table H-2 estimates the increase in the process capital investment and energy cost above the base case cost for 100% and 50% recalcination of the dolomite in the fluid bed boilers. The costs in Table H-2 are extremely sensitive to the dolomite circulation rate, which has been assumed to be the base circulation rate.

TABLE H-2

COST INCREASE FOR CALCINING BOILER CONDITIONS
TWO-STEP PROCESS

Process Sulfur Load	Increase in Capital Investment, $/kw		Increase in Energy Cost, mills/kWh	
	100% Recalcination	50% Recalcination	100% Recalcination	50% Recalcination
0.01	9.5	6.3	0.36	0.24
0.03	20.4	13.6	0.79	0.53
0.06	32.9	22.0	1.33	0.89

APPENDIX I

ONCE-THROUGH PROCESS

The capital investment and energy cost of pressurized fluid bed combustion with once-through utilization of the sulfur sorbent (dolomite or limestone) has been estimated. The parameters involved in the once-through estimate are the weight fraction of sulfur in the coal, Ws, the sulfur removal efficiency in the boiler, ε, the sorbent feed rate to the boiler, moles Ca/mole sulfur fed, m, the sorbent purchase plus disposal cost, $/ton, and the boiler conditions -- calcination or carbonation.

The cost of the regenerative boiler system has been previously estimated.[1] The once-through boiler system consists of the same components -- sorbent storage and handling, sorbent feeding, and sorbent disposal -- designed for higher sorbent rates. The once-through process excludes the cost of sorbent regeneration and circulation. The cost in $/kw for sorbent storage and handling, sorbent feeding, and sorbent disposal are estimated in Figure I-1, based on 635 MW of plant output. The costs shown do not include interest during construction or general items and engineering.

The true investment expressed as $/kw depends on the energy lost in heating the sorbent and calcining the sorbent. With a base cost of $226.62/kw for a once-through process excluding sorbent storage, handling, feeding, and disposal the total plant investment is, in $/kw,

$$[226.62 + \text{Cost of Sorbent System}] \quad 1.13 + 5.5$$

based on 635 MW plant output. This cost is corrected by an efficiency loss term which for dolomite is

$$[0.9938 - 0.286\ W_s m]^{-1}$$

with calcination of the dolomite in a boiler operated at 1750°F, or

$$[0.9959 - 0.0955\ W_s m]^{-1}$$

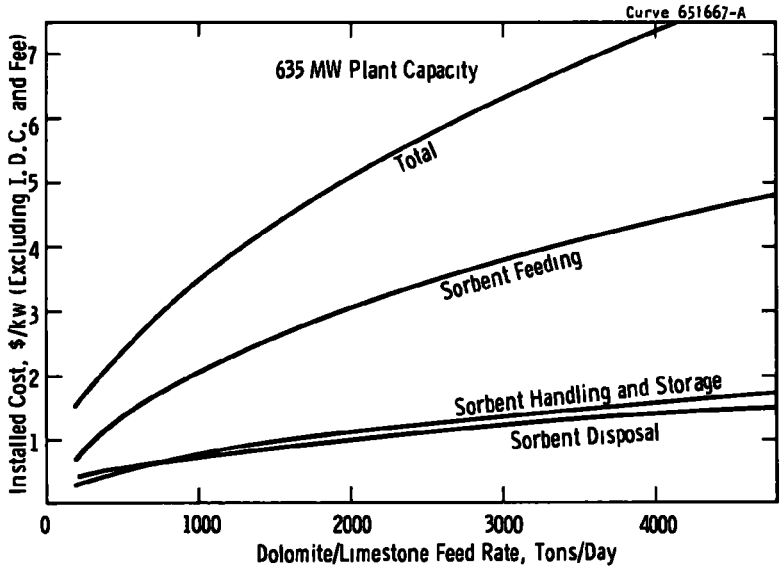

Figure I-1· Sorbent Handling and Feeding Costs

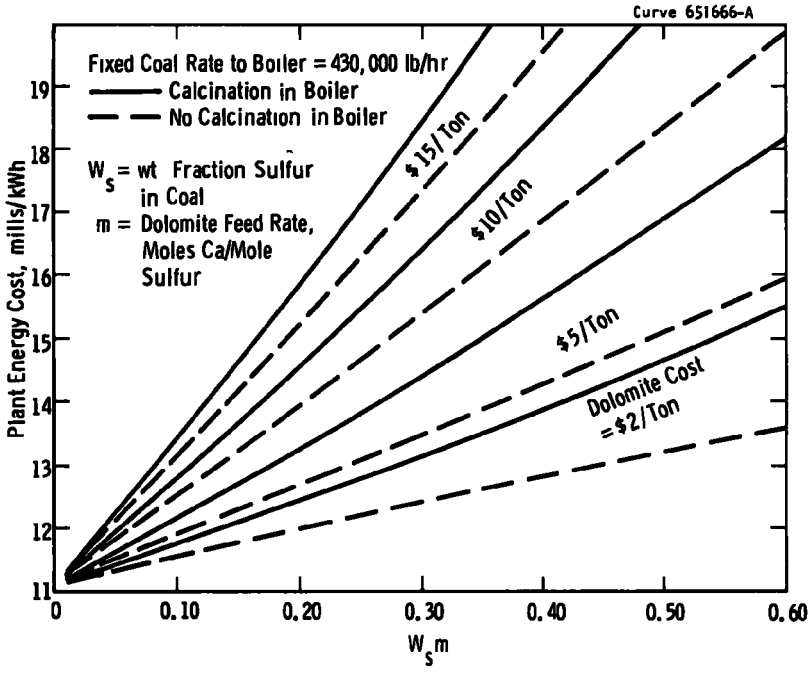

Figure I-2: Once-through Energy Cost

with no calcination of the dolomite in a boiler operated at 1750°F. The correction can be substantial for large dolomite rates.

The plant energy cost is computed using the basis previously applied. The purchase plus disposal cost of dolomite is used as a parameter having values of 2, 5, 10, and 15 $/ton. Again, the energy cost, in mills/kWh, has been corrected to reflect energy losses associated with the sensible heat of the discarded dolomite and the calcination of the sorbent. Figure I-2 shows the energy cost results for a fixed coal feed rate of 430,000 lb/hr. Note that the single variable $W_s m$ is sufficient to account for all once-through conditions, independent of sulfur removal efficiency. The variable $W_s m$ is shown for values as large as 0.60 which would correspond to, for instance, a coal containing 6 wt % sulfur requiring a dolomite feed rate of 10 mole Ca/mole sulfur. This extreme case appears to be an upper limit which would never be approached. A more realistic value of the variable would be 0.08 corresponding to a sulfur content of 4 wt % and m = 2 (calcium utilization of 45% for 90% sulfur removal). Even lower values seem probable.

The energy cost results in Figure I-2 indicate that once-through operation with high-sulfur coals and with calcium utilizations of 50% or better will yield cost advantages over regenerative operation or a conventional coal-fired power plant using limestone wet scrubbing even for dolomite costs of $15/ton.

J

APPENDIX J

CONSTANT LOAD CONCEPT

The major equipment required for the constant load concept is shown in Figure J-1 for the cases of the 1 atmosphere one-step regeneration process and the two 10 atmosphere regeneration processes. The equipment consists of circulation elements, storage vessels, sorbent heaters and coolers, and single regenerator modules rather than the multiple modules used in the variable load concept. It has been assumed that the normal load variation of the power plant is over a short time period so that a two-week storage capacity is sufficient to allow constant operation of the regeneration process. On-off control can also be used.

Table J-1 gives the capital investment for the constant load concept applied to the three regeneration processes. Figure J-2 compares the capital investment for the constant load concept and the variable load concept with the low-pressure one-step regeneration process. Because the variable load concept of the low-pressure one-step regeneration process required sorbent heaters and coolers and much of the circulation equipment shown in Figure J-1, the cost of the constant load concept is only slightly greater than that of the variable load concept. Thus, it may be advantageous from the process control standpoint to use the low-pressure one-step process as a constant load process rather than as a variable load concept.

Figure J-3 shows the comparison between the capital investment for the constant load and variable load concepts with the two high-pressure regeneration processes. The constant load concept is considerably more expensive than the variable load with these processes.

Table J-2 presents the energy cost breakdown for the three regeneration processes using the constant load concept. The energy cost for the constant load 1 atmosphere one-step regeneration process is nearly identical to the cost of the variable load concept. The energy cost of the high-pressure constant load concepts is considerably greater than that of the variable load concepts.

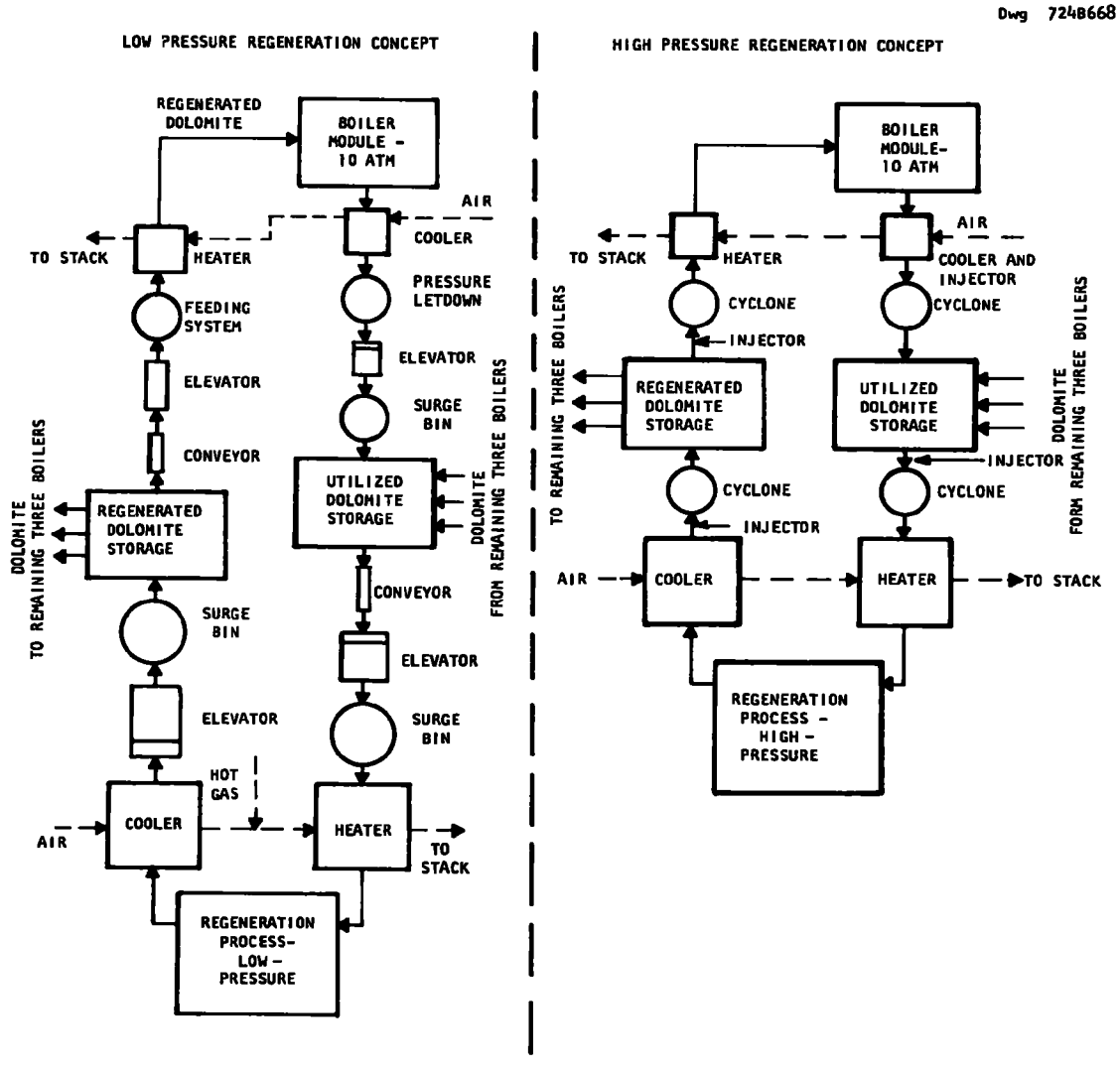

Figure J-1: Constant Load Concept Flow Diagram

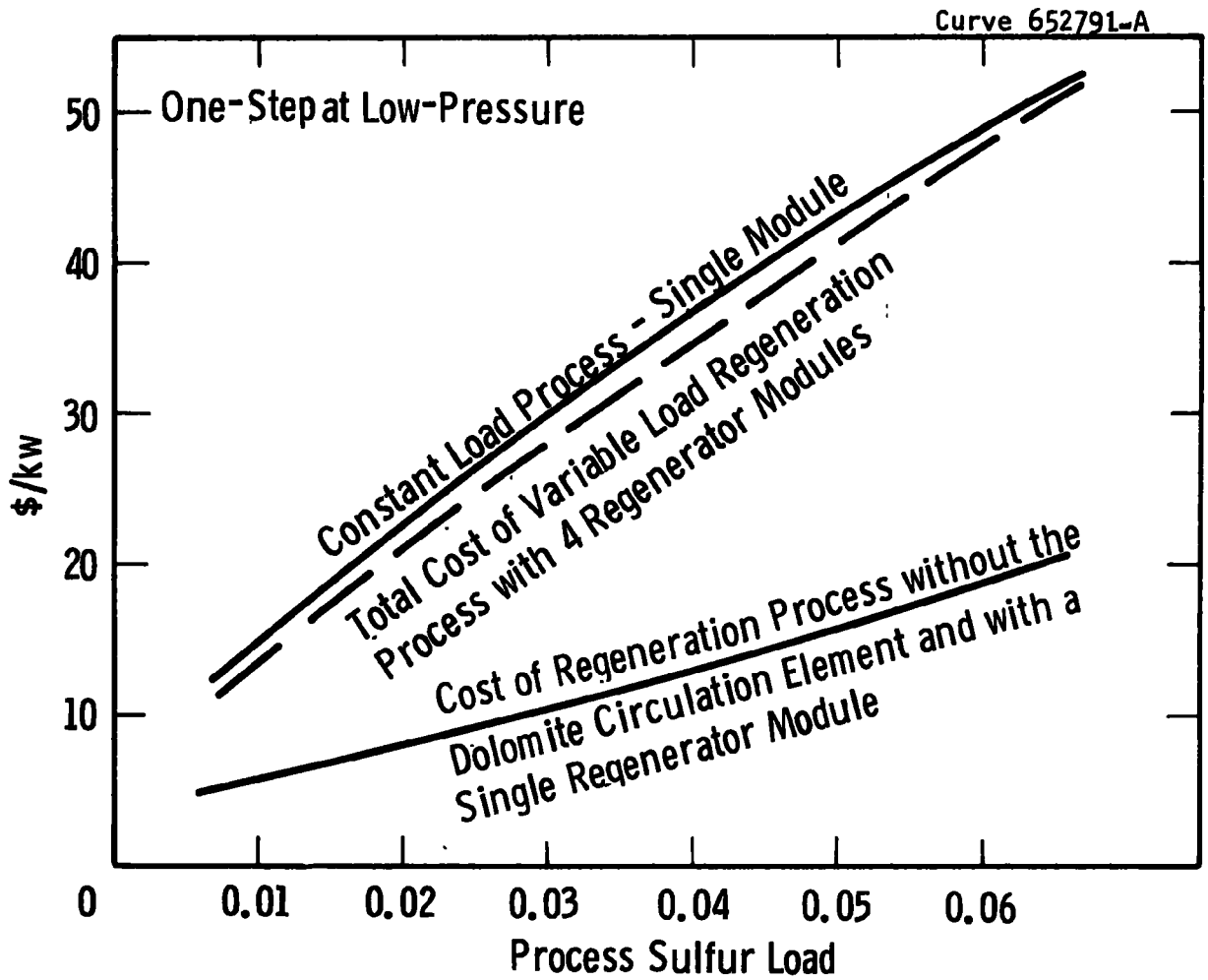

Figure J-2: Constant versus Variable Load for the Low-Pressure One-Step Process

TABLE J-1

CAPITAL INVESTMENT FOR CONSTANT LOAD CONCEPT

Process Sulfur Load	Investment, $/kw[a]			
	One-Step-1 Atm	One-Step-10 Atm		
	10% SO_2[b]	1% SO_2[c]	2% SO_2[c]	Two-Step[c]
0.01	15.1	22.1	17.6	24.2
0.03	29.9	45.8	37.5	52.9
0.06	48.9	73.4	59.0	86.8

[a] Does not include interest during constructi and fee - 635 MW(e) plant capacity, mid-1973 costs, 70% capacity factor.

[b] Incineration of process tail gas.

[c] Recycle of process tail gas to fluid bed boilers.

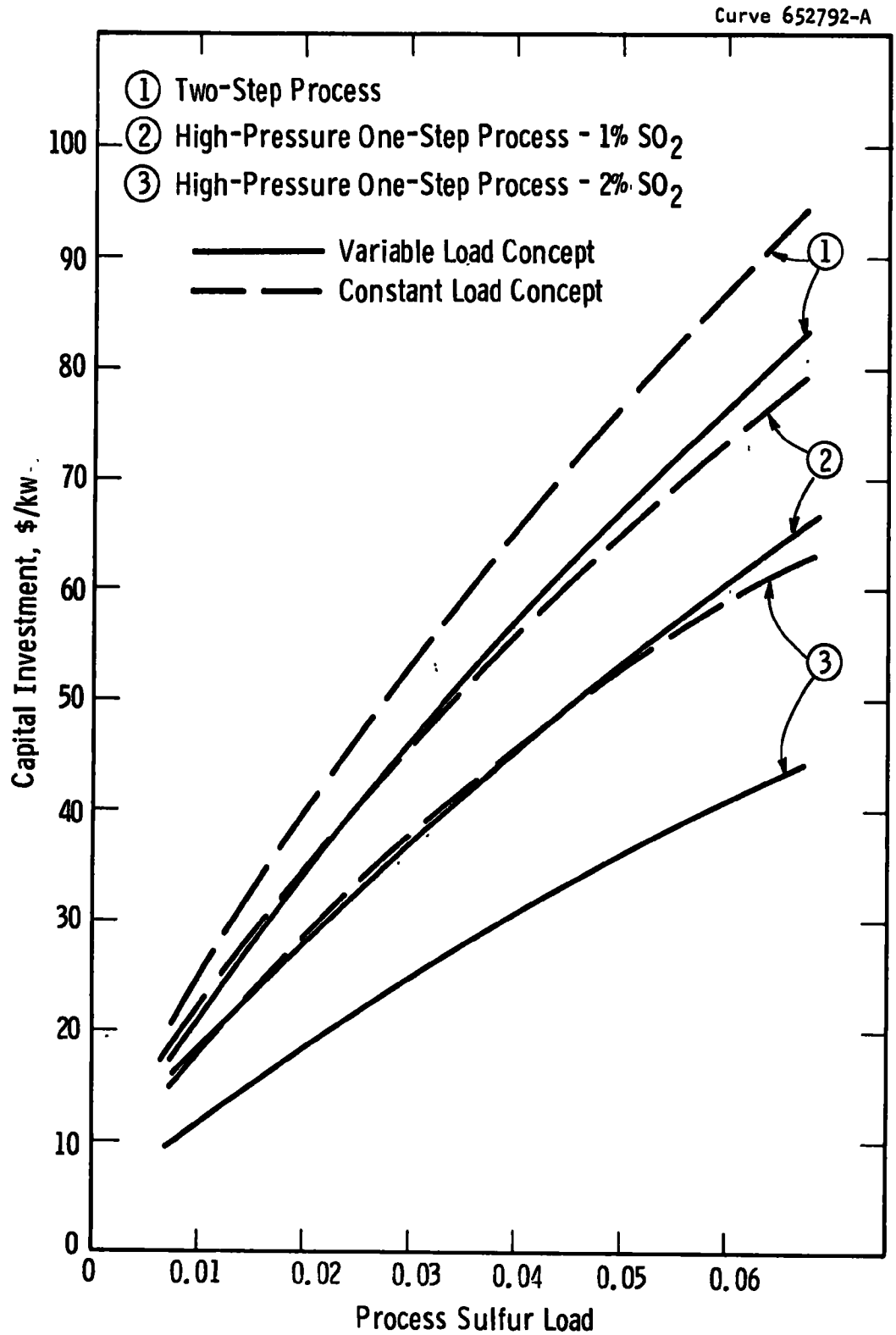

Figure J-3: Constant vs Variable Load for the High-Pressure Processes

TABLE J-2

CONSTANT LOAD CONCEPT ENERGY COSTS (mills/kWh)

Process	$W_s(-MX_s)$	Capital and O&M	Fuel	Dolomite ($2/Ton)	Total
One-Step at 1 Atm					
	0.06	1.84	0.46	0.24	2.54 + 11.30
	0.03	1.13	0.23	0.12	1.48
	0.01	0.56	0.08	0.04	0.68
One-Step at 10 Atm (1% SO_2)					
	0.06	2.75	1.30	0.24	4.29 + 11.30
	0.03	1.72	0.65	0.12	2.49
	0.01	0.83	0.22	0.04	1.09
One-Step at 10 Atm (2% SO_2)					
	0.06	2.21	0.88	0.24	3.33 + 11.30
	0.03	1.40	0.44	0.12	1.96
	0.01	0.66	0.15	0.04	0.85
Two-Step					
	0.06	3.26	0.73	0.24	4.23 + 11.30
	0.03	1.98	0.37	0.12	2.47
	0.01	0.92	0.12	0.04	1.08

K

APPENDIX K

PROCESS COMPARISONS

The costs associated with the base designs of the three regeneration processes examined are compared as a function of the process sulfur load in Figures K-1 and K-2. Figure K-1 gives the process capital investments, for both boiler carbonation and calcination conditions, for each of the processes. Figure K-2 shows the process energy costs, for a dolomite cost of $2/ton.

Figures K-2 through K-10 show the total power plant energy cost for the three regeneration processes and for the once-through dolomite operation. The costs are expressed as a function of the dolomite make-up rate, the weight fraction of sulfur in the coal, and the dolomite purchase plus disposal cost. A fixed sulfur removal efficiency of 95% in the boiler and a calcium utilization of 30% in the boiler is assumed. Figures K-3 to K-6 represent the case in which utilized dolomite is removed for disposal before the regeneration process while Figures K-7 to K-10 indicate the cost behavior for the case in which the dolomite is removed for disposal after the regeneration process. The optimum boiler condition (calcination or carbonation) is assumed for each regeneration process. The cost behavior with both calcination and carbonation conditions are shown for the once-through process.

For the case of disposal before the regeneration process (Figures K-3 to K-6) it is seen that the energy cost is reduced as the dolomite make-up rate is increased for both the $2/ton and the $5/ton dolomite. This is because the process sulfur load is reduced as the dolomite make-up rate is increased [being equal to $W_S\ (\varepsilon - mx_S^B)$], which reduces the process energy cost to a greater extent than the cost of dolomite increases the energy cost. This behavior is sensitive to the calcium utilization in the boiler, X_S^B, but is not present for the case of disposal

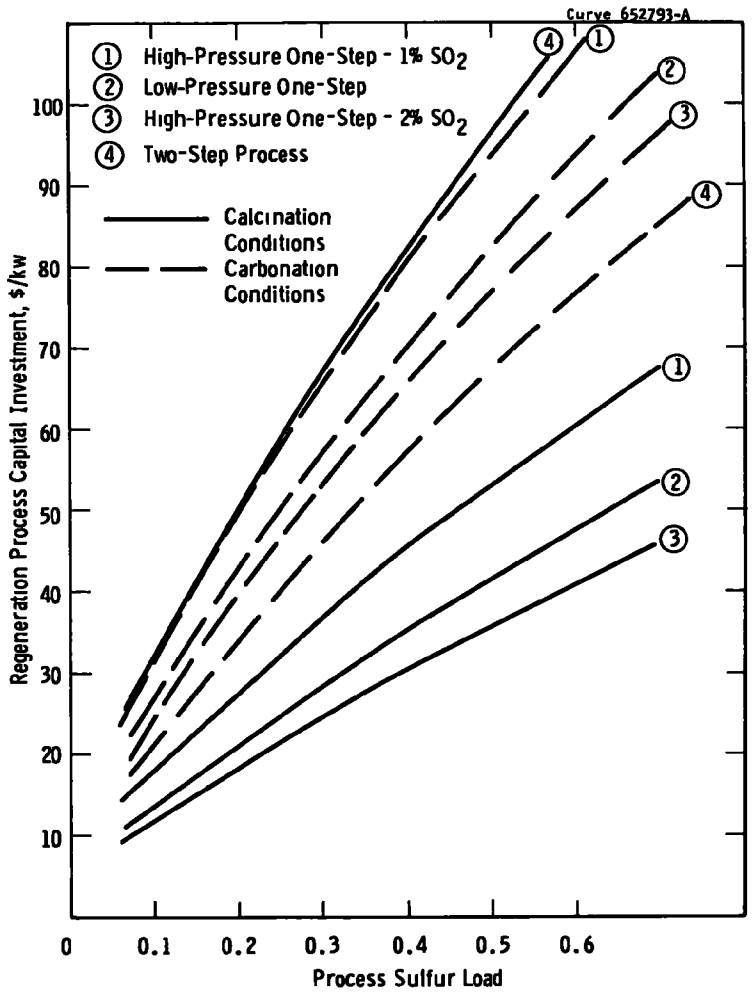

Figure K-1. Regeneration Process Investment Comparison

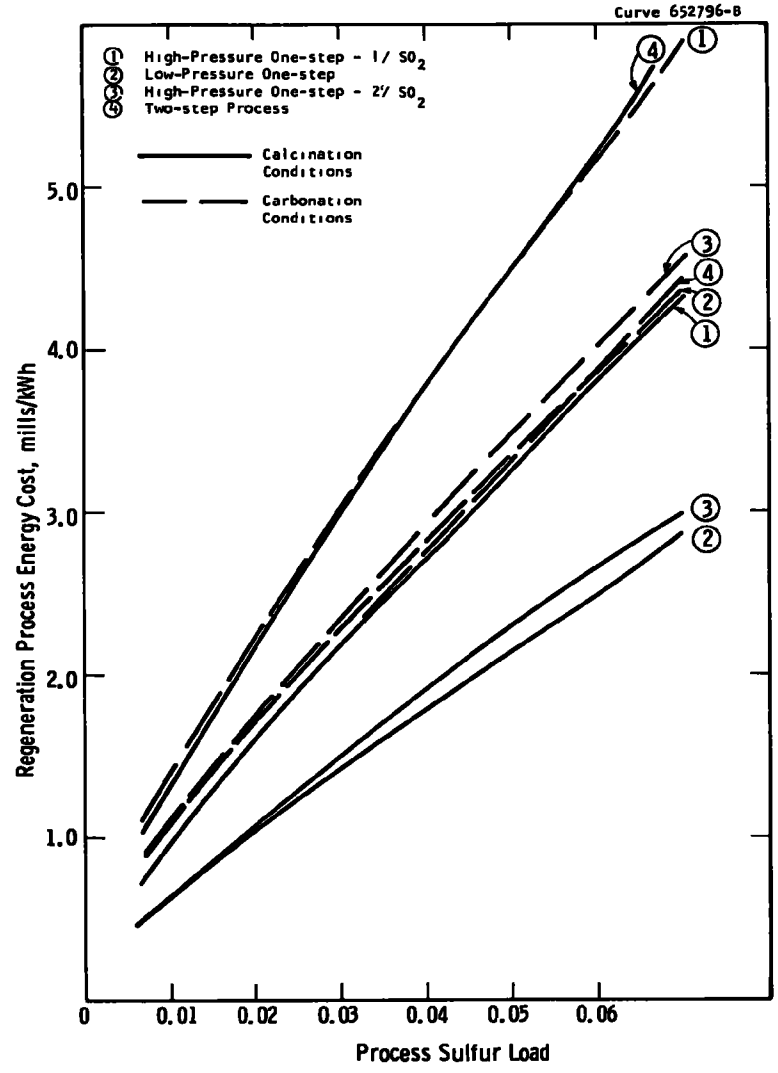

Figure K-2: Regeneration Process Energy Cost Comparison

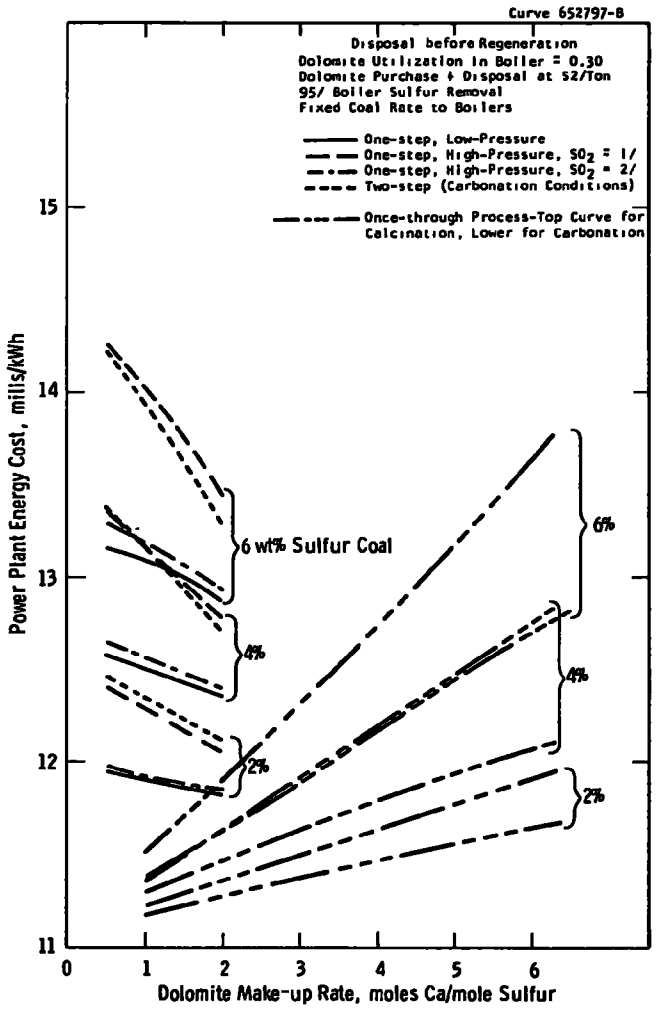

Figure K-3. Energy Cost Comparison Disposal before Regeneration $2/Ton Dolomite

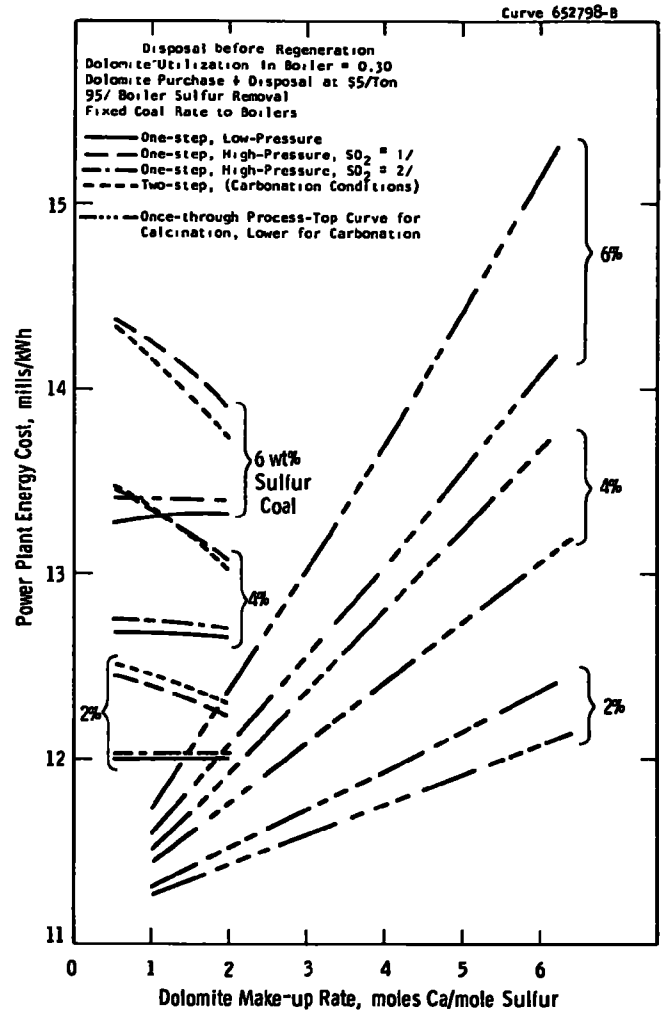

Figure K-4: Energy Cost Comparison: Disposal before Regeneration, $5/Ton Dolomite

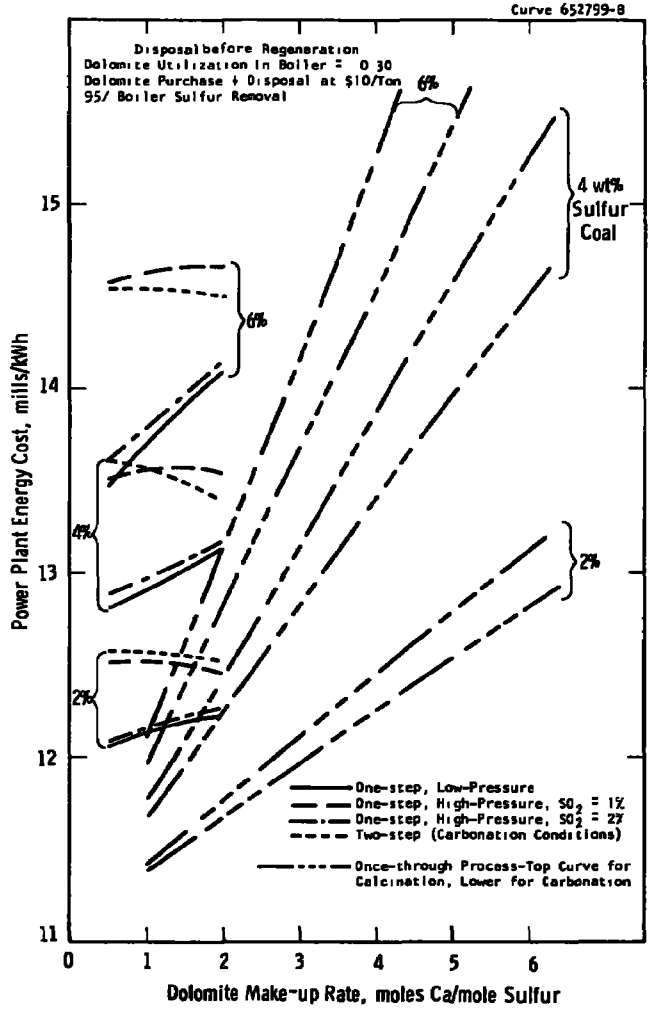

Figure K-5 Energy Cost Comparison: Disposal before Regeneration, $10/Ton Dolomite

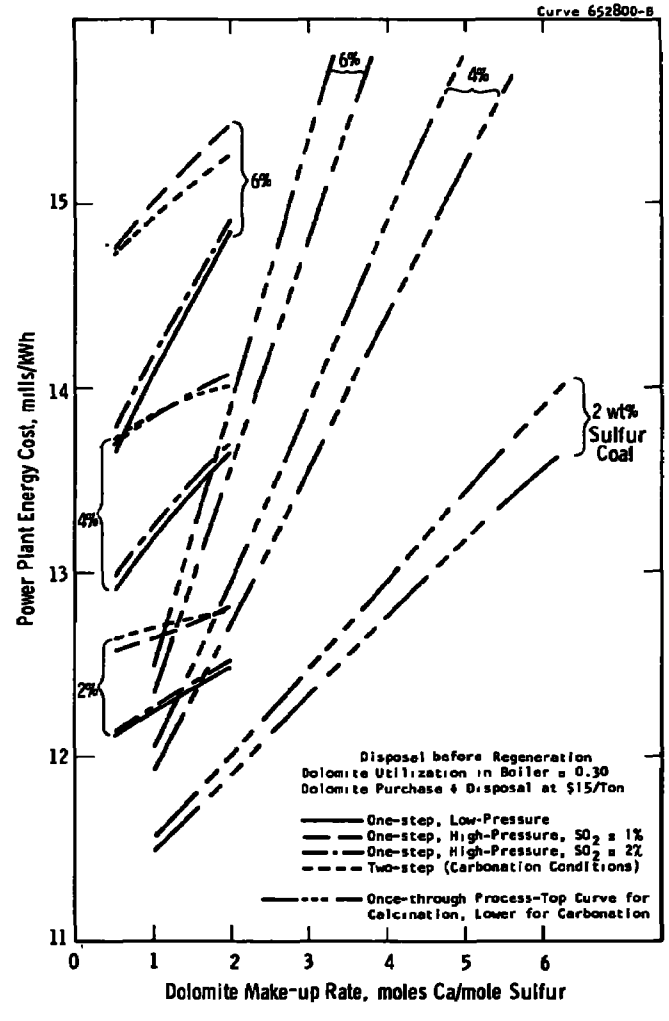

Figure K-6 Energy Cost Comparison. Disposal before Regeneration, $15/Ton Dolomite

after the regeneration process (Figures K-7 to K-12) unless the calcium utilization after regeneration, X_S^R, is large [the process sulfur load being $W_S(\varepsilon - mx_S^R)$].

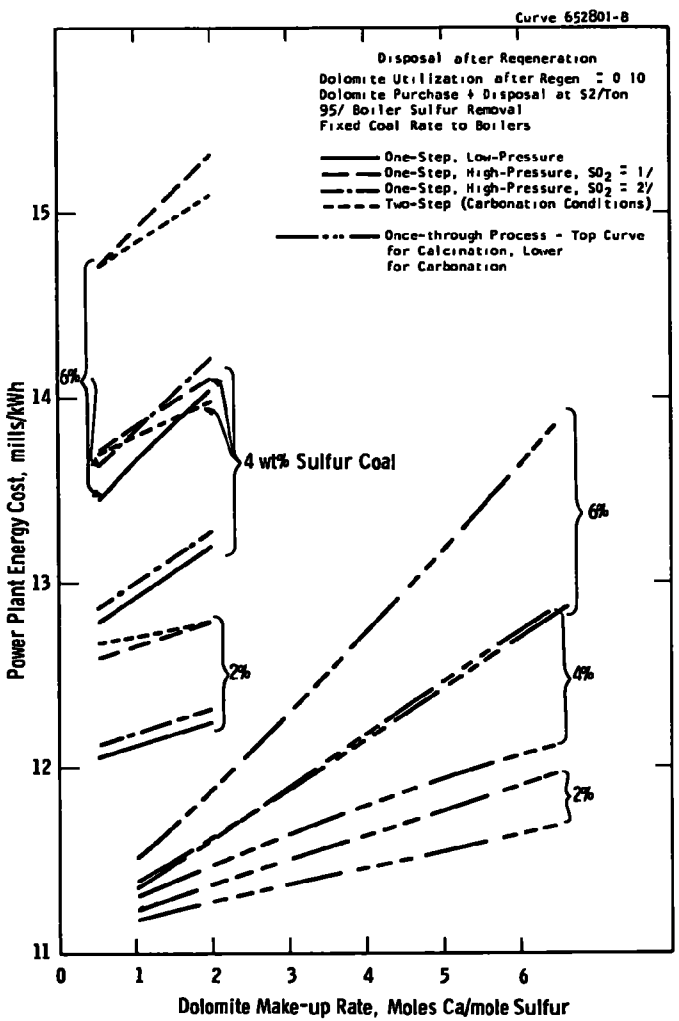

Figure K-7 Energy Cost Comparison: Disposal after Regeneration, $2/Ton Dolomite

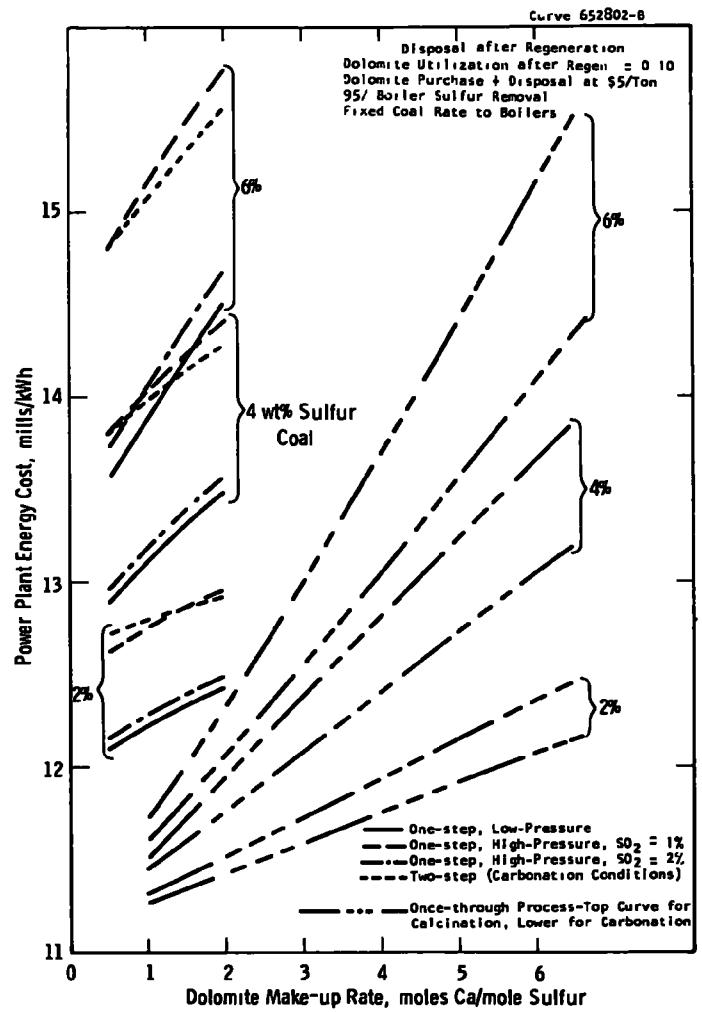

Figure K-8: Energy Cost Comparison Disposal after Regeneration, $5/Ton Dolomite

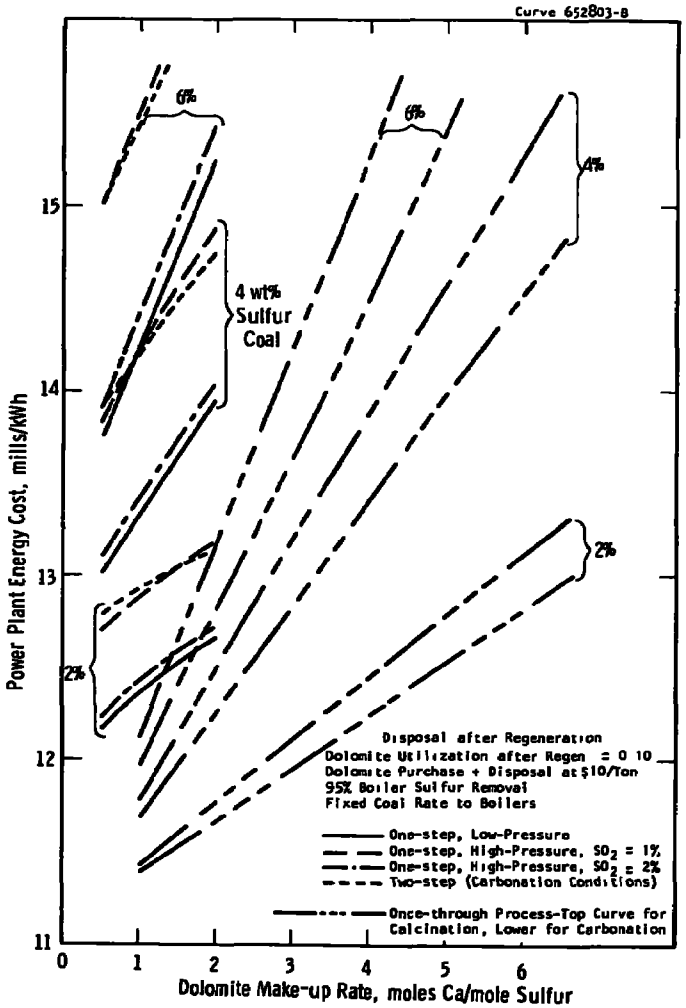

Figure K-9: Energy Cost Comparison Disposal after Regeneration, $10/Ton Dolomite

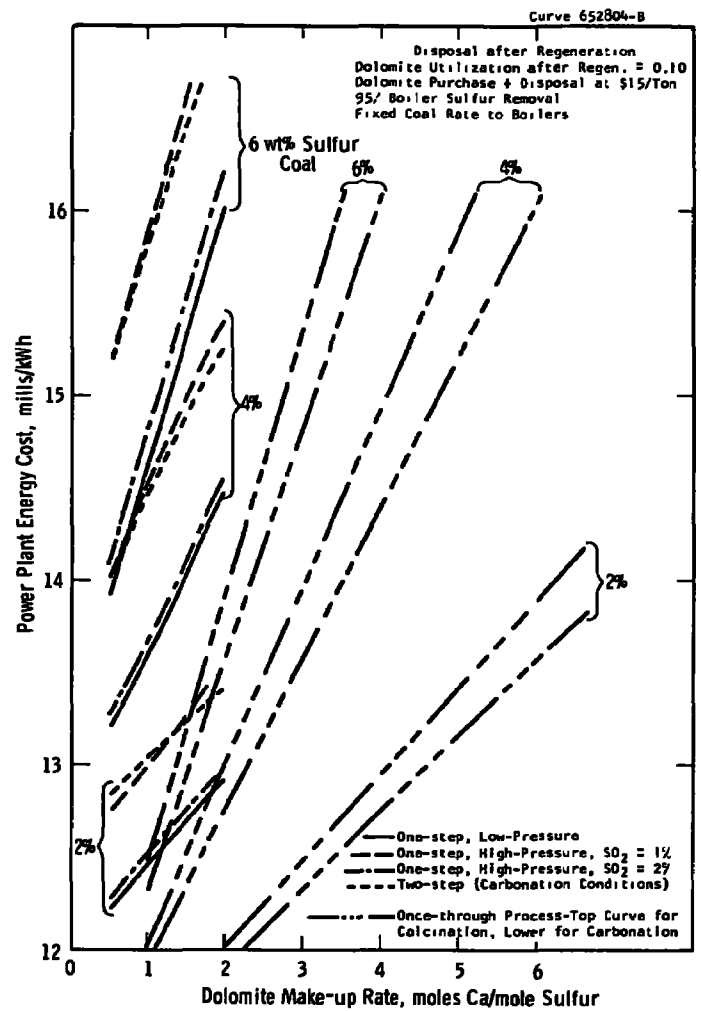

Figure K-10 Energy Cost Comparison- Disposal after Regeneration, $15/Ton Dolomite

L

APPENDIX L

A GENERAL STUDY OF THE ONE-STEP REGENERATION PROCESS

INTRODUCTION

The regeneration of dolomite or limestone sulfur sorbents is perhaps the area of greatest uncertainty in the design of the pressurized fluid bed combustion power plant. Various regeneration schemes have been proposed, but only bench-scale investigation has been carried out at this time. A two-step regeneration process has been considered in the design of a 635 MW pressurized fluid bed combustion power plant, with the regeneration process design of a preliminary nature and based on little experimental information.[1] A one-step regeneration process has also been proposed in which the $CaSO_4$ from the fluid bed boiler is reacted with a reducing gas of H_2 and CO to produce CaO and SO_2. The one-step process has been investigated by Esso with bench-scale equipment and will be utilized in a continuous pressurized fluid bed combustion miniplant which they will operate.[2]

Sensitivity analyses are being carried out to assess both the one-stage and the two-stage pressurized regeneration systems and selected alternatives -- e.g., once-through, atmospheric pressure regeneration -- and the corresponding sulfur recovery system. An analysis of the one-step dolomite regeneration process as it applies to pressurized fluidized bed combustion is being carried out first. The goals of this sensitivity analysis are to:

- Identify design parameters, operating variables, and major problem areas involved in the one-step process
- Estimate regeneration system costs and identify the critical cost factors
- Provide direction for experimental studies to be carried out by Esso

- Establish feasibility bounds on the regeneration system performance variables which can be used to evaluate the experimental results provided by Esso and Westinghouse.

ONE-STEP REGENERATION CONCEPT

The one-step dolomite/limestone regeneration process consists of a single fluidized bed reaction vessel in which utilized dolomite/limestone ($CaSO_4$) from the pressurized fluid bed boiler (coal-fired) is reacted with a H_2/CO reducing gas to produce CaO and SO_2. The reaction

$$CaSO_4 + \left\{\begin{matrix} H_2 \\ CO \end{matrix}\right\} \rightleftarrows CaO + \left\{\begin{matrix} H_2O \\ CO_2 \end{matrix}\right\} + SO_2 \qquad (1)$$

requires temperatures on the order of 2000°F to produce high levels (1 to 15%) of SO_2 at reasonable rates. The SO_2 equilibrium concentration is favored by reduced pressure since it is inversely proportional to the total pressure. The competing reaction

$$CaSO_4 + 4\left\{\begin{matrix} H_2 \\ CO \end{matrix}\right\} \rightleftarrows CaS + 4\left\{\begin{matrix} H_2O \\ CO_2 \end{matrix}\right\} \qquad (2)$$

also occurs to produce the unwanted product CaS.

The regenerated dolomite/limestone is returned to the fluid bed boiler with the required amount of fresh dolomite/limestone to supplement the regenerated sorbent's reduced activity. The SO_2 stream from the regenerator is sent to a sulfur recovery plant in which sulfuric acid or elemental sulfur is produced.

STUDY BASIS

The elements of the one-step regeneration process and the various design options which are possible should be understood before analysis of the process proceeds. In this same regard the specification for the design, and the design variables, operating variables, and performance variables, are compiled and discussed. Finally, the goals and philosophy of the study are stated.

One-Step Process Elements

For convenience, the one-step regeneration process is broken down into five interrelated elements; a regenerator element, a reducing-gas producer element, a sulfur recovery element, a Claus plant tail gas handling element, and a sorbent circulation element. These elements and their relationship to the other elements are shown in Figure L-1. Details of the equipment provided in each element are discussed later. The simple block flow diagram indicates the basic streams in the process. Fuel, air and/or steam is converted to a H_2/CO reducing gas in the reducing-gas producer element. This reducing gas is combined with tail gas recycled from the sulfur recovery element to make up the reducing gas provided to the regenerator. Utilized sorbent from the fluid bed boiler is transported to the regenerator element to produce a regenerated sorbent and an SO_2 stream. The regenerator product gas is processed in the sulfur recovery element, with the sulfur recovery tail gas being either recycled to the regenerator or processed in the tail gas handling element. The performance and design of these five regeneration process elements are interrelated in a very complex manner.

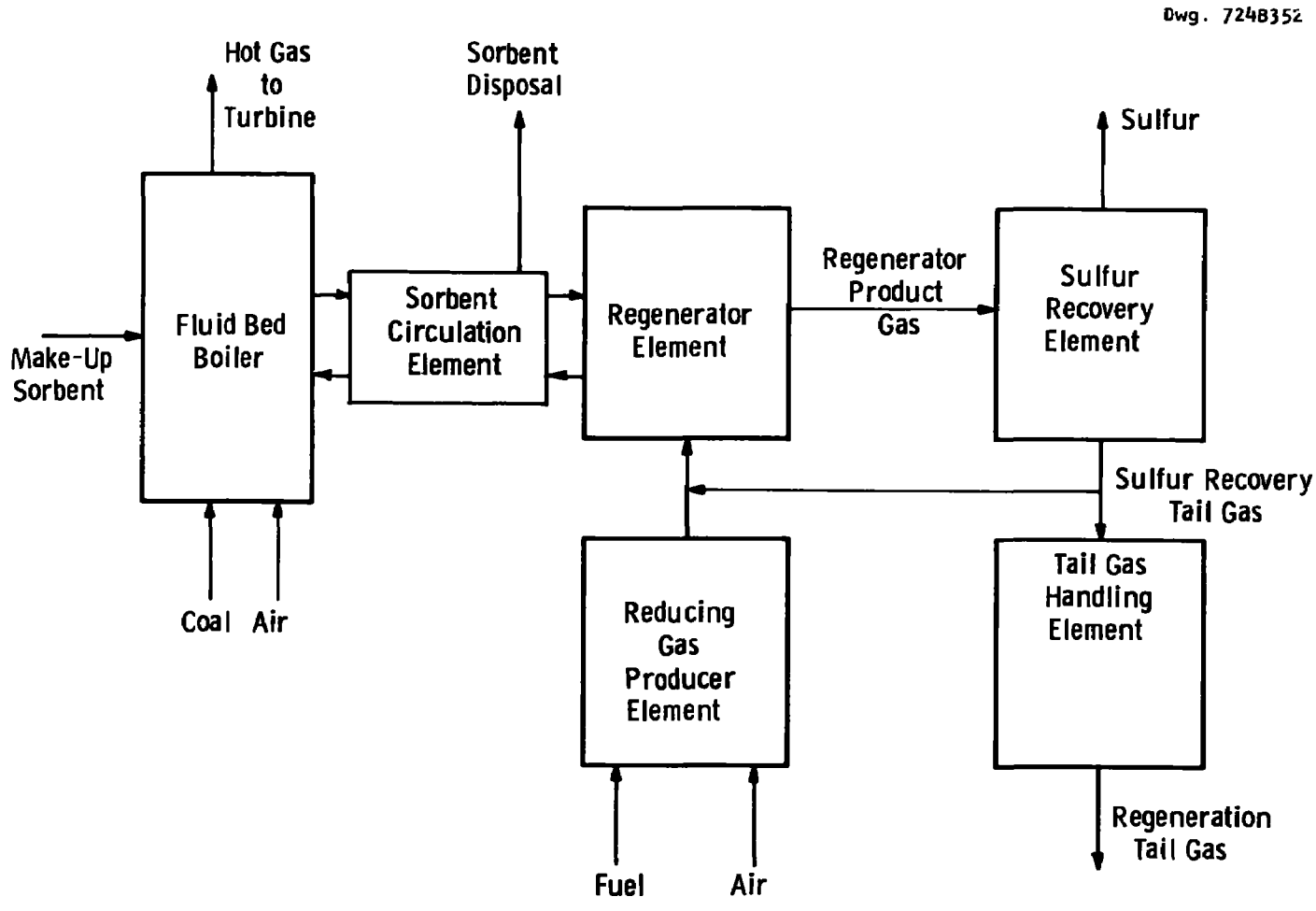

Figure L-1: One-Step Regeneration Process Elements

Process Specifications

Process specifications are presented in Table L-1. The one-step regeneration process design study is based on a coal-fired pressurized fluid bed combustion power plant capacity of 635 MW, to correspond to the preliminary plant study carried out earlier. This capacity requires a coal feed rate of 430,000 lb/hr. Dolomite is specified as the SO_2 sorbent for this study, though limestone could easily be considered in addition to the dolomite. A boiler pressure of 150 psia is specified, along with the specification that elemental sulfur rather than sulfuric acid is to be recovered and that disposal of the spent dolomite should take place before the regeneration step rather than after. The advantages of recovering elemental sulfur rather than sulfuric acid are well known. The advantages in disposing of the spent dolomite before regeneration rather than after are that the total sulfur load on the regeneration process is reduced, and the dolomite is in a more suitable form for disposal before regeneration ($CaSO_4$) than it is after (CaS).

TABLE L-1

PROCESS SPECIFICATIONS

Power Plant	coal-fired, pressurized fluid bed combustion power plant
Capacity	635 MW
Fluid Bed Boiler Pressure	150 psia
Fluid Bed Boiler Temperature	∿ 1750°F
Boiler Sorbent Condition	calcined
Coal Rate	430,000 lb/hr
Sulfur Sorbent	dolomite (50% $CaCO_3$, 50% $MgCO_3$)
Disposal of Dolomite	before regeneration
Sulfur Recovery	elemental sulfur
Plant Capacity Factor	70%
Turndown Ratio	4:1

An effort has been made to specify a minimum number of items in order to study the general cost behavior of the regeneration process.

Variables and Design Options

Operating and design variables considered in the study are listed in Table L-2. In addition to these variables, which the designer or operator can control or set, there are a number of performance variables which are dependent on the design and operating variables. These performance variables are listed in Table L-3 in very general terms.

TABLE L-2

OPERATING AND DESIGN VARIABLES

Boiler Fuel Sulfur Content
Boiler Sulfur Removal Efficiency
Regenerator Vessel Pressure
Regenerator Vessel Temperature
Regenerator Fluidization Velocity
Regenerator Bed Depth
Number of Regenerator Modules
Regenerator Vessel Design (internals, freeboard, etc.)
Gas Producer Design and Fuel Utilized
Air/fuel Ratio to Gas Produced or H_2+CO Concentration in Reducing Gas
Fraction of Claus Tail Gas Recycled to Regenerator
Regenerator Vessel Temperature Control Scheme

TABLE L-3

PERFORMANCE VARIABLES

Composition of the Regenerator Gas Product Stream
Composition of Reducing-Gas Stream
Composition of Claus Tail Gas
Composition of Stone from Boiler
Composition of Regenerated Stone
Dolomite Make-up Rate

Design options which are considered in the study are shown in Table L-4. The reducing-gas producer element may consist of a coal gasifier, an oil gasifier, a methane partial oxidation burner, or a methane reformer, all of which are conventional gas producing methods. Other reducing-gas producer options which carry out both reducing-gas production and regeneration of dolomite in the same vessel have not been considered because they depend largely on unexplored technology and may lead to many complications.

The tail gas handling element may consist of an incinerator and a turbine expander to recover some of the flue gas energy. The option of recycling the tail gas to either the fluid bed boiler or the gas-turbine combuster is also considered.

Study Philosophy

One of the purposes of this investigation is to establish feasibility bounds on the performance variables in order to aid in the evaluation of bench-scale experimentation and the Esso miniplant program. With this purpose in mind, based on preliminary considerations, the set of variables listed in Tables L-2 through L-4 has been simplified into variables of prime importance in determining the one-step process feasibility and variables of secondary importance. These two groups of variables are listed in Table L-5.

TABLE L-4

DESIGN OPTIONS

Gas Production	coal gasification oil gasification methane partial oxidation methane reforming
Claus Plant Tail Gas Handling	recycle to boiler or gas-turbine combustor, incineration and expansion

TABLE L-5

SIMPLIFIED VARIABLES

Prime Variables

- Regenerator pressure - 10, 5, 2 atmospheres
- Reducing-gas producer scheme - coal gasification, oil gasification, methane partial oxidation, methane reforming
- Process sulfur load - $W_s[\varepsilon - mX_s^B] = 0.01, 0.03, 0.06$
- Mole fraction SO_2 in regenerator product - Y_{SO_2}

  $Y_{SO_2} = 0 - 0.05$ at 10 atmospheres

  $Y_{SO_2} = 0 - 0.10$ at 5 atmospheres

  $Y_{SO_2} = 0 - 0.15$ at 2 atmospheres

Secondary Variables

- Regenerator temperature - 1800-2200°F
- Air/fuel ratio to gas producer - 40-80% of stoichiometric
- Regenerator fluidization velocity - 5-15 ft/sec.
- Regenerator vessel height - 15-65 ft
- Fraction of Claus tail gas recycled to regenerator - 0-0.50
- Tail gas recycle to boiler or incineration of tail gas
- Change in dolomite sulfur utilization across regenerator, $X_s^B - X_s^R = 0.1 - 0.3$
- Regeneration process thermal efficiency - 50-75%

The philosophy of the investigation is then to estimate capital costs and energy costs for the one-step regeneration process as a function of the prime variables. Values of the prime variables considered are included in the table. Since the secondary variables have a small effect on the capital and energy costs these variables are set to span a reasonable range of values which are designed to cover the probable situations and which are included in the table.

The final result, then, is probable ranges of capital and energy costs for the one-step regeneration process as a function of the prime variables. These ranges are narrow enough so that concise conclusions may be drawn as to the process feasibility and behavior.

The four prime variables listed are clearly the most significant, based on simple considerations. The process sulfur load, $W_s[\varepsilon - mX_s^B]$, is a combination of the fuel sulfur content, W_s, (lb sulfur/lb fuel); the boiler sulfur removal efficiency, ε; the dolomite make-up rate, m, (moles Ca/mole S fed); and the fractional utilization of the dolomite in the fluid bed boiler, X_s^B. This variable is representative of the amount of sulfur which the regeneration process must handle and, therefore, sets the scale of the process.

The mole fraction of SO_2 in the regenerator product gas is representative of the size of the regeneration process equipment and the gas producer fuel requirements, since the amount of sulfur handled is fixed by the variable $W_s[\varepsilon - mX_s^B]$. Since the equipment sizes and fuel requirements are inversely proportional to Y_{SO_2}, this prime variable has an extremely large effect.

Since the equilibrium SO_2 concentration is inversely proportional to the regenerator pressure and the equipment sizes are directly proportional to the pressure, the possible advantages or disadvantages to be gained by operating the regeneration process at pressures lower than the boiler pressure of 10 atmospheres should be investigated. This also leads to the possibility of lowering the regenerator temperature by reducing the pressure and thereby possibly improving the regenerated dolomite activity.

The type of fuel used to produce reducing gas has a great effect on the capital cost, system complexity, and energy cost associated with the one-step regeneration process.

The most important of the secondary variables is the change in dolomite sulfur utilization, $X_s^B - X_s^R$. The rate of dolomite circulation is inversely proportional to this variable.

MATERIAL AND ENERGY BALANCES

Thermodynamic studies indicate some of the behavior to be expected as a function of the regenerator pressure and the operating conditions. Energy balances around the regenerator indicate the requirements for regenerator temperature control. Using the insight gained from thermodynamics, overall material and energy balances have been carried out which allow the sizing of equipment as a function of the prime and secondary variables outlined in Table L-5.

Thermodynamics

Thermodynamics indicates that the SO_2 concentration resulting from the equilibrium of reaction 1 and 2 is inversely proportional to the regenerator pressure. This behavior provides the incentive to study the possibility of operating the regeneration process at pressures below the boiler pressure. Thermodynamics also predicts that nearly all of the H_2 and CO in the reducing gas will be utilized to produce SO_2 and CaS by reaction 1 and 2. This leads to the expectation of low CaS contents at pressures as low as 2 atmospheres and high CaS contents in the regenerated dolomite at pressures of 10 atmospheres.

The trends indicated by thermodynamics can be expected in an actual operation. For this reason the ranges of SO_2 mole fractions as noted in Table L-6 are considered at each of the pressures to be investigated.

TABLE L-6

RANGES OF SO_2 MOLE FRACTIONS

Regenerator Pressure, atm.	Range of SO_2 Mole Fractions
10	0.01-0.05
5	0.01-0.10
2	0.01-0.15

These ranges are chosen on the basis of a regenerator temperature of about 2000°F. Data collected by Esso from batch operations lie within these ranges.[2]

Regenerator Temperature Control

The temperature of the dolomite regenerator vessel may be maintained at about 2000°F by controlling the temperature of the streams entering the regenerator. This may require heating or cooling of the gas producer product, the tail gas recycle stream, or the utilized dolomite stream. The variables involved in the regenerator energy balance are numerous and, lacking direct experimental evidence, it appears that either cooling or heating may be required, depending on the regenerator pressure, the reducing-gas producer fuel, the dolomite utilization in the boiler, the temperature of the dolomite stream entering the regenerator, and the kinetic behavior of the regenerator.

In order to account for the cost of temperature control it was assumed that the energy loss or input required is not extensive, and a gas-fired heater necessary to reheat the Claus plant tail gas recycle stream would be sufficient to control the regenerator temperature at about 2000°F. It appears that the temperature control energy requirements will decrease with decreasing regenerator pressure.

Material and Energy Balances

All major streams have been characterized to the extent necessary to allow equipment capacities to be estimated as a function of the primary and secondary variables. Fuel inputs into the reducing-gas product, the tail gas recycle heater, the Claus plant, and the tail gas incinerator have been estimated. Auxiliary power requirements for the regeneration process have also been calculated. Some of the factors which limit the one-step regeneration process feasibility are brought out by simple material balances.

Material and energy balances have been computed for process sulfur loads, W_s $[\varepsilon - mX_S^B]$, of 0.06, 0.03, and 0.01. A sulfur load of 0.03 is assumed to be a reasonable value to be expected with coals having normal sulfur contents (∿4 wt %). Values of 0.06 and 0.01 are probably extremely high and extremely low, respectively, and have been chosen to allow extrapolation of the cost results to sulfur loads within the range of 0.01 to 0.06. Figure L-2 illustrates how the process sulfur load varies as a function of the fractional utilization of the dolomite in the boiler for coals having weight fractions of sulfur of 0.06, 0.04, 0.03, and 0.02. A constant sulfur removal efficiency of 0.95 is assumed and dolomite make-up rates of 1.0 and 2.0 moles Ca/Mole S are examined.

An important factor in determining the feasibility of recycling Claus plant tail gas to the fluid bed boilers or the gas-turbine combustor is the extent of modification required to the boiler or combustor in order to handle the increased load from the regeneration process. Figure L-3 is a plot of the volume of tail gas being recycled to the boiler, in percent of the boiler combustion air volume, as a function of Y_{SO_2}. Zero recycle of tail gas to the regenerator is assumed in the figure, so it represents the most drastic case. If it is assumed that a 10% volumetric load increase is permissible without modification, a mole fraction of SO_2 greater than 0.02 is required for a process sulfur load of 0.03, and 0.04 for a sulfur load of 0.06. Since no tail gas recycle to the regenerator has been assumed and the 10% limit is conservative, no boiler modification cost has been charged for recycling tail gas to the boiler. This assumption may not be valid for process sulfur loads as high as 0.06, with low SO_2 concentrations.

Fuel requirements are simply computed as a function of the process variables. The fuel imput to the gas producer is shown in Figure L-4 as the fraction of the Btu input of the boiler. Curves are shown for process sulfur loads of 0.06, 0.03, and 0.01, and for reducing-

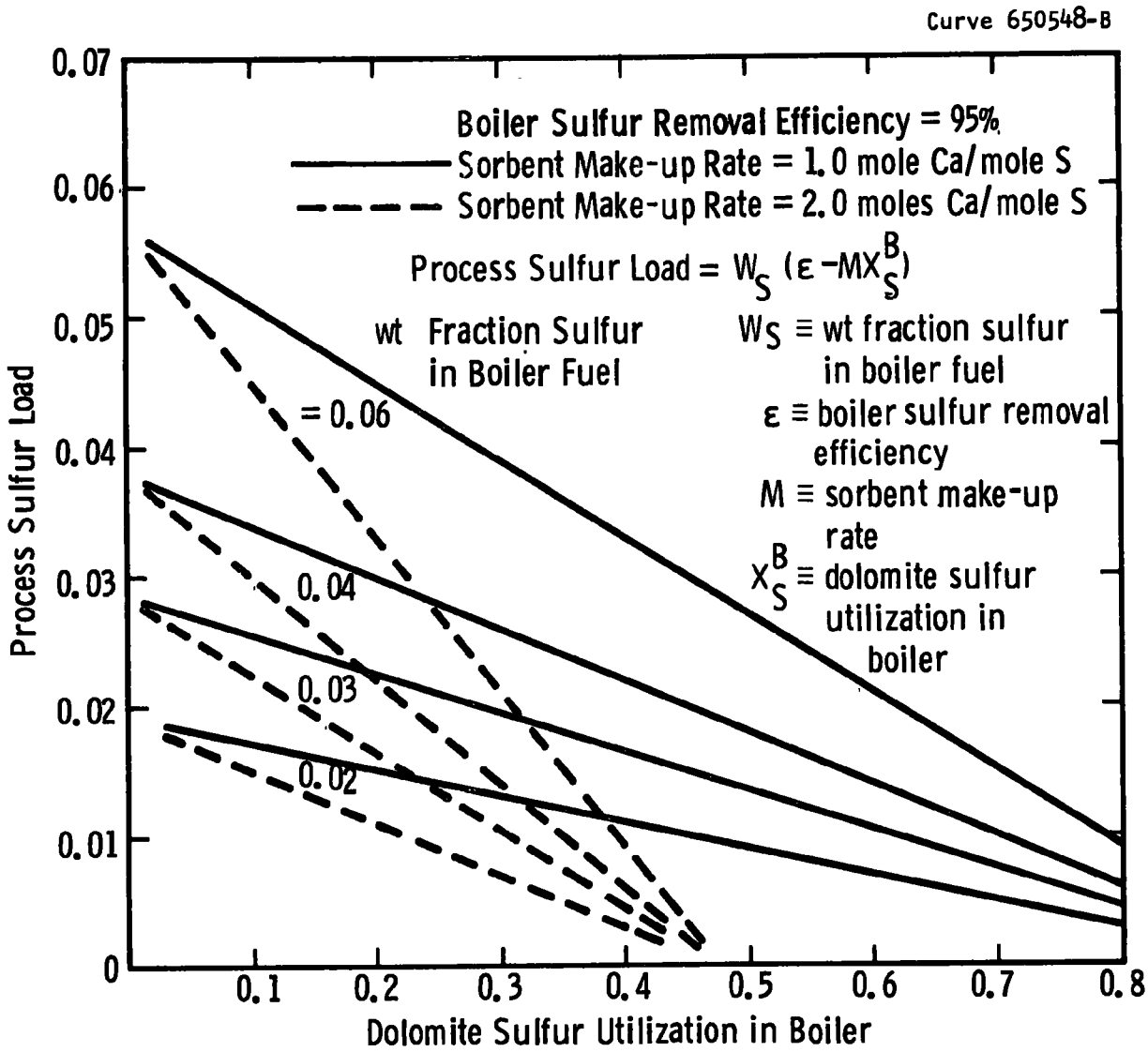

Figure L-2: Reqeneration Process Sulfur Load

Curve 650538-B

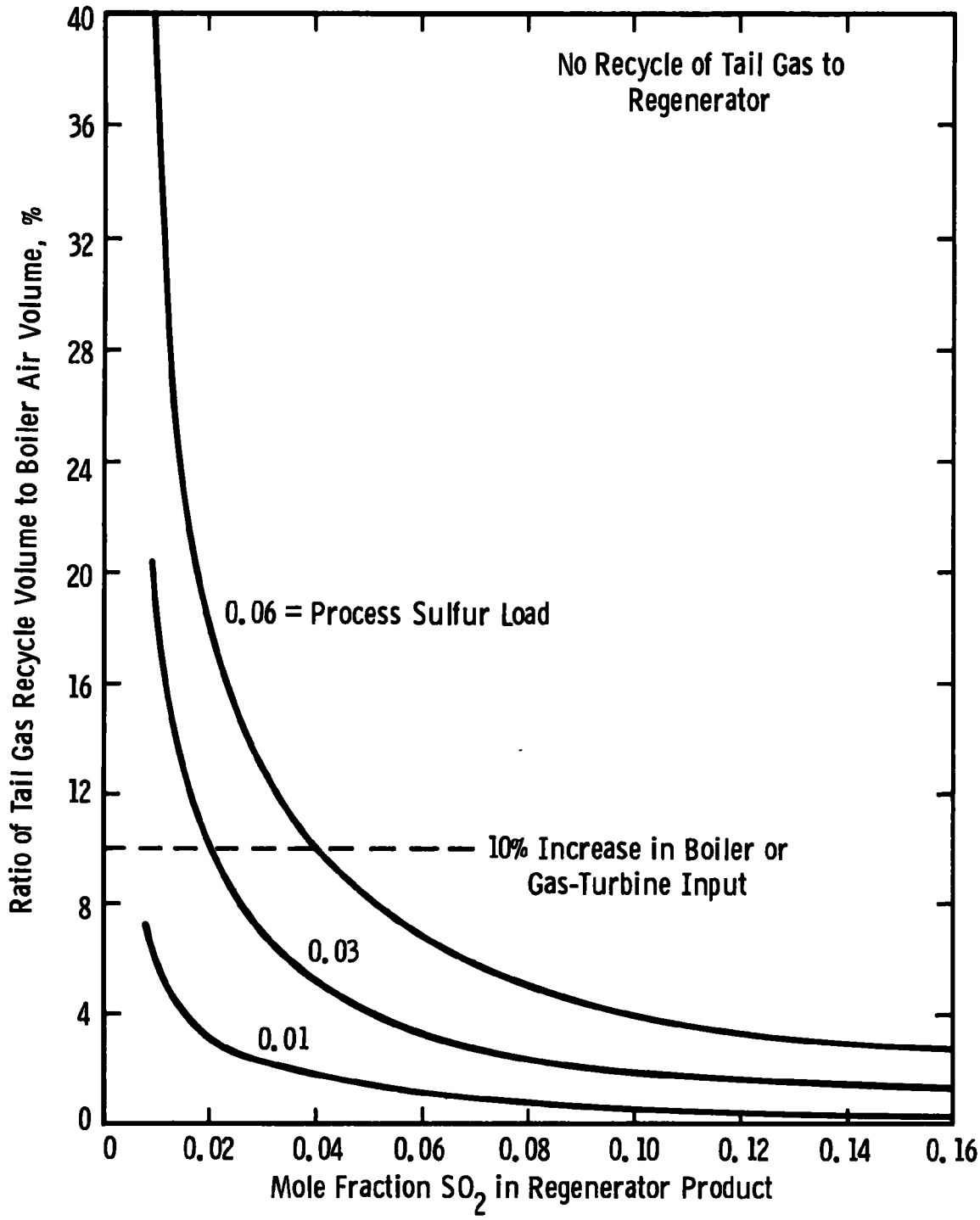

Figure L-3: Tail Gas Recycle to Boiler

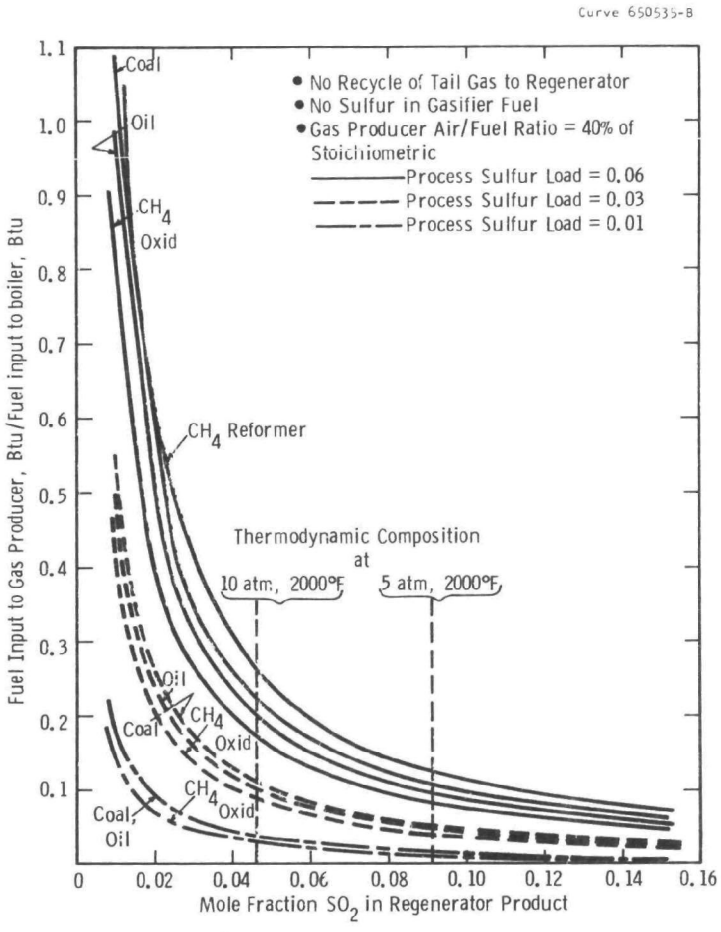

Figure L-4: Gas Producer Fuel Requirement

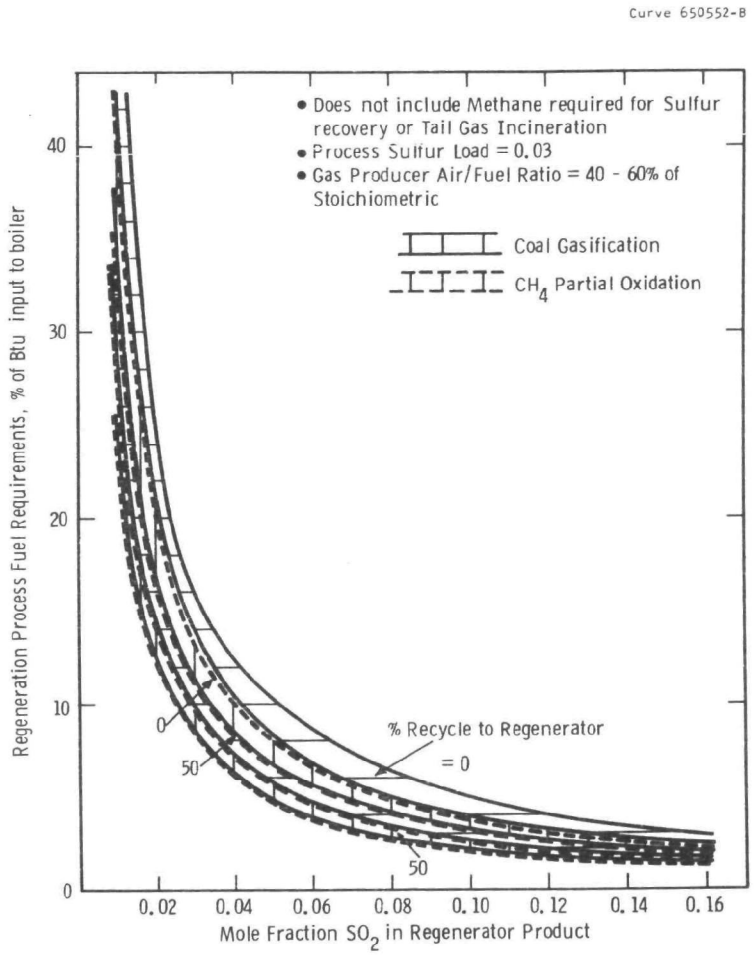

Figure L-5: Total Regeneration Process Fuel Requirement

gas production by coal gasification, oil gasification, methane partial oxidation, and methane reforming. The following assumptions have been made in generating the figure:

- An air/fuel ratio in the gas producer of 40% of the stoichiometric value
- No sulfur in the fuel used for reducing-gas production.

The fuel rate to the gasifier is directly proportional to the fraction of the tail gas which is recycled to the regenerator, so again the figure represents the most extreme case. The curves rise rapidly at lower SO_2 mole fractions and indicate that the scale of the regeneration process may approach the scale of the fluid bed combustion process at low mole fractions of SO_2. Air/fuel ratios much larger than 40% of stoichiometric may be suitable, which will reduce the fuel requirement (see Figure L-6).

Additional fuel, CH_4, is required for the reduction of SO_2 to H_2S in the sulfur recovery element, for incineration of Claus plant tail gas if that option is chosen, and for heating the tail gas being recycled to the regenerator. Figure L-5 shows the combined fuel requirements for gas production and tail gas recycle heating in percent of Btu input to the boiler. Curves are shown for coal gasification and for methane partial oxidation with fractional recycles of the tail gas to the regenerator of 0 and 0.50. The following assumptions contribute to the figure:

- The process sulfur load is 0.03 and the fuel requirement is linear in this factor.
- The recycled tail gas is heated from the 300°F Claus plant exhaust temperature to 2000°F with an 85% efficient gas-fired heater.
- The air/fuel ratio in the gas producer is taken over a range of 40% to 60% of stoichiometric.
- Sulfur in the coal used for reducing-gas production is neglected.

The total fuel required for the one-step regeneration process would be about 10% greater than that indicated in Figure L-5 if Claus plant requirements and incinerating requirements were included.

The effect of utilizing a fuel for reducing-gas production which contains a significant proportion of sulfur is shown in Figures L-6 and L-7. Figure L-6 shows the multiplication factor to be used with Figure L-4 to account for air/fuel ratios other than 40% of stoichiometric and fuels containing sulfur. Figure L-7 shows the plant sulfur production rate as a function of the gas producer fuel sulfur content. The fuel sulfur content effect can be important at small SO_2 mole fractions (< 3%). Higher air/fuel ratios will reduce the effect of sulfur in the reducing-gas fuel shown in Figure L-7. In Figures L-6 and L-7 the SO_2 mole fraction includes the sulfur contribution of the reducing-gas producer fuel.

Auxiliary power requirements for the one-step regeneration process consist of the following contributions: compression of air for reducing-gas production, compression of tail gas recycled to the regenerator, compression of tail gas recycled to the 10 atmosphere boiler, or compression of air for tail gas incineration, power for dolomite circulation, and power for cooling water, pumping, and fuel feeding. The total auxiliary power requirement shows the same characteristic increase with decreasing SO_2 mole fraction and may vary from 2 to 5 MW at high SO_2 mole fractions (∿ 10 to 15%) up to 20 to 30 MW at low SO_2 mole fractions (∿ 1%).

Not all of the fuel energy which is used for reducing-gas production, recycled tail gas heating, Claus plant SO_2 reduction, and tail gas incineration is lost. Through dolomite recycle to the boiler, steam generation in the Claus plant, recycle of the tail gas to the boiler, or energy recovery from the tail gas incineration product, it is estimated that 50 to 75% of the energy entering the regenerator vessel can be utilized as useful energy for power generation at an air/fuel ratio of ∿ 40% of stoichiometric. The necessity of insuring the recovery of the useful energy for power generation is clear from the huge energy requirements for regeneration at low SO_2 mole fractions. Including the expected

Curve 650549-b

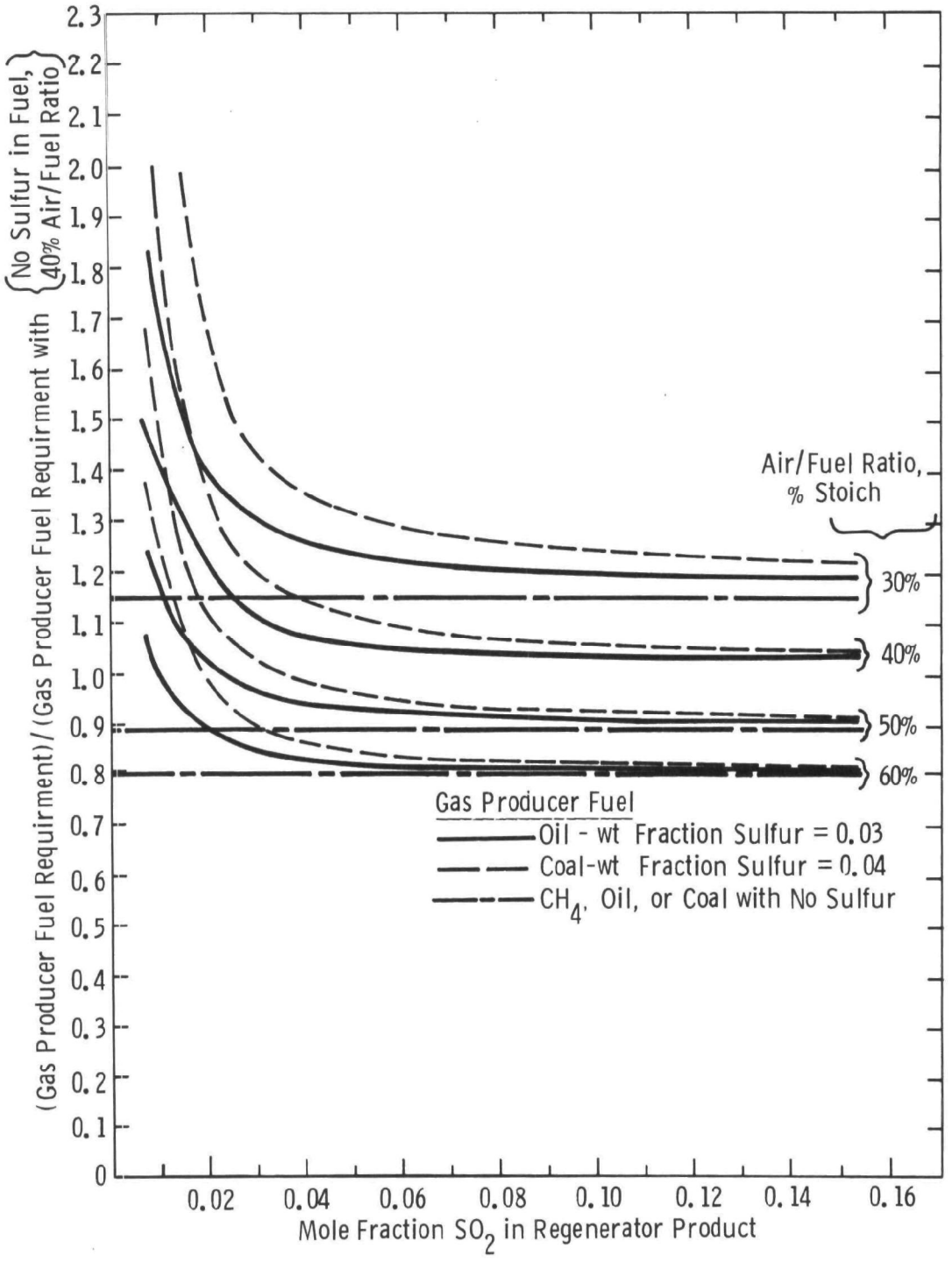

Figure L-6: Effect of Sulfur in Gas Producer Fuel

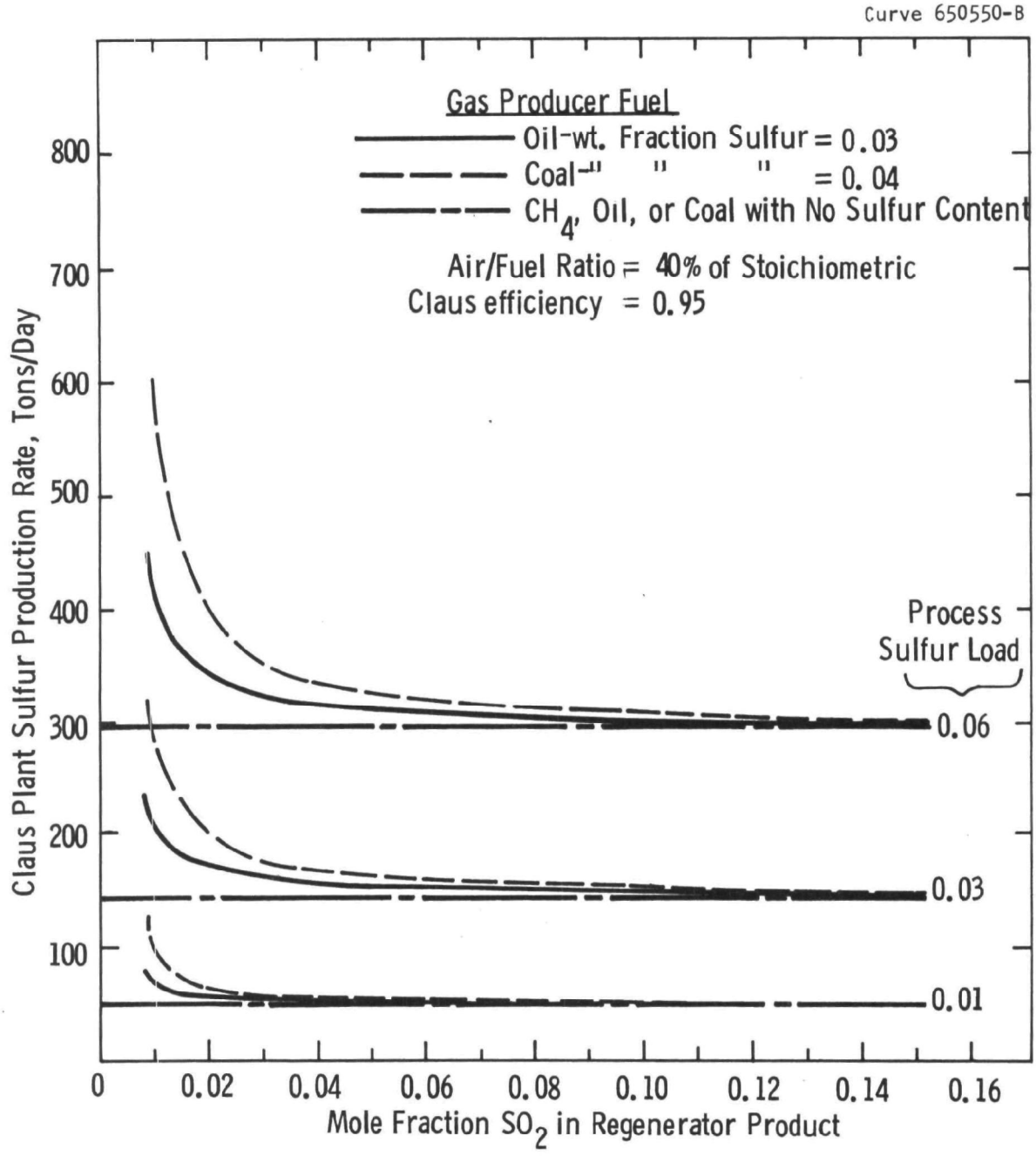

Figure L-7: Sulfur Production Rate

thermal efficiency of the reducing-gas production element, the recycle gas heater efficiency, and the process auxiliary power requirements, the regeneration process operates with an overall efficiency of 30 to 50% at an air/fuel ratio of ∿ 40% of stoichiometric. Higher air/fuel ratios will reduce both the fuel requirement and the process overall efficiency.

The factors briefly discussed here indicated some clear advantages in maximizing the SO_2 mole fraction in the regenerator product. A quantitative picture will be generated by estimating total energy costs for the one-step dolomite regeneration process.

EQUIPMENT DESIGN

The individual pieces of equipment making up the five elements of the one-step dolomite regeneration process have been designed as a function of the primary and secondary variables outlined in Table I-5. The considerations investigated and the assumptions applied to the equipment design are discussed.

Figure L-8 is a schematic flow diagram showing the equipment included in capital cost estimates. The equipment and pertinent assumptions made are as follows:

Regenerator Element

• Regenerator vessel and internals:	5-15 ft/sec fluidization velocity 15-65 ft overall height design temperature 1800-2200°F purchased equipment cost based on standard literature references and price quotations

Sulfur Recovery Element

• Claus plant with SO_2 reduction by CH_4:	does not include tail gas disposal cost based on Shell report[3]

Tail Gas Handling Element

- Boiler recycle option: tail gas recycle compressor
  no modification of boiler
  cost based on recent price quotation data
- Incineration option: tail gas incinerator
  combustion air compressor
  turbine expander (except at 2 atm)
  waste heat boiler at 2 atm pressure
  cost based on Shell report[3]

Reducing Gas Producer Element

- Tail gas recycle compressor: 0-50% recycle of tail gas
  cost based on recent price quotations
- Tail gas recycle heater: gas-fired
  0-50% recycle of tail gas
  85% efficient
  includes combustion air system
  cost taken from published information cost
- Gas producer: 0-50% recycle of tail gas
  40-80% of stoichiometric air/fuel ratio

Option: Coal Gasification

- Array of fixed-bed type gasifiers (Lurgi or McDowell-Wellman)
- Capacity: ∿320 ton coal/day per gasifier (12 ft. maximum diameter)
- Includes coal lock hoppers and ash lock hoppers
- Does not include: coal preparation or storage
  sulfur removal
  tar removal
- Thermal efficiency: ∿80%
- Gas product: 1200-1500°F
  10-25% hydrogen and carbon monoxide
- Cost taken from recent price quotations, recent references[4]
- Particle collectors
- Air compressor

Option: Oil Gasification (Gasification system cost would be essentially the same for either a residual oil or a distillate fuel.)

- Array of Shell or Texaco type heavy oil gasifiers
- Capacity: $\sim 33 \times 10^6$ scf/hr per gasifier (12 ft diameter, 20 ft. high)
- Does not include: sulfur removal
  soot recovery and recycle
- Thermal efficiency: ~85%
- Gas product: 2000-2500°F
  10-30% hydrogen and carbon monoxide
- Cost estimated from information provided by Shell Oil[4]
- Particle collectors
- Air compressor
- Oil feeding and storage (day tank and 30 day storage tank)

Option: Methane Partial Oxidation

- Refractory lined burners
- Thermal efficiency: ~95%
- Gas product: 2000-2500°F
  10-40% hydrogen and carbon monoxide
- Air compressor

Option: Methane Reforming

- Methane reformer vessels
- Thermal efficiency: ~85%
- Gas product: ~1500°F
  30-50% hydrogen and carbon monoxide
- Cost taken from quote from the Selas Corporation

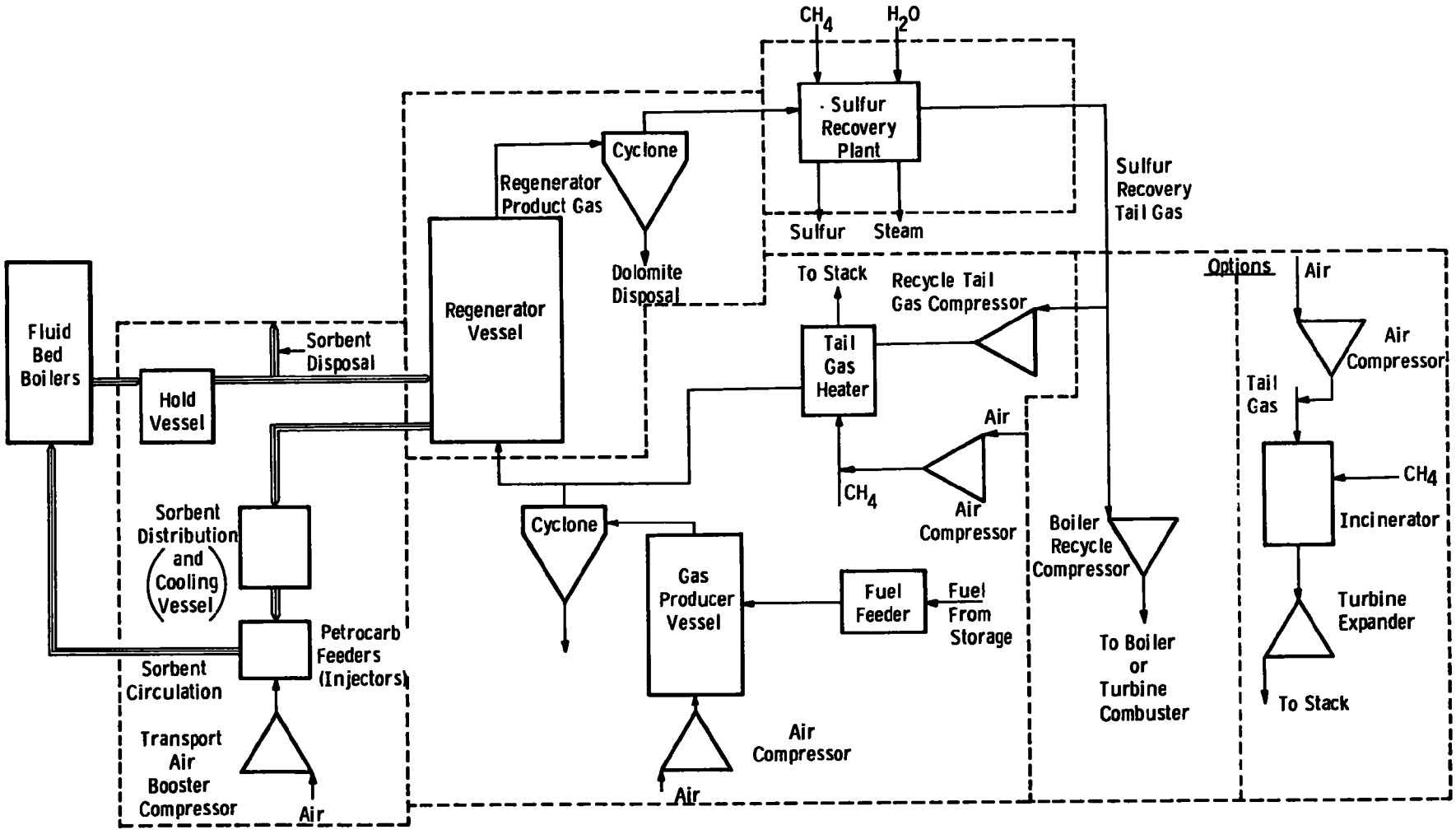

Figure L-8: One-Step Regeneration Process Flow Diagram

Sorbent Circulation Element - $X_S^B - X_S^R = 0.1\text{-}0.3$

- 10 atmosphere regenerator pressure
  - Four hold vessels (one for each boiler)
  - Sorbent distribution vessel
  - Petrocarb feeder assemblies
  - Transport air booster compressor (175 psia)
  - 2500 linear feet of solids piping
  - Costs supplied by Petrocarb
- 5 and 2 atmosphere regenerator pressure
  - Four hold vessels
  - Sorbent distribution vessel
  - Dolomite cooling vessel: counter-current flow moving bed with cooling by steam or water injection. Solids cooled to 800°F to meet valve temperature restriction.
  - Petrocarb injection and feeder assemblies
  - Transport air booster compressor (175 psia)
  - 2500 linear feet of solids piping

The capacities and dimensions of these equipment items have been estimated as a function of the four prime variables for the ranges of secondary variables indicated.

CAPITAL INVESTMENT

Equipment costs have been estimated from standard cost references appearing in the literature and from vendor quotes. Capital costs shown are total installed costs which reflect both field and shop fabrication costs. Each estimate was made based on factoring f.o.b. equipment cost to total installed cost. Each item of major equipment was priced from cost curves derived from published equipment price correlations, modified in the case of pressure vessels and compressors to reflect recent firm price quotations for these two categories of equipment.

The f.o.b. prices of major equipment were totaled, and the total was broken down into percentages for cost of vessels, compressors, mechanical equipment, heat exchange equipment, tanks, and pumps. Appropriate factors were then applied to each category of major equipment to obtain field material costs (pipe, concrete, structural steel, etc.), and field labor costs. Escalation was applied as required to material and labor costs to bring them to mid-1972 levels. The subtotal of all direct costs (equipment, material, and labor) was then factored to provide for field indirect costs, home office engineering, field supervision, freight, and contractor's contingency and fee. The total investment so arrived at is over four times the total f.o.b. equipment cost. Costs do not include interest during construction. A contractor's contingency and fee of 15% was applied.

Examples of installed costs, in $/kw, of the five process elements of the one-step regeneration process are shown in the following discussion. The importance of each element and its cost behavior is discussed. The total one-step regeneration process cost is discussed by means of a table of representative values.

Regenerator Element

The cost of the regenerator element for a 5 atmosphere regenerator pressure is shown in Figure L-9. The cost ranges refer to a single regenerator module with the secondary variables having the values shown in Figure L-5. The contribution of this element to the total process cost is small but not negligible. The cost penalty for going to two modules rather than one will be small, especially if the size of the single module is reduced from a field-fabricated size to two shop-fabricated vessels. Turndown requirements may necessitate duel regenerator vessels.

Attempts should be made to maximize the SO_2 mole fraction in the regenerator product by proper regenerator design. The overall cost penalty in using low fluidization velocities and deep beds is slight.

Curve 650551-B

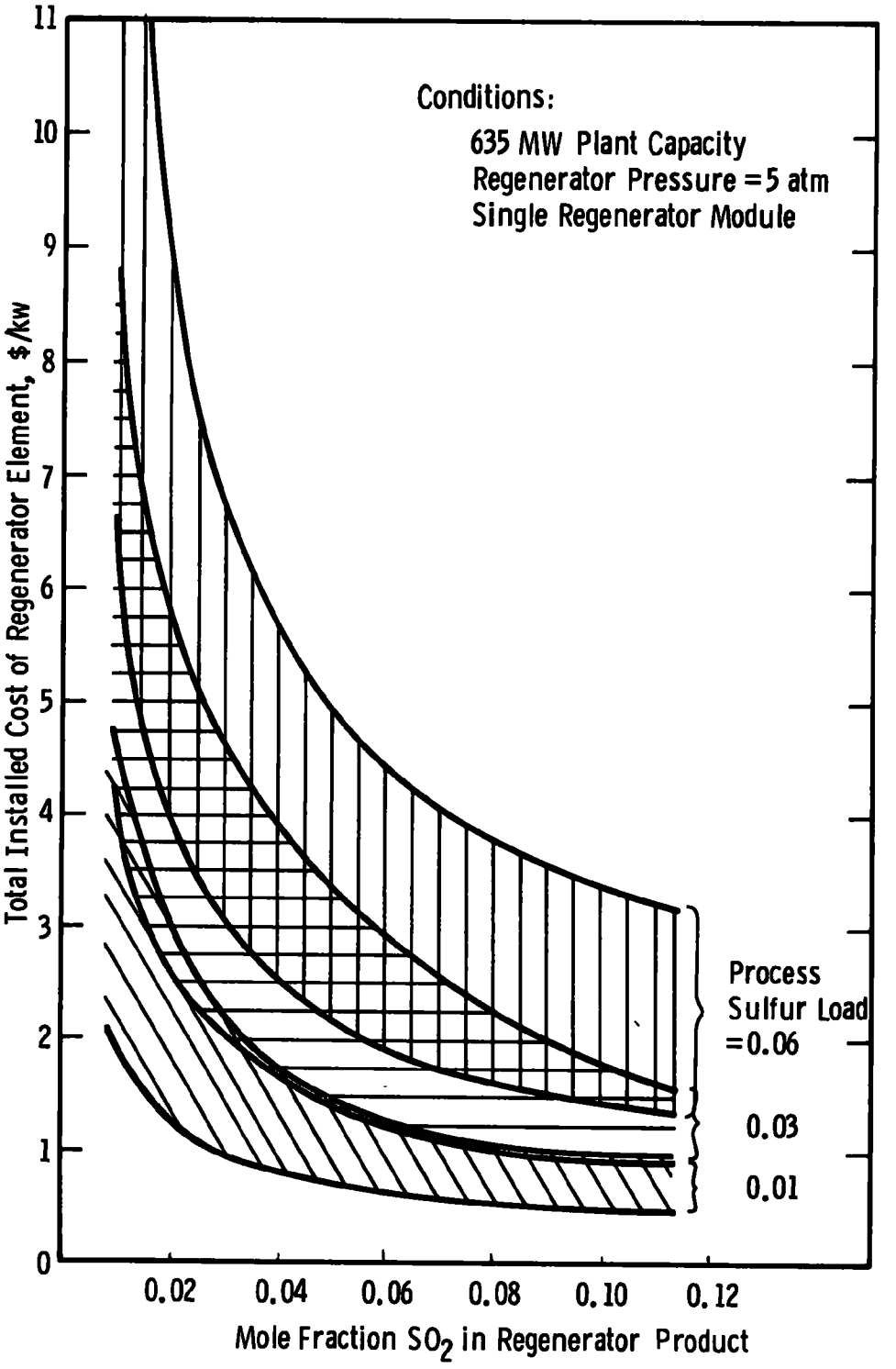

Figure L-9: Regenerator Element Capital Investment

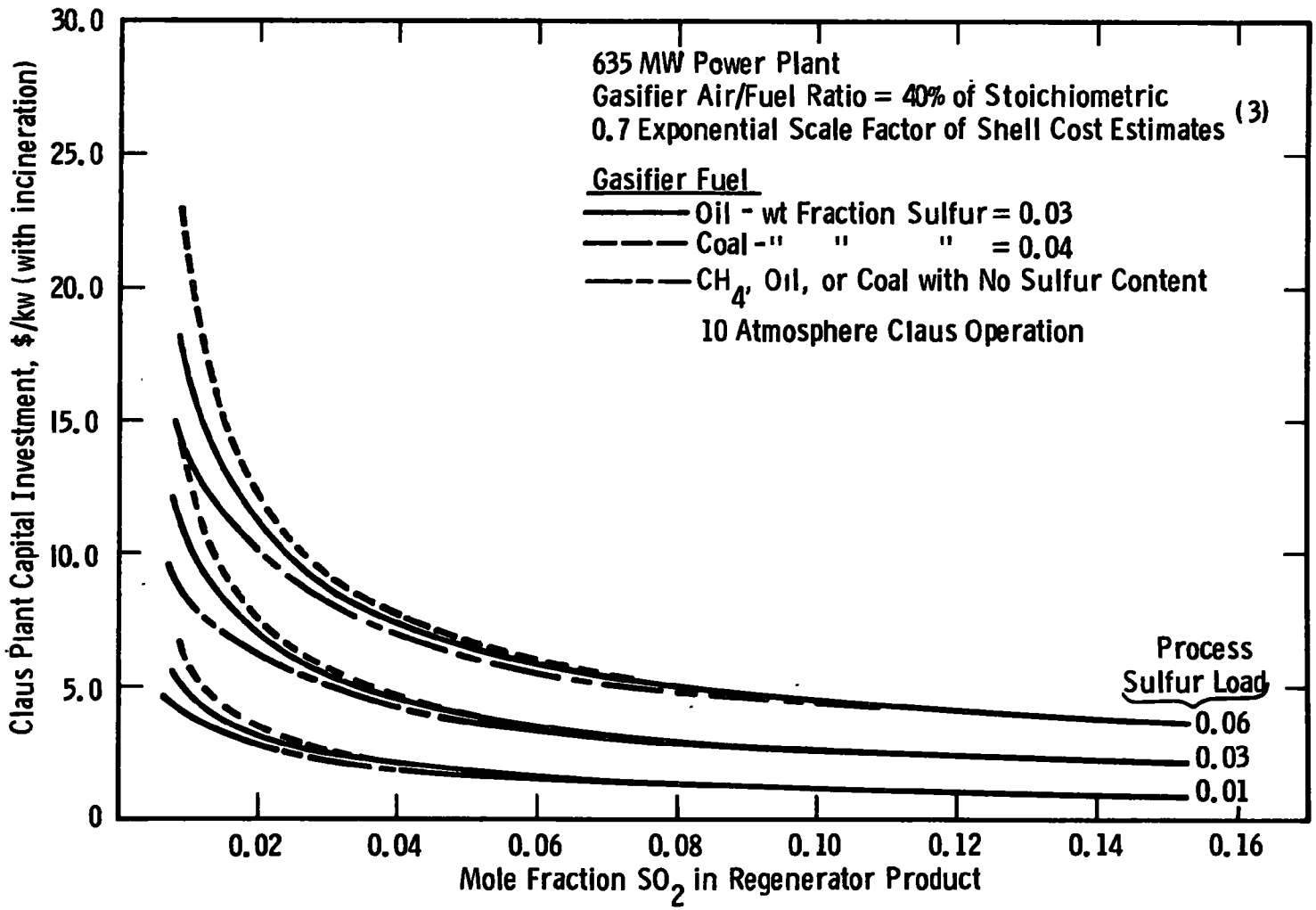

Figure L-10: Sulfur Recovery Element Capital Investment

Curve 650541-B

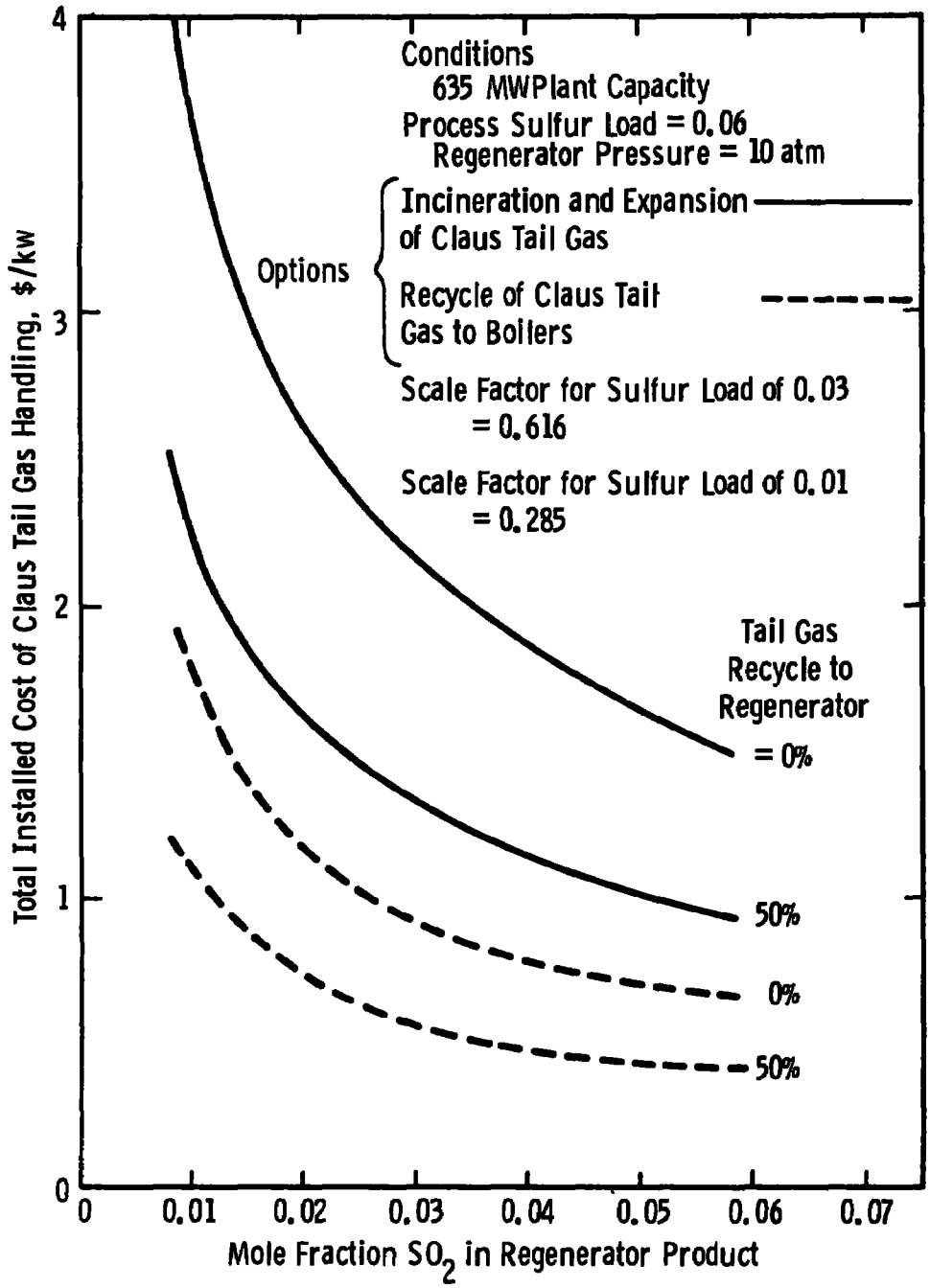

Figure L-11: Tail Gas Handling Element Capital Investment

Sulfur Recovery Element

The capital investment for the sulfur recovery element is based on a study by Shell.[3] Figure L-10 shows the cost for a 10 atmosphere Claus operation with the cost of tail gas incineration included. Incineration was assumed to amount to about 20% of the Claus plant investment. The effect of sulfur content in the gas producer fuel is included in the figure. The contribution of the sulfur recovery element to the total (process cost) is about the same as the regenerator element.

Tail Gas Handling Element

The tail gas handling element cost is shown in Figure L-11 for the two options listed in Table L-4 with a pressure of 10 atmospheres. The graph represents a sulfur load of 0.06 with scale factors for sulfur loads of 0.03 and 0.01 given in the figure. Curves are shown for percent recycles of tail gas to the regenerator of 0 and 50.

The contribution of the tail gas handling component to the total one-step regeneration process cost is the smallest of the five elements. Recycle of the Claus plant tail gas to the boiler is cheaper than incineration of the tail gas at a regenerator pressure of 10 atmospheres. The costs of the two options are similar at 5 atmospheres, and the cost of boiler recycle greatly exceeds the cost of incineration at 2 atmospheres pressure. It should be recalled that no modification to the boiler system was assumed in the case of the boiler recycle option (see Figure L-3).

The advantages of recycling the Claus flue gas to the boiler should be considered even for the low-pressure regeneration where incineration is much cheaper than recycling. These advantages are

- Improved plant sulfur removal efficiency if the tail gas is recycled to the boiler
- Possibly higher gas-turbine inlet temperatures if the tail gas is recycled to the gas-turbine combustor
- Decreased fuel requirements for the regeneration process.

These considerations should be examined in much greater detail.

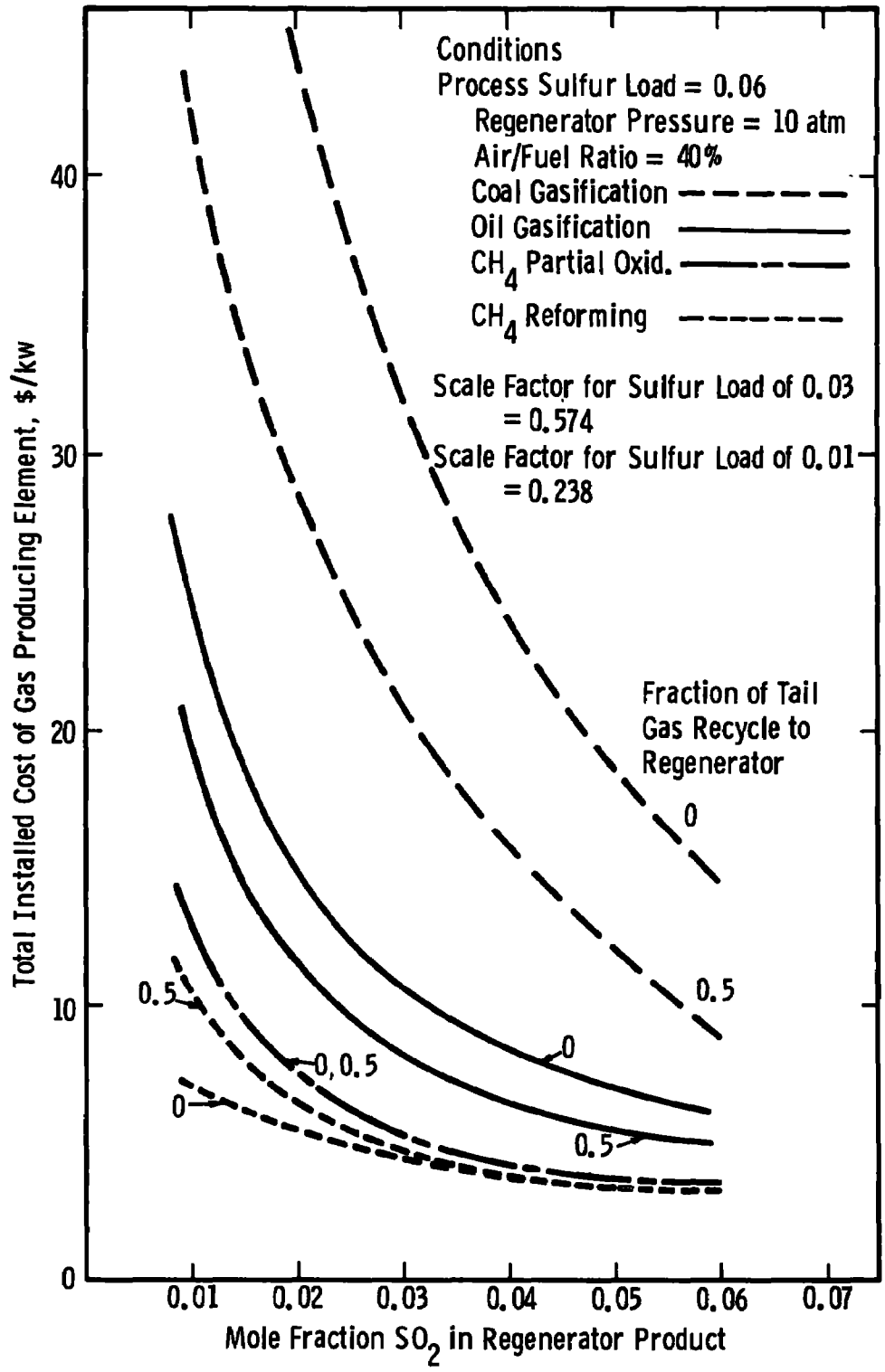

Figure L-12: Gas-Producing Element Capital Investment

Reducing-Gas Producer Elements

Reducing-gas production represents a large contribution to the total process cost. Figure L-12 gives costs for the gas producer element with the four fuel options of coal gasification, oil gasification, methane partial oxidation, and methane reforming, and with sulfur loads of 0.06, 0.03, and 0.01. Percent tail gas recycles to the regenerator of 0 and 50 are shown. Higher air/fuel ratios will reduce the cost of reducing-gas production.

The fuel options have the same order of relative cost, with coal gasification being the most expensive, at all regenerator pressures. Oil gasification is the second most expensive option at all pressures. Methane reforming is the least expensive option at 10 atmospheres pressure, and methane partial oxidation is the cheapest at 2 atmospheres pressure. The cost of coal and oil gasification is reduced by increasing the amount of tail gas recycle to the regenerator, while the cost of methane partial oxidation and methane reforming remains nearly the same as the amount of recycle is increased.

The merits of the various gas producing options can only be compared for a given regenerator performance (mole fraction SO_2 in the regenerator product). The specific performance of regeneration with the reducing gases produced by the four gas producing options is not known and must be investigated. Investigation of one-step regeneration with synthetic mixtures of hydrogen and carbon monoxide may have little relation to the performance obtained with a commercial reducing-gas source.

Sorbent Circulation Element

The capital investment for dolomite circulation at 5 and 2 atmosphere regenerator pressures is about four times the investment at 10 atmospheres. This is shown in Figure L-13 with capital investment plotted against the dolomite sulfur utilization change $X_S^B - X_S^R$. Curves for

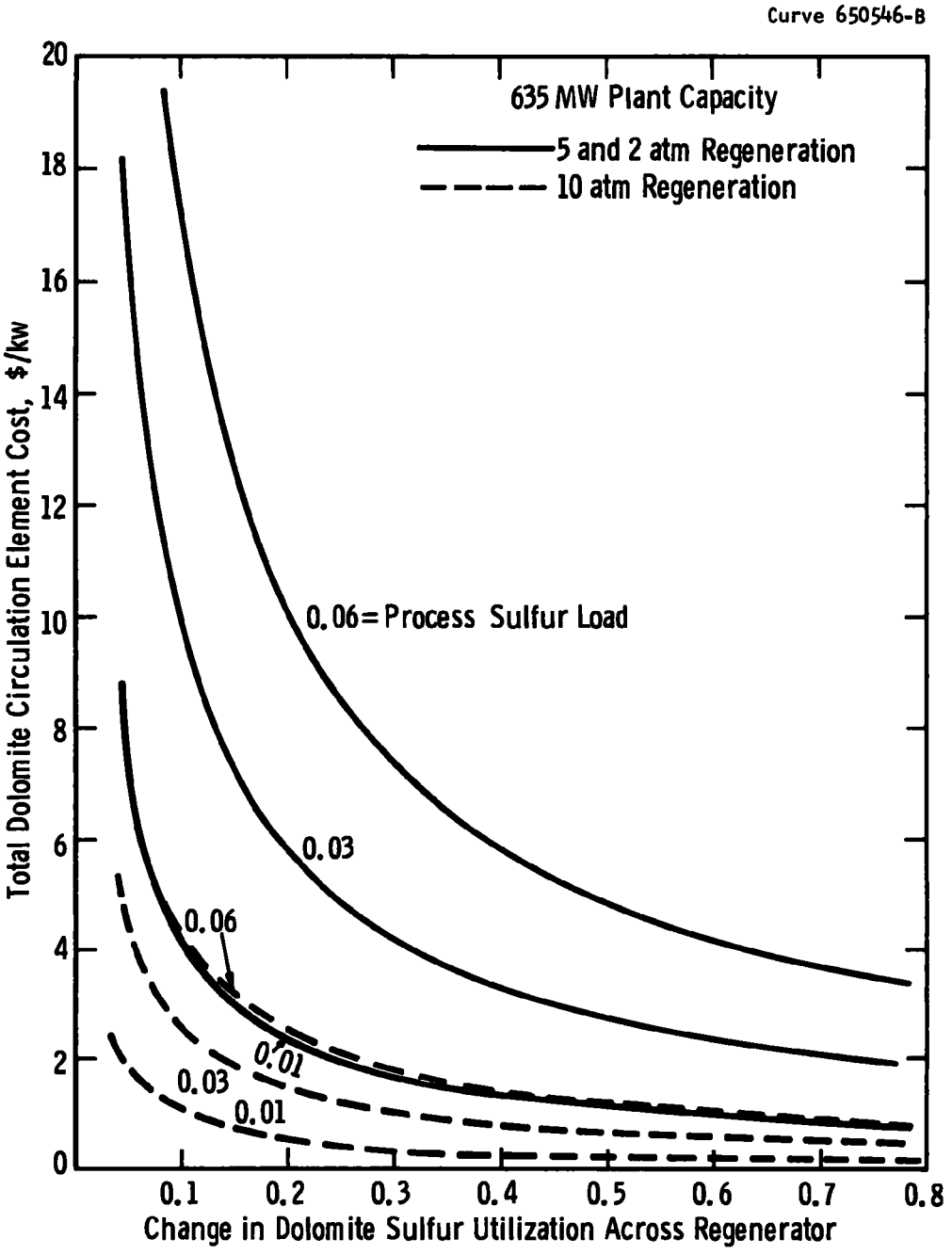

Figure L-13: Sorbent Circulation Element Capital Investment

process sulfur loads of 0.06, 0.03, and 0.01 are shown with regenerator pressures of 10 atmospheres, and 5 and 2 atmospheres.

Capital investment for dolomite circulation has been assumed identical for the 2 and 5 atmosphere pressure cases because essentially the same equipment is required with both pressures. While dolomite circulation is relatively cheap at a regenerator pressure of 10 atmospheres, the capital investment is very significant at 2 and 5 atmospheres. Part of this additional cost is due to the need to cool the dolomite down to 800°F so that existing values may be used. The introduction of high-temperature values would reduce the investment.

Total One-Step Regeneration Process Capital Investment

Samples of total process capital investments for a process sulfur load of 0.03 at pressures of 2, 5, and 10 atmospheres are shown in Table L-7. SO_2 mole fractions which might be expected at each pressure have been indicated in the table along with the corresponding capital investment ranges. For the most part the total capital investment is less than that expected for a stack gas cleaning device on a conventional coal-fired power plant (30 to 50 $/kw). Depending on the actual regenerator performance, operation at regenerator pressures lower than the boiler pressure may be justified, even with the large cost penalty paid for dolomite circulation at low pressures. The capital investment for other process sulfur loads can be estimated by extrapolation from the results for sulfur loads of 0.06 and 0.01 which have been generated.

ENERGY COSTS

Energy costs for a pressurized fluid bed combustion power plant utilizing the one-step regeneration process have been computed on the following basis:

- The cost of a 635 MW pressurized fluid bed combustion power plant, excluding dolomite regeneration, has been estimated as 228.77 $/kw (includes interest during construction).[1]

TABLE L-7

TOTAL INSTALLED REGENERATION PROCESS COST, $/kw[a]

Regenerator Pressure (atm)	SO_2 Mole Fraction	Cost Range, $/kw			
		Coal Gasification	Oil Gasification	CH_4 Oxidation	CH_4 Reforming
10	0.01	27.5-56.5	22.0-31.0	18.5-28.0	15.5-27.5
	0.03	13.5-29.0	11.5-17.0	9.0-14.5	9.0-15.0
5	0.03	20.0-42.5	18.0-29.0	16.0-26.5	16.0-26.5
	0.06	13.0-28.5	12.5-23.0	11.5-20.0	12.0-20.5
2	0.09	13.0-29.0	12.5-24.5	11.0-21.0	12.0-23.0
	0.14	10.5-23.5	10.0-20.5	9.0-18.0	10.0-19.5

[a]Conditions: 635 MW fluid bed coal combustion plant
$W_s\ [\varepsilon - m\ X_s] = 0.03$

Curve 650534-B

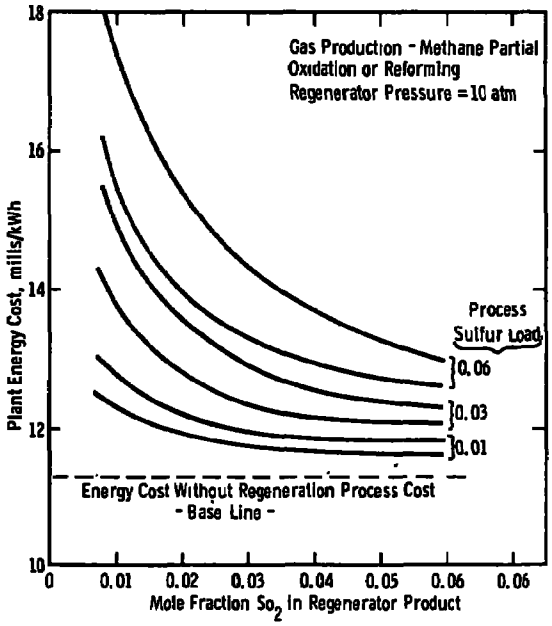

Figure L-14. Energy Cost-Methane at 10 Atmospheres

Curve 650539-B

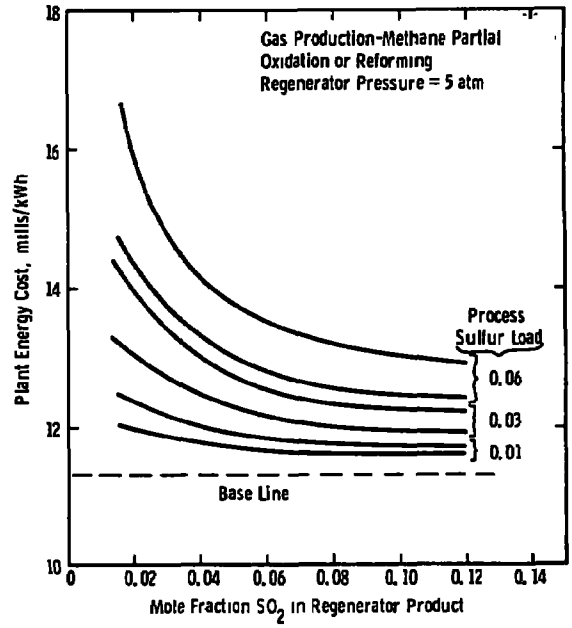

Figure L-15 Energy Cost-Methane at 5 Atmospheres

Curve 650545-B

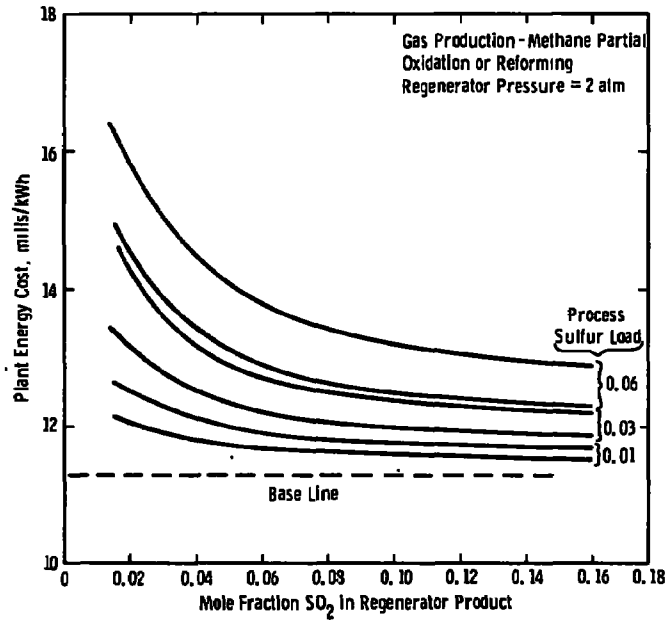

Figure L-16 Energy Cost—Methane at 2 atmospheres

Curve 650544-B

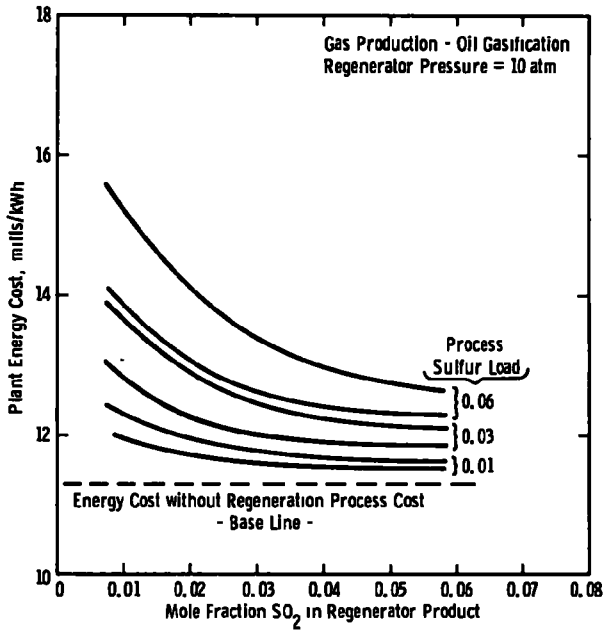

Figure L-17 Energy Cost-Oil at 10 Atmospheres

Curve 650543-B

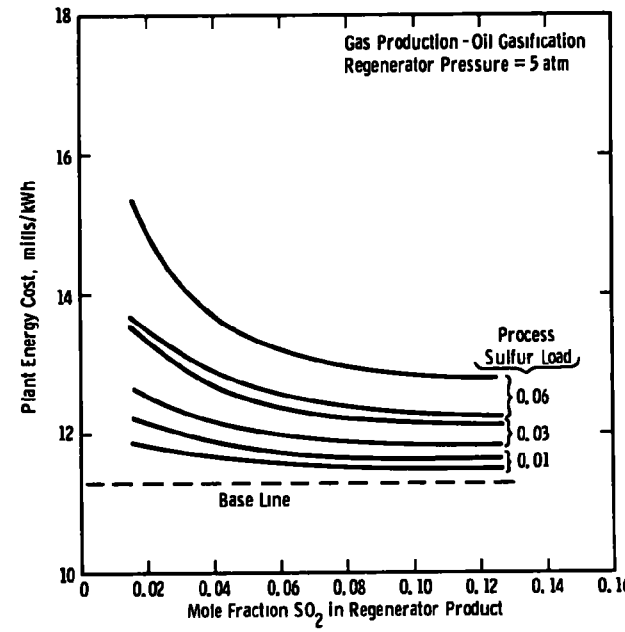

Figure L-18 Energy Cost — Oil at 5 Atmospheres

Curve 650542-B

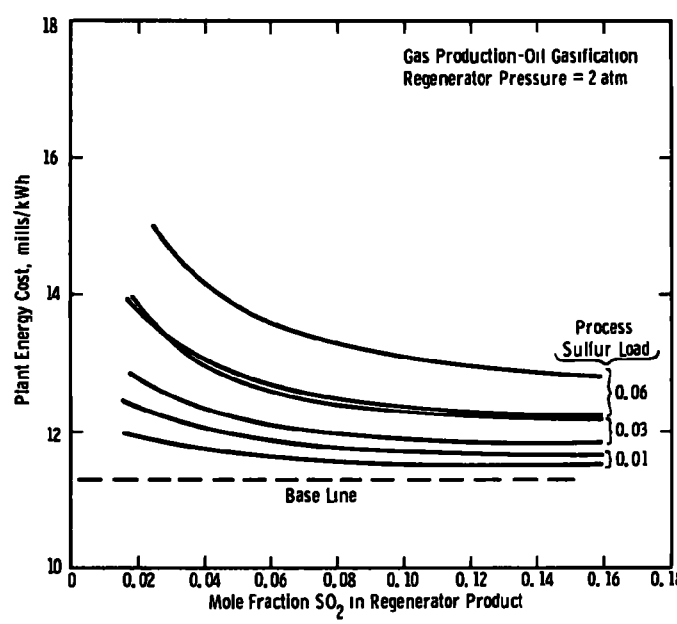

Figure L-19 Energy Cost-Oil at 2 Atmospheres

- Interest during construction is charged on the one-step regeneration process investment at 7-1/2% for 3-1/2 years construction period.
- Capital charges at 15%/yr
- O&M charges at 2%/yr
- Dolomite at $2/ton; make-up rate of 1 mole Ca/mole S fed
- 70% capacity factor
- No credit for recovered sulfur
- Plant heat rate of 8967 Btu/kWh (excluding inefficiency of regeneration process)
- Fuel costs
  - Coal at 45¢/MM Btu
  - Oil at 45¢/MM Btu
  - Methane at 80¢/MM Btu
- Operating water at 8¢/M gal

Total energy costs for a 635 MW pressurized fluid bed combustion power plant utilizing one-step dolomite regeneration is shown in the following set of graphs, Figures L-14 through L-22. Each group refers to a specific gas producer fuel and a specific regenerator pressure. Energy cost ranges are shown for process sulfur loads of 0.01, 0.03, and 0.06 as a function of the regenerator product SO_2 mole fraction.

General conclusions drawn from the set of graphs are that the use of methane by either partial oxidation or reforming is the most costly process option due to the high cost associated with methane, and coal gasification is the second most costly due to the high capital cost associated with coal gasification. Oil gasification is the least costly of the process options due to the low capital cost and low fuel cost. These conclusions are largely dependent on the cost basis used to compute energy costs,and other bases may change the relative significance of capital costs and fuel costs. Care should also be exercised in comparing the plant energy cost of the various fuel options considered because the regeneration performance with the four

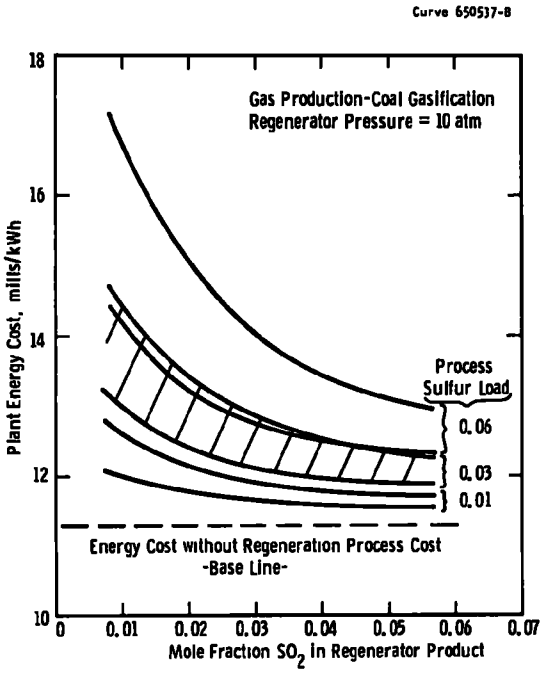

Figure L-20 Energy Cost-Coal at 10 Atmospheres

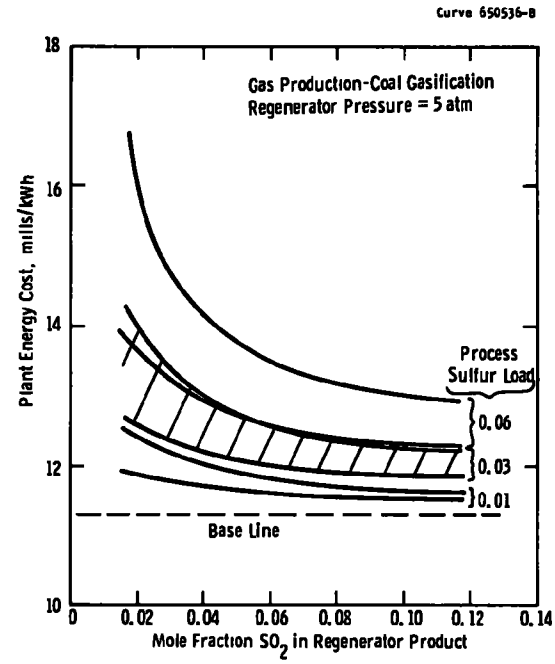

Figure L-21 Energy Cost-Coal at 5 Atmospheres

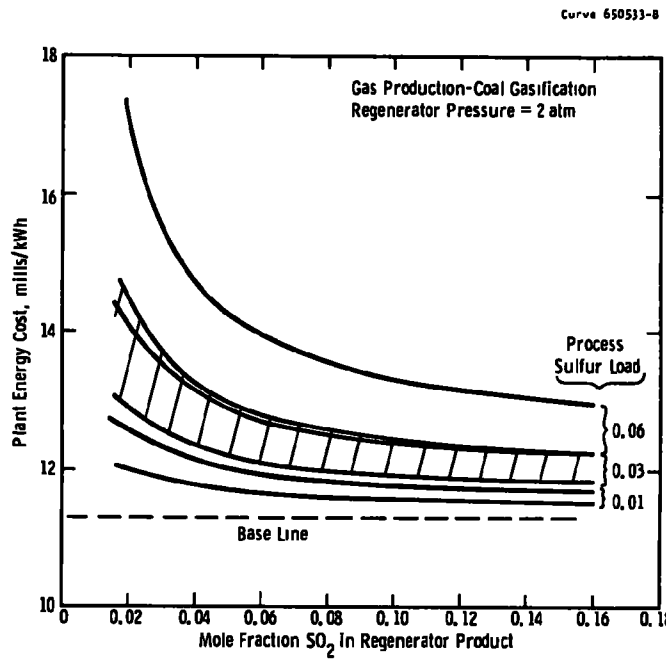

Figure L-22 Energy Cost - Coal at 2 Atmospheres

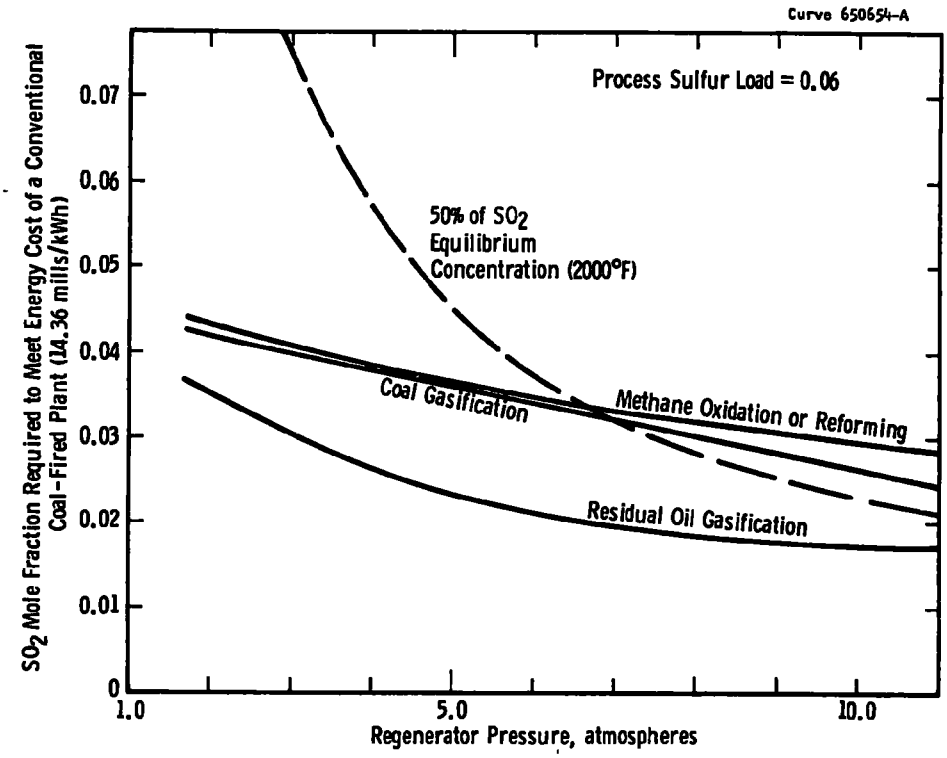

Figure L-23: Energy Cost Comparison-High-Sulfur Load

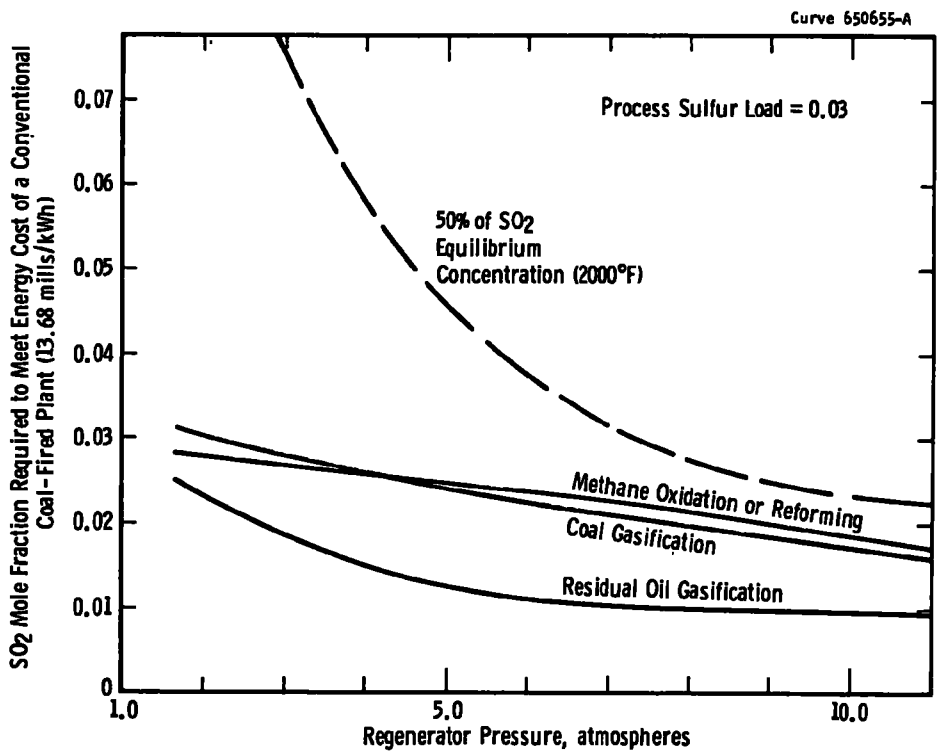

Figure L-24: Energy Cost Comparison-Medium Sulfur Load

fuel options is not known. Thus, the SO_2 mole fraction possible at a given regenerator pressure may differ among the four fuel options, and it may be possible to operate one fuel option at the lower end of the indicated cost range at a given SO_2 mole fraction while another fuel option may require operating at the high end of the cost range.

The energy cost has been computed assuming that 30 to 50% of the fuel energy input into the gas producer element can be utilized to generate power. This may be a significant consideration at low SO_2 mole fractions. For example, if none of the fuel energy input to the regeneration process can be utilized to generate power then the plant energy cost will increase about 5% at an SO_2 mole fraction of 0.01. At high SO_2 mole fractions this consideration becomes unimportant. For example, at a mole fraction of SO_2 of 0.05 the increase in plant energy cost is less than 1% if no useful energy is provided by the regeneration process fuel input. If the one-step regeneration process can be operated at SO_2 mole fractions of about 0.10 or higher, then the recovery is not required for economic feasibility. If SO_2 mole fractions no higher than 3 to 4% can be realized in practice, then every effort must be made to recover useful energy from the regeneration process since the penalty for not recovering the energy is significant.

The energy cost graphs indicate that, at a fixed SO_2 mole fraction, decreasing the pressure increases the plant energy cost. The SO_2 mole fraction may increase, though, as the pressure is decreased to an extent large enough to make the plant energy cost lower at lower pressures. Experimental evidence with each of the fuel options considered is required in order to compute the advantage or disadvantage of going to lower regeneration pressures.

The effect of the process sulfur load is also indicated in the graphs. This parameter is extremely significant at low SO_2 mole fractions. The energy cost of a pressurized fluid bed combustion power plant without the cost of the dolomite regeneration process is included in the graphs to provide a base line (11.3 mills/kWh).

CONCLUSIONS OF GENERAL STUDY

Important Assumptions

- No change in boiler performance -- no boiler modifications needed
- Constant cost (base case) of make-up dolomite feeding and handling
- Constant dolomite make-up rate of 1 mole Ca/mole S under all conditions
- Low dolomite purchase and disposal cost of $2/ton
- No sulfur in reducing-gas producer fuel; coal and oil at 45¢/MM Btu
- Constant Claus plant sulfur removal efficiency of 95% under all conditions
- Regeneration/sulfur recovery system thermal efficiency of 30 to 50%
- Temperature control requirements assumed small and not costly.

Cost Comparison with Alternative

Alternative

- The alternative would be a conventional coal-fired power plant utilizing limestone wet scrubbing for pollution control -- 635 MW with same process sulfur load.

Basis

- Highest cost in cost range selected for one-step regeneration process
- Capital costs for limestone scrubbing system taken from "Some General Economic Considerations of Flue Gas Scrubbing for Utilities," J. K. Burchard, G. T. Rochelle, W. R. Schofield, J. O. Smith, Control Systems Division, E.P.A., October, 1972.

- Capital cost of conventional coal-fired plant and energy cost basis taken from "Evaluation of the Fluidized Bed Combustion Process."

TABLE L-8

CONVENTIONAL PLANT ENERGY COST
WITH LIMESTONE WET SCRUBBING

Process Sulfur Load	Energy Cost, (mills/kWh)
0.01	13.37
0.03	13.68
0.06	14.36

TABLE L-9

ENERGY COST COMPARISON[a]

Process Sulfur Load	Regenerator Pressure Atm	Reducing-Gas Producer Fuel		
		Coal	Oil	Methane
0.03	10	1.7	0.95	1.85
	5	2.5	1.25	2.5
	2	3.0	2.3	2.8
0.06	10	2.65	1.75	2.95
	5	3.6	2.35	3.65
	2	4.2	3.5	4.3
0.01	10			
	5		< 1.0	
	2			

[a] SO_2 break-even mole percent to meet energy cost of a conventional coal-fired power plant with limestone wet scrubbing.

Cost Conclusions

- At a fixed SO_2 mole fraction, decreasing the pressure increases the capital and energy costs slightly.
- The energy and capital costs increase drastically as the SO_2 mole fraction decreases below about 5%.
- As the regenerator pressure is decreased, the equilibrium SO_2 concentration increases much faster than does the SO_2 concentration required to meet a fixed energy cost.
- The energy and capital costs increase faster with increased process sulfur load than does the cost of a conventional coal-fired power plant utilizing limestone wet scrubbing.
- The cost feasibility of one-step regeneration at all pressures, all gas producer fuels, and all process sulfur loads considered is not limited by equilibrium, though the ability to meet the cost of a conventional plant utilizing limestone wet scrubbing becomes greater at lower regenerator pressures and lower process sulfur loads.
- Low-pressure regeneration should be considered and has many potential advantages over high-pressure regeneration:
  - SO_2 mole fractions not much greater than 0.01 have been obtained in batch tests at 10 atmospheres pressure while mole fractions of 0.08 have been obtained at atmospheric pressures. One percent SO_2 is too low at a process sulfur load of 0.03 while 8% is a reasonable SO_2 level.
  - Roughly, equipment sizes are proportional to $(Y_{SO_2}P)^{-1}$ while the fuel requirements are proportional to $(Y_{SO_2})^{-1}$.
  - At low SO_2 mole fractions (< 5%), the thermal efficiency of the regeneration process must be maximized in order to maintain cost feasibility, while at high SO_2 mole fractions (> 10%), the recovery of useful energy from the regeneration process is not required. Maximum thermal efficiency is probably less than 50%

- The energy costs are optimistic for coal and oil gasification at low SO_2 mole fractions (< 3%) because the presence of sulfur in these fuels is neglected. With high-sulfur fuels the fuel requirements, Claus plant sulfur load, and energy cost will increase drastically as the SO_2 mole fraction drops below 3%. The alternatives of desulfurization of the reducing gas or the use of low-sulfur fuels will also increase the energy cost.
- Temperature control requirements (energy inputs or energy withdrawals) are reduced at higher SO_2 mole fractions.

Design Conclusions

- The incentive to develop an integrated reducing-gas producer-dolomite regeneration reactor is small unless performance is improved by integration.
  - Capital saving slight
  - No savings in energy cost unless the SO_2 fraction is increased
  - Possible introduction of complications
- Regenerator vessel modules rather than a single vessel should be considered to aid turndown.
- Recycle of tail gas to the fluid bed boiler is attractive, especially at high regenerator pressures. Further study is required.
- Dolomite circulation at low regenerator pressures is about four times the capital investment for dolomite circulation at 10 atmospheres. Further design analysis is required.

Problem Areas and Major Unknowns

Reducing-Gas Producer Element

- Composition of reducing gas
  - Tars
  - Trace metals, etc.
  - Sulfur (or desulfurization of reducing gas)
  - Particulate material
- Operability of gas producer (especially coal gasifier)
  - Control
  - Flexibility
  - Reliability.

Regenerator Element

- Effect of reducing-gas contaminants on regenerated stone
- Regenerator product gas composition and contaminants

  SO_2, H_2S, O_2, H_2O, CO, H_2, tars, metals, etc.
- Ash agglomeration
- Regenerated stone composition
- Attrition and elutriation
- Effect of pressure cycling on stone
- Temperature control.

Sulfur Recovery Element

- Effect of regenerator gas product composition (including particulates) on sulfur removal efficiency of Claus plant, catalyst life, fuel requirements, etc.
- Composition of Claus plant tail gas.

Tail Gas Handling Element

- Incineration option
  - Sulfur and other pollutant emitted
  - Fuel required and recoverable energy

- Boiler recycle option
  - Effect on boiler performance
  - Modifications to boiler required
  - Contaminants in recycle gas and effect on gas turbine.

Sorbent Circulation Element

- Operability and control
- Melt formation
- Stone cooling method
- Attrition.

Experimental Data Required

- Conditions to maximize SO_2 mole fraction
- Stone composition and activity; attrition
- Limestone or dolomite sorbent characteristics
- Maximum stone utilization capability
- Effect of pressure, temperature cycling
- Effect of reducing-gas composition (typical compositions from commercial gas sources)
- Regenerator product gas composition
- Effect of ash in regenerator
- Temperature control data, operability, sensitivity
- Sulfur recovery from product gas-fuel required, poisoning, etc.
- Analysis of Claus plant tail gas composition
- Demonstration of stone circulation between vessels with large pressure differential
- Demonstration of gas producer operability.

REFERENCES

1. "Evaluation of the Fluidized Bed Combustion Process," Vols. I-III, submitted to the Office of Air Programs E.P.A. by Westinghouse Research Laboratories, Pittsburgh, Pa., November 1971.

2. "A Regenerative Limestone Process for Fluidized Bed Coal Combustion and Desulfurization," R. C. Hoke, H. Shaw, M. S. Nutkis, L. A. Ruth, Esso Research and Engineering Company, Monthly reports under Contracts CPA 70-19 and 68-02-0617.

3. "Claus Technical and Economic Study," R. T. Shpall, Shell Development Company, OAP Contract EH SD-71-45 Task Order No. 15.

4. J. Agosta, H. F. Illian, R. M. Lundberg, O. G. Tranby, Commonwealth Edison Company, Chicago, Illinois, "Status of Low BTU Gas as a Strategy for Power Station Emission Control," A.I.Ch.E., 65th Annual Meeting, November 1972.

5. Information provided in correspondence from Shell, February 28, 1972.

M

APPENDIX M

LOW-SULFUR COAL FLUID BED COMBUSTION

The economics of fluid bed combustion of low-sulfur coal has been estimated. Two cases have been considered: the combustion of a 1 wt % sulfur coal which requires some desulfurization in order to meet SO_2 emission standards, and the combustion of a coal requiring no desulfurization. Capital investments and energy costs for the pressurized fluid bed combustion power plant have been compared to the costs of a conventional coal-fired power plant using limestone wet scrubbing in the two cases.

CASE I: 1 WT % SULFUR COAL REQUIRING DESULFURIZATION

For the pressurized fluid bed combustion plant both once-through and regenerative operations have been considered. In addition, desulfurization efficiencies of 50% and 70%, giving SO_2 emissions equivalent to 0.5 wt % and 0.3 wt % sulfur coal, respectively, are included. The cost basis is listed in Table M-1.

TABLE M-1

COST BASIS

- Fluid bed combustion capital costs and energy cost basis are taken from Reference 1.
- Conventional power plant capital costs are taken from Reference 1 and limestone wet-scrubber costs from Reference 2.
- Capital charges at 15%, fuel at 45 ¢/MM Btu, dolomite at $10/ton, 70% capacity factor, 635 MW plant.
- Once-through fluid bed combustion costs are based on 50% dolomite utilization.
- Regenerative fluid bed combustion costs are based on the one-step dolomite regeneration process at a pressure of 10 atmospheres.

- Limestone wet-scrubbing system includes reheat, bypass, pond.
- Plant heat rates (Btu/kWh) are as follows: once-through fluid bed combustion plant -- 9000; regenerative fluid bed combustion plant -- 9300; conventional plant -- 9400.

Table M-2 lists the results of the cost analysis.

TABLE M-2

COST RESULTS WITH 1 WT % SULFUR COAL

	Plant Investment, $/kw		
	Fluid Bed Combustion		Conventional Plant with
Desulfurization (%)	Once-through	Regenerative	Limestone Wet Scrubbing
50	265.0	272.5	330.5
70	265.5	278.5	331.4
	Plant Energy Cost, mills/kWh		
50	11.24	11.58	13.29
70	11.31	11.86	13.36

These results indicate that the economic advantages of fluidized bed combustion over the conventional plant using limestone wet-scrubbing are large when a 1 wt % sulfur fuel requiring desulfurization is being considered. A reduction of 15% in the energy cost is projected.

CASE II: LOW-SULFUR COAL REQUIRING NO DESULFURIZATION

With no desulfurization required, the pressurized fluid bed combustion plant can be operated without dolomite handling, storage, feeding, and disposal and without dolomite regeneration. The conventional power plant can be operated without limestone wet scrubbing but must include an electrostatic precipitator for particulate control. If the basic pressurized fluid bed combustion plant design is assumed (1) then the figures in Table M-3 result.

TABLE M-3
COST RESULTS WITH NO DESULFURIZATION

	Capital Cost, $/kw	Energy Cost, mills/kWh
Pressurized Fluid Bed Combustion	260.5	11.12
Conventional Plant	316.3	12.51

About an 11% reduction in energy cost is estimated by applying pressurized fluid bed combustion with the basic design condition used when desulfurization was an important consideration. With no desulfurization required many improvements in the pressurized fluid bed combustion design conditions could be utilized. Some of these factors are listed in Table M-4.

While it does not appear that the total plant cost could be reduced significantly by the factors in Table M-4, the plant operation with no sulfur removal would be considerably simpler than the operation with sulfur removal.

TABLE M-4

DESIGN FACTORS RESULTING FROM NO SULFUR REMOVAL REQUIREMENT

Factor	Effects
Bed Material (type of material, shape, size, or size distribution)	higher or lower fluidization velocity: may result in small cost savings even at the optimum velocity[4] (Figure M-1)
	higher heat transfer coefficient: less heat transfer surface could result in a cost saving of only about $2/kw; would insure against operating in the region of low heat transfer where costs rise rapidly (Figure M-2)
	limited attrition and elutriation of bed material: could result in a reduction in particle removal equipment of about $3.50/kw[4]
	limited tube wear
	limited solid waste material
Higher Bed Temperature (up to the ash agglomeration temperature)	higher gas-turbine inlet temperature giving a high efficiency; increasing the inlet temperature from 1600°F to 1800°F would decrease plant heat rate from 9026 to 8820 Btu/kWh
	less heat transfer surface in the bed
	could produce a soot having a less damaging nature for the gas turbine
Easier Turndown, Start-up, Control	operate at optimum cycle conditions without sulfur removal restrictions
Operate As an Agglomerating Bed - 2000°F-2100°F	new design concept
	higher gas-turbine inlet temperature
	reduced heat transfer surface
	reduced particulate removal

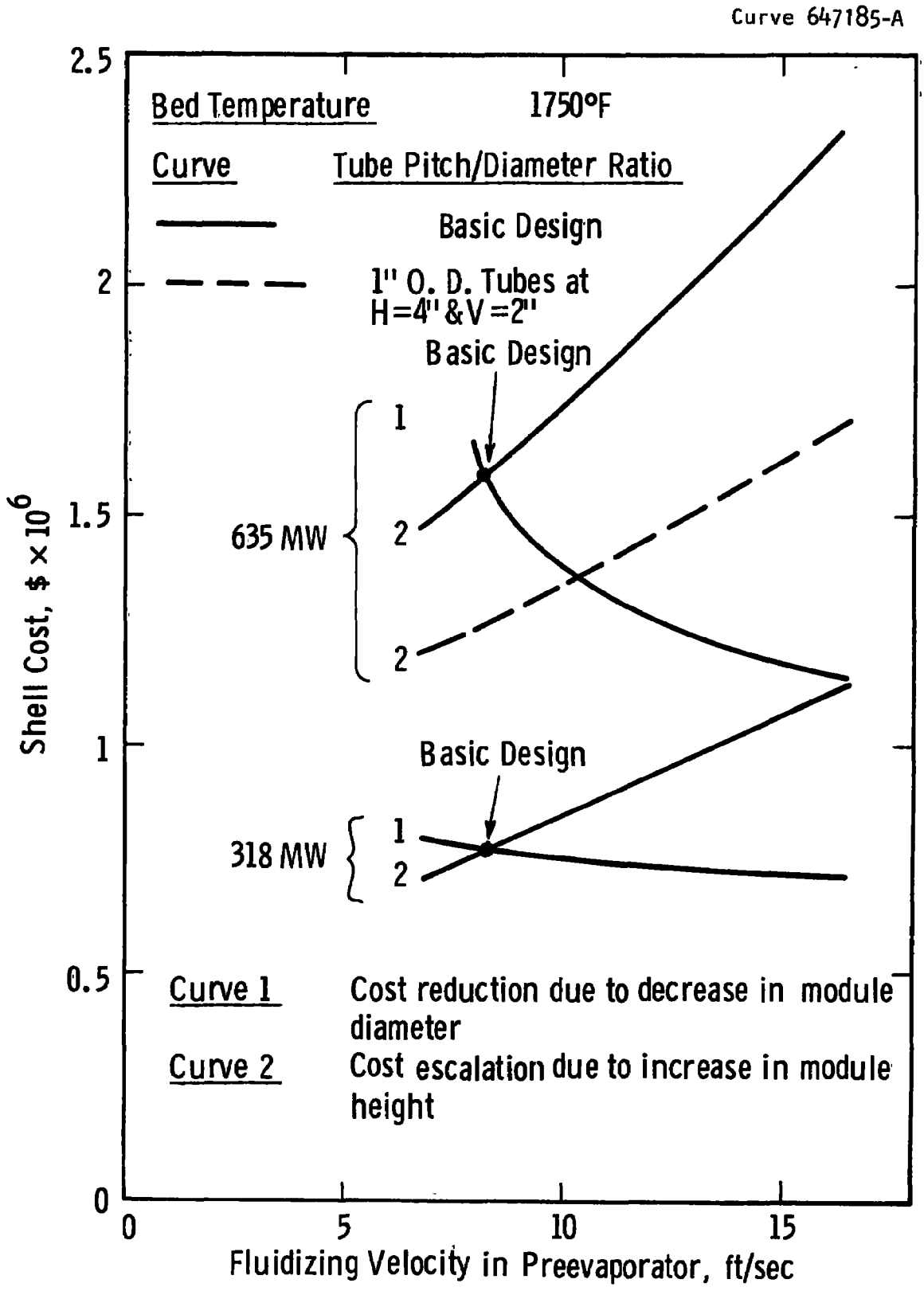

Figure M-1: Dependence of the Shell Cost on the Fluidizing Velocity

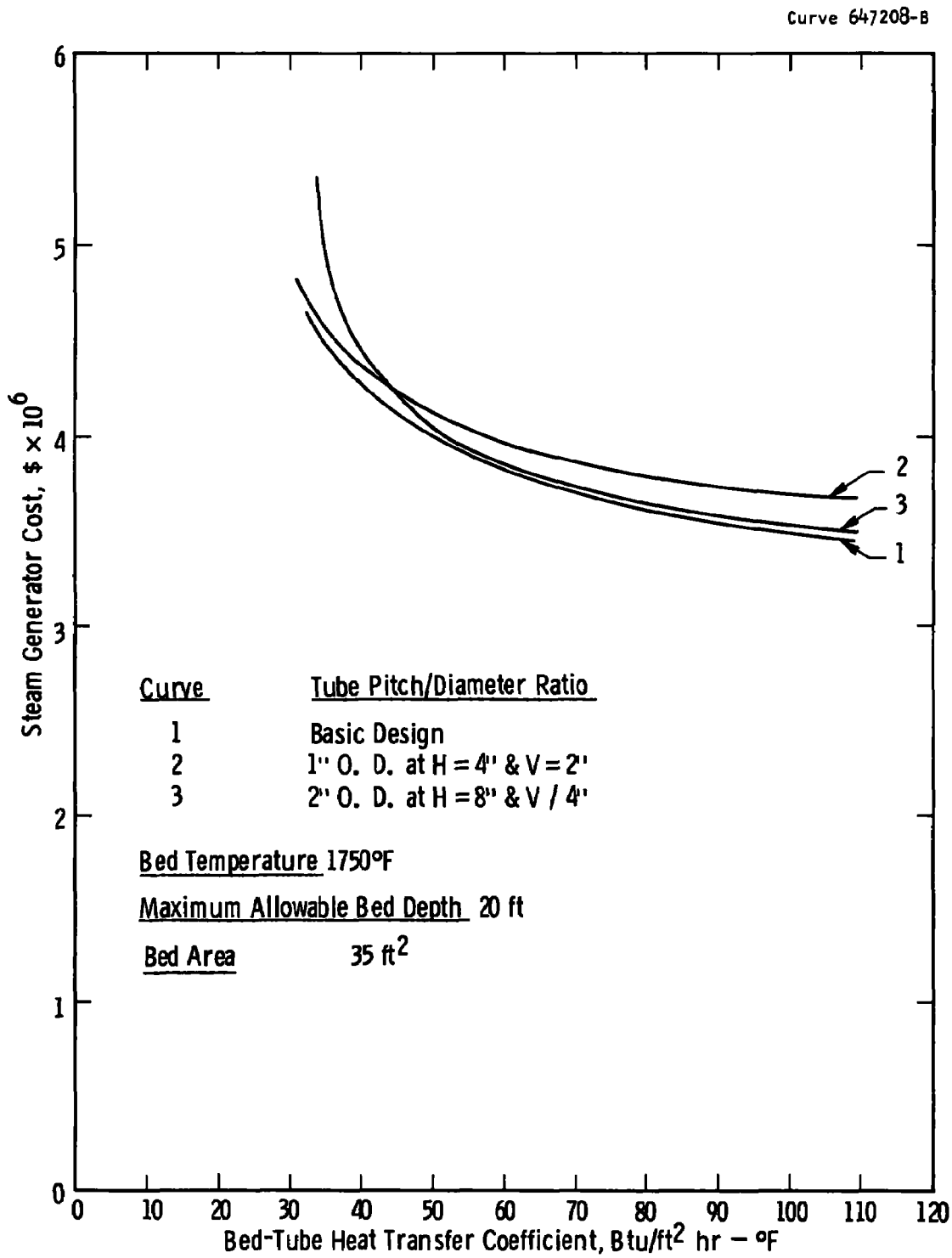

Figure M-2: Effect of Bed-Tube Heat Transfer Coefficient on the Steam Generator Cost (not including erection)

REFERENCES

1. "Evaluation of the Fluidized Bed Combustion Process," Vols. I-III, submitted to the Office of Air Programs E.P.A. by Westinghouse Research Laboratories, Pittsburgh, Pa., November 1971.

2. Burchard, J. K., Rochelle, G. T., Schofield, W. R., Smith, J. O., "Some General Economic Considerations of Flue Gas Scrubbing for Utilities," Control Systems Division, E.P.A., October 1972.

N

APPENDIX N

LIMESTONE WET SCRUBBING COSTS

The cost of power generation with a conventional coal-fired power plant using limestone wet scrubbing has been estimated for purposes of comparison with the pressurized fluid bed boiler power plant. The following basis has been used:

- Wet-scrubber costs include
  - By-pass piping
  - Disposal pond
  - No venturi scrubber
- New plant installation, 635 MW
- Coal-fired power plant cost without scrubber = 306.3 $/kw[1]
- Other factors are the same as those used to compute the capital and energy costs of the pressurized fluid bed power plant.

The limestone wet-scrubber capital investment is shown in Figure N-1 as a function of the weight fraction sulfur in the coal.[2] Table N-2 gives the energy cost breakdown for the conventional plant for a limestone purchase plus disposal cost of $2/ton. The total energy cost is shown in Figure N-1. The energy cost may be expected to vary by as much as 0.5 mills/kWh from one plant to another, but the cost in Figure N-1 is a reasonable average.

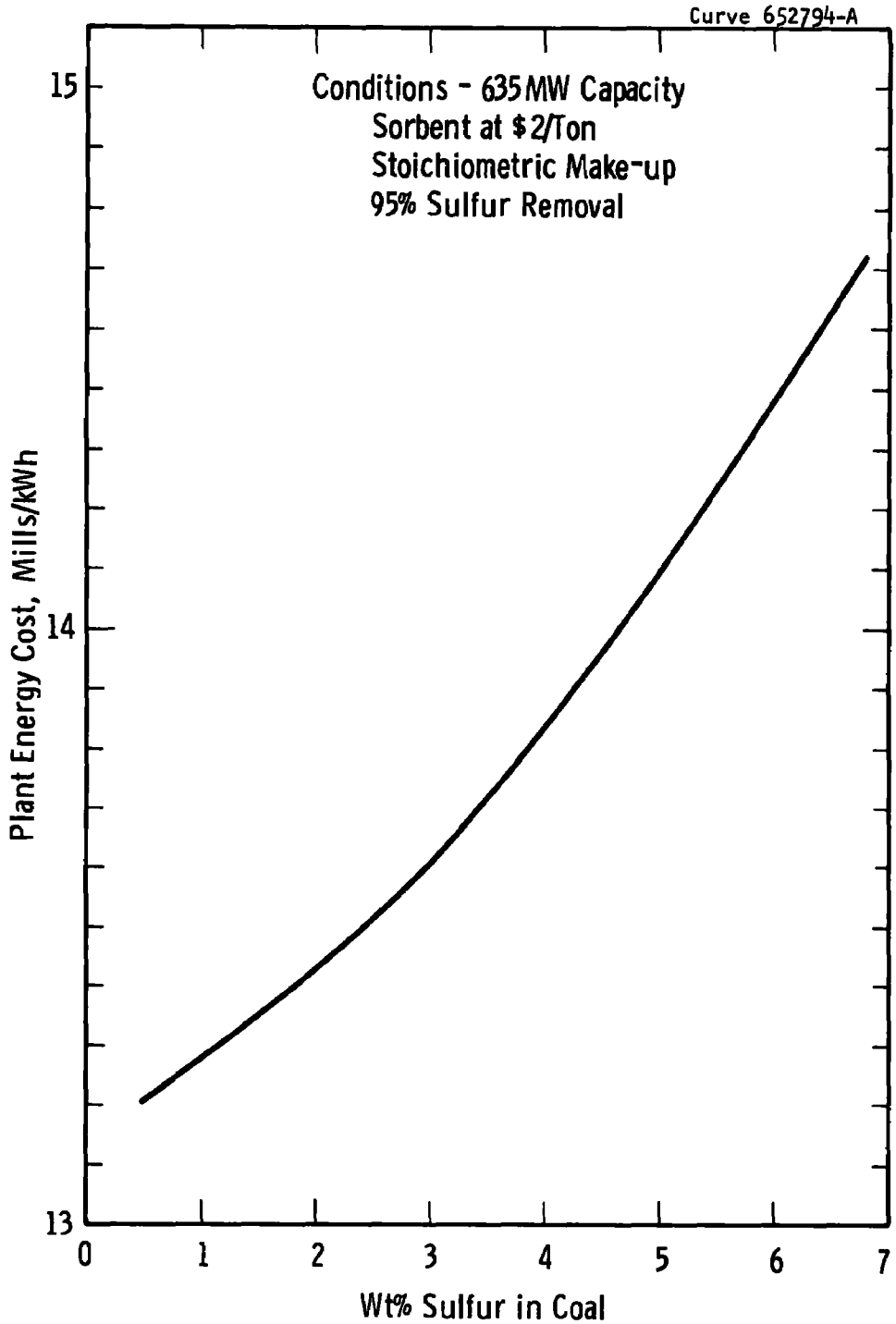

Figure N-1: Energy Cost of a Conventional Coal-Fired Power Plant with Limestone Wet Scrubbing

TABLE N-1

CONVENTIONAL PLANT CAPITAL INVESTMENT

Weight Percent Sulfur in Coal[a]	Capital Investment, $/kw	
	Scrubber System	Total Power Plant
6.0	49.6	355.9
3.0	35.0	341.3
1.0	26.8	333.1

[a]95% sulfur removal

TABLE N-2

CONVENTIONAL PLANT ENERGY COST

	Energy Cost, mills/kWh Weight % Sulfur in Coal		
	6.0	3.0	1.0
Fixed Charges	8.95	8.35	8.15
Fuel (45¢/MM Btu)	4.11	4.11	4.11
Limestone ($2/ton)	0.15	0.075	0.025
O&M	1.17	1.06	0.99
TOTAL	14.38	13.60	13.28

REFERENCES

1. "Evaluation of the Fluidized Bed Combustion Process," Vols. I-III, submitted to the Office of Air Programs E.P.A. by Westinghouse Research Laboratories, Pittsburgh, Pa., November 1971.

2. Burchard, J. K., Rochelle, G. T., Schofield, W. R., Smith, J. O. "Some General Economic Considerations of Flue Gas Scrubbing for Utilities," Control Systems Division, E.P.A., October 1972.

0

APPENDIX O

PART LOAD OPERATION

The ability to change the electrical output of a power system is necessary in order to meet the varying electrical demand. An analysis of the pressurized fluid bed boiler power plant concept has been made to determine its ability to follow load over the desired range. This analysis considers alternative turndown techniques, process limitations, and general performance projections.

To be competitive with conventional steam power plants, the high-pressure fluidized bed boiler power system should have the capability of at least a 75% turndown and a response rate of 5% per minute.

The temperature-enthalpy diagram for the pressurized boiler power system (Figure O-1) shows the energy distribution among the boiler functions, gas-turbine expander, and the heat recovery equipment at a design point of 1750°F bed temperature and 17% excess air. The power output from the system is a function of the following four process parameters:[1]

- Airflow rate
- Fuel/air ratio
- Bed temperature
- Bed depth.

Four modes of load control for the combined cycle fluidized bed boiler have been considered and are summarized in Table O-1. In order to assess these alternative operating modes quantitatively, the limitations imposed on the control variables by the process must be considered. These limitations are summarized in Table O-2.

TABLE O-1

ALTERNATIVE TURNDOWN PROCEDURES

Mode 1

- Constant fuel/air ratio and bed temperature
- Variable airflow and bed depth
- Fuel rate decreases to maintain constant fuel/air ratio.
- Bed depth is reduced simultaneously with airflow to maintain constant bed temperature; turbine inlet pressure decreases to satisfy constant turbine flow number with reduced airflow.
- Steam power decreases because of lower airflow and pressure level.

Mode 2

- Constant airflow and bed temperature
- Variable bed depth and fuel/air ratio
- Bed depth is reduced simultaneously with fuel/air ratio to maintain constant bed temperature.
- Turbine inlet pressure decreases slightly to satisfy constant turbine flow number with reduced fuel flow.
- Steam power decreases because of reduced heat transfer surface; gas-turbine power would be nearly constant.

TABLE O-1 (Continued)

Mode 3

- Constant bed depth and airflow
- Variable fuel/air ratio and bed temperature
- Gas-turbine inlet pressure reduces to satisfy constant turbine flow number with reduced temperature.
- Steam power decreases because of lower bed temperature.
- Gas-turbine power decreases because of lower gas temperature and pressure level.

Mode 4

- Constant bed depth and temperature
- Variable airflow and fuel/air ratio
- Gas-turbine inlet pressure decreases to satisfy constant turbine flow number with reduced airflow.
- Steam power constant; gas-turbine power decreases because of reduced flow and pressure.

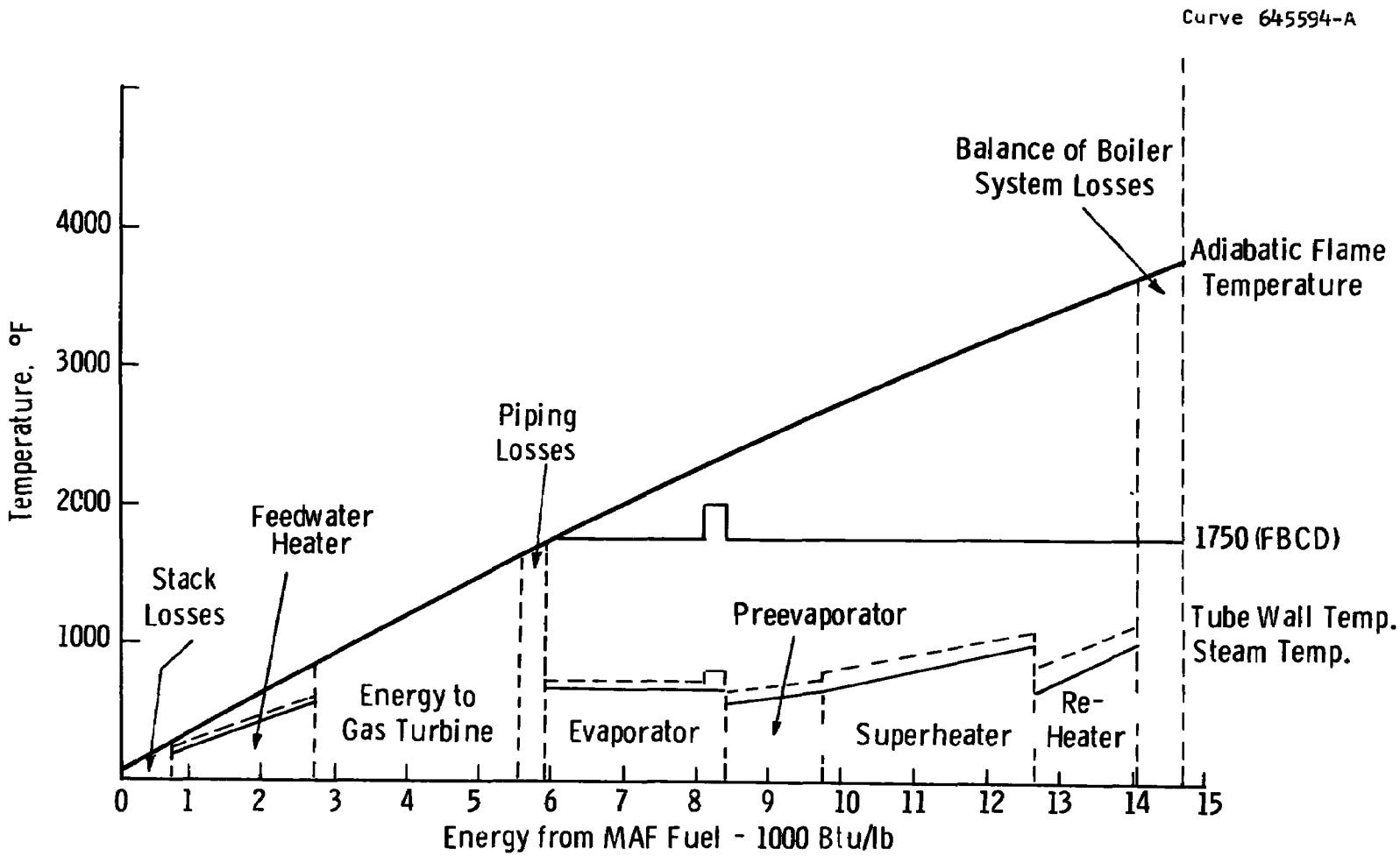

Figure O-1: Temperature-Energy Diagram for Pressurized Utility Boiler

TABLE O-2

PROCESS VARIABLE LIMITATIONS

Airflow Rate	
Fluidized bed	cannot operate at gas velocity below minimum fluidization or greater than terminal velocity of majority of bed material -- ratio ∿ 10 to 1
Combustion	airflow such that excess air greater than ∿ 5%
Gas-turbine	variable inlet guide vanes permit ∿ 33% reduction in gas-turbine airflow
Fuel/Air Ratio	
Combustion	fuel/air ratio maintained such that excess air $\geq$ 5%, <∿ 300%
Bed Temperature	
Sulfur removal	temperature less than ∿ 1750°F, greater than ∿ 1300°F
Combustion	temperature <∿ 2000°F to prevent agglomeration
Bed Depth	
Fluidized bed	depth >∿ 4 ft; upper limit not clear; additional solids handling and storage system required

Within these limitations part load plant performance for two combinations of these control modes has been estimated[1] -- modes 1 and 2 in sequence and modes 3 and 4 in sequence. In both instances, the design point conditions are 1750°F and 10% excess air. These performance estimates are shown in Figure O-2 along with the part load performance of a typical coal-fired plant. The combination of modes 1 and 2 in sequence has a part load performance which is significantly better than that of the conventional plant. The part load performance for operating modes 3 and 4 in sequence is also superior to that of the conventional plant over most of the range, but it is not as good as for operating modes 1 and 2 in sequence.

Any mode with constant bed temperature requires a variable bed depth to control steam power. As shown in Table O-2, the minimum fluidized bed depth is about 4 feet, so design point bed depths of 12 to 14 feet would give a good range. However, in practice heat transfer to the steam cycle is not proportionate to bed depth. What really controls the quantity of heat being transferred is the average heat transfer coefficient of the total heat transfer surface, and the heat transfer coefficient for the surface in the space immediately above the bed is nearly as high as it is in the bed. Because of this, and since varying the bed depth requires expensive materials handling and storage equipment, operating modes which use constant bed temperature were eliminated from consideration for the pressurized fluidized bed boiler system.

The two design point parameters which have the most effect on plant turndown capabilities are bed temperature and percent excess air. As shown in Figure O-3 for operating mode 3, there is a nearly linear relationship between plant power output and bed temperature, and the slope of the operating line is independent of the percent excess air. Operating lines for a range of design point temperatures were constructed parallel to the 1750°F line. This indicates that the turndown capability of the system under operating mode 3 is proportionate to the difference between the design point bed temperature and the minimum bed temperature.

Curve 654051-A

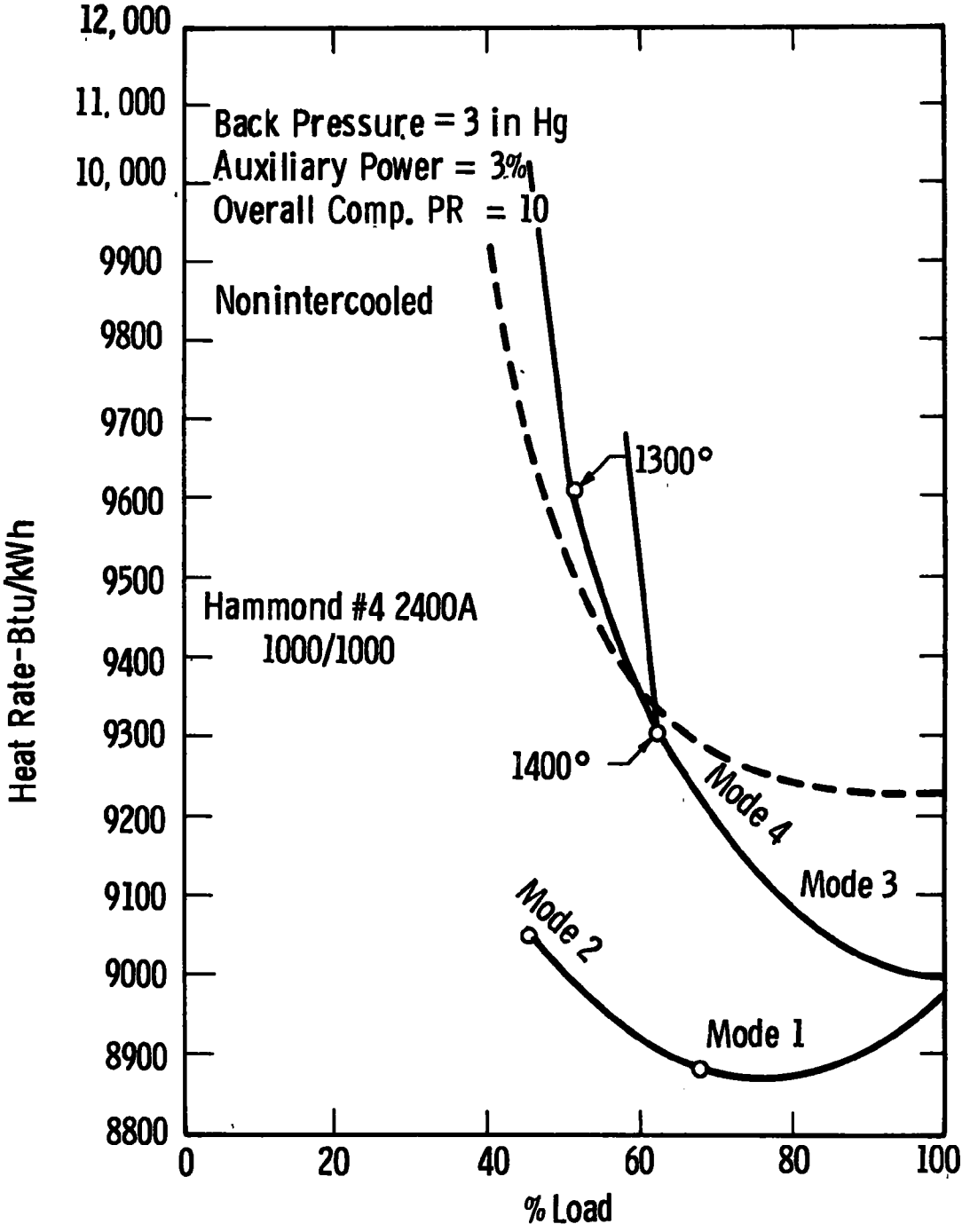

Figure O-2: Part Load Characteristics

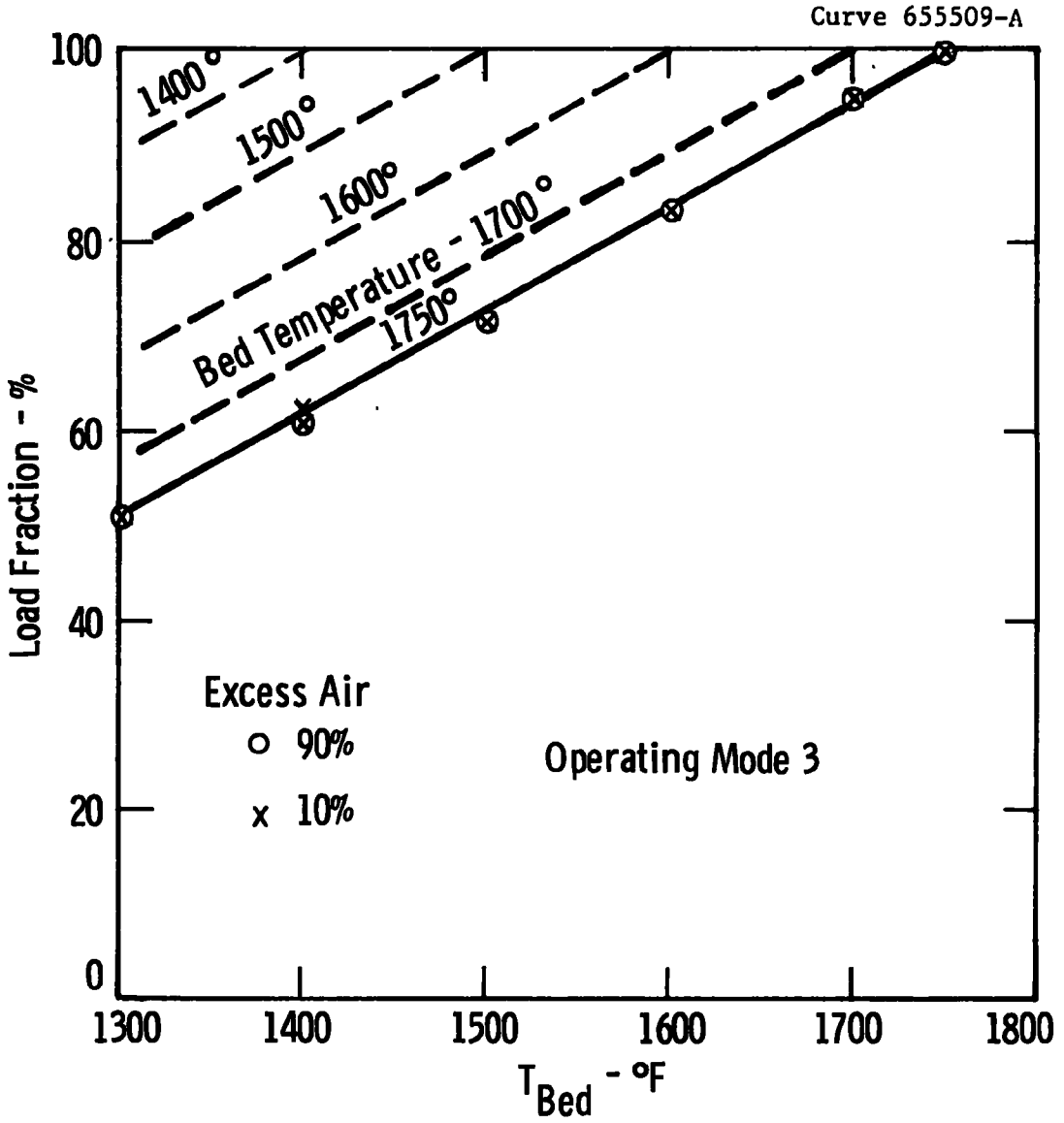

Figure O-3: Effect of Design Point Temperature and Percent Excess Air on Plant Turndown Capability

The turndown capability of the high-pressure fluidized bed boiler system under operating mode 4 is a function of the percent excess air at design point. This is because the fraction of plant power from the gas turbine increases as the percent excess air increases, and the gas-turbine power is proportionate to airflow. At 10% excess air, the gas-turbine power is 17.5% of the total plant power, and a one-third reduction in airflow reduces the plant output by about 6%. At 90% excess air, the gas-turbine power is 29% of the plant output and a similar reduction in airflow reduces the plant output by 9-1/2%. When operating mode 4 is used sequentially with mode 3, the reduction attainable in the second step is a percentage of the power output at the end of the first step, not of the design point power.

As indicated in Table 0-2, the upper limit on percent excess air is about 300%. This is the amount of excess air required to give an adiabatic flame temperature of 1750°F when burning bituminous coal and air at a temperature of 650°F.

With a design point bed temperature of 1750°F and a minimum bed temperature of 1300°F, the mode 3 turndown capability of the high-pressure fluid bed system is about 50%. With mode 4 following mode 3, the attainable turndown is as follows:

% Excess Air	Turndown %
10	53
100	55
Adiabatic case	67

This shows that a single high-pressure fluid bed module will not meet the 75% turndown objective. Therefore, two boiler modules will have to be used. If the design point bed temperature has to be decreased significantly and/or the minimum bed temperature has to be increased significantly, more than two modules may be necessary to obtain 75% turndown capability.

In the preliminary design of a high-pressure fluidized bed boiler carried out in Phase I of this program,[1] two gas-turbine

modules are used, with two boiler modules per gas turbine. The gas-turbine modules can be operated with only one boiler module with a bed temperature of 1400°F and above. This system has an overall turndown capability of about 82%. With the design point value of 10% excess air, minimum bed temperatures* of about 1350°F are necessary to avoid discontinuity in the load curve. With a minimum bed temperature of 1400°F, an excess air level of about 170% would be necessary to avoid discontinuity in the load curve.

The proposed load control system which varies bed temperature and airflow either simultaneously or sequentially is expected to achieve the desired specifications and have the following characteristics:

- Bed depth is maintained constant eliminating the need for rapid transport of solids into and out of the bed.
- Gas velocity through the fluidized bed is primarily a function of the square root of the absolute bed temperature even when the gas-turbine airflow is varied. This means that the superficial bed velocity will vary only about 15% in going from a design point bed temperature of 1750°F to a minimum bed temperature of 1300°F.
- Excess air percentage increases during turndown so that carbon carry-over will be minimized.
- Ability to change load rapidly by changing the fuel feed rate and airflow rate.
- Particulate removal system volumetric flow variations are the same as for the fluidized bed.

---

*With two boiler modules operating per gas-turbine module.

REFERENCES

1. "Evaluation of the Fluidized Bed Combustion Process," Vols. I-III, submitted to the Office of Air Programs, Environmental Protection Agency, by Westinghouse Research Laboratories, Pittsburgh, Pennsylvania, November 1971.

P

APPENDIX P

RECIRCULATING BED BOILER STUDIES

INTRODUCTION

The concept of a deep recirculating bed boiler was presented in Volume I, Section 6.2. In order to study the feasibility of using deep recirculating fluidized beds for coal combustion boiler power plants, a two-dimensional cold model was constructed from transparent acrylic sheets, to investigate solid circulation, operation characteristics, and design criteria.

The recirculating fluid bed concept is illustrated in Figure P-1. Gas is fed to the base of an open draft tube section. The superficial velocity of the gas flowing up the riser may be 10 to 60 ft/sec. The solids are picked up pneumatically in the draft tube. The effective overall density of solids and gases is less in the draft tube section than in the downcomer, which creates a solid circulation pattern upward through the draft tube and downward in the downcomer. Solids and gases from the draft tube pass into a fluid bed of the expanded cross-section. Solids from the fluid bed above the draft tube flow into the downcomers and enter the base of the draft tube. Gas is introduced at the base of the downcomer at a rate necessary to permit the downward flow of solids. The unit was operated with and without simulated imbedded heat transfer surface in the downcomers.

Several recirculating fluid bed systems have been developed and operated. The British Gas Council[1,2,3] developed deep recirculating fluidized beds for oil and coal gasification. In the gasifier this was used to smooth out the local high temperatures at the point of oxygen entry and, in the hydrogenator, to allow for the quick removal of particles wetted by the oil in the vicinity of the oil inlet, thus avoiding the

Dwg. 6197A35

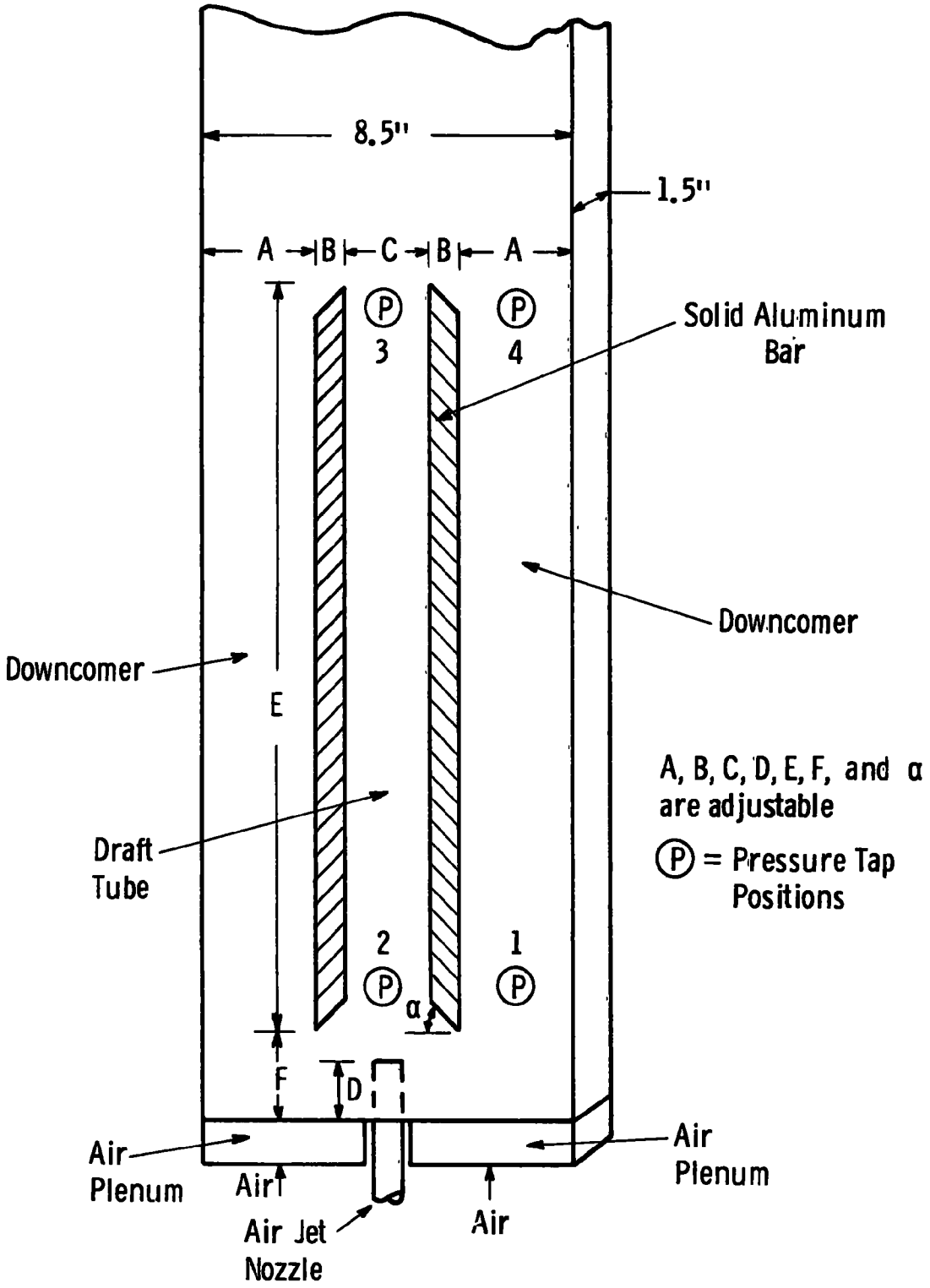

Figure P-1—Detailed Schematic of the Two-Dimensional Cold Model

formation of agglomerates as well as closely controlling temperature for process purposes. Experiments were performed in large-scale models up to 5 feet in diameter and operated at pressures and temperatures up to 70 atmospheres and 750°C (1352°F).

The same concept was also used for vertical pneumatic transportation of sticky and bridging powders.[4] A variation of this concept was utilized to promote solid mixing, circulation, heat and mass transfer in the bed,[5] and for pretreatment of caking coal.[6] Taskaev and Kozhina[7] utilized a recirculating bed for the low-temperature carbonization of coals. Product gas preheated to a temperature of 600° to 700°C (1112° to 1292°F) was recirculated to entrain the coal particles of sizes up to 1/4 in through a vertical draft tube 1 in in diameter and 20 in in length into a concentric tube 6 in in diameter and 40 in in length. The coal or char particles fell through this annular space (a downcomer) in a dense descending bed and were then reentrained by the gas and recirculated until carbonization was complete.

A recirculating fluid bed reactor is utilized in the multi-stage fluidized bed coal gasification process for production of low-Btu gas for power generation being developed by Westinghouse.[8] A recirculating bed operating near 1600°F is used in this concept to devolatilize the coal and possibly simultaneously to desulfurize the fuel gas.

This experimental and theoretical study establishes both the potential for utilizing a recirculating bed as a boiler and the initial design considerations for developing the concept. The recirculating bed boiler offers economical and environmental advantages as a second generation pressurized fluid bed boiler.

TWO-DIMENSIONAL MODEL DESIGN

A cold model was constructed from transparent acrylic sheets to facilitate visual observation of the bed operation. The detailed dimensions are shown in Figure P-1. Only the bed cross-section, 8.5 in x 1.5 in is fixed; the other dimensions (A, B, C, D, E, F, and α) in Figure P-1 can be adjusted to study the effect of these design variables. For the present investigation, the following dimensions are used

A = 2.5 in; B = 1.188 in; C = 1.125 in; D = 0 in, 1 in, and 2 in; E = 18 in; F = 3 in; $\alpha = 45°$.

Pressure taps are also provided for measuring differential pressure drops between points 1, 2, 3, and 4. The distance between pressure taps 1 and 4 (or 2 and 3) is 16 in. Pressure drops between 1 and 2, 1 and 4, and 3 and 4 were measured using U-tube manometers; the pressure drop between 2 and 3 was then obtained by difference. Water was used as manometer fluid in 1 and 2 and 3 and 4 measurements; mercury and alkazine with a specific gravity of 1.75 was used for 1 and 4 measurements. The reactor pressure was measured with a separate U-tube manometer (not shown in Figure P-1).

Air is supplied by four separate streams with their individual controls and flow meters: one for each of the two air plenums supplying air to fluidize the downcomer sections; and two for the air jet. The air jet nozzle is an open 1/2-in. copper tube with a stainless steel wire-mesh cap at the end to prevent weeping. The distributor plate consists of 1/16-in. holes spaced 11/32 in apart in a staggered arrangement. (The distributor plate is also covered with wire-mesh). The draft tube and the downcomers are separated by the two solid aluminum bars as shown in Figure P-1.

Some experiments were performed in a slightly modified two-dimensional bed as shown in Figure P-2. Two separate fluidized beds (or "boots") are created by inserting two aluminum bars of 3/4-in. thickness underneath the draft tube. The objective of this modification is to study the effect of the draft tube inlet design on the solid circulation

Dwg. 6197A36

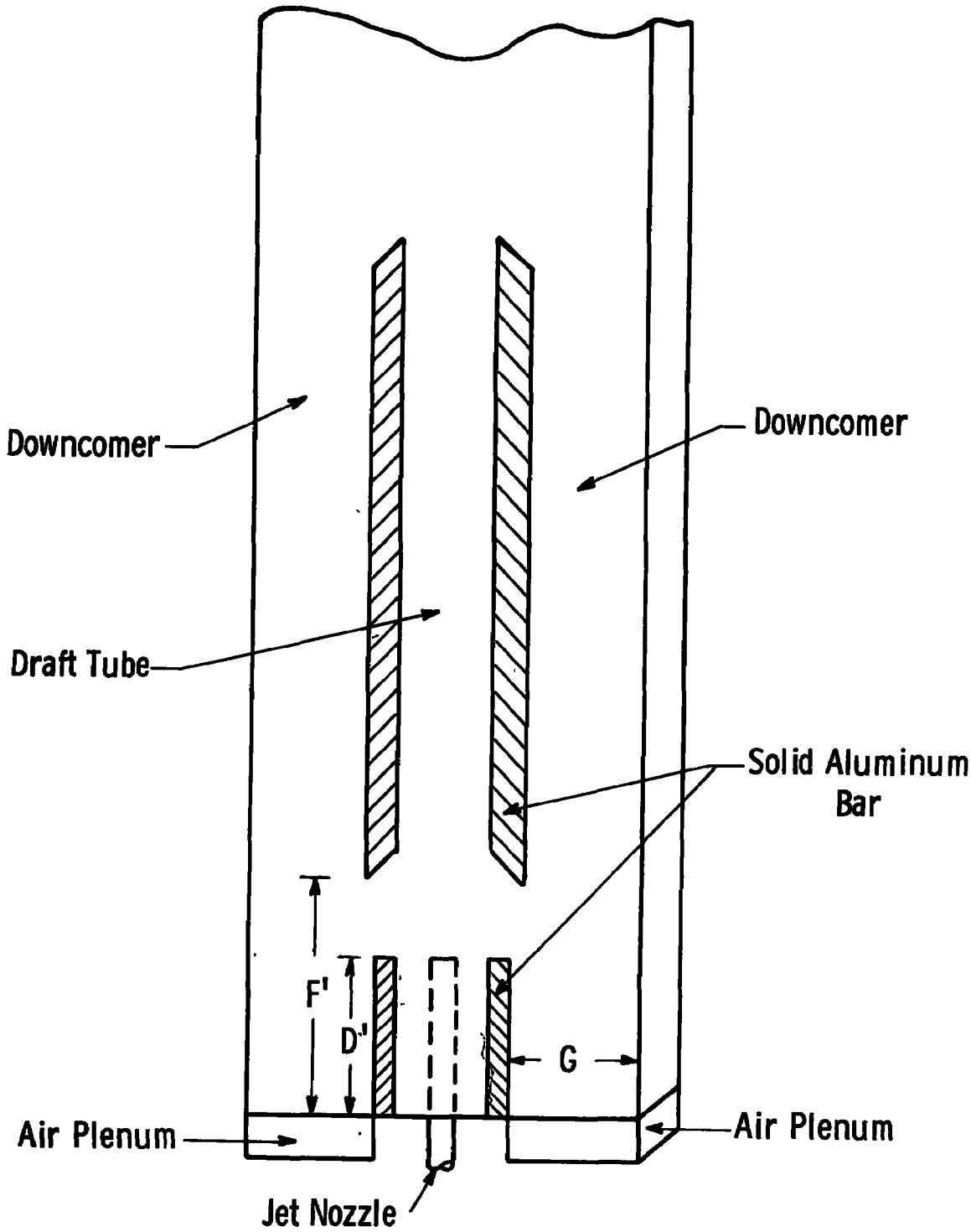

Figure P-2—Two-Dimensional Cold Model with Modified Draft Tube Inlet

rate and the air distribution between the downcomers and the draft tube. All the dimensions in the modified model are similar to the original model (Figure P-1) except now D' = 5 in., F' = 7 in., and G = 3.0 in.

To simulate imbedded heat transfer surfaces in the downcomer sections, serpentine solid copper rods of the dimensions shown in Figure P-3 were immersed in the downcomers. The rods are supported by pushing the ends of the rods into closely sized holes in the aluminum bars. Two serpentine rods are immersed in each downcomer 4.5 in. below the top of the draft tube with equal distances between the rods and between the rods and the walls. The effect of the imbedded serpentine rods on the solid circulation rate was studied by a similar method.

EXPERIMENTAL PROCEDURE

Ottawa sand was used as the bed material with the particle size distribution as shown in Table P-1. The mean particle size was calculated to be 606 μ using the following equation:

$$d_p = \frac{1}{\Sigma_i \, (X/d_p)_i} \quad , \qquad (1)$$

where

X_i = weight fraction of particles of size i and

d_{pi} = particle diameter of size i.

During operation, air is injected into the draft tube through the air jet nozzle to provide an air velocity up to ∿ 43 ft/sec in the draft tube while the downcomer sections are minimally fluidized. This creates a solid circulation pattern upward through the draft tube and downward in the downcomers. The minimum fluidizing condition in the downcomers is assured first by turning up the air supply to the downcomers until air bubbles appear in the downcomers and then turning down the air supply until the air bubbles just disappear.

Curve 653461-A

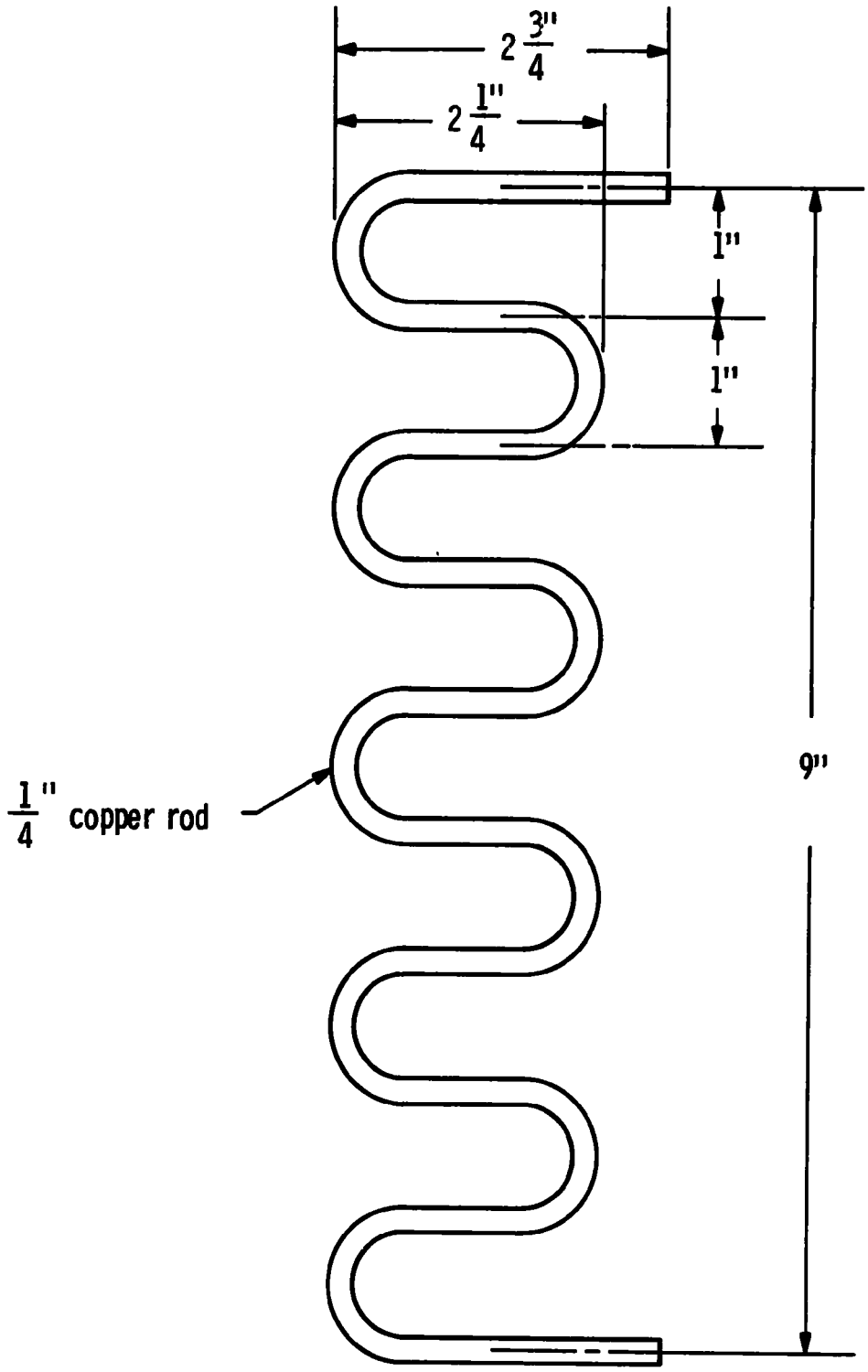

Figure P-3— Dimensions of the Serpentine Copper Rods

TABLE P-1

PARTICLE SIZE DISTRIBUTION OF THE OTTAWA SAND USED AS BED MATERIAL

U.S. Standard Mesh	Opening in μ	Opening in Inches	Wt %
20	841	0.0331	0.28
30	595	0.0234	74.82
40	420	0.0165	14.10
50	297	0.0117	8.95
60	250	0.0098	1.10
80	177	0.0070	0.75

The solid downward velocity in the downcomer was estimated by following a tracer particle for 16 inches with a stopwatch. The tracer particles are silica gel dyed with red pigment and of similar size. For every operating condition, at least ten particles in each downcomer were traced and the arithmetic average velocity was taken to be the solid particle velocity in the downcomer. The solid recirculation rate was then calculated by assuming plug flow in the downcomer.

More than 100 runs have been performed in the cold model. The variables changed are static bed height, airflow rate, and the jet nozzle position. With model configuration as shown in Figure P-1 (Case I), the experiments were divided into three series:

Test Series 1: D = 0 in.; static bed height at 20 in., 25 in., 30 in., and 37 in.

Test Series 2: D = 1 in.; static bed height at 21 in., 24 in., 27 in., and 35 in.

Test Series 3: D = 2 in.; static bed height at 22 in., 25 in., 29 in., 33 in., and 37 in.

With serpentine rods in the downcomers (Case II), the experiments were also divided into three series. The variables changed are static bed height, airflow rate, and the jet nozzle position:

Test Series 1: D = 0 in.;static bed height at 21 in.,25 in., 29 in.,33 in.,and 37 in.

Test Series 2: D = 1 in.;static bed height at 21 in.,25 in., 29 in.,34 in.,and 38 in.

Test Series 3: D = 2 in.;static bed height at 21 in.,24 in., 28 in.,33 in.,and 38 in.

With model configuration as shown in Figure P-2 (Case III), the air jet nozzle position was fixed at the same height of the boots. The variables changed were static bed height and air velocity.

EXPERIMENTAL RESULTS

The experimental data for Case I, Case II, and Case III are summmarized in Tables P-2 to P-8. The largest observed solid recirculation rate is 110,000 lb/hr-ft^2 of the downcomer area, which is comparable to the figure 113,000 lb/hr-ft^2 reported by Horsler and Thompson[2]. All the experimental data obtained so far can be approximated by equations based on the pressure drops between 1-2 ($P_1-P_2 = \Delta P_{1-2}$) as shown in Figures P-4 and P-5.

$$(Up,d)_L + (Up,d)_R = 0.107\ (2gHp)^{2/3} \text{ for Cases I and II} \qquad (2)$$

$$(Up,d)_L + (Up,d)_R = 0.025\ (2gHp) \text{ for Case III} \qquad (3)$$

$$H_p = \frac{62.43\ (\Delta P_{1-2})}{\rho_s\ (1-\varepsilon_d)} \qquad (4)$$

Since the inlet to the draft tube (point 2 in Figure P-1) is at a lower pressure compared to that at outlets of the downcomers (point 1 in Figure P-1), the air from the air plenums favors the draft tube, and, thus air by-passing into the draft tube results. The amount of air by-passing

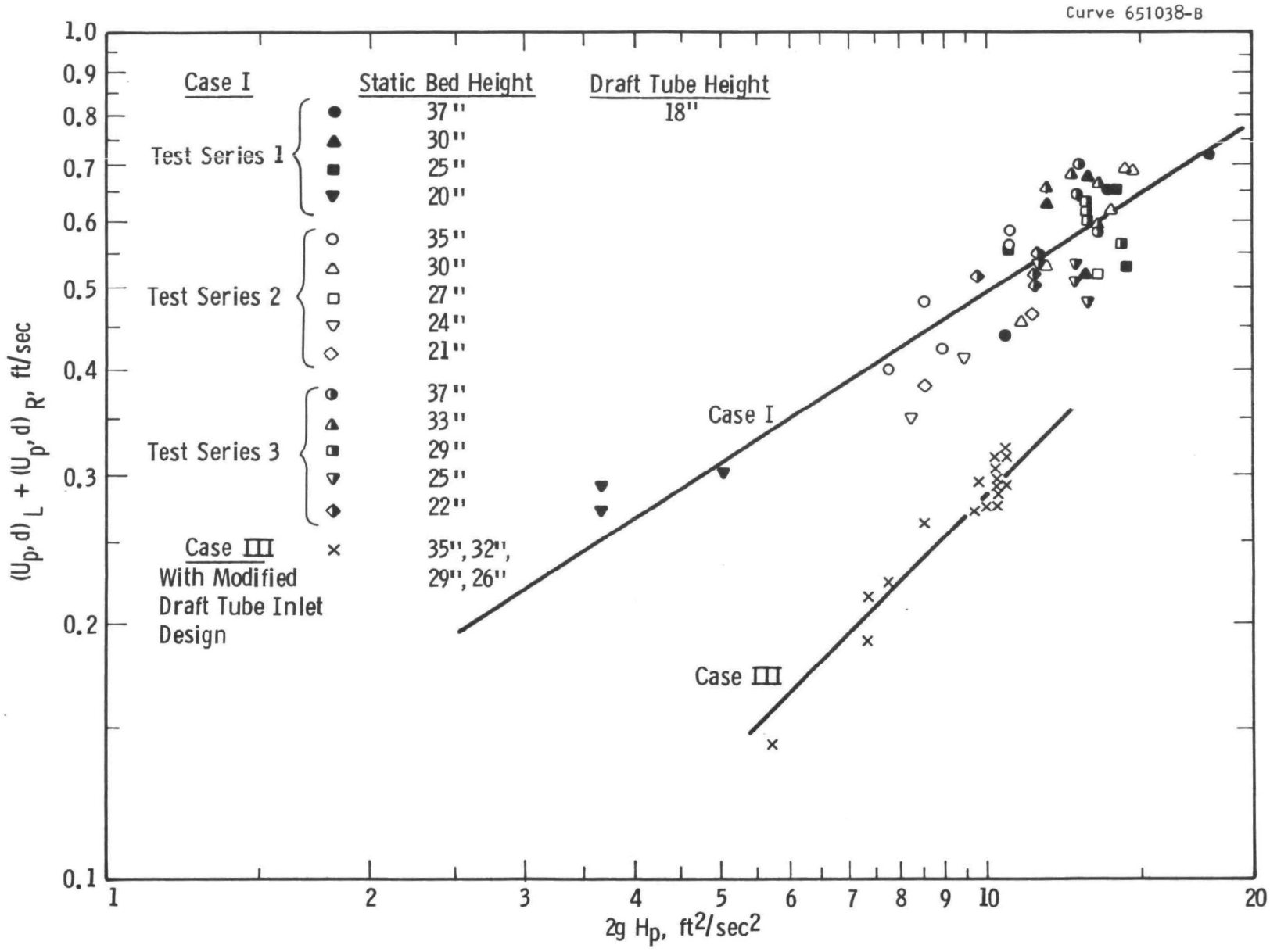

Figure P-4—Experimental Data for Case I and Case III

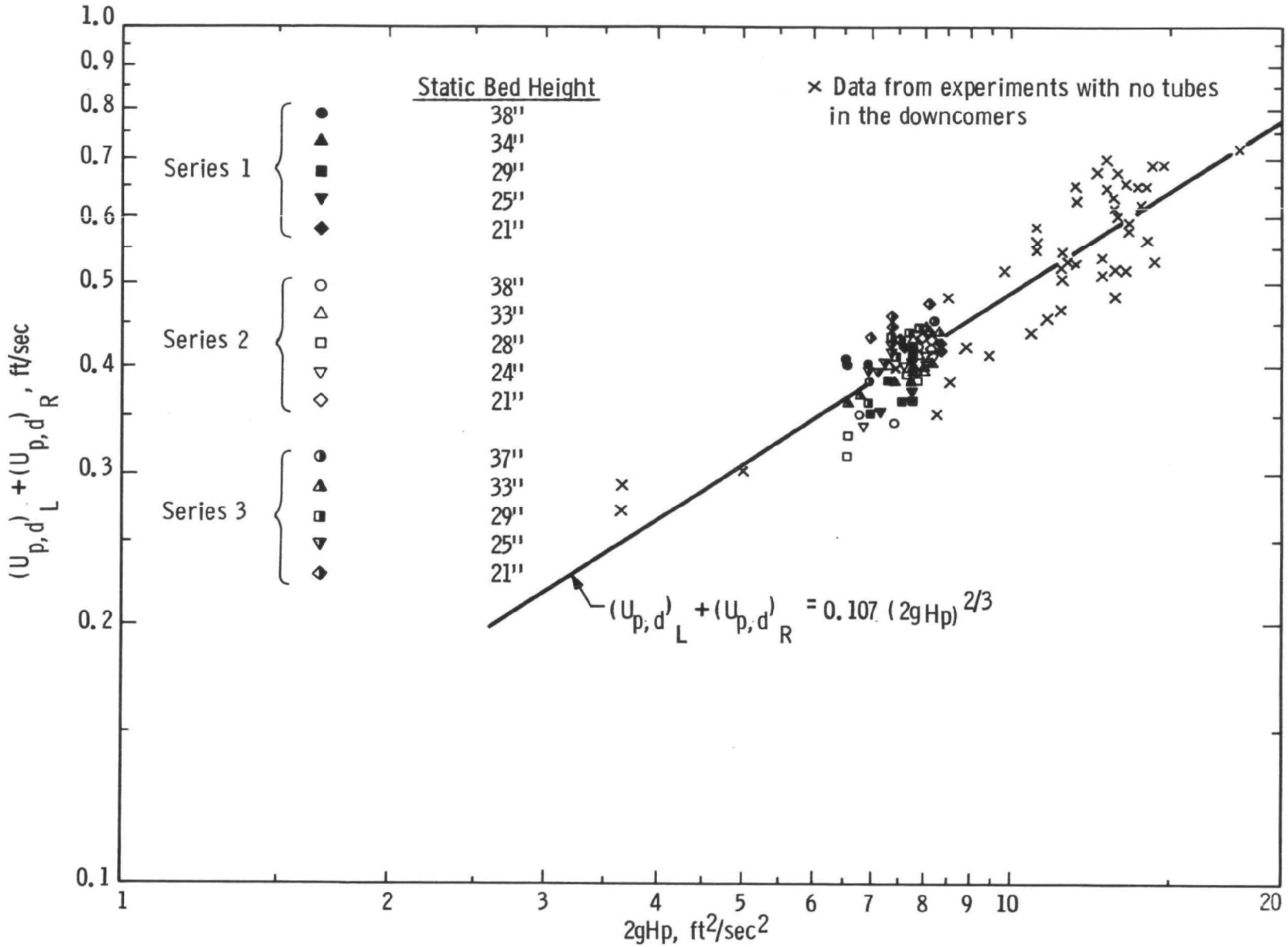

Figure P-5—Experimental Data for Case II

depends on the pressure drop ΔP_{1-2} as shown in Figure P-6. The straight line can be represented by the following equation:

$$F = 1.15\ \Delta P_{1-2}\ , \tag{5}$$

where F, the air by-passing factor is defined as

$$F = \frac{\text{Total Air input into the Air Plenums}}{\text{Total Air Required to Minimally Fluidize the Downcomers}}\ .$$

When the jet from the draft tube exit penetrates the fluid bed above the draft tube and the downcomers, the fluid bed behaves essentially like a spouting bed. When the jet does not penetrate, the fluid bed becomes a slugging bed. Due to this oscillating nature, the solid downward velocities (obtained from timing with a stopwatch) in the downcomers,at fixed operating conditions,vary for up to 10% of the average value. The solid velocities in the two separate downcomers can be adjusted to as close to each other as possible by varying air input into their separate air plenums.

The manometer readings are generally stable when the air jet penetrates the fluid bed. When the fluid bed becomes a slugging bed, the oscillation frequency of the pressure readings can be up to 20 cycles per minute. The range of pressure fluctuation is up to 10% of observed value for ΔP_{1-4} and up to 20% for ΔP_{1-2}.

After about 50 hours' operation, no visible erosion was noticed on the draft tube sides of the aluminum bars, though a slight blur appeared on the plexiglass walls.

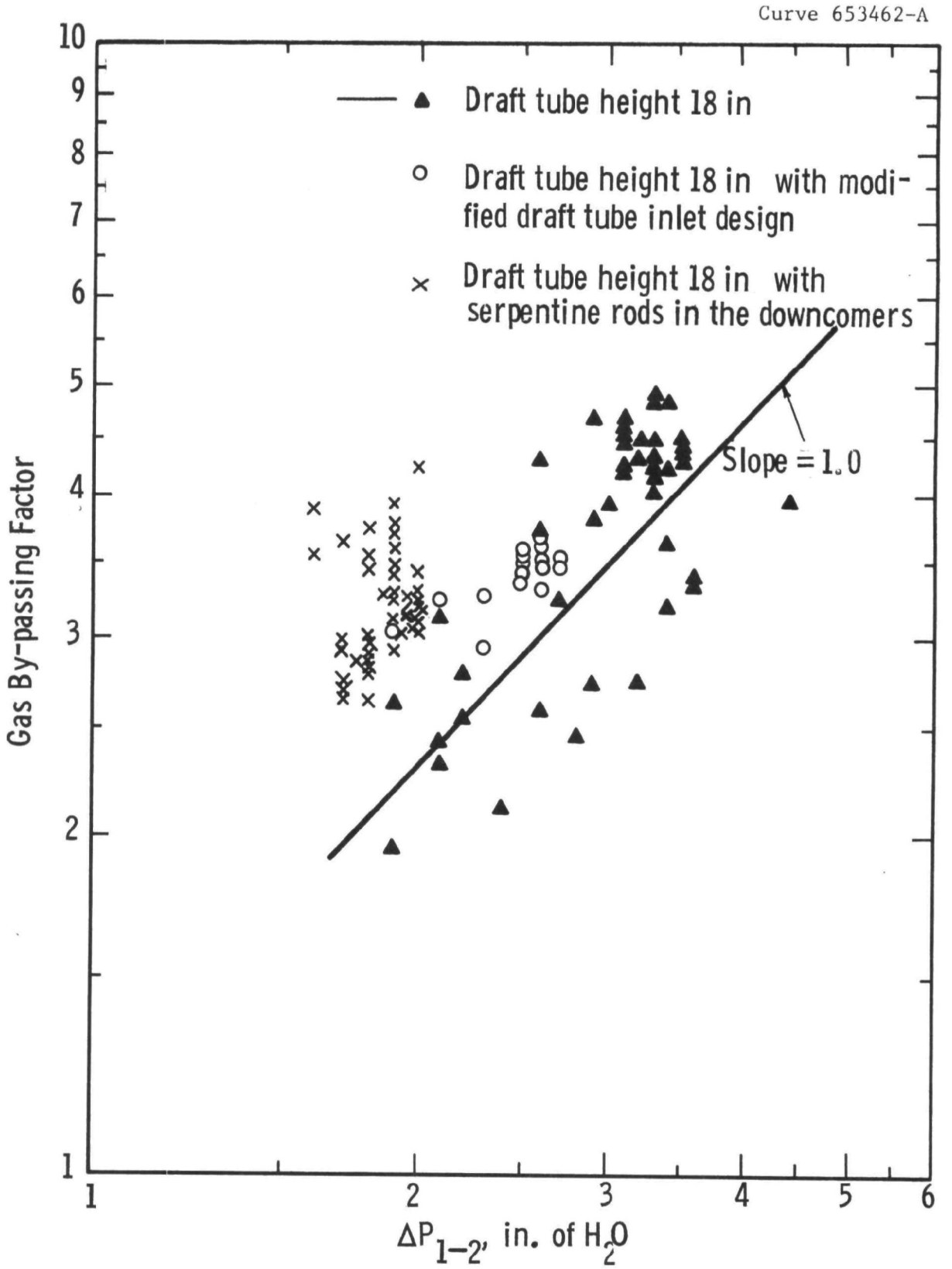

Figure P-6—Experimental Values of Total Air By-passing

TABLE P-2

EXPERIMENTAL DATA OF TEST SERIES 1 (CASE I)

Run No.	Static Bed Height, in.	Superficial Fluid Velocity in Draft Tube, ft/sec	Solid Circulation Rate, lb/sec	Specific Solid Loading in Draft Tube, lb solids/lb fluid
1-1-1	37	42.48	1.42	36.1
1-1-2	37	31.53	1.55	53.8
1-1-3	37	19.73	0.95	53.8
1-2-1	30	41.25	1.46	38.4
1-2-2	30	30.65	1.36	48.9
1-2-3	30	20.27	1.12	61.3
1-3-1	25	40.05	1.20	31.9
1-3-2	25	29.72	1.41	49.8
1-3-3	25	22.76	1.15	55.6
1-4-1[a]	20	29.06	0.631	23.0
1-4-2[a]	20	22.31	0.590	28.2

[a]Downcomers are not at minimally fluidized condition.

TABLE P-3

EXPERIMENTAL DATA OF TEST SERIES 2 (CASE I)

Run No.	Static Bed Height, in.	Superficial Fluid Velocity in Draft Tube, ft/sec	Solid Circulation Rate, lb/sec	Specific Solid Loading in Draft Tube, lb solids/lb fluid
2-1-1	35	32.58	0.912	29.6
2-1-2	35	30.69	1.21	42.0
2-1-3	35	27.34	1.27	49.1
2-1-4	35	22.06	1.04	51.0
2-2-1	30	39.96	1.50	40.0
2-2-2	30	28.49	1.49	55.4
2-2-3	30	21.73	1.34	66.2
2-3-1[a]	27	33.17	1.12	35.0
2-3-2[a]	27	22.41	0.521	24.7
2-4-1[a]	24	30.54	0.759	25.6
2-4-2[a]	24	23.05	0.895	41.0
2-5-1[a]	21	30.48	0.830	28.0
2-5-2[a]	21	24.34	1.00	43.2

[a]Downcomers are not at minimally fluidized condition.

TABLE P-4

EXPERIMENTAL DATA OF TEST SERIES 3 (CASE I)

Run No.	Static Bed Height, in.	Superficial Fluid Velocity in Draft Tube, ft/sec	Solid Circulation Rate, lb/sec	Specific Solid Loading in Draft Tube, lb solids/lb fluid
3-1-1	37	38.29	1.53	40.5
3-1-2	37	32.05	1.39	44.8
3-1-3	37	24.95	1.27	53.8
3-2-1	33	40.54	1.42	36.1
3-2-2	33	37.11	1.47	41.8
3-2-3	33	32.74	1.42	45.9
3-2-4	33	28.74	1.29	48.3
3-3-1	29	39.63	1.33	35.3
3-3-2	29	33.95	1.37	42.6
3-3-3	29	30.54	1.31	45.6
3-3-4	29	27.43	1.22	47.5
3-4-1	25	36.82	1.14	32.5
3-4-2	25	33.21	1.15	36.6
3-4-3	25	28.75	1.10	40.7
3-4-4	25	25.42	1.04	43.9
3-5-1	22	36.59	1.12	32.0
3-5-2	22	32.28	1.18	38.7
3-5-3	22	27.39	1.14	44.8
3-5-4	22	24.74	1.11	48.6

TABLE P-5

EXPERIMENTAL DATA OF TEST SERIES WITH TUBES IN DOWNCOMERS (CASE II)

Run No.	Static Bed Height, in.	Superficial Fluid Velocity in Draft Tube, ft/sec	Solid Circulation Rate, lb/sec	Specific Solid Loading in Draft Tube, lb Solids/lb Fluid
1-1-1	38	22.3	0.709	35.3
1-1-2	38	25.0	0.711	31.4
1-1-3	38	28.3	0.726	28.0
1-1-4	38	32.2	0.744	25.0
1-1-5	38	35.5	0.718	21.4
1-2-1	34	23.1	0.705	34.0
1-2-2	34	25.7	0.683	29.3
1-2-3	34	30.1	0.700	25.3
1-2-4	34	35.1	0.716	21.7
1-2-5	34	34.6	0.675	20.8
1-2-6[a]	34	31.3	0.467	15.9
1-3-1	29	20.9	0.620	33.1
1-3-2	29	26.1	0.640	26.9
1-3-3	29	29.9	0.640	23.2
1-3-4[a]	29	26.5	0.380	15.5
1-3-5	29	34.9	0.675	20.4
1-3-6[a]	29	30.1	0.417	14.7
1-4-1	25	21.5	0.625	32.4
1-4-2	25	25.8	0.713	30.5
1-4-3[a]	25	22.1	0.400	20.0
1-4-4	25	31.1	0.653	22.6
1-4-5[a]	25	30.2	0.409	14.6
1-4-6[a]	25	27.7	0.214	8.4
1-5-1	21	23.7	0.742	34.8
1-5-2	21	28.5	0.750	28.9
1-5-3	21	32.8	0.752	24.8
1-5-4[a]	21	29.2	0.400	14.9
1-5-5[a]	21	26.9	0.231	9.3

[a] Downcomers are not at minimally fluidized condition.

TABLE P-6

EXPERIMENTAL DATA OF TEST SERIES WITH TUBES IN DOWNCOMERS (CASE II)

Run No.	Static Bed Height, in.	Superficial Fluid Velocity in Draft Tube, ft/sec	Solid Circulation Rate, lb/sec	Specific Solid Loading in Draft Tube, lb Solids/lb Fluid
2-1-1	38	28.7	0.744	28.3
2-1-2	38	31.7	0.744	25.4
2-1-3[a]	38	29.7	0.610	22.2
2-1-4	38	37.2	0.750	21.5
2-1-5[a]	38	33.8	0.618	19.5
2-2-1	33	27.6	0.703	28.1
2-2-2	33	30.7	0.700	24.9
2-2-3[a]	33	27.6	0.398	15.8
2-2-4	33	35.0	0.713	21.8
2-2-5[a]	33	31.6	0.465	15.7
2-2-6[a]	33	31.3	0.316	10.7
2-3-1	28	27.9	0.742	29.2
2-3-2	28	31.0	0.690	24.3
2-3-3[a]	28	28.6	0.553	21.0
2-3-4	28	35.0	0.683	20.9
2-3-5[a]	28	33.2	0.584	18.7
2-4-1	24	27.1	0.731	29.7
2-4-2	24	31.0	0.713	25.1
2-4-3[a]	24	29.4	0.627	23.2
2-4-4	24	34.7	0.707	22.5
2-4-5[a]	24	33.1	0.597	20.0
2-5-1	21	27.0	0.731	29.8
2-5-2	21	31.2	0.759	26.6
2-5-3	21	34.1	0.759	24.0

[a]Downcomers are not at minimally fluidized condition.

TABLE P-7

EXPERIMENTAL DATA OF TEST SERIES WITH TUBES IN DOWNCOMERS (CASE II)

Run No.	Static Bed Height, in.	Superficial Fluid Velocity in Draft Tube, ft/sec	Solid Circulation Rate, lb/sec	Specific Solid Loading in Draft Tube lb Solids/lb Fluid
3-1-1	37	26.9	0.977	40.4
3-1-2	37	31.1	0.977	34.7
3-1-3	37	35.5	0.977	29.9
3-1-4	37	34.1	0.834	26.5
3-2-1	33	26.5	0.943	39.4
3-2-2	33	30.9	0.953	33.9
3-2-3	33	32.7	0.949	31.5
3-2-4[a]	33	31.0	0.787	27.5
3-2-5	33	34.5	0.971	30.3
3-2-6[a]	33	33.4	0.796	25.7
3-3-1	29	26.2	0.940	39.7
3-3-2	29	30.8	0.951	33.7
3-3-3	29	33.0	0.962	31.6
3-3-4[a]	29	30.3	0.744	26.7
3-3-5	29	33.5	0.895	28.9
3-3-6[a]	29	32.4	0.787	26.2
3-4-1	25	25.3	0.852	37.3
3-4-2	25	27.2	0.858	34.9
3-4-3	25	29.8	0.930	34.1
3-4-4	25	31.8	0.908	31.0
3-4-5	25	34.0	0.892	28.3
3-4-6[a]	25	33.1	0.789	25.7
3-5-1	21	25.5	0.940	40.9
3-5-2	21	26.6	0.934	38.8
3-5-3	21	29.3	0.994	37.2
3-5-4	21	30.9	0.977	34.5
3-5-5	21	34.2	1.053	33.3
3-5-6[a]	21	33.2	0.971	31.6

[a]Downcomers are not at minimally fluidized condition.

TABLE P-8

EXPERIMENTAL DATA OF TEST SERIES WITH BOOT (CASE III)

Run No.	Static Bed Height, in.	Superficial Fluid Velocity in Draft Tube, ft/sec	Solid Circulation Rate, lb/sec	Specific Solid Loading in Draft Tube, lb solids/lb fluid
B-1-1	35	29.16	0.681	25.9
B-1-2	35	32.56	0.638	21.5
B-1-3	35	33.94	0.586	18.8
B-1-4	35	37.06	0.662	19.3
B-2-1	32	29.02	0.679	26.1
B-2-2	32	32.85	0.662	22.2
B-2-3	32	34.93	0.614	19.2
B-2-4	32	35.93	0.601	18.1
B-2-5[a]	32	34.65	0.467	14.6
B-3-1	29	28.90	0.685	26.4
B-3-2	29	32.40	0.631	21.3
B-3-3[a]	29	31.48	0.566	19.7
B-3-4	29	34.18	0.598	19.1
B-3-5	29	36.94	0.610	17.8
B-3-6[a]	29	33.85	0.413	13.2
B-4-1	26	28.24	0.694	27.4
B-4-2	26	31.98	0.644	22.2
B-4-3	26	34.07	0.640	20.6
B-4-4[a]	26	32.13	0.484	16.5
B-4-5	26	36.08	0.681	20.4
B-4-6[a]	26	33.20	0.311	10.1

[a]Downcomers are not at minimally fluidized condition.

DEVELOPMENT OF MATHEMATICAL MODEL

Pressure Drop in the Downcomer

During operation, the downcomers are minimally fluidized. The pressure drop through a minimally fluidized bed can be calculated from the Ergun equation:[9]

$$\Delta P_D = \frac{L}{g_c}\left[150\,\frac{\mu U_f(1-\varepsilon_d)^2}{d_p^{\,2}\phi_s^{\,2}\varepsilon_d^{\,2}} + 1.75\,\frac{\rho_f U_f^{\,2}(1-\varepsilon_d)}{d_p\phi_s\varepsilon_d}\right] . \quad (6)$$

Yoon and Kunii[10] found that the Ergun equation can correlate the pressure drop through a moving bed if the fluid velocity, U_f, is substituted with the fluid-solid slip velocity, $U_{sl} = U_f + U_{p,d}$. Thus the downcomer pressure drop can be estimated from the following equation:

$$\Delta P_D = \frac{L}{g_c}\left[150\,\frac{\mu(U_{f,d}+U_{p,d})(1-\varepsilon_d)^2}{\bar{d}_p^{\,2}\phi_s^{\,2}\varepsilon_d^{\,2}} + 1.75\,\frac{\rho_f(U_{f,d}+U_{p,d})^2(1-\varepsilon_d)}{\bar{d}_p\phi_s\varepsilon_d}\right] . \quad (7)$$

Pressure Drop in the Draft Tube

The draft tube in the present design is essentially a vertical pneumatic transport tube. There are many correlations available for estimating the pressure drop of pneumatic transport in a vertical line.[11,12,13,14,15] All the correlations invariably consist of different combinations of the following terms:

$$\Delta P_R = \Delta P_{kg} + \Delta P_{hg} + \Delta P_{fg} + \Delta P_{fs} + \Delta P_{ks} + \Delta P_{hs} . \quad (8)$$

ΔP_{kg} and ΔP_{hg} are usually negligible compared to other terms. ΔP_{fg} can be estimated by the Fanning equation

$$\Delta P_{fg} = \frac{2f\rho_f U_o^2 L}{g_c D} \quad . \tag{9}$$

The friction factor, f, is calculated from

$$f = 0.0791 \left(\frac{\rho_f U_o D}{\mu}\right)^{-0.25} \text{ for } 3 \times 10^3 < Re < 10^5 \ , \tag{10}$$

and

$$f = 0.0008 + 0.0552 \left(\frac{\rho_f U_o D}{\mu}\right)^{-0.237} \text{ for } 10^5 < Re < 10^8 \ . \tag{11}$$

Jones et al[12] correlated numerous vertical pneumatic transport data and found out the solid friction term, ΔP_{fs}, can be expressed with an equation similar to the Fanning equation with a solid friction factor, f_s:

$$\Delta P_{fs} = \frac{2f_s \rho_f U_o^2 L}{g_c D} \tag{12}$$

with

$$f_s = 1.89 \times 10^{-6} \frac{A_o}{\phi_s^{0.5}} \theta^x \quad . \tag{13}$$

The kinetic and the static energy terms, ΔP_{ks} and ΔP_{hs}, can be expressed as

$$\Delta P_{ks} = \frac{\rho_s (1 - \varepsilon_r) U_{p,r}^2}{2g_c} \tag{14}$$

$$\Delta P_{hs} = \rho_s (1 - \varepsilon_r) \frac{g}{g_c} L \quad . \tag{15}$$

The solid kinetic energy term, ΔP_{ks}, is very important when the pressure drop is measured over a section of pipe closely downstream of the point of introduction of the solids, because the solid particles are accelerated from zero velocity to their final velocities in this section of the pipe. Kolpakov and Donat[13] have made a detailed experimental study of the pressure drop associated with the acceleration of solid particles in vertical pneumatic conveying pipes. They conclude that the simple expression for ΔP_{ks} of the form of Equation 14 is inadequate and correlate their data through a complex empirical relationship involving the terminal velocity of the particles, mean gas velocity and the specific solid loading in the gas stream. Extrapolating their correlation for the present application yields some unreasonable results and thus is not used here.

Ignoring the negligible terms, the total pressure drop in the draft tube can be represented by

$$\Delta P_R = (f + f_s)\left(\frac{2\rho_f U_o^2}{g_c}\right)\frac{L}{D} + \frac{\rho_s(1 - \varepsilon_r)\, U_{p,r}^2}{2g_c} + \rho_s(1 - \varepsilon_r)\frac{g}{g_c} L \ . \qquad (16)$$

There are two unknowns in Equation 16, i.e., the voidage ε_r and the solid particle velocity $U_{p,r}$. The solid particle velocity in the draft tube can be estimated through the correlation derived from the experiments by Richardson and Zaki.[16] The correlation is very similar to that of Wen and Yu:[17]

$$U_{sl} = \frac{\varepsilon_r^{n-1}}{10^{(d_p/D)}} U_t = U_{f,r} - U_{p,r} \qquad (17)$$

or

$$U_{p,r} = \frac{U_o}{\varepsilon_r} - \frac{\varepsilon_r^{n-1}}{10^{(d_p/D)}} U_t \ . \qquad (18)$$

To find n, the following equation can be used:[18]

$$n = (4.45 + 18 \frac{d_p}{D}) \, Re_t^{-0.1} \text{ for } 1 < Re_t < 200 \, , \tag{19}$$

and

$$Re_t = \frac{U_t d_p \rho_f}{\mu} \quad . \tag{20}$$

For the present system (using Ottawa sand as bed material), n was calculated to be 2.86.

The terminal velocity, U_t, was estimated from:[18]

$$U_t = \frac{(\rho_s - \rho_f) \, g_c d_p^{\,2}}{18\mu} \text{ for } \frac{d_p U_o \rho_f}{\mu} < 2.0 \quad , \tag{21}$$

and

$$U_t = \frac{0.153 (d_p)^{1.14} g_c^{\,0.71} (\rho_s - \rho_f)^{0.71}}{\mu^{0.43} \, \rho_f^{\,0.29}} \text{ for } 2.0 < \frac{d_p U_o \rho_f}{\mu} < 500 \, , \tag{22}$$

with a correction factor, η, for nonspherical particles,

$$\eta = 0.843 \log \left(\frac{\phi_s}{0.065}\right) \quad . \tag{23}$$

Voidage in the draft tube, ε_r, can be calculated by writing a material balance between the downcomers and the draft tube:

$$U_{p,r}(1 - \varepsilon_r)\rho_s A_r = 2U_{p,d}(1 - \varepsilon_d)\rho_s A_d = W_s \quad . \tag{24}$$

Substituting Equation 18 into Equation 24, we have

$$(1 - \varepsilon_r) = \frac{W_s}{\rho_s A_r} \cdot \frac{1}{\left(\frac{U_o}{\varepsilon_r} - \frac{\varepsilon_r^{\,n-1}}{10^{(d_p/D)}} U_t\right)} \quad . \tag{25}$$

The only unknown in Equation 25 is ε_r; however, a trial and error procedure is required to calculate ε_r.

With f_s, $U_{p,r}$, and ε_r calculated from Equations 13, 18, and 25, respectively, the pressure drop in the draft tube can now be estimated from Equation 16.

Hinkle[19] measured particle velocities experimentally by means of a high-speed photographic technique and found the following relationship correlated his data within $\pm$ 5%:

$$U_{p,r} = U_{f,r}(1 - 0.179\ d_p^{0.3}\rho_s^{0.5}) \ . \tag{26}$$

He also proposed a way to calculate the solid friction term (ΔP_{fs}):

$$\Delta P_{fs} = f_p \frac{2\ U_{p,r} GL}{gD} \ , \tag{27}$$

with

$$f_p = \frac{3\rho_f C_D D}{2\rho_s d_p} \left[\frac{U_{f,r} - U_{p,r}}{U_{p,r}} \right]^2 \ . \tag{28}$$

The largest specific solid loading in Hinkle's experiments was 6.02 compared to 23 to 66 in the present experiments. Equation 26 probably has limited applicability because of the low specific solid loading covered in his experiments; however, Hinkle's model was also utilized to estimate the pressure drop in the draft tube for comparison with predictions from other models.

Another model utilized to estimate the pressure drop in the draft tube is the model by Curran and Gorin.[11] The model is rather complex; the readers should refer to the original reference for details. The predictions by Curran and Gorin are also presented for comparison.

Jet Penetration

When the fluid-solid stream leaves the top of the draft tube, it penetrates into the fluid bed above. The depth of this penetration depends on the stream velocity, specific loading of the solid, and particle and fluid properties. Due to the oscillating nature of the bed operation, the penetration will vary for given operating conditions. The average penetration depth, however, can be estimated by applying the Bernoulli equation between the top of the draft tube and the end of the penetration. The particle velocity was assumed to start to decrease at the top of the draft tube, and the voidage in the jet starts to decrease also. At the end of penetration, the solid particle velocity is essentially zero and the voidage becomes equal to that of the fluidized bed above the draft tube. The energy recovered from the deceleration of the solid particles is dissipated by friction. The Bernoulli equation gives

$$\frac{\rho_s(1 - \varepsilon_r)U_{p,r}^2}{2g_c} = (f + f_s)\left(\frac{2\rho_f U_o^2}{g_c}\right)\frac{J}{D_j} + \rho_s(1 - \varepsilon)\frac{g}{g_c}L \quad . \tag{29}$$

The voidage, ε, is the average voidage in the jet and is calculated from the equation

$$\varepsilon_{ave} = \frac{\varepsilon_r[J\exp(-J) + \exp(-J) - 1] - \varepsilon_b[\exp(-J) + J - 1]}{J[\exp(-J) - 1]} \quad . \tag{30}$$

Equation 30 was obtained by assuming the voidage change in the jet can be approximated by an exponential equation of the form

$$\varepsilon = a + be^{-H} \tag{31}$$

with boundary conditions

$$\begin{aligned} &\text{at} \quad H = 0 \quad \varepsilon = \varepsilon_r \\ &\text{at} \quad H = J \quad \varepsilon = \varepsilon_b \quad . \end{aligned} \tag{32}$$

Preliminary experimental data indicate that jet penetration depth can be estimated from Equations 29 and 30 as presented in Tables P-9 to P-11 if the jet diameter, D_j, is taken to be the draft tube diameter.

Comparison with the Experimental Data

The experimental data were correlated with the mathematical model described in the last section for the pressure drop in the downcomers, in the draft tube, and for jet penetration depth. Hinkle's and Curran and Gorin's model were also used to estimate the pressure drop in the draft tube for comparison with the predictions by the present model for Case I.

The pressure drop in the downcomer at minimum fluidization was calculated from Equation 7 with $\varepsilon_d = 0.467$ and $\phi_s = 0.86$ and compared with the experimental measurement in columns 11 and 12 of Tables P-12, P-13, and P-14 for Case I. Comparisons between the experimental and the theoretical values for Case III are presented in Table P-16. For Case II (Table P-15) where additional serpentine copper rods were inserted into the downcomers, the pressure drop calculations from Equation 7 were corrected with the following correction factor:

$$F_c = \frac{(H_o - H) + H \cdot \frac{(A_d - A_t)}{A_d}}{H_o} \quad . \tag{33}$$

The pressure drop in the draft tube was calculated from Equation 16, from Hinkle's model, and from Curran and Gorin's model for Case I. Their relative predictions were compared with the experimental measurement in Table P-12 to P-14. Columns 1 through 6 were defined in the previous section. Experimental observation shows that the pressure difference between 3 and 4, ΔP_{3-4}, can be taken as zero except when the jet penetrates the fluid bed above the draft tube. (When the jet penetrates the bed, ΔP_{3-4} has a value ranging from 0 to 0.5 H_2O.) The pressure drop between 1 and 2 can then be calculated from the difference between the pressure drops in the downcomer and in the draft tube. The calculated pressure drop in the draft tube, ΔP_R, from all models deviates considerably from the experimental values, $(\Delta P_D)_{exp} - (\Delta P_{1-2})_{exp}$, especially

TABLE P-9

COMPARISON BETWEEN EXPERIMENTAL AND CALCULATED
JET PENETRATION DEPTH (CASE I)

Run No.	Jet Penetration Depth	
	Experimental (inches)	Calculated (inches)
1-1-1	7-10	12.9
1-1-2	6-9	9.5
1-1-3	4-8	2.18
1-2-1	9-13	12.9
1-2-2	4-7	8.1
1-2-3	3-6	3.5
1-3-1	1-through	through
1-3-2	1-4	through
1-3-3	2-4	4.4
1-4-1	1-through	through
1-4-2	1-through	2.1
2-1-1	3-14	6.2
2-1-2	5-14	7.3
2-1-3	5-11	6.5
2-1-4	2-6	3.8
2-2-1	through	through
2-2-2	through	8.0
2-2-3	2-4	4.7
2-3-1	through	through
2-3-2	through	1.9
2-4-1	through	through
2-4-2	through	through
2-5-1	through	through
2-5-2	through	through

TABLE P-9 (Continued)

Run No.	Jet Penetration Depth	
	Experimental (inches)	Calculated (inches)
3-1-1	7-11	12.1
3-1-2	6-9	8.8
3-1-3	4.5-7.5	5.6
3-2-1	7-through	through
3-2-2	5-through	11.2
3-2-3	4-through	9.2
3-2-4	3.5-8	7.0
3-3-1	through	through
3-3-2	through	through
3-3-3	through	through
3-3-4	4-through	6.2
3-4-1	through	through
3-4-2	through	through
3-4-3	through	through
3-4-4	through	through
3-5-1	through	through
3-5-2	through	through
3-5-3	through	through
3-5-4	through	through

[a]"Through" means the jet penetrates through the bed.

TABLE P-10

COMPARISON BETWEEN EXPERIMENTAL AND CALCULATED
JET PENETRATION DEPTH (CASE II)

Jet Penetration Depth, Inches

Run No.	Experimental	Calculated
1-1-1	0.5-2.5	2.6
1-1-2	2.0-3.5	3.2
1-1-3	4.0-7.0	4.0
1-1-4	5.5-9.0	4.9
1-1-5	7.0-12.0	5.5
1-2-1	3.0-5.0	2.7
1-2-2	3.0-6.5	3.2
1-2-3	4.0-8.0	4.3
1-2-4	6.0-through[a]	5.4
1-2-5	9.0-through	5.0
1-2-6[b]	8.0-through	3.0
1-3-1	3.0-7.0	2.0
1-3-2	4.0-through	3.1
1-3-3	5.0-through	3.8
1-3-4[b]	4.0-through	1.9
1-3-5	6.0-through	5.1
1-3-6[b]	through	2.5
1-4-1	through	2.1
1-4-2	through	3.3
1-4-3[b]	through	1.4
1-4-4	through	through
1-4-5[b]	through	2.5
1-4-6[b]	through	1.1
1-5-1	through	through
1-5-2	through	through
1-5-3	through	through
1-5-4[b]	through	through
1-5-5[b]	through	through
2-1-1	4-9	4.2
2-1-2	6-14	4.9
2-1-3[b]	7-through	3.6
2-1-4	7-through	6.1
2-1-5[b]	8-through	4.4
2-2-1	5-9	3.8
2-2-2	7-through	4.4
2-2-3[b]	7-through	2.1
2-2-4	9-through	5.4
2-2-5[b]	9-through	3.0
2-2-6[b]	5-8	2.0
2-3-1	5-through	4.0
2-3-2	through	4.3
2-3-3[b]	through	3.1
2-3-4	through	5.1
2-3-5[b]	through	4.1

TABLE P-10 (Continued)

Run No.	Experimental	Calculated
2-4-1	through	through
2-4-2	through	through
2-4-3[b]	through	through
2-4-4	through	through
2-4-5[b]	through	through
2-5-1	through	through
2-5-2	through	through
2-5-3	through	through
3-1-1	4-8	4.9
3-1-2	5-10	6.1
3-1-3	7-through	7.4
3-1-4	8-through	6.0
3-2-1	5-9	4.6
3-2-2	5-through	5.9
3-2-3	8-through	6.5
3-2-4[b]	7-through	5.0
3-2-5	5-through	7.1
3-2-6[b]	7-through	5.6
3-3-1	4-through	4.5
3-3-2	6-through	5.9
3-3-3	5-through	6.6
3-3-4[b]	through	4.6
3-3-5	5-through	6.3
3-3-6[b]	5-through	5.3
3-4-1	through	3.8
3-4-2	through	through
3-4-3	through	through
3-4-4	through	through
3-4-5	through	through
3-4-6[b]	through	through
3-5-1	through	through
3-5-2	through	through
3-5-3	through	through
3-5-4	through	through
3-5-5	through	through
3-5-6[b]	through	through

[a]"Through" means the jet penetrates through the bed.
[b]Downcomers are not at minimally fluidized condition.

TABLE P-11

COMPARISON BETWEEN EXPERIMENTAL AND CALCULATED
JET PENETRATION DEPTH (CASE III)

Run No.	Jet Penetration Depth, Inches	
	Experimental	Calculated
B-1-1	4.0-through[a]	3.9
B-1-2	6.0-through	4.3
B-1-3	7.0-through	4.2
B-1-4	8.0-through	5.4
B-2-1	5.0-through	3.9
B-2-2	5.0-through	4.6
B-2-3	through	4.6
B-2-4	through	4.7
B-3-1	through	through
B-3-2	through	through
B-3-4	through	through
B-3-5	through	through
B-4-1	through	through
B-4-2	through	through
B-4-3	through	through
B-4-5	through	through

[a]"Through" means the jet penetrates the fluid bed above the draft tube.

at lower air velocities in the draft tube. This is because of the short draft tube (18 inches) used in the cold model. Experimental data[12,13,15,19] show that the solid concentration in the gas stream takes up to several feet to attain the final equilibrium value. At lower gas velocities, the solid acceleration is slower, and thus the voidage in the draft tube increases to the final equilibrium value more slowly. Hence, the actual average voidage in the draft tube is lower than the equilibrium value. To obtain this average voidage, the exponential equation of the form of Equation 31 is again assumed with boundary conditions

$$\begin{aligned} &\text{at} \quad H = 0 \quad \varepsilon = \varepsilon_d \\ &\text{at} \quad H = L \quad \varepsilon = \varepsilon_r \ . \end{aligned} \tag{33}$$

Average voidage can then be found to be

$$\varepsilon_{ave} = \frac{\varepsilon_d[L \exp(-L) + \exp(-L) - 1] - \varepsilon_r[\exp(-L) + L - 1]}{L[\exp(-L) - 1]} \ . \tag{34}$$

The corrected static head term, $(\Delta P_{hs})_c$, is then calculated through the following equation

$$(\Delta P_{hs})_c = \rho_s(1 - \varepsilon_{ave})L_a + \rho_s(1 - \varepsilon_r)(L - L_a) \ , \tag{35}$$

where

$$L_a = \frac{(3U_t - U_o)}{(U_o - U_t)} L \ . \tag{36}$$

For superficial gas velocity, U_o, larger than three times the terminal velocity, no correction is necessary for the static head term based on the experimental pressure measurements.

Theoretically, the distance required to accelerate a spherical particle to a specific velocity should be evaluated from the following integration equation:

TABLE P-12

COMPARISON OF PRESSURE DROP PREDICTIONS IN THE DRAFT TUBE
(inches H_2O)

Run No.		(1) Up. r (ft/sec)	(2) ϵ_r	(3) ΔP_{ks}	(4) ΔP_{hs}	(5) ΔP_f	(6) ΔP_R	(7) $(\Delta P_{hs})_c$	(8) $(\Delta P_R)_c$	(9) $(\Delta P_{1-2})_{exp}$	(10) $(\Delta P_{1-2})_{calc.}$	(11) $(\Delta P_D)_{exp}$	(12) $(\Delta P_D)_{calc.}$
1-1-1	(a)†	30.80	0.975	11.25	1.02	5.26	17.53	1.02	17.53	3.40	2.30	21.66	19.83
	(b)	27.82		9.18	1.02	0.88	11.08						
	(c)	31.31	0.975	11.57	1.00	2.29	14.86						
1-1-2	(a)	20.48	0.959	8.04	1.64	4.29	13.97	5.85	18.19	4.40	1.96	19.04	20.15
	(b)	20.65		8.18	1.64	1.31	11.14						
	(c)	23.03	0.962	9.37	1.51	2.34	13.22						
1-1-3	(a)	8.94	0.942	2.15	2.31	1.68	6.14	6.43	10.26	2.60	8.52	19.04	18.78
	(b)	12.92		4.50	2.31	0.86	7.67						
	(c)	12.50	0.957	3.10	1.71	1.80	6.61						
1-2-1	(a)	29.68	0.973	11.24	1.09	5.27	17.60	1.09	17.60	3.20	2.33	19.04	19.93
	(b)	27.02		9.32	1.09	0.96	11.38						
	(c)	30.61	0.973	11.71	1.08	2.30	15.09						
1-2-2	(a)	19.38	0.962	6.66	1.52	3.69	11.87	6.34	16.69	2.90	3.01	19.04	19.70
	(b)	20.08		7.14	1.52	1.17	9.83						
	(c)	22.00	0.965	7.82	1.39	2.11	11.32						
1-2-3	(a)	9.76	0.937	2.80	2.52	2.02	7.34	6.95	11.77	3.20	7.40	19.04	19.17
	(b)	13.28		5.19	2.52	1.04	8.75						
	(c)	13.23	0.952	3.89	1.91	2.04	7.84						

TABLE P-12 (Continued)

Run No.		(1) Up. r (ft/sec)	(2) ε_r	(3) ΔP_{ks}	(4) ΔP_{hs}	(5) ΔP_f	(6) ΔP_R	(7) $(\Delta P_{hs})_c$	(8) $(\Delta P_R)_c$	(9) $(\Delta P_{1-2})_{exp}$	(10) $(\Delta P_{1-2})_{calc.}$	(11) $(\Delta P_D)_{exp}$	(12) $(\Delta P_D)_{calc.}$
1-3-1	(a)	28.18	0.976	8.71	0.94	4.15	13.79	1.02	13.87	2.60	5.47	21.66	19.34
	(b)	26.24		7.54	0.94	0.85	9.33						
	(c)	29.08	0.977	9.14	0.92	1.99	12.05						
1-3-2	(a)	18.59	0.959	6.60	1.64	3.53	11.77	7.07	17.20	3.40	2.61	21.66	19.81
	(b)	19.47		7.24	1.64	1.20	10.09						
	(c)	21.34	0.963	7.86	1.47	2.19	11.52						
1-3-3	(a)	11.91	0.947	3.51	2.12	2.31	7.94	8.06	13.89	3.60	5.32	21.66	19.21
	(b)	14.91		5.49	2.12	1.20	8.81						
	(c)	15.27	0.958	4.59	1.67	1.95	8.21						
1-4-1*	(a)	16.77	0.979	2.70	0.82	1.59	5.12	6.99	11.28	0.90	2.26	13.54	--
	(b)	19.03		3.48	0.82	0.58	4.89						
	(c)	18.96	0.981	3.13	0.76	1.15	5.04						
1-4-2*	(a)	10.37	0.969	1.54	1.23	1.15	3.92	7.22	9.91	0.90	3.63	13.54	--
	(b)	14.61		3.07	1.23	0.62	4.92						
	(c)	13.63	0.976	2.10	0.96	1.18	4.24						

‡ Row (a): Predictions by the present model.
" (b): " " the Hinkle's model.
" (c): " " the Curran and Gorin's model.
* Downcomers are not minimally fluidized .

TABLE P-13

COMPARISON OF PRESSURE DROP PREDICTIONS IN THE DRAFT TUBE

(inches H_2O)

Run No.		(1) Up. r (ft/sec)	(2) ε_r	(3) ΔP_{ks}	(4) ΔP_{hs}	(5) ΔP_f	(6) ΔP_R	(7) $(\Delta P_{hs})_c$	(8) $(\Delta P_R)_c$	(9) $(\Delta P_{1-2})_{exp}$	(10) $(\Delta P_{1-2})_{calc.}$	(11) $(\Delta P_D)_{exp}$	(12) $(\Delta P_D)_{calc.}$
2-1-1	(a)†	20.59	0.975	4.85	0.98	2.55	8.38	4.68	12.08	2.20	6.61	16.25	18.69
	(b)	21.34		5.21	0.98	0.79	6.98						
	(c)	23.18	0.978	5.53	0.88	1.56	7.97						
2-1-2	(a)	19.21	0.966	5.91	1.37	3.19	10.47	6.20	15.30	2.60	4.07	18.96	19.37
	(b)	20.10		6.47	1.37	1.05	8.89						
	(c)	22.33	0.969	7.09	1.23	1.92	10.24						
2-1-3	(a)	16.21	0.957	5.24	1.71	2.95	9.90	8.94	17.14	2.60	2.32	19.04	19.49
	(b)	17.91		6.40	1.71	1.10	9.21						
	(c)	19.70	0.964	6.53	1.43	2.03	9.99						
2-1-4	(a)	11.11	0.948	2.98	2.07	2.00	7.05	7.67	12.64	2.10	6.34	18.28	18.98
	(b)	14.45		5.04	2.07	1.06	8.17						
	(c)	14.87	0.961	4.05	1.55	1.85	7.45						
2-2-1	(a)	28.44	0.971	10.87	1.15	5.13	17.15	1.26	17.27	3.50	2.76	20.40	20.03
	(b)	26.17		9.21	1.15	1.04	11.40						
	(c)	29.69	0.972	11.68	1.12	2.36	15.16						
2-2-2	(a)	17.59	0.954	6.68	1.85	3.60	12.13	8.13	18.42	3.60	1.57	21.76	19.99
	(b)	18.66		7.52	1.85	1.29	10.66						
	(c)	20.46	0.959	7.97	1.63	2.28	11.88						
2-2-3	(a)	11.36	0.936	3.84	2.55	2.50	8.89	7.84	14.18	3.40	5.47	18.96	19.65
	(b)	14.23		6.04	2.55	1.33	9.92						
	(c)	14.75	0.949	5.16	2.03	2.27	9.46						

TABLE 13 (Continued)

Run No.		(1) Up. r (ft/sec)	(2) ϵ_r	(3) ΔP_{ks}	(4) ΔP_{hs}	(5) ΔP_f	(6) ΔP_R	(7) $(\Delta P_{hs})_c$	(8) $(\Delta P_R)_c$	(9) $(\Delta P_{1-2})_{exp}$	(10) $(\Delta P_{1-2})_{calc}$	(11) $(\Delta P_D)_{exp}$	(12) $(\Delta P_D)_{calc}$
2-3-1*	(a)	21.43	0.971	6.09	1.14	3.11	10.34	4.45	13.66	3.40	2.66	16.32	--
	(b)	21.73		6.26	1.14	0.95	8.35						
	(c)	23.51	0.973	6.88	1.08	1.81	9.77						
2-3-2*	(a)	10.31	0.972	1.36	1.10	1.02	3.48	7.18	9.56	1.90	2.68	12.24	--
	(b)	14.68		2.76	1.10	0.56	4.42						
	(c)	13.46	0.978	1.84	0.88	1.05	3.77						
2-4-1*	(a)	18.39	0.977	3.59	0.91	1.95	6.45	5.96	11.50	2.10	3.46	14.96	--
	(b)	20.00		4.24	0.91	0.68	5.83						
	(c)	20.51	0.979	4.08	0.84	1.34	6.26						
2-4-2*	(a)	11.68	0.958	2.67	1.68	1.76	6.11	7.91	12.34	2.40	5.34	17.68	--
	(b)	15.10		4.47	1.68	0.77	6.92						
	(c)	15.02	0.967	3.52	1.31	1.64	6.47						
2-5-1*	(a)	18.46	0.975	3.97	1.00	2.12	7.09	6.06	12.15	2.10	2.13	14.28	--
	(b)	19.96		4.64	1.00	0.74	6.38						
	(c)	20.70	0.977	4.50	0.92	1.42	6.84						
2-5-2*	(a)	13.04	0.958	3.34	1.68	2.06	7.09	8.48	13.89	2.80	3.11	17.00	--
	(b)	15.95		5.00	1.68	0.87	7.55						
	(c)	16.30	0.965	4.28	1.39	1.73	7.40						

‡ Row (a): Predictions by the present model.
" (b): " by the Hinkle's model.[19]
" (c): " by the Curran and Gorin's[11] model.
* Downcomers are not minimally fluidized .

TABLE P-14

COMPARISON OF PRESSURE DROP PREDICTIONS IN THE DRAFT TUBE
(inches H_2O)

Run No.	Up.	(1) r (ft/sec)	(2) ε_r	(3) ΔP_{ks}	(4) ΔP_{hs}	(5) ΔP_f	(6) ΔP_R	(7) $(\Delta P_{hs})_c$	(8) $(\Delta P_R)_c$	(9) $(\Delta P_{1-2})_{exp}$	(10) $(\Delta P_{1-2})_{calc}$	(11) $(\Delta P_D)_{exp}$	(12) $(\Delta P_D)_{calc.}$
3-1-1	(a)†	26.87	0.969	10.44	1.24	4.78	16.46	2.02	17.24	3.10	2.85	19.04	20.09
	(b)	25.08		9.10	1.24	1.12	11.46						
	(c)	28.38	0.970	11.35	1.20	2.35	14.90						
3-1-2	(a)	20.75	0.963	7.32	1.46	3.71	12.49	5.39	16.41	3.10	3.36	19.04	19.77
	(b)	20.99		7.49	1.46	1.18	10.13						
	(c)	23.18	0.966	8.44	1.35	2.14	11.93						
3-1-3	(a)	14.05	0.950	4.56	1.98	2.69	9.23	8.91	16.16	3.30	3.33	19.04	19.49
	(b)	16.35		6.17	1.98	1.09	9.24						
	(c)	17.26	0.959	5.72	1.63	2.09	9.44						
3-2-1	(a)	28.93	0.973	10.64	1.09	4.79	16.52	1.09	16.52	2.90	3.31	19.60	19.83
	(b)	26.55		8.96	1.09	0.96	11.01						
	(c)	29.94	0.973	11.11	1.08	2.23	14.42						
3-2-2	(a)	25.66	0.969	9.58	1.25	4.64	15.47	2.53	16.75	3.10	3.20	20.30	19.95
	(b)	24.31		8.59	1.25	1.12	10.96						
	(c)	27.34	0.970	10.50	1.20	2.27	13.97						
3-2-3	(a)	21.43	0.964	7.71	1.44	3.96	13.11	4.95	16.62	3.30	3.21	19.60	19.83
	(b)	21.45		7.71	1.44	1.19	10.34						
	(c)	23.82	0.967	8.84	1.31	2.21	12.36						
3-2-4	(a)	17.50	0.960	5.69	1.59	3.21	10.49	7.76	16.66	3.30	2.88	19.43	19.54
	(b)	18.83		6.59	1.59	1.12	9.30						
	(c)	20.34	0.964	6.86	1.43	2.03	10.32						
3-3-1	(a)	27.95	0.973	9.65	1.06	4.49	15.20	1.30	15.44	3.4	4.2	19.9	19.6
	(b)	25.96		8.32	1.06	0.95	10.33						
	(c)	29.01	0.975	9.82	1.00	4.28	15.10						
3-3-2	(a)	22.52	0.967	7.84	1.32	3.96	13.12	4.17	15.97	3.2	3.7	19.4	19.7
	(b)	22.24		7.64	1.32	1.13	10.10						
	(c)	24.61	0.970	8.59	1.19	2.09	11.87						
3-3-3	(a)	19.22	0.963	6.38	1.48	3.43	11.29	6.38	16.20	3.2	3.4	19.4	19.6
	(b)	20.01		6.92	1.48	1.13	9.53						
	(c)	21.77	0.967	7.25	1.31	2.04	10.60						
3-3-4	(a)	16.19	0.959	4.98	1.63	2.88	9.49	8.82	16.68	3.5	2.7	19.4	19.4
	(b)	17.97		6.14	1.63	1.07	8.83						
	(c)	19.12	0.965	5.94	1.39	1.92	9.25						

TABLE P-14 (Continued)

Run No.		(1) Up. r (ft/sec)	(2) ε_r	(3) ΔP_{ks}	(4) ΔP_{hs}	(5) ΔP_f	(6) ΔP_R	(7) $(\Delta P_{hs})_c$	(8) $(\Delta P_R)_c$	(9) $(\Delta P_{1-2})_{exp}$	(10) $(\Delta P_{1-2})_{calc.}$	(11) $(\Delta P_D)_{exp}$	(12) $(\Delta P_D)_{calc.}$
3-4-1	(a)	24.99	0.975	7.37	1.01	3.58	11.96	2.44	13.39	2.9	5.8	19.2	19.2
	(b)	24.12		6.86	1.01	0.90	8.78						
	(c)	26.38	0.976	7.65	0.96	1.79	10.40						
3-4-2	(a)	21.52	0.971	6.32	1.17	3.27	10.76	4.46	14.05	3.1	5.1	19.4	19.2
	(b)	21.76		6.45	1.17	0.98	8.60						
	(c)	23.57	0.973	6.90	1.08	1.77	9.75						
3-4-3	(a)	17.23	0.965	4.82	1.39	2.72	8.94	7.61	15.16	3.1	3.9	18.9	19.1
	(b)	18.83		5.76	1.39	0.97	8.12						
	(c)	19.94	0.970	5.58	1.19	1.86	8.53						
3-4-4	(a)	14.08	0.959	3.75	1.62	2.29	7.67	8.85	14.92	3.2	4.1	18.5	19.0
	(b)	16.65		5.25	1.62	0.91	7.78						
	(c)	17.17	0.967	4.55	1.31	1.73	7.59						
3-5-1	(a)	24.73	0.975	7.14	1.00	3.48	11.62	2.54	13.16	2.4	6.0	18.7	19.2
	(b)	23.97		6.70	1.00	0.89	8.59						
	(c)	26.15	0.977	7.45	0.92	1.83	10.20						
3-5-2	(a)	20.67	0.969	6.18	1.24	3.26	10.69	5.07	14.52	2.8	4.8	18.9	19.3
	(b)	21.14		6.47	1.24	1.01	8.72						
	(c)	22.90	0.972	6.88	1.11	1.86	9.85						
3-5-3	(a)	16.03	0.961	4.62	1.54	2.72	8.88	8.80	16.14	2.8	3.1	18.4	19.2
	(b)	17.94		5.79	1.54	1.00	8.34						
	(c)	18.94	0.967	5.50	1.31	1.79	8.60						
3-5-4	(a)	13.59	0.955	3.87	1.79	2.40	8.06	8.71	14.98	2.8	4.1	18.7	19.1
	(b)	16.21		5.50	1.79	0.96	8.26						
	(c)	16.76	0.964	4.74	1.43	1.83	8.00						

† Row (a): Predictions by the present model.
" (b): " by the Hinkle's model.[19]
" (c): " by the Curran and Gorin's [11] model.

TABLE P-15

COMPARISON BETWEEN THEORETICAL PREDICTIONS
AND EXPERIMENTAL VALUES IN THE DOWNCOMER (CASE II)

Run No.	Pressure Drop in Downcomer, in. H_2O	
	Experimental	Theoretical
1-1-1	15.4	14.8
1-1-2	15.2	14.8
1-1-3	15.4	14.8
1-1-4	15.6	14.9
1-1-5	15.4	14.8
1-2-1	15.4	14.8
1-2-2	15.4	14.8
1-2-3	15.6	14.8
1-2-4	15.4	14.8
1-2-5	15.0	14.8
1-3-1	15.2	14.6
1-3-2	15.4	14.7
1-3-3	15.4	14.7
1-3-5	15.0	14.8
1-4-1	15.2	14.7
1-4-2	15.4	14.8
1-4-4	15.4	14.7
1-5-1	15.2	14.9
1-5-2	15.0	14.9
1-5-3	14.7	14.9
2-1-1	15.6	14.9
2-1-2	15.4	14.9
2-1-4	15.4	14.9
2-2-1	15.4	14.8
2-2-2	15.2	14.8
2-2-4	15.0	14.8
2-3-1	15.6	14.9
2-3-2	15.6	14.8
2-3-4	15.4	14.8
2-4-1	15.6	14.8
2-4-2	15.4	14.8
2-4-4	15.4	14.8

TABLE P-15 (Continued)

Run No.	Pressure Drop in Downcomer, in. H_2O	
	Experimental	Theoretical
2-5-1	15.4	14.9
2-5-2	15.4	14.9
2-5-3	15.4	14.9
3-1-1	15.8	15.3
3-1-2	15.4	15.3
3-1-3	15.2	15.3
3-2-1	15.4	15.2
3-2-2	15.2	15.3
3-2-3	15.2	15.3
3-2-5	15.4	15.3
3-3-1	15.2	15.2
3-3-2	15.6	15.3
3-3-3	15.6	15.3
3-3-5	15.0	15.2
3-4-1	15.0	15.1
3-4-2	15.2	15.1
3-4-3	15.4	15.2
3-4-4	15.4	15.2
3-4-5	14.9	15.2
3-5-1	15.2	15.2
3-5-2	15.0	15.2
3-5-3	15.4	15.3
3-5-4	15.0	15.3
3-5-5	15.4	15.4

TABLE P-16

COMPARISON BETWEEN THEORETICAL PREDICTIONS
AND EXPERIMENTAL VALUES IN THE DOWNCOMER (CASE III)

Run No.	Downcomer Pressure Drop, in. H_2O	
	Predicted	Experimental
B-1-1	18.2	18.9
B-1-2	18.1	18.4
B-1-3	18.0	18.4
B-1-4	18.1	18.4
B-2-1	18.2	18.9
B-2-2	18.1	18.9
B-2-3	18.0	18.7
B-2-4	18.0	18.2
B-3-1	18.2	19.2
B-3-2	18.1	18.9
B-3-4	18.0	18.9
B-3-5	18.0	18.9
B-4-1	18.2	19.2
B-4-2	18.1	18.7
B-4-3	18.1	18.7
B-4-5	18.2	18.5

$$\Delta L = \int_{U_{p1}}^{U_{p2}} \frac{U_p \, d(U_p)}{\frac{3 \rho_f C_D (U_o - U_p)^2}{4 d_p \rho_s} - \frac{f_p U_p^2}{2 D}} \quad . \tag{37}$$

However, this requires a relation between the particle friction factor, f_p, and the particle velocity, U_p. There is no proven and reliable correlation existing so far. It is also difficult to isolate the solid friction term from the pressure measurements of a short draft tube. Because of these uncertainties, Equation 38 was not used in calculating the pressure drop in the draft tube. Fortunately, this correction is negligible when the draft tube is sufficiently long (i.e., > 10 ft).

The corrected static pressure drop, $(\Delta P_{hs})_c$, is presented in column 7 . Column 8 , $(\Delta P_R)_c$, is the corrected total pressure drop in the draft tube by taking into account the term $(\Delta P_{hs})_c$. Columns 9 and 10 compare the experimental and calculated values of ΔP_{1-2}. The calculated pressure drop between 1 and 2, $(\Delta P_{1-2})_{calc}$, is determined by subtracting $(\Delta P_R)_c$ from $(\Delta P_D)_{calc}$. It is noticed that Curran and Gorin's model predicts a higher solid kinetic loss, a lower solid static loss, and a lower solid friction loss, resulting in a lower overall pressure drop in the draft tube. The difference, however, is usually less than 2.5 in H_2O. Hinkle's model gives either a higher or a lower kinetic loss, depending on the gas velocity range in question; the friction loss, however, is much lower when compared to the predictions of the other two models, resulting in a still lower pressure drop. The difference in total pressure drop ranges up to 6.5 in H_2O at high gas velocities in the draft tube.

Excluding the runs with superficial air velocity in the draft tube less than ∿ 22 ft/sec, the calculated pressure drop, $(\Delta P_{1-2})_{calc}$, is within ± 37% of the experimental value in 70% of the data taken. When the superficial air velocity in the draft tube is less than 22 ft/sec,

TABLE P-17

COMPARISON BETWEEN THE CALCULATED AND THE OBSERVED SOLID FLOW RATE

Run No.	Observed Solid Flow Rate, lb/sec*	Calculated Solid Flow Rate, lb/sec	Deviation %
1-1-1	1.42	1.02	- 28.2
1-1-2	1.55	0.917	- 40.8
1-2-1	1.46	1.03	- 29.5
1-2-2	1.36	1.22	- 10.3
1-3-1	1.20	1.82	+ 51.7
1-3-2	1.41	1.11	- 21.3
1-4-1	0.631	1.01	+ 60.1
2-1-1	0.912	2.06	+125.9
2-1-2	1.21	1.49	+ 23.1
2-1-3	1.27	1.03	- 18.9
2-2-1	1.50	1.15	- 23.3
2-2-2	1.49	0.79	- 47.0
2-3-1	1.12	1.12	+ 0
2-4-1	0.759	1.34	+ 76.5
2-5-1	0.830	0.969	+ 16.7
2-5-2	1.00	1.25	+ 25.0
3-1-1	1.53	1.18	- 22.9
3-1-2	1.39	1.31	- 5.8
3-1-3	1.27	1.31	+ 3.1
3-2-1	1.42	1.30	- 8.5
3-2-2	1.47	1.27	- 13.6
3-2-3	1.42	1.27	- 10.6
3-2-4	1.29	1.18	- 8.5

TABLE P-17 (Continued)

Run No.	Observed Solid Flow Rate, lb/sec[a]	Calculated Solid Flow Rate, lb/sec	Deviation %
3-3-1	1.33	1.52	+ 14.3
3-3-2	1.37	1.40	+ 2.2
3-3-3	1.31	1.32	+ 0.8
3-3-4	1.22	1.13	- 7.4
3-4-1	1.14	1.89	+ 65.7
3-4-2	1.15	1.73	+ 50.5
3-4-3	1.10	1.45	+ 31.8
3-4-4	1.04	1.49	+ 43.2
3-5-1	1.12	1.93	+ 72.2
3-5-2	1.18	1.66	+ 40.6
3-5-3	1.14	1.24	+ 8.8
3-5-4	1.11	1.49	+ 34.2

[a]Includes both downcomers.

the largest particles of the bed material which have terminal velocity close to 22 ft/sec are likely to accumulate in the draft tube and form a slugging bed. This phenomenon was actually observed in the experiments. For those runs, the pressure drop prediction using a vertical pneumatic transport correlation is no longer valid.

From the experimental relationship for the solid velocities in the downcomers as shown in Equation 2, the solid circulation rate can be calculated through the following equation:

$$W_s = 0.107\ \rho_s\ A_d\ (1 - \varepsilon_d)(2\ gH_p)^{2/3}, \text{for Case I,}$$

$$W_s = 0.107\ \rho_s\ A_c\ (1 - \varepsilon_d)(2\ gH_p)^{2/3} \text{ for Case II,} \qquad (39)$$

and

$$W_s = 0.025\ \rho_s\ A_d\ (1 - \varepsilon_d)(2\ gH_p) \text{ for Case III,}$$

where

$$A_c = F_c \cdot A_d\ .$$

By using the predicted pressure drop between 1 and 2, $(\Delta P_{1-2})_{calc}$, the calculated solid flow rates are compared to the observed ones in Table P-17 for Case I. About 75% of the calculated solid flow rate comes within $\pm$ 35% of the observed solid flow rate.

The calculated jet penetration depth was compared to the observed value in Tables P-9 through P-11. Due to the oscillating nature of the actual bed operation, the observed bed penetration depth has a 3 to 5 in range. The predictions from Equation 29 are good.

DISCUSSION

By analogy with liquid, the flow rate of minimally fluidized particles during outflow through a small orifice in a thin wall with constant bed height above the orifice is given by Massimilla[18] as

$$W_s = C_o A \rho_s (2 g H_{mf})^{1/2} \quad . \tag{40}$$

The solid discharge coefficient increases with the increase of d_o/d_p up to 40 and then levels off to a value of about 0.5. If the orifice is a high vertical slot partially filled with fluidized particles, the solid discharge rate is $W_s \alpha H_{mf}^{3/2}$. If the orifice is profiled to a quadratic hyperbola equation, the discharge rate is $W_s \alpha H_{mf}$.

In the present set-up, the discharge of solid particles from the downcomers into the draft tube is very similar to solid discharge from a minimally fluidized bed. Thus, the solid recirculation rate in the bed should be in a form as shown in Equation 40. Comparing Equation 40 with the experimental equations obtained, Equations 2 and 3 conform with Equation 40 but with a different dependence on H_{mf}. This is understandable because of the different designs of the draft tube inlets and the much larger orifice openings. However, when the solid discharge coefficients (Co) are evaluated from Equations 2 and 3 by using the open area between the draft tube and the downcomers as the orifice openings (A), the coefficients are $\sim$ 0.05 for Cases I and II and $\sim$ 0.01 for Case III, which are much less than the 0.5 from Equation 40. Apparently, the solid recirculation rate in a recirculating bed involves some other complicated mechanisms which are explained below.

In a recirculating bed, the solid recirculation rate is controlled not only by the rate of solid discharge from the downcomers but also by the rate of solid pick-up in the draft tube. At steady state,

the solid discharge rate from the downcomers should equal the solid pick-up rate in the draft tube. Thus, the solid recirculation rate can be controlled either by the solid discharge rate from the downcomers or by the solid pick-up rate in the draft tube, depending on the operating conditions. The pressure drop in a minimally fluidized downcomer is relatively independent of the solid circulation rate, because the actual air velocity is much higher than the solid velocity (see Equation 7); the pressure drop in the draft tube, however, is sensitive to the air velocity in the draft tube and the total solid circulation rate as shown in Figure P-7. There exists a choking air velocity for every solid flow rate. An air velocity lower than the choking velocity will result in the collapse of solid particles into a slug and will eventually choke the vertical pneumatic conveying line. Thus, the solid loading at the choking velocity represents the saturation carrying capacity of the air stream.

The saturation carrying capacity of a gas stream can be calculated from the empirical correlation by Zenz and Weil.[20] The saturation carrying capacities of the draft tube at different air velocities are compared with the experimental solid recirculation rates for Cases I and III in Figure P-8. Only the data for "minimally fluidized" downcomers are included. It is interesting to notice that at lower air velocities, the experimental solid circulation rate is much larger than the saturation carrying capacity of the air stream. This can be easily understood if we see the downcomers as solid feeders of capacities depending on ΔP_{1-2}. When the air velocity in the draft tube is low, ΔP_{1-2} is large. The downcomers feed the solid into the draft tube at a rate much larger than that which can be handled by the air stream. Thus, the solid transport in the draft tube takes a form of slugging transport rather than pneumatic transport in the conventional sense. The slugging imposes an additional pressure drop in the draft tube. This explains why the pressure drop predictions for the draft tube from all existing mathematical models are much less than the experimental observations at lower

Curve 651039-A

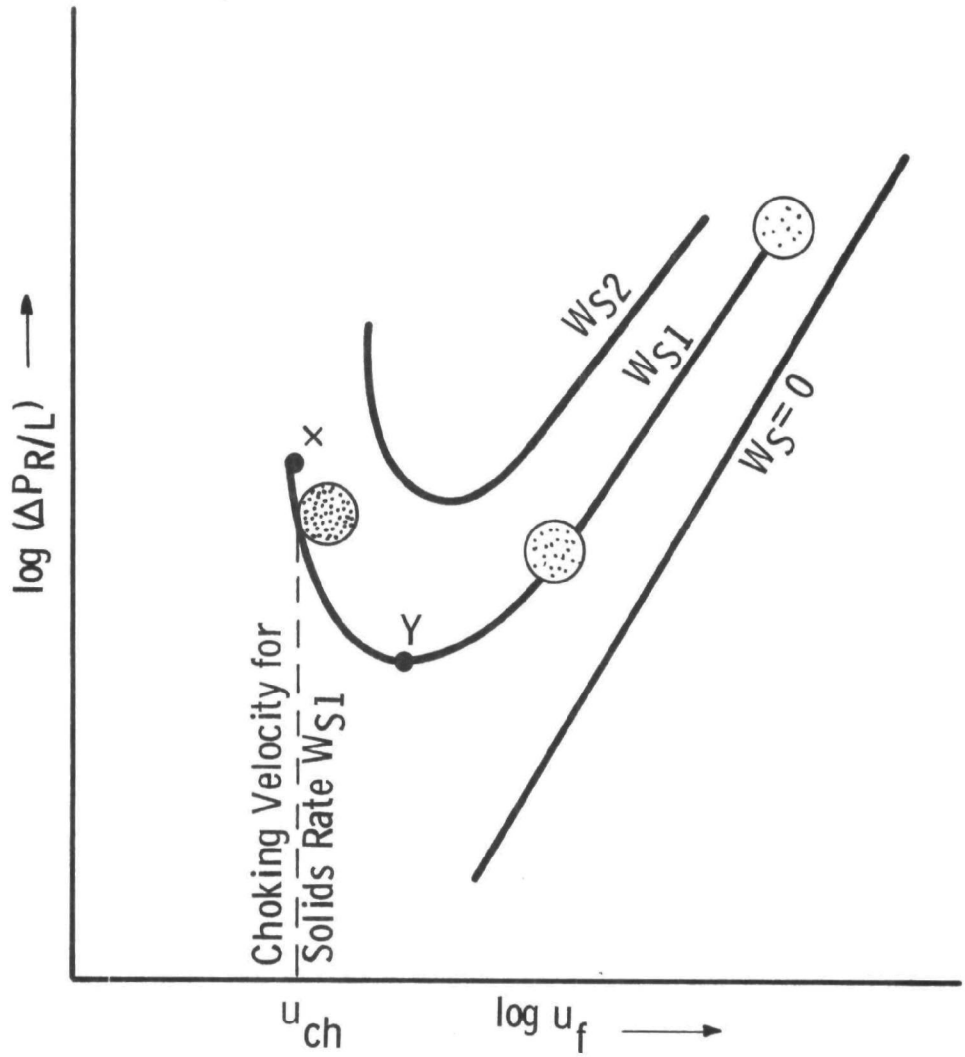

Figure P-7— Schematic Representation of Flow Characteristics in Vertical Pneumatic Transport[22]

From Fluidization and Fluid Particle Systems by F. Zenz & D. Othmer
© 1960 by Litton Educational Publishing, Inc.

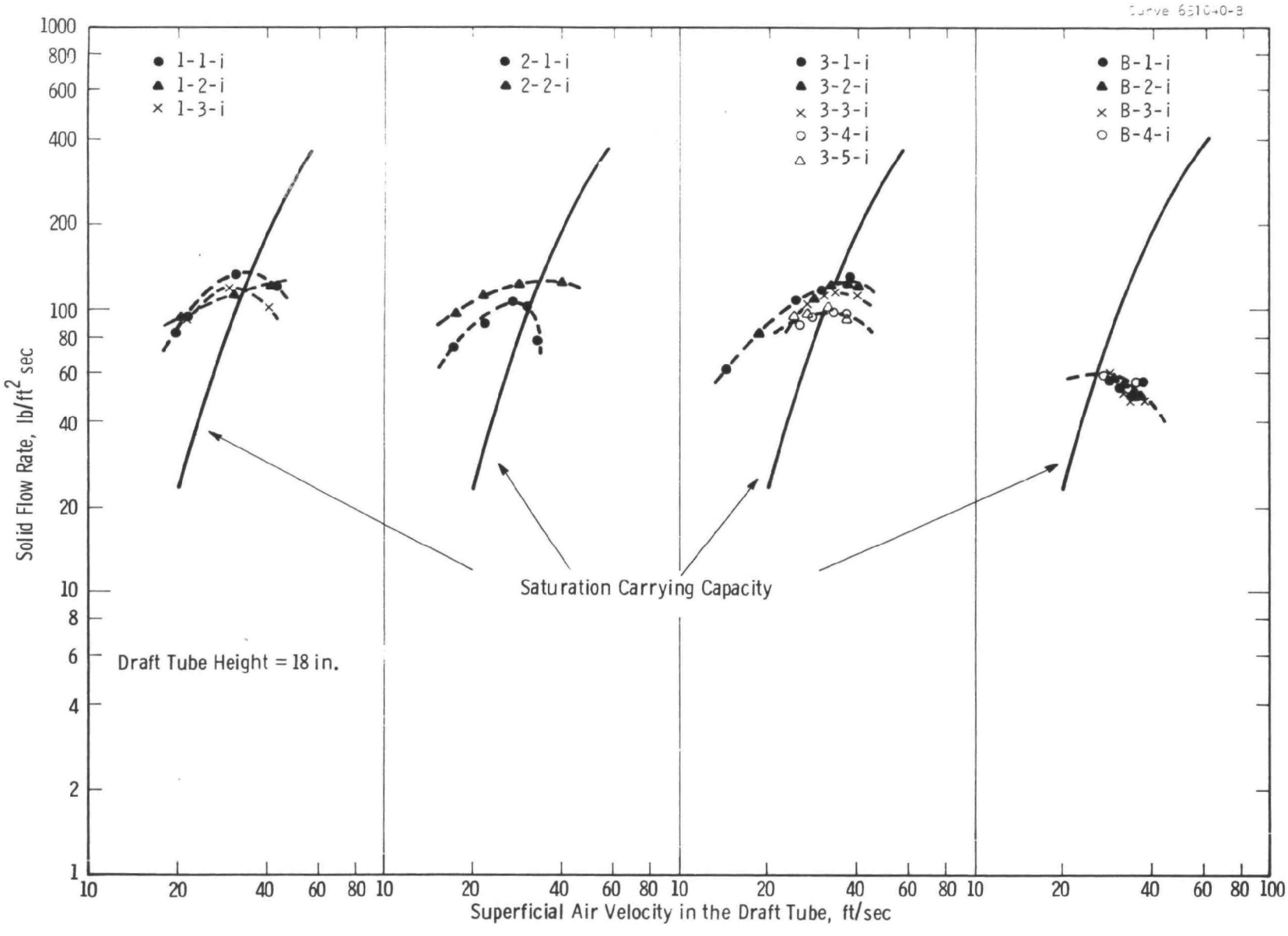

Figure P-8— Comparison between the Experimental Data and the Saturation Carrying Capacity

draft tube velocities. In fact, the pressure loss due to this slugging depends linearly on the theoretical pressure difference between the downcomers and the draft tube. Figure P-9 plots the pressure difference between the downcomers and the draft tube, $(\Delta P_D)_{exp} - (\Delta P_{2-3})_{calc}$, and the slugging pressure loss, $(\Delta P_D)_{exp} - (\Delta P_{2-3})_{calc} - (\Delta P_{1-2})_{exp}$. The straight line can be expressed by the following equation:

$$(\Delta P)_c = 3.23 + 1.025\ [(\Delta P_D)_{exp} - (\Delta P_{2-3})_{calc}] \text{ for Cases I and III,}$$
and
$$(\Delta P)_c = 2.10 + 1.025\ [(\Delta P_D)_{exp} - (\Delta P_{2-3})_{calc}] \text{ for Case II.} \qquad (41)$$

If Equation 41 is used, but $(\Delta P_D)_{calc}$ exchanged for $(\Delta P_D)_{exp}$, to predict the solid circulation rate, most predictions are good to $\pm$ 20% of the experimental values for those runs with downcomers minimally fluidized. The results are presented in Tables P-18 through P-20.

When the air velocity in the draft tube is increased, eventually an air velocity is reached where the solid discharge rate from the downcomers equals the saturation carrying capacity of the air stream. This is the point of intersection between the experimental curve and the curve for the saturation carrying capacity in Figure P-8. This point also corresponds to the point of choking in Figure P-7 (point X). The choking point does not coincide with the point of lowest pressure drop, Y. Thus, a further increase in air velocity will result in a slightly higher solid recirculation rate; the recirculation rate decreases quickly, however, at even higher velocities because of the increasing pressure drop in the draft tube. At this region, the solid discharge from the downcomers becomes the controlling factor in solid circulation. The optimum air velocity in the draft tube which corresponds to the maximum solid circulation rate can be found by maximizing the pressure drop between the downcomers and the draft tube, ΔP_{1-2}.

When the draft tube inlet design is as shown in Figure P-2, the solid circulation rate is much smaller. This is because the air input

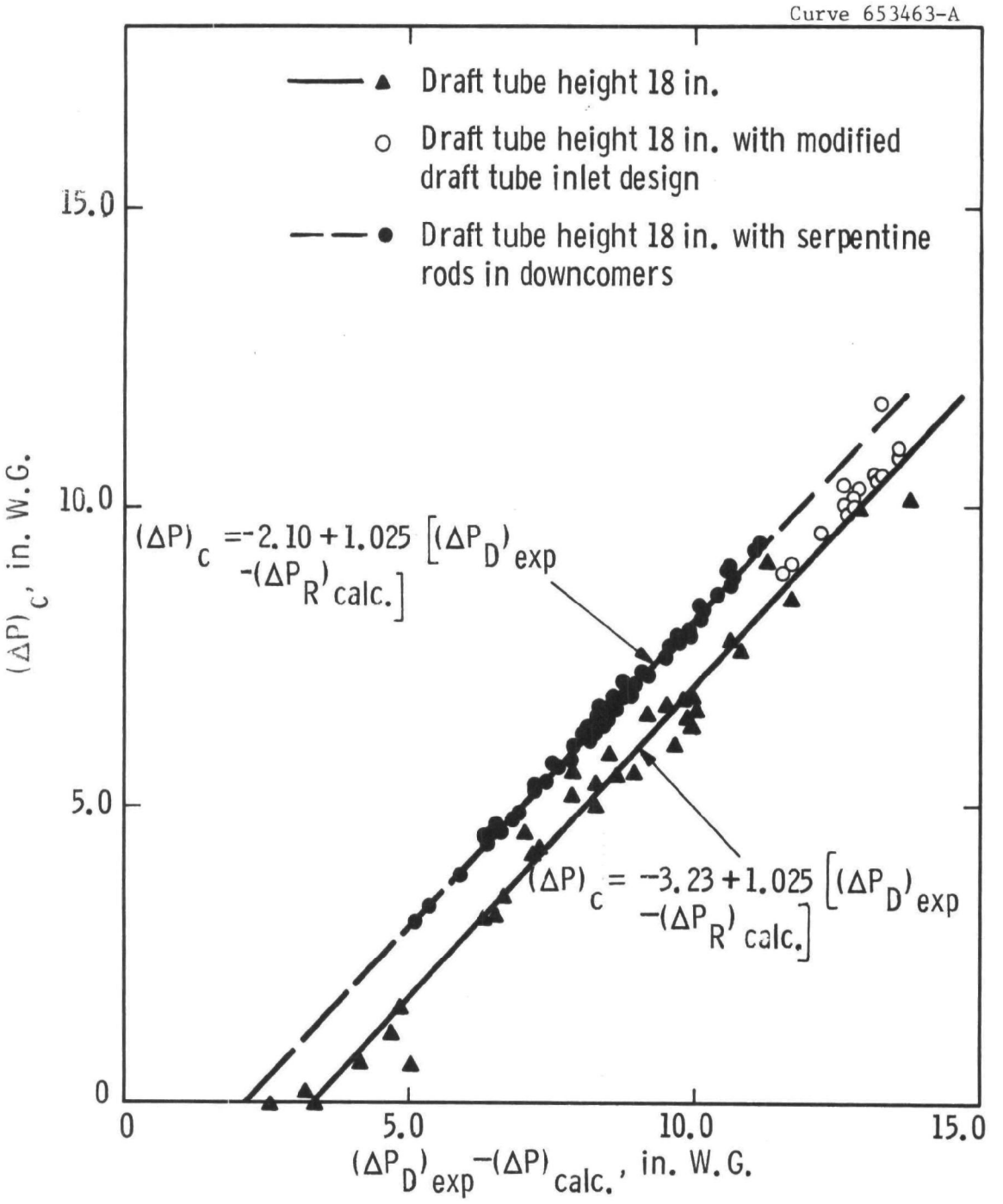

Fig. 9—Pressure Loss Due to Slugging Transport

TABLE P-18

COMPARISON BETWEEN THE PREDICTED
AND THE EXPERIMENTAL SOLID RECIRCULATION RATE (CASE I)

Solid Recirculation Rate, lb/sec

Run No.	Predicted	Experimental	Deviation
1-1-1	1.27	1.42	- 10.6
1-1-2	1.24	1.55	- 20.0
1-2-1	1.27	1.46	- 13.0
1-2-2	1.23	1.36	- 9.6
1-3-1	1.24	1.20	+ 3.3
1-3-2	1.23	1.41	- 12.8
2-1-1	1.21	0.912	+ 32.7
2-1-2	1.22	1.21	+ 0.8
2-1-3	1.22	1.27	- 3.9
2-2-1	1.26	1.50	- 16.0
2-2-2	1.23	1.49	- 17.4
3-1-1	1.26	1.53	- 17.6
3-1-2	1.23	1.39	- 11.5
3-1-3	1.21	1.27	- 4.7
3-2-1	1.26	1.42	- 11.3
3-2-2	1.25	1.47	- 15.0
3-2-3	1.24	1.42	- 12.7
3-2-4	1.22	1.29	- 5.4
3-3-1	1.25	1.33	- 6.0
3-3-2	1.24	1.37	- 9.5
3-3-3	1.22	1.31	- 6.9
3-3-4	1.21	1.22	- 0.8
3-4-1	1.23	1.14	+ 7.9
3-4-2	1.22	1.15	+ 6.1
3-4-3	1.21	1.10	+ 10.0
3-4-4	1.21	1.04	+ 16.0
3-5-1	1.23	1.12	+ 9.8
3-5-2	1.22	1.18	+ 3.4
3-5-3	1.21	1.14	+ 6.1
3-5-4	1.21	1.11	+ 9.0

TABLE P-19

COMPARISON BETWEEN THE PREDICTED
AND THE EXPERIMENTAL SOLID RECIRCULATION RATE (CASE II)

Solid Recirculation Rate, lb/sec

Run No.	Predicted	Experimental	Deviation, %
1-1-1	0.723	0.709	+1.97
1-1-2	0.725	0.711	+1.97
1-1-3	0.731	0.726	+0.69
1-1-4	0.733	0.744	-1.48
1-1-5	0.738	0.718	+2.79
1-2-1	0.723	0.705	+2.55
1-2-2	0.725	0.683	+6.15
1-2-3	0.731	0.700	+4.43
1-2-4	0.738	0.716	+3.07
1-2-5	0.733	0.675	+8.59
1-3-1	0.720	0.620	+16.13
1-3-2	0.723	0.640	+12.97
1-3-3	0.728	0.640	+13.75
1-3-5	0.733	0.675	+ 8.59
1-4-1	0.720	0.625	+15.20
1-4-2	0.725	0.713	+ 1.68
1-4-4	0.731	0.653	+11.94
1-5-1	0.725	0.742	-2.29
1-5-2	0.731	0.750	-2.53
1-5-3	0.736	0.752	-2.13
2-1-1	0.731	0.744	-1.75
2-1-2	0.733	0.744	-1.48
2-1-4	0.740	0.750	-1.33
2-2-1	0.727	0.703	+3.41
2-2-2	0.730	0.700	+4.29
2-2-4	0.738	0.713	+3.51
2-3-1	0.730	0.742	-1.62
2-3-2	0.730	0.690	+5.80
2-3-4	0.735	0.683	+7.61
2-4-1	0.727	0.731	-0.55
2-4-2	0.733	0.713	+2.81
2-4-4	0.735	0.707	+3.96

TABLE P-19 (Continued)

Run No.	Predicted	Experimental	Deviation, %
2-5-1	0.727	0.731	-0.55
2-5-2	0.735	0.759	-3.16
2-5-3	0.738	0.759	-2.77
3-1-1	0.738	0.977	-24.46
3-1-2	0.743	0.977	-23.95
3-1-3	0.753	0.977	-22.93
3-2-1	0.735	0.943	-22.06
3-2-2	0.743	0.953	-22.04
3-2-3	0.745	0.949	-21.50
3-2-5	0.751	0.971	-22.66
3-3-1	0.735	0.940	-21.81
3-3-2	0.743	0.951	-21.87
3-3-3	0.745	0.962	-22.56
3-3-5	0.743	0.895	-16.98
3-4-1	0.730	0.852	-14.32
3-4-2	0.733	0.858	-14.57
3-4-3	0.740	0.930	-20.43
3-4-4	0.743	0.908	-18.17
3-4-5	0.745	0.893	-16.57
3-5-1	0.733	0.940	-22.02
3-5-2	0.735	0.934	-21.31
3-5-3	0.743	0.994	-25.25
3-5-4	0.743	0.977	-23.95
3-5-5	0.753	1.053	-28.49

TABLE P-20

COMPARISON BETWEEN THE PREDICTED
AND THE EXPERIMENTAL SOLID RECIRCULATION RATE (CASE III)

Run No.	Solid Recirculation Rate, lb/sec		
	Predicted	Experimental	Deviation, %
B-1-1	0.640	0.681	- 6.0
B-1-2	0.640	0.638	+ 0.3
B-1-3	0.640	0.586	+ 9.2
B-1-4	0.645	0.662	- 2.6
B-2-1	0.640	0.679	- 5.8
B-2-2	0.642	0.662	- 3.0
B-2-3	0.642	0.614	+ 4.6
B-2-4	0.642	0.601	+ 6.8
B-3-1	0.640	0.685	- 6.6
B-3-2	0.640	0.631	+ 1.4
B-3-4	0.640	0.598	+ 7.0
B-3-5	0.645	0.610	+ 5.7
B-4-1	0.640	0.694	- 7.8
B-4-2	0.640	0.644	- 0.6
B-4-3	0.642	0.640	+ 3.1
B-4-5	0.647	0.681	- 5.0

into the air plenums appears as air bubbles which occupy almost the whole cross-section right above the distributor plate. These bubbles either by-pass into the draft tube and contribute to slugging or ascend into the downcomers and interfere with the solid downward flow. This phenomenon also creates severe pressure fluctuation in the downcomers and the draft tube.

Even when the length of the draft tube is increased, slugging is still expected to occur in the lower part of the draft tube at low air velocities to make up the additional pressure drop. Predictions of solid recirculation rate, at low air velocities, from pressure drop calculations of the vertical pneumatic transport without taking into account the slugging will give high values when compared with experimental data. Thus, in designing and operating a recirculation bed, it is preferable to operate at around the maximum solid recirculation rate, not only to take advantage of the high recirculation rate but also to prevent slugging in the draft tube.

CONCLUSIONS

- A mathematical model has been developed which can be used to predict recirculation or to select operating conditions to achieve a given recirculation rate for a given reactor configuration.
- The draft tube inlet design, draft tube height, downcomer draft tube area ratio are critical design variables for a recirculating fluid bed reactor.

ACKNOWLEDGEMENT

Calculations of the pressure drops in the draft tube using Curran and Gorin's model were performed by Dr. J.P.L. Chen. His help is hereby acknowledged.

REFERENCES

1. Dent, F. J., "Methane From Coal," 9th Coal Science Lecture, BCURA (1960).

2. Horsler, A. G., and Thompson, B. H., "Fluidization in the Development of Gas Making Processes," Tripartite Chem. Engr. Conf., Montreal (Sept. 1968).

3. Horsler, A. G., Lacey, J. A., and Thompson, B. H., "High Pressure Fluidized Beds," CEP, 65 (10), 59-64 (1969).

4. Decamps, F., Dumont, G., and Goossens, W., "Vertical Pneumatic Conveyor with a Fluidized Bed as Mixing Zone," Power Technol., 5, 299 (1971/72).

5. Buchanan, R. H. and Wilson, B., "The Fluid-Lift Solids Recirculator," Mech. & Chem. Eng., Trans. (Australia), 117, May (1965).

6. Curran, G. P., and Gorin, E., "The CO_2 Acceptor Gasification Process - A Status Report - Application to Bituminous Coals," Paper presented at the Third International Conference on Fluidized Bed Combustion, Hueston Woods, Ohio (1972).

   Curran, G. P., Pasek, B., Pell, M., and Gorin, E., "Pretreatment of Bituminous Coals for Pressure Gasification," Paper presented at the Fluidized Bed Combustion Symposium, American Chemical Society Meeting, Chicago, Illinois (1973).

7. Taskaev, N. D., and Kozhina, M. I., Trudy Akad. Nauk Kirgiz S.S.R., 7, 109 (1956).

8. Archer, D. H., Vidt, E. J., Keairns, D. L., Morris, J. P., and Chen, J. L. P., "Coal Gasification for Clean Power Production," Proceedings of the Third International Conference on Fluidized Bed Combustion, Hueston Woods, Ohio, October 1972.

9. Ergun, S., CEP 48, 89 (1952).

10. Yoon, S. M. and Kunii, D., "Gas Flow and Pressure Drop Through Moving Beds," Ind. Eng. Chem. Process Des. Develop. 9 (4), 559 (1970).

11. Curran, G. P. and Gorin, E., "Studies on Mechanics of Flow-Solids Systems," report prepared for Office of Coal Research by Consolidation Coal Company (1968).

12. Jones, J. H., Braun, W. G., Daubert, T. E., and Allendorf, H. D., "Estimation of Pressure Drop for Vertical Pneumatic Transport of Solids," AIChE Journal, 13 (3), 608 (1967).

13. Kolpakov, V. M. and Donat, E. V., "An Investigation of the Pressure Drop in the Acceleration Zone of a Vertical Pipeline for Conveying Solid Particles," Intern. Chem. Eng., 10 (3), 394 (1970).

14. Papai, L., "Velocity and Pressure in Vertical Pneumatic Conveying," Acta. Tech. Aca. Sci, Hungaricae, 69, 83 (1970).

15. Stemerding, S., "The Pneumatic Transport of Cracking Catalyst in Vertical Risers," Chem. Eng. Sci., 17 599 (1962).

16. Richardson, J. F. and Zaki, W. N., "Sedimentation and Fluidization: Part I," Trans. Instn. Chem. Engrs., 32, 35 (1954).

17. Wen, C. Y. and Yu, Y. H., "Mechanics of Fluidization," CEP Symposium Series 62, 62 (1966).

18. Davidson, J. F., and Harrison, D., Fluidization, Academic Press (1971).

19. Hinkle, B. L., Ph.D. Thesis, Georgia Institute of Technology, Atlanta, Georgia (June 1953).

20. Zenz, F. A. and Weil, N. A., "A Theoretical-Empirical Approach to the Mechanism of Particle Entrainment from Fluidized Beds," AIChE Journal, 4 (4), 472 (1958).

21. Leung, L. S., Wiles, R. J., and Nicklin, D. J., "Correlation for Predicting Choking Flowrates in Vertical Pneumatic Conveying," Ind. Eng. Chem. Process Des. Develop., 10 (2), 183 (1971).

22. Zenz, F. A. and Othmer, D. F., Fluidization and Fluid Particle Systems, New York: Reinhold Publishing Co., (1960).

NOMENCLATURE

A = area of orifice opening, ft^2

A_o = specific surface area of the solid particles and can be expressed as $A_o = 6/\phi_s \bar{d}_p$, ft^2

A_d = cross-sectional area of the downcomer, ft^2

A_r = cross-sectional area of the draft tube, ft^2

A_t = cross-sectional area occupied by the serpentine tubes

C_o = solid discharge coefficient defined in Equation 40

C_D = drag coefficient on solid particles

d_o = orifice diameter, ft

$\bar{d}_p$ = mean particle size, ft

d_{pi} = particle diameter of size i, ft

D = draft tube diameter, ft

D_j = diameter of the jet, ft

f = Fanning friction factor

f_p = solid friction factor from Equation 28

f_s = solid friction factor from Equation 13

F = air by-passing factor

F_c = correction factor for downcomer pressure drop

g = gravitational acceleration, ft/sec^2

G = solid mass flow rate, lb/ft^2-sec

H = length in downcomer occupied by the serpentine tubes

H_o = distance between the two pressure taps in the downcomer

H_{mf} = bed height at minimum fluidizing condition, ft

J	=	jet penetration depth, ft
L	=	height of the draft tube, ft
ΔL	=	distance required to accelerate a spherical particle to a specific velocity, ft
n	=	empirical constant defined in Equation 19
ΔP_{1-2}	=	pressure drop between 1 and 2 (see Figure P-1), lb/ft^2
$(\Delta P_{1-2})_{calc}$	=	calculated pressure drop between 1 and 2, lb/ft^2
$(\Delta P_{1-2})_{exp}$	=	experimental pressure drop between 1 and 2, lb/ft^2
ΔP_{1-4}	=	pressure drop between 1 and 4 (see Figure P-1), lb/ft^2
ΔP_D	=	pressure drop in the downcomer, lb/ft^2
$(\Delta P_D)_{calc}$	=	calculated pressure drop in the downcomers, lb/ft^2
$(\Delta P_D)_{exp}$	=	experimental pressure drop in the downcomers, lb/ft^2
ΔP_{fg}	=	pressure drop due to gas-pipe wall friction, lb/ft^2
ΔP_{fs}	=	pressure drop due to solid-solid friction and solid-pipe wall friction, lb/ft^2
ΔP_{hg}	=	pressure drop due to the static head of the gas, lb/ft^2
ΔP_{hs}	=	pressure drop due to static head of the solid particles, lb/ft^2
$(\Delta P_{hs})_c$	=	corrected pressure drop due to static head of the solid particles, lb/ft^2
ΔP_{kg}	=	pressure drop due to kinetic energy change of the gas, lb/ft^2
ΔP_{ks}	=	pressure drop due to kinetic energy change of the solid particles, lb/ft^2
ΔP_R	=	pressure drop in the draft tube, lb/ft^2
$(\Delta P_R)_c$	=	corrected pressure drop in the draft tube, lb/ft^2
Re	=	$\rho_f U_o D/\mu$, the Reynolds number

Re_t	=	Reynolds number based on the terminal velocity of the solid particles
U_o	=	superficial fluid velocity, ft/sec
U_f	=	actual fluid velocity in the bed; $U_f = U_o/\varepsilon$, ft/sec
$U_{f,d}$	=	actual fluid velocity in the downcomers, ft/sec
$U_{f,r}$	=	actual fluid velocity in the draft tube, ft/sec
$U_{p,d}$	=	solid particle downward velocity in the downcomers, ft/sec
$U_{p,r}$	=	solid particle velocity in the draft tube, ft/sec
$(U_{p,d})_L$, $(U_{p,d})_R$	=	solid particle downward velocities in two downcomers, ft/sec
U_{sl}	=	slip velocity between fluid and solid particle in the draft tube, ft/sec
U_t	=	terminal velocity of the solid particle, ft/sec
W_s	=	solid flow rate, lb/sec
X	=	empirical exponent; $X = 1.0$ when $A_o < 6300\ ft^2/ft^3$
X_i	=	weight fraction of particles of size i
ε_b	=	voidage of the fluid bed above the draft tube
ε_d	=	voidage in the downcomers
ε_r	=	voidage in the draft tube
μ	=	viscosity of the fluid, lb/sec-ft
ρ_f	=	density of the fluid, lb/ft^3
ρ_s	=	solid particle density, lb/ft^3
η	=	correction factor for nonspherical particles (Equation 23)
θ	=	specific solid loading, lb solids/lb fluid
ϕ_s	=	sphericity of the solid particle

BIBLIOGRAPHIC DATA SHEET	1. Report No. EPA-650/2-73-048a thru -d	2.	3. Recipient's Accession No.
4. Title and Subtitle Pressurized Fluidized-Bed Combustion Process Development and Evaluation, Volumes I, II, III, and IV (Vol II, Appendices; Vol III, Boiler Development Plant Design; Vol IV, Oil Gasification/Desulfurization)			5. Report Date December 1973
			6.
7. Author(s) D. L. Keairns, D. H. Archer et al.			8. Performing Organization Rept. No.
9. Performing Organization Name and Address Westinghouse Research Laboratories Pittsburgh, Pennsylvania 15235			10. Project/Task/Work Unit No. ROAP 21ADB-09
			11. Contract/Grant No. 68-02-0217
12. Sponsoring Organization Name and Address EPA, Office of Research and Development NERC-RTP, Control Systems Laboratory Research Triangle Park, North Carolina 27711			13. Type of Report & Period Covered Final
			14.

15. Supplementary Notes

16. Abstracts The report presents: results of a process evaluation of the pressurized fluidized-bed combustion (FBC) system for power generation; preliminary plans and a cost estimate for a 30-MW pressurized FBC boiler development plant; identification of a project team and program to demonstrate FB oil gasification/desulfurization for power generation on a 50-MW plant; and evaluation of pressurized oil gasification for combined-cycle power generation. It identifies no problems which preclude the development of pressurized FBC combined-cycle power plants and FB oil gasification power plants which can generate electrical energy within environmental goals at lower energy costs than competitive systems. Work reported here, a continuation of earlier FBC process evaluation efforts, is aimed at the development and demonstration of these FB fuel processing systems.

17. Key Words and Document Analysis 17a. Descriptors

Air Pollution
Combustion
Gasification
Fluidized Bed Processing
Desulfurization
Oils
Fossil Fuels
Wastes
Electric Power Generation

17b. Identifiers/Open-Ended Terms

Air Pollution Control
Stationary Sources
Fluidized-Bed Combustion

17c. COSATI Field/Group 13B, 14A, 21B

18. Availability Statement	19. Security Class (This Report)	21. No. of Pages
Unlimited	UNCLASSIFIED	258
	20. Security Class (This Page) UNCLASSIFIED	22. Price

FORM NTIS-35 (REV. 3-72) USCOMM-DC 14952-P72